DTU Library

Advances in high-gradient magnetic fishing for bioprocessing

Goncalves Gomes, Claudia Sofia

Publication date:
2006

Document Version
Early version, also known as pre-print

[Link back to DTU Orbit](#)

Citation (APA):
Goncalves Gomes, C. S. (2006). *Advances in high-gradient magnetic fishing for bioprocessing*. Technical University of Denmark.

Advances in High-Gradient Magnetic Fishing for Bioprocessing

Cláudia Sofia Gonçalves Gomes

Ph.D. Thesis
April 2006

BioCentrum-DTU
TECHNICAL UNIVERSITY OF DENMARK

Advances in High-Gradient Magnetic Fishing for Bioprocessing

Ph.D. Thesis

Cláudia Sofia Gonçalves Gomes

Center for Microbial Biotechnology

Biocentrum-DTU

Technical University of Denmark

Dansk Resumé

"High-gradient magnetic fishing" (HGMF) er en metode til processering af fødestrømme med biologiske molekyler. HGMF integrerer brugen af superparamagnetiske adsorbenter med separation og processering med høj-gradient magnetisk separation (HGMS) i et magnetisk filter med høj (≥90 %) "voidage". Adsorbenterne er uporøse (med lave diffusionsbegrænsninger og mindre tilbøjelighed til "fouling") og meget små, hvilket tilsikrer en stor specifik bindingsoverflade. Siden sin begyndelse i 2001, har forskning indenfor HGMF fokuseret på undersøgelse af teknikkens basale principper og udbredelse af dens anvendelighed til direkte produktfangst - med det langsigtede mål at udvikle et egentligt redskab til biotekindustrien til hurtig og effektiv (og dermed økonomisk) rensning af værdifulde makromolekyler. På trods for betydelige fremskridt, er rejsen ikke overstået endnu. Selv om HGMF har vundet større anerkendelse som redskab til bioprocessering, og for nylig har været underkastet opskaleringsforsøg, har teknologien endnu ikke nået biotekindustrien til trods for, at HGMS har været etableret i mineral- og spildevandsbehandlingsindustrierne siden 70'erne. En del af forklaringen på, at HGMF ikke har bevæget sig fra laboratoriet og pilot plant til industrien er den manglende fundamentale forståelse af teknikkens generelle natur, særligt dens potentielle anvendelsesområde men også viden om adsorbenthåndtering med det magnetiske højgradientfilter.

Målet med denne afhandling er at undersøge, hvorledes HGMF kan anvendes til direkte fangst af højværdi produkter i fødestrømme ved høje koncentrationer, og hvorvidt HGMF kan udbredes til brug ved andre bioprocesseringsopgaver end direkte fangst, samt at besvare fundamentale spørgsmål om, hvorledes magnetiske adsorbenter pakker sig i og frigør sig fra magnetiske højgradientfiltre.

Afhandlingen begynder med at introducere HGMS, efterfulgt af en oversigt af basale koncepter med betydning for HGMF og den seneste udvikling i feltet (Kapitel 1). Derefter gennemføres et studie om design af en ny type magnetisk adsorbent til oprensning af immunoglobulin G (IgG), som anvendes i diagnostik, og som er tæt beslægtet med den nye generation af værdifulde monoklonal antistofbaserede

lægemidler. Disse adsorbenter anvender en velkendt omend relativ nyudviklet ligand kaldet MEP (4-mercaptoethylpyridine), som er vist selektivt at kunne binde IgG fra forskellige fødestrømme, når den er koblet til "packed bed" kromatografimedier. I nærværende arbejde, blev en HGMF proces udviklet med MEP magnetiske adsorbenter til oprensning af IgG fra kanin antiserum (Kapitel 2).

Selv om arbejdet beskrevet i kapitel 2 var succesfuldt, belyste det en række andre forhold, som HGMF ikke tidligere havde været stillet overfor, særligt hvordan fødestrømme med høje produktkoncentrationer kan processeres ikke alene til at give oprensede produkter, men også koncentrerede produkter. I HGMF, som i andre adsorptive metoder er kapacitet og selektivitet af adsorbenterne kritiske parametre, men gode adsorbenter er som sådan ikke tilstrækkeligt i HGMF. For at udnytte de optimerede adsorbenters egenskaber, er det vigtigt at processen ikke begrænses af det magnetiske filters kapacitet. Kapaciteten betinger mængden af adsorbent, som kan processeres i en cyklus og korrelerer derfor med protein koncentration og procesproduktivitet. Disse vigtige parametre i processering af fødestrømme med biologiske molekyler adresseres i kapitel 3 og 4. To strategier til forudsigelse af filterkapaciteter beskrives i kapitel 3 og derefter studeres, hvorledes de magnetiske højgradient filtre opfører sig igennem flere cykler af semikontinuerlig processering (Kapitel 4).

I kapitel 5 gennemføres et systematisk studie for at undersøge, om HGMFs unikke egenskaber kan anvendes til at kontrollere proteinhydrolyseprocesser. Med dette sigte, anvendes en HGMF process med optimerede benzamidineforbundne magnetiske adsorbenter sammen med filtrene fra kapitel 3 og 4 til at standse tryptisk hydrolyse af ostevalleproteiner på et defineret punkt.

Thesis outline

High-gradient magnetic fishing (HGMF) is a technique for the downstream processing of biological molecules. HGMF integrates the use of superparamagnetic adsorbents with separation and processing by high-gradient magnetic separation (HGMS) in a high voidage (≥90 %) magnetic filter. The adsorbents are non-porous (low diffusion limitations and less prone to fouling) and very small, ensuring a large specific area available for binding. Since its inception in 2001, the research on HGMF has been focused on proof-of-principle studies and broadening its application for direct product capture with the long term view of developing an industrial biotech tool for quick and efficient (i.e. economic) recovery of valuable macromolecules (Hubbuch *et al.*, 2001; Hubbuch and Thomas, 2002; Heebøll-Nielsen *et al.*, 2003, 2004a, 2004b; Meyer *et al.*, 2005; Ferré, 2005; Ebner, 2005). Despite significant progress, the journey is not over. Although HGMF has been gaining recognition as a bioprocessing tool and has recently been the subject of scale-up studies (Ebner, 2005), it has not yet reached the biotech industry, despite the conventional applications of HGMS that have been established in the mineral and waste water treatment industries since the 1970's (Svoboda, 1987). Part of the reason that HGMF has not made the transition from laboratory and pilot plant to industry is the lack of fundamental understanding about the generic nature of the technique, in particular the potential scope of its application and knowledge of adsorbent handling using the high-gradient magnetic filter.

The aim of this thesis is to examine how HGMF can be used for direct capture of high value products present in feedstocks at high concentrations, whether HGMF can be extended to bioprocessing tasks apart from direct product capture, and to answer fundamental questions about how magnetic adsorbents pack in and release from high-gradient magnetic filters.

This thesis begins by introducing HGMS followed by providing an overview of the basic concepts related to HGMF and recent developments in the field (Chapter 1). A study is then conducted on the design of a new type of magnetic adsorbent for the purification of immunoglobulin G (IgG) used in diagnostic applications, and which is

very similar to the new generation of valuable monoclonal antibody-based pharmaceuticals. These adsorbents employ a well known, although recently developed, ligand called MEP (4-mercaptoethylpyridine) that has been shown to selectively capture IgG from various feedstocks when coupled to packed bed chromatography media (Boschetti, 2002). In the current work, a HGMF process was developed using MEP magnetic adsorbents for the purification of IgG from rabbit anti-serum (Chapter 2).

Although the work conducted in chapter 2 was successful, it highlighted a number of issues not previously faced by HGMF, in particular how feedstocks with high concentrations of product can be processed to not only give purified products, but concentrated ones. In HGMF, like in other adsorptive techniques, the capacity and selectivity of the adsorbents are critical parameters. However, in HGMF good adsorbent performance is not enough. In order to take advantage of the optimised properties of the adsorbents it is important that the process is not limited by the capacity of the magnetic filter. The magnetic filter capacity determines the amount of adsorbent that can be processed in one cycle and therefore correlates to protein concentration and process productivity. These two important parameters in downstream processing of biological molecules are addressed in chapters 3 and 4. Two strategies are introduced in chapter 3 for predicting filter capacities and the performance of high-gradient magnetic filters are subsequently studied in semi-continuous multicycle processing over a number of cycles (Chapter 4).

In chapter 5, a systematic study is conducted to examine whether the unique properties of HGMF can be applied for controlling protein hydrolysis processes. For that purpose, an HGMF process employing optimised benzamidine-linked magnetic adsorbents together with a filter selected from the studies in chapter 3 and 4 is used for halting the tryptic hydrolysis of cheese whey proteins at a defined point.

References

Boschetti, E. (2002) Antibody separation by hydrophobic charge induction chromatography. *Trends Biotechnol*., 20(8), 333-337

Ebner, N. (2006) *Einsatz von Magnettechnologie bei der bioprodukt.* Ph.D. Thesis. University of Karlsruhe, Germany.

Ferré, H. (2005) *Development of novel processes for continuous protein refolding and primary recovery - A case study on the major histocompatibility complex class I receptor and its individual subunits.* Ph.D. Thesis. Technical University of Denmark, Denmark.

Hubbuch, J.J., Matthiesen, D.B., Hobley, T.J., Thomas O.R.T. (2001) High gradient magnetic separation versus Expanded bed adsorption: A first principle comparison. *Bioseparation*, 10, 99-112.

Hubbuch, J.J., Thomas, O.R.T. (2002) High-gradient magnetic affinity separation of trypsin from crude porcine pancreatin. *Biotechnol. Bioeng.*, 79, 301-313.

Heebøll-Nielsen, A., Choe, W-S., Middelberg, A.P.J., Thomas, O.R.T. (2003) Efficient inclusion body processing using chemical extraction and high-gradient magnetic fishing. *Biotechnol. Progr.,* 19(3), 887-898.

Heebøll-Nielsen, A., Dalkiær, M., Hubbuch, J.J., Thomas, O.R.T. (2004) Superparamagnetic adsorbents for high-gradient magnetic fishing of lectins out of legume extracts. *Biotechnol. Bioeng.,* 87(3), 311-32.

Heebøll-Nielsen, A., Justesen, S.F.L., Hobley, T.J., Thomas, O.R.T. (2004) Superparamagnetic cation-exchange adsorbents for bioproduct recovery from crude process liquors by high-gradient magnetic fishing. *Sep. Sci. Technol.,* 39(12), 2891-2914.

Meyer, A., Hansen, D.B., Gomes, C.S.G., Hobley, T.J., Thomas, O.R.T., Franzreb, M. (2005) Demonstration of a strategy for product purification by high-gradient magnetic fishing: Recovery of superoxide dismutase from unconditioned whey. *Biotechnol. Progr.*, 21, 244-254.

Svoboda, J. (1987) Magnetic methods for the treatment of minerals. *Developments in Mineral Processing* (Ed. Fuerstenau, D.W.), 8, Elsevier Sci. Publ. Co., Amsterdam.

Preface

This thesis is the outcome of my work done as a PhD student in the Bioseparations group at the Center for Microbial Biotechnology (CMB), DTU. During this period I counted with the necessary financial support to perform my research activities through a grant awarded to me by the Portuguese Foundation for Science and Technology.

First of all, I wish to thank Owen R. T. Thomas for having accepted me as a student in his group and for supervising me during the initial period of my PhD. During that period I counted with the support of Timothy Hobley who then continued supporting me as my main supervisor in the last years of the PhD, and whom I thank for giving me the necessary motivation to complete this work.

Part of my work was conducted in the group of Matthias Franzreb in the Forschunszentrum Karlsruhe in Germany. There, I had the opportunity to initiate two of the projects integrated in this thesis, in close collaboration with the PhD student Niklas Ebner. I would like to thank both Matthias and Niklas for making my stay in Germany such a good working experience and for the inspiring discussions about magnetics.

Another part of my work was done in collaboration with Anders Heebøll-Nielsen, whom I thank for the useful criticism and prompt feedback.

Trine Lütken Petersen and Inga Pakalnyte have conducted their master's projects under my supervision and have contributed to part of the work in this thesis with excellent technical skills and enthusiasm. I'm grateful to them for that.

Most experiments done in connection with HGMF involved a great deal of 'unseen' preparations, such as equipment set-up and programming. These were accomplished with the help of Martin Nielsen and the people from the pilot plant, to whom I would like to thank for their efforts.

The experimental results used in the first part of this thesis were made possible by Hanne Bak, who developed and gave me access to an immunoturbidimetric assay that permitted the quantification of the immunoglobulins that I purified. Hanne also provided me with the rabbit anti-serum used in the work and shared with me her

experience with that feedstock. In connection with this project I also wish to thank Fanny Guillaumie and Paulo Vital for scientific advice on the matters related to organic chemistry.

I would like to thank my friends in Denmark and Portugal, with whom I could always count. I am especially grateful to Luis Lomelino Fernandes.

Finally I want to express my sincere gratitude to Christian Hansen and my family for their unconditional support.

<div align="right">

Cláudia Sofia Gonçalves Gomes

April 2006

</div>

List of publications, oral and poster presentations during the thesis

Publications

1. Gomes, C.S.G., Petersen, T.L., Hobley, T.J., Thomas, O.R.T. (2005) Controlling enzyme reactions in unclarified bioprocess liquors using high-gradient magnetic fishing (HGMF). In *Proceedings of the 7th World Congress of Chemical Engineering*. ISBN 085295 494 8.

2. Meyer, A., Hansen, D.B., Gomes, C.S.G., Hobley, T.J., Thomas, O.R.T., Franzreb, M. (2005) Demonstration of a strategy for product purification by high-gradient magnetic fishing: Recovery of superoxide dismutase from unconditioned whey. *Biotechnol. Progr.*, 21, 244-254.

3. Ebner, N., Gomes, C.S.G., Hobley, T.J., Thomas. O.R.T., Franzreb, M. Filter capacity predictions for the capture of superparamagnetic microparticles by high-gradient magnetic separation (HGMS). Submitted to *IEEE Trans. Magn.*

4. Gomes, C.S.G., Pakalnyte, I., Thomas, O.R.T., Hobley, T.J. Construction and application of mercaptoethylpyridine–linked magnetic adsorbents for the purification of immunoglobulins from crude rabbit antiserum by high-gradient magnetic separation. *In preparation*

5. Gomes, C.S.G., Ebner, N., Thomas. O.R.T., Franzreb, M., Hobley, T.J. Protein purification using high-gradient magnetic fishing: Impact of magnetic filter performance. *In preparation*

6. Gomes, C.S.G., Heebøll-Nielsen, A., Petersen, T.L., Thomas, O.R.T, Hobley, T.J. Control of protein hydrolysis in unclarified liquors: application of high-gradient magnetic fishing (HGMF) employing improved magnetic adsorbents. *In preparation*

The articles 1 and 2 are published and are in appendices 1 and 2, respectively. Publication 3 (submitted) including small modifications is chapter 3 of this thesis. Publications 4, 5 and 6 (in preparation) are based on chapters 2, 4 and 5, respectively.

Oral presentations

Cláudia S.G. Gomes, Trine L. Peteresen, Niklas Ebner, Andrea Meyer, Matthias Franzreb, Owen R.T. Thomas, <u>Timothy Hobley</u>. Using magnetic filters for downstream processing of bioproducts. *AFS 2005 Annual Conference & Exposition*, Atlanta, USA, 11-13 April.

<u>Cláudia S.G. Gomes</u>, Niklas Ebner, Andrea Meyer, Owen R.T. Thomas, Timothy J. Hobley, Matthias Franzreb. Advances in High-Gradient Magnetic Fishing for protein purification: impact of filter design on bioprocessing. *Biotechnology 2004*, Santiago, Chile, 17-22 October 2004.

<u>Cláudia S.G. Gomes</u>, Inga Pakalnyte, Timothy J. Hobley, Owen R.T. Thomas. Mercaptoethylpyridine–linked magnetic adsorbents for the purification of immunoglobulins from crude rabbit antiserum. *12th International Conference on Bio-Partitioning and Purification (BPP)*, Vancouver, Canada, 22-27 June 2003. (Poster and oral presentation)

Poster presentations

<u>Timothy J. Hobley</u>, Henrik Ferré, Cláudia S.G. Gomes, Dennis B. Hansen, Trine L. Petersen, Søren Buus, Owen R.T. Thomas. The potential of magnetic adsorbents for downstream processing. *European Symposium on Biochemical Engineering Science (ESBES 5)*, Stuttgart, Germany, 8-11 September 2004.

<u>Cláudia S.G. Gomes</u>, Inga Pakalnyte, Timothy J. Hobley, Owen R.T. Thomas. Mercaptoethylpyridine–linked magnetic adsorbents for the purification of immunoglobulins from crude rabbit antiserum. *PREP Symposia on Preparative / Process Chromatography*, San Francisco, USA, 29 June - 2 July 2003.

Contents

1. Introduction

1.1 What is HGMF?

High-gradient magnetic fishing (HGMF) is a technique designed for recovering macromolecules directly from biological feedstocks. It results from the combination of two basic processes: (i) binding of a biological molecule to a magnetic based adsorbent, and (ii) handling of the magnetic adsorbents by a technique known as high-gradient magnetic separation (Hubbuch *et al.*, 2001) (Fig. 1.1).
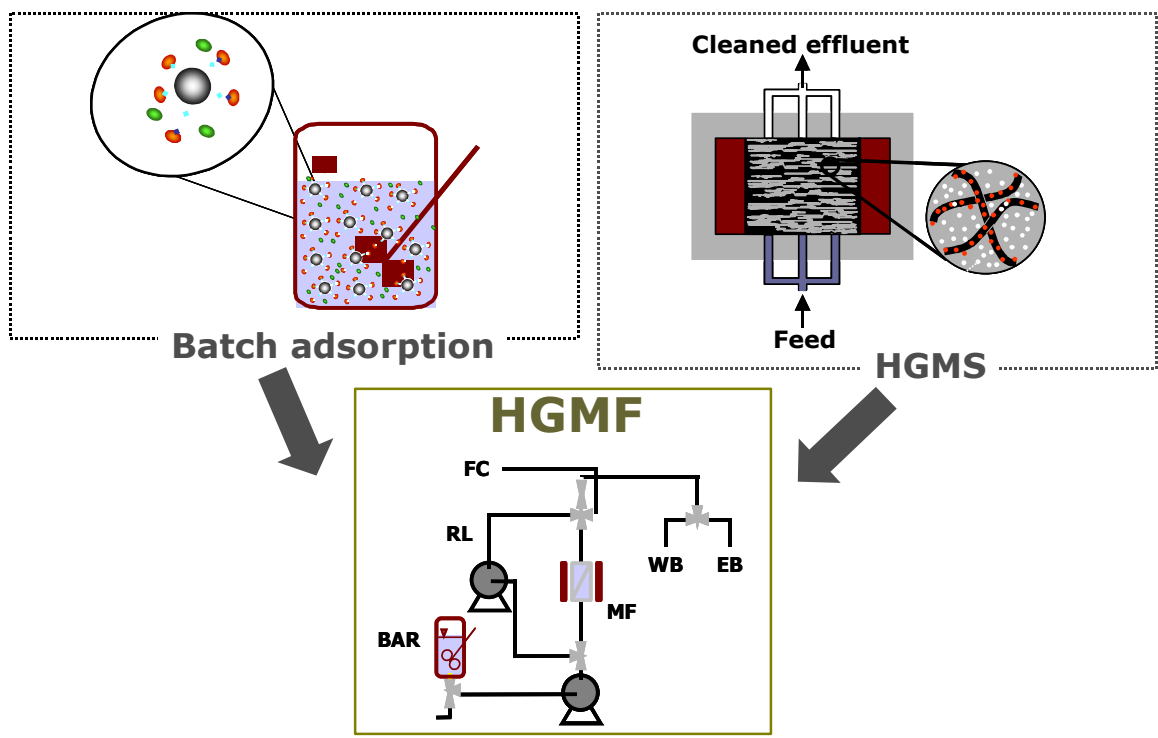
Fig. 1.1 Illustration of HGMF as a result of the integration of HGMS and batch adsorption. MF = magnetic filter, FC = fraction collector, WB = washing buffer container, EB = elution buffer container, RL = recycle loop, BAR = batch adsorption reactor.

In HGMF, the general steps involved in a downstream processing operation based on adsorptive methods can be performed, i.e., equilibration of the adsorbents, binding, wash, elution, and regeneration. A typical process conducted at laboratory scale is initiated by a batch binding step with the molecule of interest to previously equilibrated adsorbents. The loaded adsorbents are then collected on a high-gradient

20

magnetic filter placed in a loop (Fig. 1). By switching the magnetic field off whilst pumping, the magnetic adsorbents can be released from the filter into the closed loop containing buffer (e.g. wash, elution, etc) and mixed. Subsequently the adsorbents can be collected in the filter by reinstating the field and the contents (e.g. the buffer containing the eluted protein) collected. In a HGMF recovery process it therefore is possible to control the conditions to which the adsorbent will be exposed in the different steps and to repeat these steps in a closed system to give a complete cycle of adsorbent loading, wash, elution and regeneration. Since high voidage (~85-93 %) filters are typically used (Hubbuch *et al.*, 2001; Hubbuch and Thomas, 2002; Heebøll-Nielsen, 2003, 2004a, 2004b; Meyer *et al.*, 2005; Ebner *et al.*, 2006; Gomes *et al.*, 2006a, 2006b, 2006c), crude feedstreams can be processed without prior clarification and often without conditioning, thus combining clarification and direct capture in one unit operation.

An advantage that HGMF has over other adsorptive techniques, such as conventional batch mode adsorption with chromatography like adsorbents, packed bed or expanded bed chromatography, is the possibility of employing non-porous adsorbents of small sizes and still being able to separate them easily. Non-porous adsorbents not only have the property of being more resistant to fouling (Halling and Dunnill, 1979, 1980) and therefore are more suited to use in the presence of crude feedstocks, but also allow for fast binding kinetics due to the elimination of internal diffusion limitations (Ferré, 2005; Hoffmann, 2002). However, in order to compensate for less pore area available for binding, the sizes of non-porous adsorbents must be much smaller than those of conventional chromatographic type adsorbents. The main disadvantage of HGMF from a process point of view is that, in principle, binding and elution can only be done in batch mode, therefore limiting the possibility of achieving high resolution, and placing extra demands on the affinity of the adsorbents during binding and elution. Thus, the role of HGMF is to act primarily as a direct capture step offering clarification, concentration and intermediate purification. If required, high resolution can be obtained in later operations of a typical downstream process, namely during the purification stage. Substitution of HGMF for conventional clarification and

concentration steps, while at the same time increasing product purity, reduces the total number of unit operations and could thus potentially reduce costs.

1.2 High-Gradient Magnetic Separation

High-gradient magnetic separation (HGMS) forms the basis of the current generation of magnetic filters used in HGMF. The basic principle underlying HGMS is that the introduction of a magnetisable wire perpendicular to the field lines of a homogeneous magnetic field gives rise to a strong magnetic field gradient around the wire (Fig. 1.2) which attracts magnetically susceptible particles. This principle permits the use of moderate magnetic fields for the recovery of small or weakly magnetic particles, not only by generating high field gradients but also by providing large surface areas for capture. This technique was introduced in the early seventies (Kolm, 1972) and amongst many applications, it has been used extensively in the mineral and waste water treatment industries (Svoboda, 1987; Oberteuffer, 1973, 1974, Oberteuffer *et al.*, 1975). In more recent years, it has been applied to laboratory-scale bioprocessing, as will be discussed later.
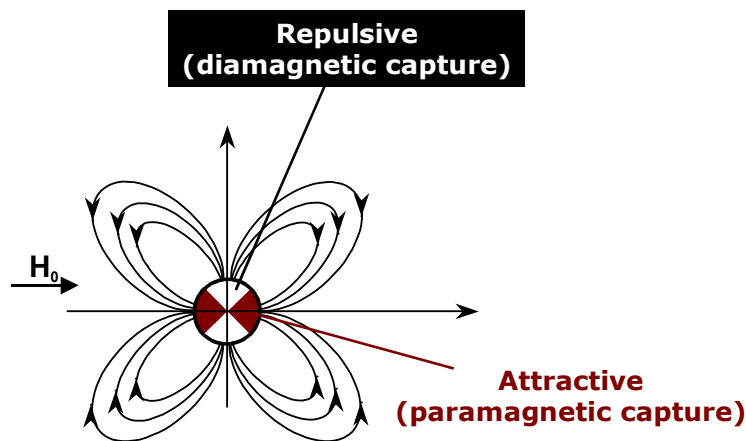
Fig. 1.2 Magnetic force field around a cylindrical wire with axis perpendicular to the page (adapted from Cummings *et al.*, 1976). The existence of the repulsive zones perpendicular to the applied magnetic field have been confirmed experimentally by Himmelblau (1974).

1.2.1 Single wire theory

Motion of a paramagnetic particle around a magnetised wire

The single wire model, as the name indicates, describes the dynamic behaviour of a paramagnetic particle in the vicinity of a magnetised single cylindrical ferromagnetic wire and it was first introduced by Watson (1973). In this theory, the field is always represented perpendicularly to the axis of the wire since this is the arrangement that yields maximum distortion of the field around the wire. The theory considers the application of a uniform magnetic field H_0 strong enough to saturate the wire of radius a, i.e., a field that magnetises the wire to the magnetisation M_S, and a spherical paramagnetic particle of radius b at a distance r from the centre of the wire axis carried by a fluid with a velocity v_0 as depicted in figure 1.3. Two arrangements concerning the fluid direction with respect to the wire and the field directions can be described by this model: (i) $\alpha=0$, where the fluid flows parallel to the magnetic field in the opposite direction and (ii) $\alpha=\pi/2$, where the fluid flows perpendicularly to the field. These two cases are defined as the longitudinal (L) and the transversal (T) configurations, respectively. A third possibility, the axial (A) configuration, occurs when the fluid moves parallel to the wire axis. An illustration of the three ideal configurations and the effect of these on the build up of the paramagnetic particles are presented in figure 1.3.
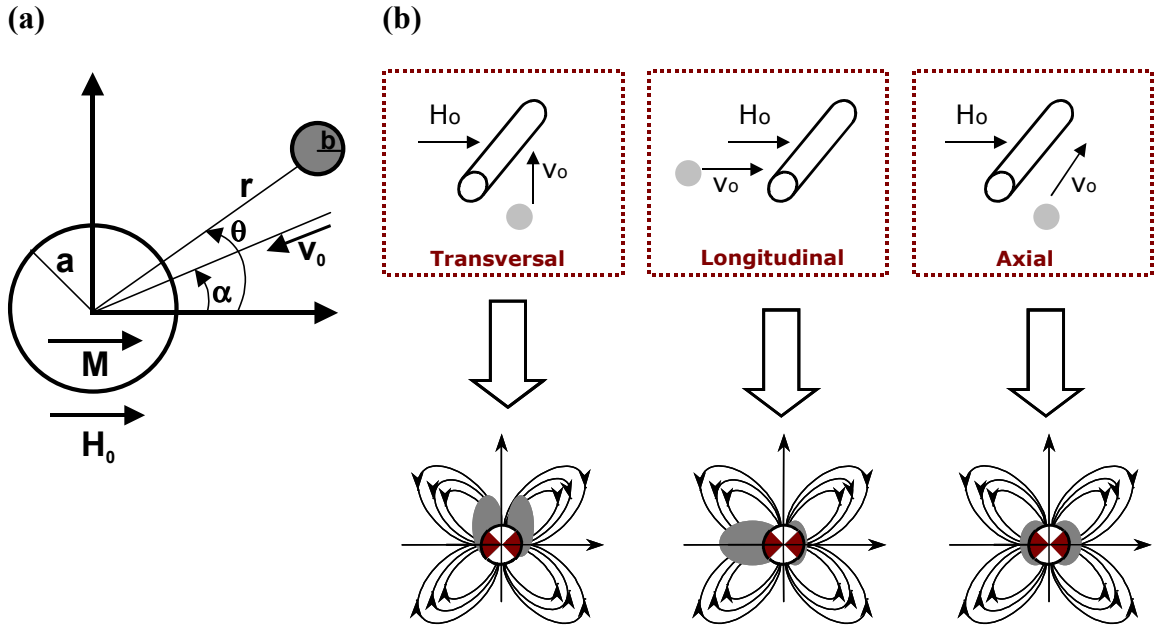
Fig. 1.3 (a) Cross section of a ferromagnetic wire with axis into the page and radius a placed perpendicularly to the external magnetic field H_0 interacting with a paramagnetic particle of radius b in a fluid moving in a perpendicular direction with respect to the wire at a velocity v_0. (b) Arrangements concerning the fluid, magnetic field and ferromagnetic wire directions, and illustration of the particle build up on the wire for each configuration. The figure is adapted from Cummings *et al.* (1976), Friedlaender *et al.* (1978) and Svoboda (1987).

A number of forces act on a paramagnetic particle in a magnetic separator: inertial ($\vec{F}_i$), viscous drag ($\vec{F}_d$), magnetic ($\vec{F}_m$) and gravitational ($\vec{F}_g$) forces, and the equation for the motion of a particle can therefore be written in the following way:

$$\vec{F}_i = \vec{F}_d + \vec{F}_m + \vec{F}_g \qquad \text{(Eq. 1.1)}$$

Under the conditions at which HGMS is operated, i.e., small particles (≤ 10 μm, Cummings *et al.*, 1976), the inertial and gravitational forces can be neglected (Watson, 1973; Cummings *et al.*, 1976, 1980) and the particle motion depends solely on the viscous drag force, $\vec{F}_d$, (given by Stokes equation) and the magnetic force, $\vec{F}_m$:

$$\vec{F}_d = -6\pi\eta b v_0 \qquad \text{(Eq. 1.2)}$$

$$\bar{F}_m = \frac{1}{2}\mu_0 \chi V_p \nabla (H \cdot H)$$

(Eq. 1.3)

Thus, the forces acting on a paramagnetic particle depend on the viscosity (η) and velocity (v_0) of the liquid, on the radius of the magnetic particle (b), according to equation 1.2, and on the volume magnetic susceptibility (χ) and volume (V_p) of the particle and on the magnetic field gradient induced by the magnetic field strength (H), according to equation 1.3.

Considering a time-independent equation for particle motion in a fluid moving perpendicularly to the wire axis (i.e., for the L- and T- configurations) the behaviour of a magnetic particle over a magnetisable wire was obtained[1] (Eq. 1.4). The works of Gerber and Birss (1983) or Svoboda (1987) are recommended for simple and clear descriptions of the physical and mathematical principles used for deriving equation 1.4.

$$\frac{1}{r_a}\frac{dr_a}{d\theta} = \frac{\left(1 - \frac{1}{r_a^2}\right)\cos(\theta - \alpha) - \frac{v_m}{v_0}\left(\frac{M_S}{2\mu_0 H_0 r_a^5} + \frac{\cos 2\theta}{r_a^3}\right)}{\left(1 + \frac{1}{r_a^2}\right)\sin(\theta - \alpha) + \frac{v_m}{v_0}\frac{\sin 2\theta}{r_a^3}}$$

(Eq. 1.4)

Where μ_0 is the permeability of the free space, r_a is the normalised distance to the axis of the wire r/a and v_m is the magnetic velocity. These last two parameters were introduced by Watson (1973) and the second is given by the following equation:

$$v_m = \frac{2\chi M_S H_0 b^2}{9\eta a}$$

(Eq. 1.5)

Where η the viscosity of the liquid, χ the volume magnetic susceptibility of the particle, H_0 is the external magnetic field strength and M_S the saturation magnetisation of the wire.

---

[1] The viscous drag force component of equation 1.1 has been derived under the assumption that the liquid is frictionless with respect to the wire. Therefore, this equation is valid for potential flow, i.e., for Reynolds numbers >> 1 (Watson (1975) considers this to be > 10) where the effect of fluid viscosity can be neglected and no friction around the wire is considered.

Equation 1.4 shows that for the longitudinal and transversal configurations, the motion of a magnetic particle in the vicinity of a magnetised wire will depend solely on the initial position and initial velocity of the particle, the ratios v_m/v_0 and $M_S/(2\mu_0 H_0)$. The solution of the equation (Eq. 1.4) permits the critical radius (R_c) to be determined, i.e., the maximum distance from the axis of the wire at which a magnetic particle will be captured. According to this model, R_c depends on the ratio v_m/v_0 but not on the magnetic velocity or fluid velocity alone, and this dependency is higher when particles are away from the wire. $M_S/(2\mu_0 H_0)$ has a high impact close to the wire, and is thus commonly called the short range term. Quantification of these two parameters and their impact on the critical radius for the longitudinal configuration and the transversal configuration has been reported by Watson (1975). The critical capture radius is an important parameter since, by comparing its values at different conditions, one can extrapolate the information to compare efficiency of collection of magnetic particles by a wire, and in turn by a magnetic filter consisting of magnetisable wires under those conditions. However, a first problem encountered with the equations of motion developed by Watson was the fact that they could only be solved numerically. Soon other authors (Uchiyama and Hyashi, 1979; Birss and Parker, 1981; Gerber and Birss, 1983) introduced some simplifications and thus could calculate analytically approximate solutions that were close to the ones obtained numerically.

The second problem was encountered when the values of R_c for transversal and longitudinal configurations calculated for the same conditions were compared. It was found that the capture radius of the transversal configuration was always the largest although experimental studies indicated that filters with the longitudinal configuration performed better in the conditions tested ($0.3 < vm/v_0 < 10$) (Watson, 1975). It was argued that the inferior experimental performance of filters employing the T-configuration had to do with collection of particles occurring in a region exposed to high shear, contrary to the L-configuration.

Nevertheless, the trends observed for the calculated R_c values according to the equations of motion were in agreement with experimental observations for filter

performance (Watson, 1975). Furthermore, for large values of v_m/v_0 (>8, Gerber and Birss, 1983) a good approximation for the normalised critical capture radius in both longitudinal and transversal configurations can be given by the following equation (Gerber and Birss, 1983):

$$ R_{ca} \approx \frac{3}{4}\sqrt{3}\left(\frac{v_m}{v_0}\right)^{\frac{1}{3}}\left[1-\frac{2}{3}\left(\frac{v_m}{v_0}\right)^{-\frac{2}{3}}\right] \qquad \text{(Eq. 1.6)} $$

The single wire model has later been extended to the axial configuration by Birss *et al.* (1976). The axial configuration describes the situation where the flow of the magnetic particle suspension and the wire are parallel as illustrated in figure 1.3. From the three possible configurations, the axial configuration results in the lowest collection efficiency, both theoretically and experimentally. The assumption of potential flow (see footnote 1 in page 25) has been examined, and computational models for low speed flow, assuming viscous flow near the wire, were developed (Cummings e*t al.*, 1976, 1980; Lawson and Gerber, 1990).

In general, the models mentioned up to here were critical for understanding the basic mechanisms of magnetic capture since they provided information about the behaviour of a single particle in the vicinity of a ferromagnetic wire.

Particle build-up

A breakthrough in the HGMS field occurred when high quality visual observations of particle capture on a single magnetised wire were made possible by Friedlaender *et al.* (1978) using a television camera coupled to a specially constructed microscope. Particle capture on a nickel wire was observed for particle slurries consisting of $Mn_2P_2O_7$, Mn_2O_3 and Cr_2O_3 with sizes ranging between 1 and 20 μm using the three main orientations of wire, field and flow illustrated in figure 1.3. This technology enabled accurate measurements of particle build-up radius over time and the determination of maximum build-up radius, i.e., the saturation accumulation radius R_s (or R_{as} for relative values to the wire radius).

Visualisation of particle behaviour around a ferromagnetic wire supported a new approach in the study of particle capture in HGMS: the description of particle build-up on individual collecting wires. Theoretical models developed by Luborsky and Drummond (1976) and by others (Friedlander *et al.*, 1978a; Nesset and Finch, 1979) could be tested experimentally. These models, contrary to the equations of motion presented above, take into consideration the changes in the flow pattern around a wire as particles start accumulating. For the axial configuration a relatively simple analytical model developed by Friedlander *et al.* (1978a) was shown to adequately describe experimental data based on optic studies of saturation build-up as a function of v_m/v_0 (McNeese *et al.*, 1979), although a coefficient related to particle density had to be estimated empirically. Experimental data was also obtained for the other two configurations, but in these cases, a description of the collection process was more difficult to obtain (McNeese *et al.*, 1980). It was, however, shown that realistic calculations of the saturation radius for the longitudinal configuration were made possible by using a model called the static equilibrium build-up model (Nesset and Finch, 1979; Nesset *et al.*, 1980). Furthermore, the build-up profiles predicted by this model were in close agreement with optic measurements of $Mn_2P_2O_7$ particle collection at different velocities for a variety of ferromagnetic wires (Nesset and Finch, 1981).

Another important observation that Friedlander's technology permitted, was the capture of particles on the rear of the wire in the longitudinal configuration when operating at moderate Reynolds numbers (~6-40) (McNeese *et al.*, 1980; Friedlaender *et al.*, 1978). This is due to a wake formation, a phenomenon already known from fluid mechanics and that had already been described as 'vortex capture' (Cummings *et al.*, 1976). An increase of the capture area of the wire could be observed for the L-configuration simply due to the fact that some particles escaping the build-up upstream of the wire are again captured downstream of the wire where they are protected from sheer forces. Experimental tests have later shown that for Reynolds numbers between 4 and 30, the introduction of turbulence enhancers in the form of a grid results in an improvement of the filter performance (Watson and Bahaj, 1989).

The determination of the build-up radius might not be the best method to determine the filter efficiency since this parameter does not always correlate with the experimental performance of filters. For example, Leiterman *et al.* (1984), in a comparison between different geometries show that particle build-up reaches the smallest accumulation radius for the longitudinal configuration, when this type of filter was the best performing in terms of particle recovery. Friedlander *et al.* (1978b) observed larger R_{as} values for the axial configuration as compared to any other. These inconsistencies are mainly due to the density of the 'cake' of particles agglomerated around the wire not being taken into consideration. In this way, a larger capture radius does not necessarily mean that the wire is capable of capturing a larger amount of particles per unit of wire area. Furthermore, the volume of the build-up might be of more interest than the simple measurement of the radius, especially for the transversal configuration where a wake is formed.

1.2.2 Filter performance

There are two approaches to dealing with the study of magnetic separation in a real filter: the microscopic approach and the phenomenological approach. The first, based on the single wire theories, tries to extrapolate the description of particle trajectories and wire capture efficiencies to an array of wires. The second approach, describes the dynamic behaviour of a filter by use of parameters that can be measured experimentally, such as the breakthrough of magnetic particles during loading to the filter. The microscopic approach is not of great use in practical terms due to its complexity, whereas the phenomenological, being a simpler approach, is less rigorous. A combination of both, however, is possible (Svoboda, 1987; Gerber and Birss, 1983).

The performance of a filter with respect to the recovery of a given magnetic particle suspension can be experimentally evaluated by conducting breakthrough studies. These consist of filter loading experiments under controlled conditions of magnetic field and fluid velocity, while monitoring the concentration of particles in the inlet and outlet over time. The particle breakthrough, at the filter-end, according to deep bed filtration studies, can be described by the following equation (Herzig, 1970):

$$\frac{c}{c_0} = \frac{\exp\left(\sigma_S^{-1} c_0 v_0 \lambda_0 \tau\right)}{\exp\left(\sigma_S^{-1} c_0 v_0 \lambda_0 \tau\right) + \exp\left(\lambda_0 L_F\right) - 1} \qquad \text{(Eq. 1.7)}$$

where c_0 and c are the particle concentrations of the suspension in the inlet and outlet of the filter, respectively, σ_S is the saturation or maximum capacity of the filter, v_0 is the liquid velocity in the filter and τ is the displacement filter time, which equals the filtration time, t, minus the time, t_F, the suspension needs to cover the filter length, L_F. λ_0 is the filter coefficient of the empty filter and is given by the following equation (Gerber and Birss, 1983):

$$\lambda_0 = \frac{f_{M,T} \cdot F_{V,T} \cdot R_{ca}}{a} \qquad \text{(Eq. 1.8)}$$

where, $f_{M,T}$ is geometric coefficient of the wire ($2/\pi$ for transversal wires and 0.12 for random wires), $F_{V,T}$ is the volume fraction of the transverse filter element wires, a is the wire radius and R_{ca} is the normalised critical capture radius.

By using this approach, it is possible to link experimental filter performance results to the properties of the magnetic particle suspension and of the magnetic filter. Examination of equation 1.7 shows that for a given filter length, the filter coefficient affects the breakthrough curve steepness which, according to equation 1.8, depends on filter properties such as orientation and thickness of the wires, voidage, and on the size of the critical capture radius R_{ca}.

1.3 Critical parameters in HGMF

When looking separately at all components of a HGMF process, it is possible to relate the critical parameters affecting HGMF to: (i) the magnetic adsorbents, (ii) the magnetic filter and (iii) the magnetic separator. In this section these parameters will be evaluated. Keeping in mind that this work deals only with proteins, no specific consideration will be given to other types of molecules, such as DNA.

1.3.1 Magnetic adsorbents

There are a number of affinity magnetic adsorbents commercially available which are mainly intended for laboratory applications. The authors Safarik and Safarikova (2004) recently published a comprehensive review of magnetic adsorbents available commercially and reported in the literature. As mentioned in section 1.1, small sizes and non-porosity are believed to be the properties necessary for magnetic adsorbents when used in crude feedstocks, and for guaranteeing fast kinetics during binding and desorption. Additionally, if a HGMF process is to be competitive in industry it is necessary to take into consideration other properties of the adsorbents, such as binding capacity, re-usability and chemical resistance. As we will see later, the size and shape of the supports also play an important role.
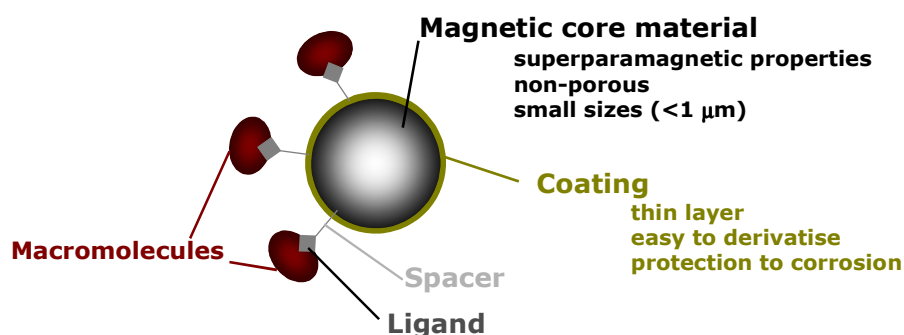
Fig. 1.4 Illustration of magnetic adsorbent components and main properties with relevance to bioprocessing.

Most magnetic base supports consist of colloidal magnetite particles embedded in a polymer or of coated iron-oxide crystal clusters. The magnetic adsorbents used in the current work, PGF (poly-glutaraldehyde ferrite) based, are of the second type. These are prepared from the alkaline precipitation of iron oxides followed by a silane polymerisation reaction using 3-aminopropyltriethoxysilane that leads to the formation of amine terminated magnetic beads of sizes bellow 1 μm (Zulqarnain, 1999, Hubbuch; 2000; Hoffmann, 2002). The free-amine groups on the surface of the silanised magnetic beads enable the attachment of another coating layer formed by alkaline polymerisation of the bi-functional chemical glutaraldehyde (Halling and Dunnill, 1979). The poly-glutaraldehyde coating confers corrosion protection to the

particles, and leaves reactive groups (aldehyde groups) on the surface of the particles that can be used for attachment of ligands for selective targeting of proteins (Fig. 1.4).

The adsorbents mentioned above have been described in more detail by Hubbuch and Thomas (2002). It is important to consider two other important aspects of these adsorbents : the superparamagnetic and geometric properties.

The iron oxide core prepared from optimised ratios of Fe(II) and Fe(III) (1:2, respectively) confers superparamagnetic behaviour and high surface area to the supports (Zulqarnain, 1999). Paramagnetic materials have no magnetic behaviour in the absence of a magnetic field, but they respond to magnetic fields with quite low magnetisation values due to their low magnetic susceptibility[2]. Ferromagnetic particles of very small size become superparamagnetic (Whitesides et $al.$ 1983). These materials (i.e. superparamagnetic types) have the advantage of having no magnetic memory and of reaching higher magnetisation values than simple paramagnetic materials. After silane coating of iron oxide clusters, the specific surface area of the superparamagnetic particle agglomerates is roughly 100 m^2 g^{-1} (Zulquarnain, 1999), which is 10 times higher than would be expected given the sizes of these particles (<1μm, Hubbuch and Thomas 2000; Gomes et $al.$, 2006c). Given this high specific surface area, it can be concluded that these particles cannot have smooth non-porous surfaces. This assumption is supported by the scanning electron microscopy (SEM) picture of a single polyglutaraldehyde coated particle presented in figure 1.5. These adsorbents, being essentially non-porous, possess a rough surface that increases the surface to volume ratio. Moreover, the binding kinetics are fast. A simple binding test using derivatised PGF adsorbents and an antibody system showed that the binding reached equilibrium faster than the 45 s monitoring interval (Gomes et $al.$, 2006c). A precise study of binding a histidine-tagged protein to magnetic adsorbents derivatised

---

[2] Magnetic susceptibility (χ) is a proportionality constant that defines the dependency of magnetisation of a given material from the external field applied. Ferromagnetic materials are capable of achieving high magnetisation values but reach saturation at high magnetic fields. The magnetic susceptibility of these materials varies with the external magnetic field. Paramagnetic materials have constant but low magnetic susceptibilities (10^{-6} to 10^{-3}) and contrary to ferromagnetic materials, do not have magnetic memory, i.e., they lose their magnetic properties immediately when an external magnetic field is removed (Thomas and Franzreb, 2006).

with metal chelators has been performed by Ferré *et al.* (2005). They reported that binding equilibrium was reached after 10 s in a well mixed pipe reactor, and showed, by use of mass transfer models and experimental data, that binding is limited by external mass transfer, a characteristic property of non-porous adsorbents.
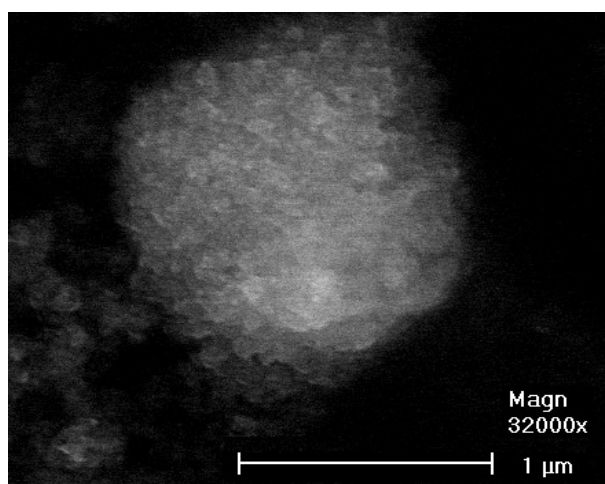
Fig. 1.5 SEM picture of a single polyglutaraldehyde coated ferrite magnetic support (magnification 32000×) (Hoffmann, 2002).

The size of the magnetic adsorbents has an impact in HGMF in two ways. First, smaller particle size causes higher surface to volume ratio, which in turn leads to higher binding capacity. For example, Bucak *et al.* (2003) have reported capacities of up to 800 mg of protein per g of adsorbent using colloidal nanoparticle adsorbents with a core size of 8 nm. The binding capacities reported for PGF micro-size adsorbents are in the range of 50 to 300 mg of protein per g of support, whereas commercial perfectly spherical non-porous adsorbents of 1-2 μm, have capacities of less than 10 mg protein g^{-1} adsorbent (Heeboel-Nielsen, 2002). Second, smaller particle size reduces the magnetic capture capability due to a lower magnetic velocity (*cf.* Eq. 1.5). In fact, individual iron oxide nanoparticles have been shown to be poorly retained in a magnetic filter, whereas permanent capture could be observed for aggregates ranging from 60 to 125 nm (Moeser *et al.*, 2004). Based on those experiments a threshold value of 20 nm has been estimated for efficient capture. Finally, in relation to size, it is important to stress the impact of size distribution. More monodisperse magnetic adsorbents will be captured with the same magnetic

33

velocity (Eq. 1.5), enabling therefore a higher predictability of filter performance (Franzreb *et al.*, 2006a).

The amount of magnetic particles that can be captured by a magnetic filter, (i.e., the filter capacity) also depends on the shape of the adsorbents. Particles that are close to being perfectly spherical are capable of compacting better than irregular particles. The PGF base adsorbents are highly irregular (Ebner *et al.*, 2006; Gomes *et al.* 2006a), and comparison of these with a more regular type of adsorbent with similar magnetic properties showed that the latter led to higher filter capacities (Ebner *et al.* 2006). Furthermore, monodisperse magnetic adsorbents will be captured with the same magnetic velocity (Eq. 1.5), thereby enabling a higher predictability of filter performance. Another important feature of HGMF is the ability of releasing the adsorbents from the filter during the desorbing steps and during recovery of the adsorbents at the end of an operating cycle. It was also found that more regularly shaped adsorbents could be released more efficiency from the magnetic filters (Gomes *et al.*, 2006a).

In addition to the properties of magnetic adsorbents mentioned above, the properties that characterize surface interactions with the molecules of interest are of crucial importance if the adsorbents are to be used in bioprocesses. As was mentioned earlier, a large surface area on the magnetic adsorbents that is available for binding is an advantage. However, in order to use the full potential of a large surface area, it is necessary to ensure appropriate chemical modification that guarantees a large number of binding sites. Usually, functionalised magnetic adsorbents are constructed by introducing a hydrophilic spacer that connects the base matrix to a functional group, i.e., the ligand (Hubbuch, 2000). The hydrophilic nature of the spacer and the high affinity of the ligand, enhanced by high ligand density covering the base matrix, minimize unspecific binding and ensure high selectivity of the adsorbent for a protein of interest (Hermanson *et al.*, 1992). In HGMF, the single plate nature of the binding process requires the adsorbent-protein interaction to be strong. Extensive work on spacer design for PGF based adsorbents has been reported by Hubbuch (2000), Hoffmann (2002), Hubbuch and Thomas (2002) and Heebøll-Nielsen *et al.* (2003,

2004a, 2004b, 2004c). Binding properties of the adsorbents were modified by employing different spacer chemistries and lengths, such as epichlorohydrin (Hermanson *et al.*, 1992), allyl bromide and allyl glycidyl ether (both introduced by Burton and Harding, 1997a, 1997b).

Characterization of adsorbent binding properties is usually performed by the construction of Langmuir (1918) type isotherms described by the following equation:

$$Q^* = Q_{max} \frac{C^*}{K_d + C^*}$$
(Eq. 1.9)

In equation 1.9 the equilibrium concentrations of the adsorbed and bulk-phase protein are represented by Q^* and C^* respectively, K_d is the dissociation constant and Q_{max} is the maximum binding capacity of the adsorbents. This simple model is based on the assumption of formation of a monolayer and on homogeneous site interaction energies. Although this is not always true, this model is a useful tool for monitoring ligand design and optimising process conditions (Franzreb *et al.* 2006a, 2006b). Evaluation of Langmuir parameters provides information about the strength of binding (K_d), the maximum binding capacity (Q_{max}). Furthermore, the shape of the curve, namely the formation of a plateau, indicates if the monolayer assumption is fulfilled. It has been argued that dissociation constant values in the nanomolar range are necessary for magnetic adsorbents to be efficient (Franzreb *et al.*, 2006a).

1.3.2 High-gradient magnetic filters

The magnetic filter capacity is a critical parameter in HGMF since it determines the amount of adsorbent that can be processed in a cycle and therefore affects the productivity of the process as well as the concentrating power. The capacity is dependent on operational conditions such as magnetic particle suspension velocity, magnetic field, magnetic particle properties (see section 1.3.1) and filter properties. This section will focus on the latter.

Until recently, the filters used for HGMF applications consisted of a ferromagnetic knitted mesh rolled in a cylindrical canister. Knitted meshes have the advantage of having small wire diameters (~100 μm) providing a large area for particle capture, as

well as being able to pack quite densely and still provide the filter with a high voidage. Voidages of ~85-93 % have been reported using this type of filter (Hubbuch *et al.*, 2001; Hubbuch and Thomas, 2002; Heebøll-Nielsen, 2003, 2004a, 2004b; Meyer, 2005). For the purpose of demonstrating the applications of the technique and proving of principles in the laboratory, these filters were suitable and simple to manufacture.

The magnetic force exerted on a particle is dependent on the magnetic field gradient (Eq. 1.3) and the latter depends on the diameter, shape and material of the ferromagnetic wire generating the gradient. Calculations of the optimal wire size to maximize the magnetic force on a particle indicate that the wire radius should be 3 times larger than the particle radius (Oberteuffer, 1974). Other authors (Svoboda, 1987, and references therein) have determined optimal theoretical wire:particle radius ratios in the range of 1 to 10. These estimates are based on single-collector-single-particle calculations and do not consider the effect of particle deposition on the wires or hydrodynamic conditions. Optimal wire dimension determinations should not be taken into consideration blindly. In fact, those values would indicate that the matrix elements selected to construct a magnetic filter to deal with magnetic supports in the range of sizes employed in HGMF (~1 μm) should consist of wires with diameters of 3 to 10 μm. These values are not realistic, since such filter packing would be exceptionally fragile.

The filter matrices are usually ferromagnetic due to the high magnetisation values for this type of material in the presence of a magnetic field. The magnetisation of the wires and the particle are, according to equations 1.4 and 1.5, two of the main parameters affecting particle capture, and depend only on the magnetic susceptibility of the material and the magnetic field strength applied. However, at low fields (<0.1 T) the PGF particles become saturated (Zulqarnain, 1999), and at a higher field (~1.2 T) the ferromagnetic wires become saturated (Nesset and Finch, 1979). It has been argued that filter capacity varies only slightly when operating at fields higher than the saturation value of the matrix material (Hubbuch, 2000). Thus, the choice of

ferromagnetic filter packing material should involve consideration of the saturation magnetisation properties of the wire materials.

The symmetry of paramagnetic attractive and repulsive areas on a wire (Fig. 1.2) will be affected by the transversal shape of the wire. The wire components usually available are not perfectly cylindrical and a magnetic field generated around an elliptic wire will, depending on the direction of magnetisation, narrow (if the field is applied along the minor axis) or enlarge (if the field is applied along the major axis) the capture region for paramagnetic particles. This has been confirmed experimentally by Leitermann (1984) who observed that particle build-up had different shapes depending of the shape of the wire.

(a)   **(b)**
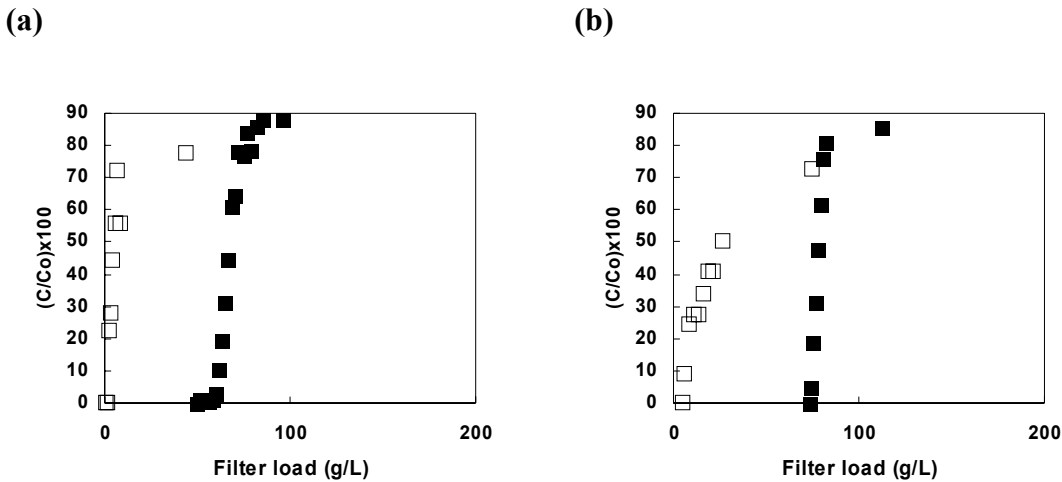
Fig. 1.6 Comparison of magnetic and mechanical particle retention in a magnetic filter. Breakthrough curves for loading of (1 g L^{-1}) glutaraldahyde-coated PGF magnetic supports resuspended in water into a 4.5-mL cylindrical magnetic filter (1 cm internal diameter and 5.8 cm long) at a field strength of 0.4 Tesla (full symbols) and zero field (open symbols) consisting of (a) Knitted mesh of 110 μm diameter, stainless steel 430 wires, 90 % voidage; (b) woven stainless steel 430, 50 μm diameter fibres, 85 % voidage. v_0: 24 m h^{-1}.

When constructing a magnetic filter some of the considerations mentioned above will become less important than considerations of a practical nature. For example, decrease in size of the wires will be limited by the mechanical strength necessary during exposure to a magnetic field, and the need to resist hydrostatic compression during operation. In spite of their high voidage (~90 %), magnetic filters constructed

with very fine wires, such as woven mesh, are more likely to retain non-magnetic particles. A simple test, performed using two different types of matrix filling, as illustrated in figure 1.6., shows that although small diameter wire materials will probably lead to an increase in the amount of magnetic particles captured per filter volume, a higher degree of mechanical entrapment is likely to occur.

Resistance to corrosion is of utmost importance in bioprocesses. Stainless steel 430 has been the most widely used material for filter matrices in general applications of HGMS. It combines the necessary magnetic properties for efficient particle retention, i.e., high magnetisation values and magnetic saturation properties for background fields $\geq$ 1 Tesla (Nesset and Finch, 1979), and it presents good corrosion resistance in the presence of chemicals typically used for cleaning-in-place of bioprocessing equipment, such as nitric acid and sodium hydroxide (Svoboda, 1987).

As mentioned above (section 1.2.1) the generation of a strong magnetic field gradient occurs when a ferromagnetic wire is positioned perpendicularly to a magnetic field. Thus, the orientation of the wires in a filter will have an impact on capture of magnetic particles (Eq. 1.3). It is well established that when the wires are positioned orthogonally to the applied field, the capture efficiency of a filter will be enhanced as compared to filters with random wire orientation (Too, 1986). Furthermore, use of wires with well-defined orientations can be regarded as a tool for aiding design of filters (Parker and Li, 1989). An example of filter performance studies using orientation of arrays of wires as a fixed parameter is presented by Ebner at al. (2006) and Gomes *et al.* (2006a) later in this work.

The impact of wire orientation according to the three possible theoretical cases illustrated in figure 1.3 on magnetic capture has been discussed by a number of authors (Watson, 1975; Briss *et al.*, 1980; McNeese *et al.*, 1979, 1980; Friedlander, 1978, Leiterman, 1984; Birss *et al.*, 1980) using different approaches. Calculations of the critical capture radius (R_{ca}) by study of magnetic particle trajectories using single-wire models indicate that under comparable operational conditions, i.e., for the same values of v_m/v_0 and $M/(2\mu_0H_0)$, the configuration where the suspension flow is perpendicular to the wires and the magnetic field (transversal configuration), results

38

in larger values of R_c, whereas the longitudinal configuration is known to lead to higher capture efficiency (Watson, 1975 and references therein). However, Birss *et al.* (1980) show in their work that filter capture efficiencies for longitudinal and transversal configurations (assumed to depend equally on the critical capture radius according to Watson, 1973) in fact correlate differently and R_c is found to be greater for the T- than in the equivalent L-configuration, resulting therefore in the superior performance of the longitudinal configuration. Evaluation of filter performance based in single-wire model parameters for axial filters, shows that these filters are not expected to perform as well as the other two configurations (Birss *et al.*, 1976). However, there is some discrepancy between these results and experimental studies using optical visualisation of actual particle build up. The largest saturation collection build-up on a single wire observed by Friedlander *et al.* (1978) was for the axial configuration, which is, however, known to give the worst performing type of filter. The smallest build-up observed was for the longitudinal configuration both in single-wire and multi-wire studies (Friedlander *et al.*, 1987; Leitermann *et al.*, 1987), although this configuration is expected to have a better performance than filters with wires in the axial orientation. Furthermore, it has been argued that the density of magnetic particle build-up is greater when particles are collected on the upstream side of a wire when the direction of the fluid is the same as the magnetic field (Leitermann, 1984). However, an observation that still holds (Friedlander *et al.*, 1987; McNeese *et al.*, 1980), as a qualitative evaluation of different wire orientations, is the fact that for filters with wires in the longitudinal configuration, the particle accumulation radii are less affected by variations of the liquid velocity or viscosity of the slurry, suggesting that the higher performance for filters in this orientation are due to less susceptibility of the particle build-up to drag forces. Nevertheless, filters operating with particle flow perpendicular to the magnetic field are more practical to employ. This has to do with filter and magnet integration rather than with the filter itself.

In general, HGMS filters can be thought of as a magnetic deep bed filter. Analogous to conventional deep bed filters, HGMS capacity is increased by extending the length of the filter (L_F). Computational studies using equation 1.8 under typical HGMF operation conditions (and keeping λ_0 constant) show that the breakthrough curve

becomes steeper when L_F increases, indicating that the filter separation will be more efficient (Hubbuch 2000; Hoffman, 2002). However, the length of a magnetic filter can only be increased to the extent allowed by the magnet generating the magnetic field.

One issue that has been given little attention, both in the HGMS literature and in HGMF studies, is particle release from the filters, although drops in capacity of 20 % have been reported when filters were re-used, apparently due to non-release of the magnetic particles from the filter after flushing (Hubbuch and Thomas, 2002). Other studies have shown that product release from the adsorbents is inefficient if they are not released from the filter (Heeboell-Nielsen, 2002). Thus, inefficient release of adsorbents from a magnetic filter during HGMF is likely to have serious consequences, including losses of valuable products and adsorbents, reduction in capture capacity, as well as issues of carry over from batch to batch. Replacement of filters between cycles of a process would be time consuming and would probably have an impact on process economics. In light of the above, an evaluation of filter performance in bioprocessing taking into consideration particle release is given later in this work (Gomes *et al.*, 2006a). There are very many parameters that affect filter performance and most of them are inter-related, thus designing the perfect filter, i.e., a filter that maximizes the capture of magnetic particles with 100 % recovery and their subsequent full release would seem to be a difficult task. Up till now, there has been much focus on studying the trajectories of magnetic particles and build-up profiles around a ferromagnetic wire, however, little has been done on the performance of 'real-life' filters with bioprocessing in mind. Thus, later in the current work (Ebner *et al.*, 2006), studies on magnetic filter capacity based on experimental data by use of ordered arrays of wires in the transversal configuration will be presented.

Magnetic separators for bioprocessing

According to Franzreb *et al.* (2006b), the high-gradient magnetic separators currently available do not meet the requirements necessary for the bioprocessing industry, such as hygienic design, prevention of product contamination, efficient cleaning-in-place and low running costs. There are two main types of magnetic separators: the solenoid and permanent types. The first can produce very high magnetic fields by use of two wound electric coils and has the advantage of having the field turned off to enable filter flushing. These separators are, however, usually associated with very high running costs. A prototype laboratory permanent magnetic separator has been developed that can be switched on and off, combining in this way the more convenient operating mode of the solenoid magnets with lower running costs (Hoffmann *et al.*, 2002; Meyer *et al.*, 2005). This magnetic separator has been used to process volumes of 0.3-0.6 L (Ebner, 2006; Gomes *et al.*, 2006a, 2006b). Although this magnet can generate the necessary magnetic field intensity of 0.3 to 0.6 Tesla required for a HGMF process, it will be difficult to maintain the field when greater pole gaps are necessary to accommodate the larger filters required for large scale processing (Franzreb *et al.*, 2006a). An alternative to the switchable permanent magnetic separator is the use of reciprocating permanent magnetic filter separators. These permanent separators are constructed so that a movable filter can be introduced in the field gap for particle capture, and subsequently removed from the field to perform the steps where particle release is necessary. Separators of this type have been reported to accommodate larger filters that can process up to 20-L batches (Franzreb *et al.*, 2006b).

1.4 Recent progress in HGMF

Several case studies during the last years have addressed various aspects of HGMF as a bioprocessing tool. From these studies, significant achievements have been reported with respect to adsorbent surface design and employment to HGMF (Hubbuch *et al.* 2001; Hoffmann, 2002; Hubbuch and Thomas, 2002; Heebøll-Nielsen *et al.*, 2003, 2004a, 2004b, 2004c), as well as to process design (Meyer, 2004; Meyer *et al.*, 2005; Ferré, 2005; Ebner, 2006; Franzreb *et al.*, 2006a, 2006b).

41

Adsorbent surface design

Application of a range of functionalisation chemistries to the PGF type of supports - characterised by having a large area to volume ratio (see section 1.3.1) - have introduced surface modifications that resulted in adsorbents with high capacity and selectivity. Binding properties of the adsorbents were shown to be closely related to the degree of ligand substitution on the surface of the particles (Hubbuch and Thomas, 2002). Furthermore, it was shown, by comparing identical supports activated with 1,4-butanediol diglycidyl ether and epichlorodydrin (both epoxy-activating agents) in the preparation of *p*-aminobenzamidine (a trypsin inhibitor) linked magnetic adsorbents, that the former (12 atoms) had better trypsin binding properties (Q_{max}=125 mg g^{-1}, K_d=0.3 μM) than with activation with the latter (3 atoms) (Hubbuch and Thomas, 2002). This possibly was due the longer spacer arm. However, for other type of magnetic adsorbents, namely ethane suphonic acid-based cation exchangers, use of the epichlorohydrin chemistry gave excellent results when tested with lysozyme solutions (Q_{max}=222 mg g^{-1}, K_d=0.6 μM). These results were further improved by introducing epichlorohydrin oligomers prior to coupling of the ligand (Heebøll-Nielsen *et al.*, 2004b).

Later work done with *p*-aminobenzamidine adsorbents showed that employment of allyl chemistries improved the performance of PGF adsorbents, probably because of the quantitative coupling of these as compared to the epoxy reactions. Introduction of a shorter spacer arm consisting 7 atoms through a reaction with allyl glycidyl ether resulted in an increased binding capacity and stronger binding to trypsin (Heebøll-Nielsen, 2002; Gomes *et al.*, 2006b). In support of these observations, comparison between ally glycidyl ether activated and 1,4-butanediol diglycidyl ether activated supports to prepare Cu^{2+} metal chelators by attachment of the ligand iminodiacetic acid, indicated the superiority of the former chemistry (Q_{max}=58 mg g^{-1} and K_d=0.08 μM for the first and Q_{max}=26 mg g^{-1} and K_d=0.5 μM for the latter, when tested with bovine serum albumine) (Heebøll-Nielsen *et al.*, 2003). Good performance of adsorbents prepared by allyl activations (allyl glycidyl ether and allyl bromide - 3 atoms) was also found in the preparation of anion exchangers by attachment of trimethyl amine. (Heebøll-Nielsen *et al.*, 2004c).

All of the magnetic adsorbents described above were tested with 'real' feedstocks, and even in those complex protein systems, the performance was still good. Some examples are (i) the employment of the *p*-aminobenzamidine adsorbents for the recovery of trypsin from porcine pancreatine and spiked cheese whey (Hubbuch and Thomas, 2002; Heebøll-Nielsen, 2002; Gomes *et al.*, 2006b); (ii) the use of magnetic metal chelators for the recovery of superoxide dismutase from cheese whey (Meyer *et al.*, 2005), and for targeting histidine tagged proteins expressed in the form of inclusion bodies (Heebøll-Nielsen, 2003; Ferré, 2005), and (iii) application of cation exchangers for the recovery of lactoperoxidase and lactoferrin from cheese whey (Heebøll-Nielsen, 2004b, 2004c; Meyer, 2004). In the cases mentioned here, purification factors reported for the target protein after elution ranged between 12 and 36 for starting materials with target protein content lower than 10 % of the total protein and 1.4 to 3.5 for less contaminated feedstocks.

As discussed before (1.3.1), adsorbent capture on a magnetic filter is an important parameter in HGMF, for which essentially spherical adsorbents with narrow size distributions have a better performance. However, these have a lower surface to volume ratio than the irregular supports presented above (PGF type), and therefore have lower binding capacities. This said, encouraging results were recently reported, where capacities of ~40 mg g^{-1} were achieved for binding green fluorescent protein from a cell homogenate to improved polyvinyl-alcohol-based magnetic metal chelators (1 μm, monodispersed) (Ebner, 2006).

Application of adsorbents to HGMF

When using improved magnetic adsorbents in HGMF processing, purity of the recovered proteins from complex feedstocks was generally in agreement with the results from test tube studies. Not surprisingly, the concentration factor depended on the initial concentration of target protein in the biological feedstock, since the desorption loops had usually similar sizes. Two extreme cases were reported where similar HGMF set-ups were used. In one case a concentration of 2.5 mg mL^{-1} of magnetic cation exchange adsorbents was used to recover lactoperoxidase from cheese whey (a protein typically present at low concentrations, <0.03 mg mL^{-1}). The

combined elution fractions resulted in a lactoperoxidase concentration 4.7 times higher than initially (Heebøll-Nielsen, 2004b). Contrary to these results, stands another HGMF study, where 28 mg of magnetic Cu^{2+} metal chelator per mL of an *E. coli* extract was needed to purify the target recombinant protein, a 2 fold dilution of the protein was obtained after elution (Heebøll-Nielsen, 2003).

Although handling of high support concentrations might be a challenge to HGMF, studies with diluted protein targets in complex systems (Heebøll-Nielsen, 2004b; Hubbuch and Thomas, 2002; Meyer, 2005) indicate that this technique can achieve both concentration and purification in a single step. The concentration power can be further increased by either decreasing the volume of the desorption loop or by conducting bench scale binding and desorption optimisation tests at the same conditions as the ones dictated by the desorption loop of the equipment (Meyer, 2005). A potential application of HGMF could be, for example, the new generation of protein based therapeutics produced in mammalian cell culture.

Process design

Recently, multicycle processing has been tested for HGMF, which enable the study of a more real bioprocessing scenario: (Meyer, 2004; Ebner, 2006; Gomes *et al.*, 2006a). Multicycle processing is likely to be necessary if HGMF is to be used for industrial applications, and therefore, the impact of this processing mode has been investigated. Using this approach, Meyer (2004) studied the dependency of process productivity on filter occupancy, taking into account the loss of particles that occurs when loading a filter to the maximum capacity, and the lower amount of protein that can be processed if less adsorbent is loaded to the filter. Hubbuch and Thomas (2002) have called attention to the importance of particle release from magnetic filters, based on the observation that after a HGMF processing cycle using a laboratory type filter (a cylinder consisting of a rolled knitted mesh), only 80 % of the adsorbents could be recovered in-line. The impact of poor adsorbent release takes larger proportions if the adsorbents and the magnetic filter are expected to operate over a number of cycles. This issue, and its impact on a model system, namely the recovery of lactoperoxidase

from cheese whey using cation exchangers, are discussed later in this work (Gomes, 2006a).

A new HGMF- based process was recently developed for continuous protein refolding of an inclusion body preparation containing a histidine tagged protein termed HAT-hβ2m (Ferré, 2005). The system consisted of a pipe reactor for time controlled refolding of protein followed by continuous mixing with a flowing magnetic chelate affinity adsorbent into a second pipe reactor. The length of the second pipe reactor and the flow velocity give the suspension the necessary time for binding to occur. The suspension was then loaded to a HGMF filter and processed as described above (1.1). This processing mode enables control of contact time between a target protein and the magnetic adsorbents, opening the possibility of extending the application of HGMF to other bioprocesses, using the full potential of the fast kinetics and low susceptibility to fouling of non-porous and small adsorbents. One example would be the novel application of HGMF to the control of protein hydrolysis, demonstrated later in this work (Gomes *et al.*, 2006b). In that process, it was shown for the scale used (0.4 L of cheese whey), that hydrolysis could be successfully halted to the desired degree by the selective removal and recovery of trypsin, the enzyme mediating hydrolysis. Given that the hydrolytic process is only halted by complete removal of the enzyme (i.e., some activity was still present when the adsorbents were still in solution), the loading time will clearly limit the efficiency of the process when scale-up is considered. A solution could then be the use of the continuous HGMF process introduced by Ferré (2005), where binding times and loading to the filter can be performed in a pipe reactor at controlled residence time.

1.5 Aims and scope of this thesis

The aim of this thesis is to advance the following aspects of HGMF: (i) extending its application to biological systems not explored before; (ii) evaluating its limitations, (iii) understanding the performance of practically applicable magnetic filters; (iv) evaluating the impact of filter performance on a bioprocess; and (v) demonstrating new process applications.

The potential of HGMF for the recovery of valuable biomolecules is examined in chapter 2 by studying for the first time the design and use of magnetic adsorbents for the HGMF processing of antibodies. In light of the challenges posed by processing antibodies by HGMF (high particle concentrations, dilution effects during elution), the performance of the current state-of-the-art prototype magnetic filter, as well as packing of two particle types during capture, are studied (Chapter 3). This study is extended to examine magnetic particle release and filter flushing in model solutions and during the multicycle processing of cheese whey (Chapter 4). Subsequently, the generic applicability and versatility of HGMF for bioprocessing tasks other than direct capture is examined for the first time by studying the control of tryptic protein hydrolysis of whey combined with the recovery of enzyme catalysts mediating the hydrolytic process (Chapter 5).

Acknowledgements

References

Birss, R.R., Gerber, R., Parker, M.R. (1976) Theory and design of axially ordered filters for high intensity magnetic separation. *IEEE Trans. Magn.*, Mag-12(6), 892-894.

Birss, R.R., Parker, M.R. (1981) High intensity magnetic separation. *Progress in filtration and separation* (Ed. Wakeman, R.J.), 2, Elsevier Sci. Publ. Co., Amsterdam.

Birss, R.R., Parker, M.R., Sheerer, T.J. (1980) Statistics of particle capture in HGMS. *IEEE Trans. Magn.*, Mag-16(5), 830-832.

Bucak, S., Jones, D.A., Laibinis, P.E., Hatton, T.A. (2003) Protein separations using colloidal magnetic nanoparticles. *Biotechnol. Prog.*, 19, 477-484.

Burton, S.C., Harding, D.R.K. (1997a) Bifunctional etherification of a bead cellulose for ligand attachment with allyl bromide and allyl glycidyl ether. *J. Chromatogr. A*, <u>775</u>, 29-38.

Burton, S.C., Harding, D.R.K. (1997b) High density ligand attachment to brominated allyl matrices and application to mixed mode chromatography of chymosin. *J. Chromatogr. A*, <u>775</u>, 39-50.

Cummings, D.L., Himmelblau, D.A., Oberteuffer, J.A. (1976) Capture of small paramagnetic particles by magnetic forces from low speed fluid flows. *AIChE Journal*, <u>22</u>(3), 569-575.

Cummings, D.L., Prieve, D.C., Powers, G.J. (1980) High gradient magnetic separation in a viscous flow field. *AIChE Journal*, <u>26</u>(6), 1041-1044.

Ebner, N. (2006) *Einsatz von magnettechnologie bei der bioproduktaufarbeitung*. Ph.D. Thesis. Forschunszentrum Karlsruhe, Germany.

Ebner, N., Gomes, C.S.G., Hobley, T.J., Thomas. O.R.T., Franzreb, M. (2006) Filter capacity predictions for the capture of superparamagnetic microparticles by high-gradient magnetic separation (HGMS). *Chapter 3*.

Ferré, H. (2005) *Development of novel processes for continuous protein refolding and primary recovery - A case study on the major histocompatibility complex class I receptor and its individual subunits*. Ph.D. Thesis. Technical University of Denmark, Denmark.

Franzreb, M., Ebner, N., Siemann-Herzberg, M., Hobley, T.J., Thomas, O.R.T. (2006a) Product recovery and high-gradient magnetic fishing. *Process-scale bioseparations for the biopharmaceutical industry* (Ed. Shukla, A., Gadam, S., Etzel, M.) Marcel Dekker, New York (in press).

Franzreb, M., Siemann-Herzberg, M., Hobley, T.J., Thomas, O.R.T. (2006b) Protein purification using magnetic adsorbent particles. *Appl. Microbiol. Biotech.* (in press).

Friedlaender, F.J., Takayasu, M., Rettig, J.B., Kentzer, C.P. (1978) Particle flow and collection process in single wire HGMS studies. *IEEE Trans. Magn.*, Mag-14(6), 1158-1164.

Gerber, R., Birss, R.R. (1983) *High gradient magnetic separation*. Research Studies Press, UK.

Gomes, C.S.G., Ebner, N., Thomas. O.R.T., Franzreb, M., Hobley, T.J. (2006a) Protein purification using high-gradient magnetic fishing: Impact of magnetic filter performance. *Chapter 4*.

Gomes, C.S.G., Heebøll-Nielsen, A., Petersen, T.L., Thomas, O.R.T., Hobley, T.J. (2006b) Control of protein hydrolysis in unclarified liquors: application of high-gradient magnetic fishing (HGMF) employing improved magnetic adsorbents. *Chapter 5*.

Gomes, C.S.G., Pakalnyte, I., Thomas, O.R.T., Hobley, T.J. (2006c) Construction and application of mercaptoethylpyridine–linked magnetic adsorbents for the purification of immunoglobulins from crude rabbit antiserum by high-gradient magnetic separation. *Chapter 2*.

Halling, P.J., Dunnill, P. (1979) Improved nonporous magnetic supports for immobilized enzymes. *Biotechnol. Bioeng.*, 393-416.

Halling, P.J., Dunnill, P. (1980) Magnetic supports for immobilized enzymes and bioaffinity adsorbents. *Enzyme Micro. Technol.*, 2, 2-10.

Heebøll-Nielsen, A (2002) *High gradient magnetic fishing – support functionalisation from unclarified bioprocess liquors*. Ph.D. Thesis. Technical University of Denmark, Denmark.

Heebøll-Nielsen, A., Choe, W.S., Middelberg, A.P.J., Thomas, O. R.T. (2003) Efficient inclusion body processing using chemical extraction and high-gradient magnetic fishing. *Biotechnol. Progr.*, 19(3), 887-898.

Heebøll-Nielsen, A., Dalkiær, M., Hubbuch, J.J., Thomas, O. R.T. (2004a) Superparamagnetic adsorbents for high-gradient magnetic fishing of lectins out of legume extracts. *Biotechnol. Bioeng.,* 87(3), 311-323.

Heebøll-Nielsen, A., Justesen, S.F.L. Hobley, T.J., Thomas, O.R.T. (2004b) Superparamagnetic cation-exchange adsorbents for bioproduct recovery from crude process liquors by high-gradient magnetic fishing. *Sep. Sci. Technol.,* 39(12): 2891-2914.

Heebøll-Nielsen, A., Justesen, S.F.L., Thomas, O.R.T. (2004c) Fractionation of whey proteins with high-capacity superparamagnetic ion-exchangers. *J. Biotechnol.,* 113, 247-262.

Hermanson, G.T., Mallia, A.K., Smith, P.K. (1992) *Immobilized affinity ligand techniques.* Academic Press, London.

Herzig, J.P., Leclerc, D.M., Le Goff, P (1970) Flow of suspensions through porous media. *Ind. Eng. Chem.,* 62(5), 8-35.

Himmelblau, D.A. (1974) M.Sc. Thesis. Department of Chemical Engineering, Massachusetts Institute of Technology, Cambridge. *In* Cummings, D.L., Himmelblau, D.A., Oberteuffer, J.A. (1976) Capture of small paramagnetic particles by magnetic forces from low speed fluid flows. *AIChE Journal,* 22(3), 569-575.

Hoffmann, C. (2002) *Einsatz magnetischer Separationsverfahren zur biotechnologischen produktaufarbeitung.* Ph. D. Thesis. Forschunszentrum Karlsruhe, Germany.

Hoffmann, C., Franzreb, M., Höll, W.H. (2002) A novel high-gradient magnetic separator (HGMS) design for biotech applications. *IEEE Trans. Appl. Supercond.,* 12(1), 963- 966.

Hubbuch, J.J. (2000) *Development of adsorptive separation systems for recovery of proteins from crude bioprocess liquors.* Ph.D. Thesis. Technical University of Denmark. Denmark.

Hubbuch, J.J., Matthiesen, D.B., Hobley, T.J., Thomas O.R.T. (2001) High gradient magnetic separation versus expanded bed adsorption: A first principle comparison. *Bioseparation*, 10, 99-112.

Hubbuch, J.J., Thomas, O.R.T. (2002) High-gradient magnetic affinity separation of typsin from porcine pancreatin. *Biotechnol. Bioeng.,* 79, 301-313.

Kolm, H.H. (1972) Process for magnetic separation. US Patent 3 676 337.

Langmuir, I. (1918) The adsorption of gases on plane surfaces of glass, mica and platinum. *J. Am. Chem. Soc.*, 40, 1361-1403.

Lawson, P., Gerber, R. (1990) Viscosity effects in multi-wire HGMS. *IEEE Trans. Magn.*, Mag-26(5), 1861-1863.

Leitermann, W., Friedlaender, F.J., Gerber, R., Hwang, J.Y., Emory, B.B. (1984) Collection of micron-sized particles at high velocities in HGMS. *IEEE Trans. Magn.*, Mag-20(5), 1174-1176.

Luborsky, F.E., Drummond, B.J. (1976) Build-up of particles on fibres in a high field – high gradient separator. *IEEE Trans. Magn.*, Mag-12(5), 463.

McNeese, W.H., Wankat, P.C., Friedlaender, F.J., Nakano, T., Takayasu, M. (1979) Viscosity effects in single wire studies. *IEEE Trans. Magn.*, Mag-15(6), 1520-1522.

McNeese, W.H., Wankt, P.C., Friedlaender, F.J. (1980) Viscosity effects in single wire HGMS studies II. *IEEE Trans. Magn.*, Mag-16(5), 843-845.

Meyer A. (2004) *Einsatz magnettechnologischer trennverfahren zur arbereitung von molkereiprodukten*. Ph.D. Thesis. Forschunszentrum Karlsruhe, Germany.

Meyer, A., Hansen, D.B., Gomes, C.S.G., Hobley, T.J., Thomas, O.R.T., Franzreb, M. (2005) Demonstration of a strategy for product purification by high-gradient magnetic fishing: Recovery of superoxide dismutase from unconditioned whey. *Biotechnol. Prog.*, 21, 244-254.

Moeser, G.D., Roach, K.A., Green, W.H., Hatton, T.A., Laibinis, P.E. (2004) High-gradient magnetic separation of coated magnetic nanoparticles. *AIChE Journal*, 50(11), 2835-2848.

Nesset, J.E., Finch, J.A. (1979) A static model of HGMS based on forces within the fluid boundary layer. *In* Hubbuch J.J. (2000) *Development of adsorptive separation systems for recovery of proteins from crude bioprocess liquors*. Ph.D. Thesis. Technical University of Denmark, Denmark.

Nesset, J.E., Finch, J.A. (1981) The static (build-up) model of particle accumulation on single wires in high gradient magnetic separation: Experimental confirmation. *IEEE Trans. Magn.*, Mag-17(4), 1506.

Nesset, J.E., Todd, I., Hollingworth, M., Finch, J.A. (1980) A loading equation for high gradient magnetic separation. *IEEE Trans. Magn.*, Mag-16(5), 833-835.

Oberteuffer, J.A. (1973) High gradient magnetic separation. *IEEE Trans. Magn.*, Mag-9(3), 303-306.

Oberteuffer, J.A. (1974) Magnetic separation: a review of principles, devices and applications. *IEEE Trans. Magn.*, Mag-10(2), 223-238.

Oberteuffer, J.A., Wechsler, I., Marston, P.G., McNallan, M.J. (1975) High gradient magnetic filtration of steel mill process and waste waters. *IEEE Trans. Magn.*, Mag-11(5), 1591-1593.

Parker, M.R., Li, J. (1989) Use of orthonomic principles in HGMF matrix design. IEEE publication no. CH2731, New York.

Safarik, I., Safarikova, M. (2004). Magnetic techniques for the isolation and purification of proteins and peptides. *BioMagnetic Research and Technology*, 2, 7.

Svoboda, J. (1987) Magnetic methods for the treatment of minerals. *Developments in Mineral Processing* (Ed. Fuerstenau, D.W.), 8, Elsevier Sci. Publ. Co., Amsterdam.

Thomas, O.R.T., Franzreb, M. (2006) Magnetic Separations. *Bioseparation Processes*. (Ed. Kieran, P., Cabral, J., Jungbauer, A.) Wiley Inc. *Accepted for publication*

Too, C.O. (1986) Optimisation of matrix design in high gradient magnetic separation. *J. Phys. D: Appl. Phys.*, 19, L1-L4.

Watson, J.H.P. (1973) Magnetic filtration. *J. Appl. Phys.*, 44(9), 4209-4213.

52

Watson, J.H.P. (1975) Theory of capture of particles in magnetic high-intensity filters. *IEEE Trans. Magn.*, Mag-11(5), 1597-1599.

Watson, J.H.P., Bahaj, A.S. (1989) Vortex capture in high gradient magnetic separators at moderate Reynolds number. *IEEE Trans. Magn.*, Mag-25(5), 3803-3805.

Whitesides, G.M., Kazlauskas, R.J., Josephson, L. (1983) Magnetic separations in biotechnology. *Trends. Biotechnol.*, 1(5), 144-148.

Zulqarnain, K. (1999) *Scale-up of affinity based separation based on magnetic support particles*. Ph. D. thesis. University College London, UK.

2. Mercaptoethylpyridine–linked magnetic adsorbents for the purification of immunoglobulins from crude rabbit antiserum by high-gradient magnetic fishing

Cláudia S. G. Gomes[1], Inga Pakalnyte[1], Owen R.T. Thomas[1,2], Timothy J. Hobley[1]

[1] Center for Microbial Biotechnology, Technical University of Denmark, 2800 Lyngby, Denmark.

[2] Department of Chemical Engineering, The University of Birmingham, Edgbaston, Birmingham B15 2TT, United Kingdom.

Abstract

We have constructed superparamagnetic adsorbents functionalised with 4–mercaptoethylpyridine (MEP), a new ligand recently introduced for the purification of immunoglobulins (Ig) by hydrophobic charge induction chromatography. A variety of different activation and ligand coupling approaches were compared for the preparation of effective IgG binding adsorbents. The best of these (prepared by activation with allyl glycidyl ether prior to coupling) was selected for further studies, i.e determination of suitable conditions for: product sorption; magnetic collection of loaded adsorbents; removal of entrained/loosely adsorbed contaminants; and product elution. In batch binding tests with diluted rabbit antiserum, these adsorbents bound IgG at levels of up to 160 mg/g, together with 220 mg/g of other serum proteins. However, the main contaminant, serum albumin, was readily desorbed from 'loaded' adsorbent particles, prior to product elution, in a single rapid washing step of <45 s duration. When operated at a working capacity of 80 mg IgG/g of adsorbent, over 90 % of the immunoglobulins present could be removed from the feedstock, and >70 % of the antibodies were recovered in two elution cycles in a highly purified state, as judged by reducing SDS–PAGE analysis.

2.1 Introduction

Polyclonal antibodies, traditionally produced in immunised mammals, have been used for passive immunotherapy, experimental research, clinical investigation and diagnosis for decades. Today, 30 years after the production of monoclonal antibodies by introduction of the hybridoma technology (Köller and Milstein, 1975), a range of new applications of antibodies is possible, namely as highly specific and potent pharmaceuticals. The initial problems associated with the partially murine antibodies derived from the hybridoma technology, i.e., the anti-mouse Ig reactions triggered in human patients, have been addressed since 1990 and new technologies enable the construction of antibodies with less mouse protein sequences and therefore less antigenicity for humans. Thus, advances in antibody engineering now permits the large scale manufacture of fully human antibodies for therapeutic use (van Dijk and van de Winkel, 2001). 18 antibody-based drugs including murine, chimeric and humanised monoclonal antibodies have reached the market (Medarex) for treating and/or diagnosing a variety of diseases, such as cancer, rheumatoid arthritis, Crohn's disease and others (GenMab; Medarex; van Dijk and van de Winkel, 2001). The potential market is large and growing rapidly, revenue of the four top-selling antibody-based drugs surpassing US$3.5 billion in 2003. Hundreds of newly developed antibodies are currently in clinical trials (GenMab).

Downstream processing accounts for at least 50 % of the cost associated with the production of monoclonal antibodies (Morrow, 2002), and there is considerable pressure for improving purification procedures. Furthermore, current antibody production costs are high and there is an ongoing discussion about whether the present worldwide downstream processing capacity is sufficient for the expected volume of production of these new pharmaceuticals. These are problems that can be minimised by introducing high throughput techniques or techniques capable of reducing the number of unit operations. High-gradient magnetic fishing (HGMF) addresses both of these goals. The technique is designed for dealing with crude feedstocks and enables direct capture of specific proteins from complex biologic broths. Clarification and concentration are combined with initial purification in one step. This advantage is

derived from the use of submicron non-porous superparamagnetic adsorbents with high surface areas and resistance to fouling (Halling and Dunnill, 1979). When integrated with a traditional batch binding process and a suitable magnetic separator, these adsorbents can be easily processed at high flow rates (typically 24 m h^{-1}) in the generic technique called high-gradient magnetic fishing (HGMF) for purification of proteins.

Use of 4-mercaptoethylpyridin (MEP) as ligand in chromatography was first reported by Burton and Harding (1998) when introducing a new form of protein chromatography called hydrophobic charge induction (HCI). The dual-mode behaviour of this molecule at different pH conditions is responsible for the mechanism characteristic to HCI. In this particular case, MEP is uncharged at higher pH (pKa=4.8) enabling hydrophobic interaction with proteins and positively charged at lower pH values causing desorption by ionic repulsion. The application of HCI using MEP for the purification of a variety of antibodies has been demonstrated by Boschetti and his co-workers (Schwartz *et al.*, 2001; Boschetti, 2002; Guerrier *et al.*, 2000, 2001) with the introduction of the commercial chromatography media HyperCel. MEP constitutes an alternative to the most widely used ligand for antibody purification, protein A, in response to the high cost of the latter and its known leakage problems that consequently require the use of additional purification steps. Furthermore, the less costly MEP has been shown to be robust to harsh cleaning procedures, to have low sensitivity to ionic strength and it does not require severe elution conditions (typically pH ~ 4). Furthermore the fact that MEP, like protein A, binds Fc fragments from IgG (Guerrier *et al.*, 2001) argues for the broad applicability of this ligand in the purification of various antibody species.

Thus, MEP is an attractive ligand for several reasons and, in this work, we use it to develop a new magnetic adsorbent and apply that in an HGMF-based procedure to purify antibodies for the first time.

2.2 Materials and methods

2.2.1 Materials

$FeCl_3 \cdot 6H_2O$ and DMSO (99.5 %) were obtained from Merck (Darmstadt, Germany). $FeCl_2 \cdot 4H_2O$ was bought from Mallinckrodt Baker B.V. (Deventer, the Netherlands). $NaBH_4$, allyl glycidyl ether (AGE), allyl bromide (AB), epichlorohydrin (ECH), divinyl sulphone (DVS), arginine, and 3-aminopropyltriethoxysilane, glutaraldehyde (50 %, photographic grade), N-bromosuccinimide (NBS), thiolacetic acid, 4-vinylpyridine and bovine serum albumin standards (Fluka, 82516) were purchased from Sigma-Aldrich Chemie GmbH (Steinheim, Germany). The bicinchoninic acid (BCA) protein assay kit was supplied by Pierce (Rockford, IL, USA). All the reagents for the rabbit Ig immunoturbidimetric assay, i.e., dilution buffer (S2005), reaction buffer (S2008), dilution buffer for goat anti-rabbit immunoglobulins (TO 0463), goat anti-rabbit immunoglobulins (Z0421) and IgG standard (X903), were obtained from Dako Cytomation Norden A/S (Glostrup, Denmark). The mesh of stainless steel 430 wires (~100 μm diameter, KnitMesh type 9029), used for preparing the magnetic filter, was a gift from C. Barnes (KnitMesh Ltd., South Croydon, Surrey, UK). The rabbit antiserum was a gift from Dako Cytomation Norden A/S (Glostrup, Denmark). This was a rabbit anti-human transferrin anti-serum that was provided undiluted and free of solid matter. It had a composition of 25 ($\pm$ 2) g L^{-1} Ig and 93 ($\pm$ 2) g L^{-1} total protein according to our measurements. The same type of feedstock unclarified and undiluted was used for the HGMF processing experiment.

2.2.2 Batch-wise magnetic support separation

A neodymium-iron-boron magnet block (B ~ 0.7 T) from Danfysik A/S (Jyllinge, Denmark) was used to separate magnetic particles from liquid phases during preparation of the magnetic adsorbents. In all bench-scale binding studies a side-pull permanent magnet rack (B $\leq$ 0.15 T, PerSeptive Diagnostics, Cambridge, MA, USA) was employed.

2.2.3 Synthesis of 4-mercaptoethylpyridine HCl

4-mercaptoethylpyridine HCl (Fig. 2.1) was prepared with some modifications by the
method described by Burton (1996). 4-vinylpyridine (95 %, 125 mL) was prechilled
under stirring to −30°C with a methanol/dry ice bath. Thiolacetic acid (85 mL) was
then added dropwise over a period of 3 hours. The reaction temperature increased and
it was controlled with a water bath (18-22°C) in order to keep it at approximately
23°C. The reaction was stirred at room temperature overnight. The product was split
in two equal parts and each part was diluted in ether (100 mL), extracted with sat. aq.
$NaHCO_3$ (4 × 80 mL) and washed with sat. aq. NaCl (2 × 75 mL). The two organic
phase fractions were combined, treated with activated charcoal to reduce colour and
dried over $MgSO_4$. The mixture was then filtered and evaporated under vacuum. The
resulting oil was stirred for 4 hours with aq. 6M HCl (400 mL). Then it was
concentrated under vacuum, recrystallised at -18°C overnight from isopropanol (150
mL), filtered and finally dried under vacuum to a dark creamy solid. The salt was
dissolved in aq. 6M HCl (400 mL), stirred at room temperature and the reaction was
monitored by TLC. After 40 h the reaction was stopped and then concentrated,
recrystallised from isopropanol (150 mL), filtered and dried to a creamy solid. This
solid (81 g, 40 % yield) was identified as the desired compound; R_f 0.38; ^{1}H NMR
(D_2O, 300 MHz) δ 2.89 (t, 2 H, CH_2-SH, J 7.1 Hz), 3.18 (t, 2 H, Pyr-CH_2, J 7.1 Hz),
7.89 (d, 2 H, H-2, H-2', Pyr, J 6.6 Hz), 8.59 (d, 2 H, H-3, H-3', Pyr, J 6.8 Hz). ^{13}C
NMR (D_2O, 300 MHz) δ 23.27 (CH_2-SH), 39.22 (Pyr-CH_2), 127.85 (Pyr, C-3, C-3'),
140.64 (Pyr, C-2, C-2'), 162.44 (Pyr, C-4).
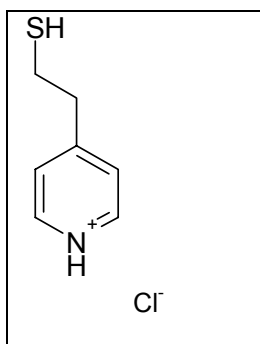
Fig. 2.1 Structure of 4-mercaptoethylpyridine HCl molecule

2.2.4 Preparation of 4-mercaptoethylpyridine-linked adsorbents

Preparation and activation of superparamagnetic base matrix

Sub-micron sized superparamagnetic iron oxide particles were prepared by a procedure based on alkaline precipitation of Fe^{2+} and Fe^{3+} followed by silanisation with 3-aminopropyltriethoxysilane, using the chemicals and methods of Hubbuch and Thomas (2002), and subsequently coated by polyglutaraldehyde as described by O'Brien *et al.* (1996). Prior to polyglutaradehyde coating, the particle sizes of the silanised supports were determined by laser diffraction on a Mastersizer 2000 coupled with a Hydro SM sample loader (Malvern Instruments Ltd., UK), in order to verify the success of the preparation. Sizes of 0.3-0.4 μm ($d_{0.5}$) were found for all batches.

Polyglutaraldehyde-coated (PG) supports were activated (at 0.2 g scale) with DVS as has been described by Heebøll-Nielsen *et al.* (2004a). In this procedure DVS was added at regular intervals over 10 min to the particles suspended at a concentration of 25 g L^{-1} in 0.5 M Na_2CO_3 containing 18 mM $NaBH_4$ to a final amount of 8 mL g^{-1} particles. The reaction was subsequently allowed to proceed for 1 h. The activation with AGE and AB was a modification of the procedures suggested by Burton and Harding (1997a). Following suspension of the magnetic base matrix (up to 0.75 g scale) in a solution containing 0.15 M NaOH and 36 mM $NaBH_4$ in 50 % (v/v) DMSO at a particle concentration of 33 g L^{-1}, AGE or AB was added to a final concentration of 50 % (v/v), and the reaction allowed to proceed for 48 h at ambient temperature. The allyl derivatised particles were washed extensively with water, and the double bonds of the allyl groups brominated with NBS to produce bromohydrin moieties. This step was performed for 1 h at room temperature in a 0.14 M aqueous solution of NBS and at a support concentration of 20 g L^{-1}. Activation of PG coated supports with ECH was conducted using a procedure described by Heebøll-Nielsen *et al.* (2004c). Sufficient amounts of particles (up to 0.2 g scale) to give a final concentration of 25 g L^{-1} were suspended in a solution of 0.5 M NaOH, 19 mM $NaBH_4$. ECH was added to a final concentration of 5 % (v/v) and the reaction allowed to proceed for 6 h at room temperature. All activated supports were washed extensively in water before the final derivatisation step.

Ligand coupling

4-mercaptoethylpyridine HCl was dissolved in 1 M sodium phosphate buffer containing 18 mM $NaBH_4$ and the pH was subsequently adjusted to 10.5 with 2 M NaOH. The 4 different types of activated adsorbents were suspended in the MEP reaction solution to a final concentration of 25 g L^{-1} (at a scale up to 0.75 g of support) and allowed to react for 35 h at ambient temperature. All reactions were performed in closed glass vessels on a vibrating shaker. The finished supports were washed thoroughly with NaCl 0.5 M and water, and stored at 4 ºC in 20 mM sodium phosphate, 1 M NaCl, pH 6.8 until use. These adsorbents were used for the initial screening studies (data presented in section 2.3.1).

The coupling conditions for preparing MEP adsorbents linked through the AGE activation route were later modified according to the following procedure. A 0.7 M solution of MEP HCl in water was adjusted to pH 11.5 with sat. aq. NaOH and subsequently diluted to 55 mM in a 0.5 M sodium carbonate solution supplemented with 28 mM $NaBH_4$. A suspension of 6 g L^{-1} AGE activated supports in this solution was allowed to react for 48 h at room temperature. The adsorbents prepared under these coupling conditions were used for all experiments in this work except for the initial screening studies. The presence of 4-mercaptoethylpyridine in the final adsorbent preparation was checked by IR spectroscopy. A transmittance peak at 800 cm^{-1}, also present for pure dry 4-mercaptoethylpyridine HCl and in solution, could be observed for MEP adsorbents. As a control, magnetic adsorbents were subjected to the same reactive conditions as for the preparation of the MEP adsorbents but in absence of 4-mercaptoethylpyridine HCl in the final coupling step. The control adsorbents showed no peak at 800 cm^{-1}.

2.2.5 Batch binding studies with magnetic adsorbents

In all batch binding experiments, an initial equilibration step was performed by thoroughly washing the supports in the binding buffer. Except for experiments where binding conditions were being tested, the binding buffer used was 50 mM Tris/HCl, pH 8. Prior to binding, the supports were resuspended in a defined volume of binding buffer and subsequently aliquoted to 2 mL Eppendorf style tubes. A sample was taken

for dry weight measurement and used for determining the exact amount of support in the tubes. After removal of the liquid phase by magnetic settlement of the supports, 1.5 mL of diluted anti-serum was added and binding was allowed to occur for 30 min at ambient temperature on a vibrating shaker. Added serum and collected supernatants were analysed by SDS-PAGE and the contents of Ig and total protein were determined in order to estimate the amount of bound protein.

Screening of different types of MEP adsorbents

MEP adsorbents prepared through the four different activation routes were compared with regard to their binding properties by conducting batch binding studies with rabbit anti-serum. The feedstock was diluted 5 fold in binding buffer and added to the equilibrated supports present at a final concentration of $6 - 8$ g L^{-1}. Following binding, the adsorbents were washed with binding buffer and then incubated in 50 mM sodium acetate, pH 4 for 30 min in order to elute the bound protein.

Characterization of binding properties of AGE activated MEP adsorbents

The MEP adsorbents prepared via activation of the matrix with AGE, were characterised by performing batch binding studies with 4.6 g L^{-1} adsorbent at a 1.5 mL scale in a range of rabbit anti-serum solutions diluted from 5 to 1000 fold in binding buffer. The amounts of adsorbed Ig and total protein were calculated by difference and the adsorption isotherm for Ig was plotted and fitted with the Langmuir model[1] (Langmuir 1918). The supports were subsequently washed with 1.5 mL of binding buffer followed by two identical elution steps using 0.75 mL of 50 mM sodium acetate, pH 4. The wash and elutions were performed by successive suspension in the appropriate buffer and magnetic settlement of magnetic supports for removal of the liquid phase. The supernatants were collected and analysed for total protein content.

---

[1] The Langmuir model is represented by the equation $Q* = Q_{max} \dfrac{C*}{K_d + C*}$. The equilibrium concentration of the adsorbed and bulk-phase protein are represented by $Q*$ and $C*$ respectively, K_d is the dissociation constant and Q_{max} is the maximum binding capacity of the adsorbents. The fit of the data to the Langmuir equation was done with the aid of the software SigmaPlot (Systat Software, Inc).

Optimization of binding conditions

The binding efficiency of Ig from rabbit anti-serum to the AGE activated MEP adsorbents was evaluated by studying the impact of support concentration, binding time, pH and presence of salt in the feedstock. Batch binding studies in a 1.5-mL scale were performed as described above using rabbit anti-serum diluted 10-fold in the appropriate binding buffer. The same buffer was used to equilibrate the adsorbents prior to binding. During a 20 min experiment employing support concentrations of 8.5 g L^{-1}, binding occurring in parallel test tubes was successively stopped by quickly (< 60 s) separating the supports and collecting the supernatants. The influence of support concentration was studied by varying the support amount (in a range between 3 and 30 mg of support per mL of diluted serum) in the batch binding experiments. The impact of pH and salt on binding was tested by employing the following binding buffers in the equilibration of the supports and dilution of the anti-serum: 50 mM sodium citrate, pH 6; 50 mM Tris/HCl, pH 7-9; 50 mM Tris/HCl, pH 8 supplemented with 0 – 150 mM NaCl; and 50 mM Tris/HCl, pH 8 supplemented with 0 – 150 mM $(NH_4)_2SO_4$.

2.2.6 Desorption of bound protein and optimization of elution conditions

Prior to elution studies, the AGE activated MEP adsorbents were loaded by binding with serum diluted 10-fold in binding buffer (50 mM Tris/HCl, pH 8). Binding was conducted at 1.5 mL scale using 30 mg adsorbent per mL diluted serum (described in section 2.2.5). Subsequently the supports were washed for 30 sec with 1.5 mL of binding buffer followed by a 2-step elution employing 0.75 mL of 500 mM sodium acetate, pH 4 in each step (corresponding to a support concentration of 60 mg per mL). Samples from the added serum, unbound material, wash and elution were collected for SDS-PAGE analysis and for determination of Ig and total protein content. A similar experiment was performed with 25 mg mL^{-1} of supports (during the binding step) but varying the concentration of sodium acetate at pH 4 in the elution buffer between 50 mM and 1 M. In this case the volumes of wash and elution buffers were 1.95 mL yielding a support concentration of 19 mg mL^{-1} in both steps.

The elution efficiency values are calculated with based on the Ig remaining on the supports after binding and the subsequent wash step.

2.2.7 HGMF processing

HGMF apparatus and system set-up

The system employed for HGMF processing is described in detail by Meyer *et al.* (2005). A laboratory type 'on-off' permanent magnet based high-gradient magnetic separator (Steinert HGF-10, Steinert Elektromagnetbau GmbH, Köln, Germany) designed for biological applications was employed (Hoffmann *et al.* 2002). The separator was set to have a 1.5 cm gap between the poles with a magnetic flux density of 0.56 T. The magnetic filter, placed vertically between the poles, consisted of a 4.4 mL (56 mm long × 10 mm internal diameter) canister, filled with a rolled mat of woven mesh composed of '430' stainless steel fibres (~110 μm thickness) to give a voidage of 0.89.

The HGMF system, depicted in figure 2.2, enables the performance of the following operations: i) an adsorption step with magnetic adsorbents in the batch reactor (BR), ii) loading of the magnetic adsorbent suspension to the magnetic filter (MF) while the magnetic field is 'on', iii) filling the system with buffer (WB or EB) to replace the solution previously present in the system while the adsorbents are kept on the filter, iv) release of the adsorbents from the filter by turning 'off' the magnetic field and recycle of them in a 16 mL closed loop (RL), v) recollection of the adsorbents in the recycling loop by switching 'on' the magnetic field. In all cases the magnetic adsorbent suspension and buffers were loaded upwards through the magnetic filter towards the fraction collector.
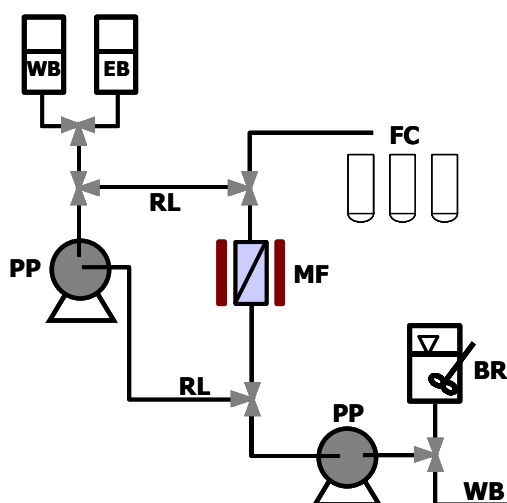
Fig. 2.2 Schematic diagram of the HGMF system employed in this work. MF = magnetic filter, FC = fraction collector, PP = peristaltic pump, WB = washing buffer container, EB = elution buffer container, RL = recycle loop, BR = batch adsorption reactor.

Determination of filter capacity

The breakthrough capacity of the HGMF filter was determined with mercaptoethylpyridine adsorbents suspended in 10-fold diluted rabbit antiserum at a flow rate of 24 m h^{-1}. The adsorbents (636 mg) were first equilibrated in 50 mM Tris/HCl, pH 8 buffer before mixing with 23 mL feedstock to a final volume of 27.5 mL. The suspension was loaded to the magnetic filter with the field 'on' and the breakthrough was monitored by measuring the dry weight content of samples collected from the fraction collector. At 5 % breakthrough, 430 mg of supports had been loaded to the filter, corresponding to a filter capacity of 98 g/L based on the total volume of the filter.

Recovery of immunoglobulins from rabbit anti-serum by HGMF processing

MEP adsorbents (380 mg) were equilibrated in binding buffer (50 mM Tris/HCl, pH 8) and subsequently mixed with 11.5 mL of rabbit antiserum (diluted 1:10 in the same buffer) giving a final volume of 13 mL. Binding was allowed to proceed for 10 min in a batch reactor with an overhead stirrer. The suspension was subsequently loaded at 24 m h^{-1} to the magnetised filter and 365 mg adsorbents were captured while the unbound material passed through. The adsorbents were then washed by performing the following operations consecutively: filling the system with binding buffer, closing the recycle loop and turning 'off' the field, recycling the adsorbents for 1 min at a velocity of 92 m h^{-1} upwards with respect to the filter and finally recollecting the

adsorbents on the filter by switching 'on' the field and lowering the velocity to 24 m
h^{-1}. The system was subsequently filled with elution buffer (500 mM sodium acetate,
pH 4) while the solution containing the washed material was collected in the fraction
collector. A new cycle of support release, recycle, support capture and collection of
the eluate was performed as described above with the only modification being that the
supports were allowed to recycle in the loop for 10 min in order to guarantee
maximum desorption of bound material. Four more elution cycles were conducted in
this way. The volumes of all collected fractions were accurately measured for mass
balance calculations. All fractions, i.e., loaded feedstock, flowthrough, wash and six
eluates were analysed by SDS-PAGE for immunoglobulins and total protein
quantification.

Quantification of rabbit immunoglobulins

The concentration of antibodies was determined by an immunoturbidimetric assay
based on a manual micro titre plate based assay developed by Bak (2004). This
method is based on the scattering of light caused by the formation of different sizes of
immune complexes by different ratios of antibody : antigen. The procedure was scaled
to be performed automatically by a Cobas Mira robot spectrophotometer (Roche
Diagnostic Systems, Rotkreutz, Switzerland) in the following way. 35 µL samples
were mixed with 126 µL of reaction buffer (S2008, DAKO A/S) and incubated at 37
ºC. After 5 min, the absorbance was recorded at 340 nm and 84 µL of a GoaRbIg
solution was added. The GoaRbIg was previously prepared by diluting a concentrated
stock (Z0421, DAKO A/S) in TO 0463 buffer (DAKO A/S) to a final concentration of
1.8 g L^{-1}, followed by a 2-fold dilution in dilution buffer (S2005, DAKO A/S). After 5
min incubation at 35 ºC, the absorbance was again recorded at 340 nm. Standards of
purified immunoglobulins from non-immunised rabbits (x903, DAKO A/S), prepared
in dilution buffer to a final concentration ranging from 6.6 to 500 mg L^{-1}, were treated
in exactly the same way as the samples. Figure 2.3 shows the average and standard
deviation of 10 different standard curves obtained over a period of 1 year. When
necessary, the samples were first diluted in dilution buffer to be within the range of

the standard curve. This procedure was incorporated in the methods programmed in the Cobas Mira robot and could be performed automatically.
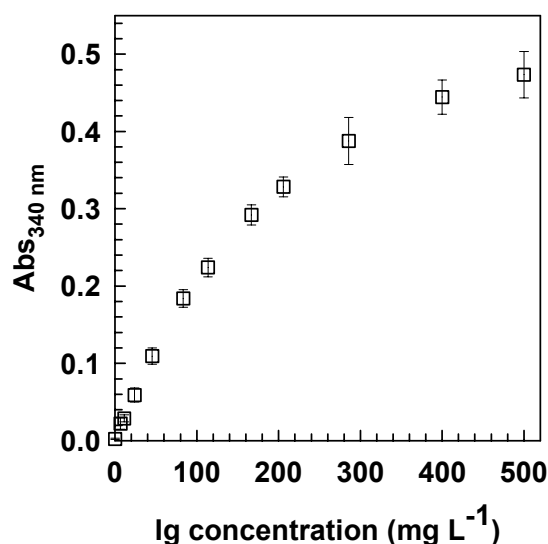
Fig. 2.3 Standard curve constructed from analysis of immunoglobulin standards (x903, DAKO A/S) by the immunoturbidimetric assay. Results are the average and standard deviation of 10 different runs.

2.2.8 Other analytical methods

Total protein was measured with a BCA protein assay (Pierce Rockford, IL, USA) following the directions of the manufacturer with the exception that a Cobas Mira robot spectrophotometer (Roche Diagnostic Systems, Rotkreutz, Switzerland) was used. All protein concentrations were expressed in mg bovine serum albumin standards (BSA) equivalents.

Visualization of the protein composition was done by reducing SDS-PAGE analysis in NuPAGE® Novex Bis-Tris (4-12 %) gels. Precast SDS-PAGE gels, sample buffer, running buffers (MES SDS running buffer), Coomassie stain (Colloidal Blue staining kit) and ladder Mark 12™ were purchased from Invitrogen (Groningen, The Netherlands), and used according to the manufacturer's instructions. Alternatively, a protein standard ladder from Bio-Rad was used (broad range, 161-0317). Scanning densitometry was performed using Quantity One® software (ver. 4.1.0, Bio-Rad

Laboratories, Hercules, CA, USA) with the help of a GelDoc2000 documentation system (Bio-Rad Laboratories).

Magnetic particle content was determined using a dry weight method. The samples were filtered on previously dried and weighed 0.2 µm filters (PALL Corporation, Ann Arbor, MI, USA) and washed thoroughly with water. Subsequently, the filters were dried for 10 min at 150 W in a microwave oven and then cooled for 2-15 h in a desiccator. The masses of the filters were measured on an analytical balance (Sartorius LA230S, Sartorius AG, Göttingen, Germany) and the dry weight determined by difference in weight of the filters before and after sample application.

2.3 Results

2.3.1 Screening of MEP adsorbents prepared via different activation routes

In this work, 4-mercaptoethylpyridine-linked magnetic adsorbents were initially prepared employing four different activation routes prior to coupling of the ligand through its thiol group. Two of the strategies modify the hydroxyl groups on the base matrix with brominated derivatives of allyl reagents (AGE and AB) and introduce 7- or 3-atom hydrophilic spacer arms between the matrix and the ligand (Fig.2.4). Use of allyl reagents for producing chromatography beads with high activation levels has been reported by Burton and Harding (1997a). Furthermore, these chemistries have been successfully applied to polyglutaraldehyde coated superparamagnetic base matrices, i.e., the type of base matrix used in this work, to produce magnetic adsorbents such as anion exchangers and metal chelators (Heebøll-Nielsen, 2003 and 2004c). Heeboell-Nielsen (2004b) also produced high binding capacity magnetic adsorbents through epoxy activation of the base matrix. Reaction of the hydroxyl groups from the polyglutaraldehyde-coated supports with epichlorohydrin (ECH) prior to coupling of 4-mercpatoethylpyridine, which was the third activation strategy selected in this work, results in a final support with a short hydrophilic spacer arm with the same structure as the adsorbents produced by AB activation (Fig.2.4). A fourth type of 4-mercpatoethylpyridine-linked adsorbent was prepared by prior

activation of the base matrix with divinylsulfone (DVS). The activation chemistry
employing DVS introduces a sulfone group in close proximity to the thioether formed
after coupling of the ligand (Fig. 2.4). This is a property that characterises the
thiophilic adsorbents introduced by Porath *et al.* (1985), which have been efficiently
employed in the purification of immunoglobulins. Moreover, adsorbents
functionalised with sulfone-aromatic ligands have been reported to possess a high
selectivity towards immunoglobulins (Knudsen *et al.* 1992).
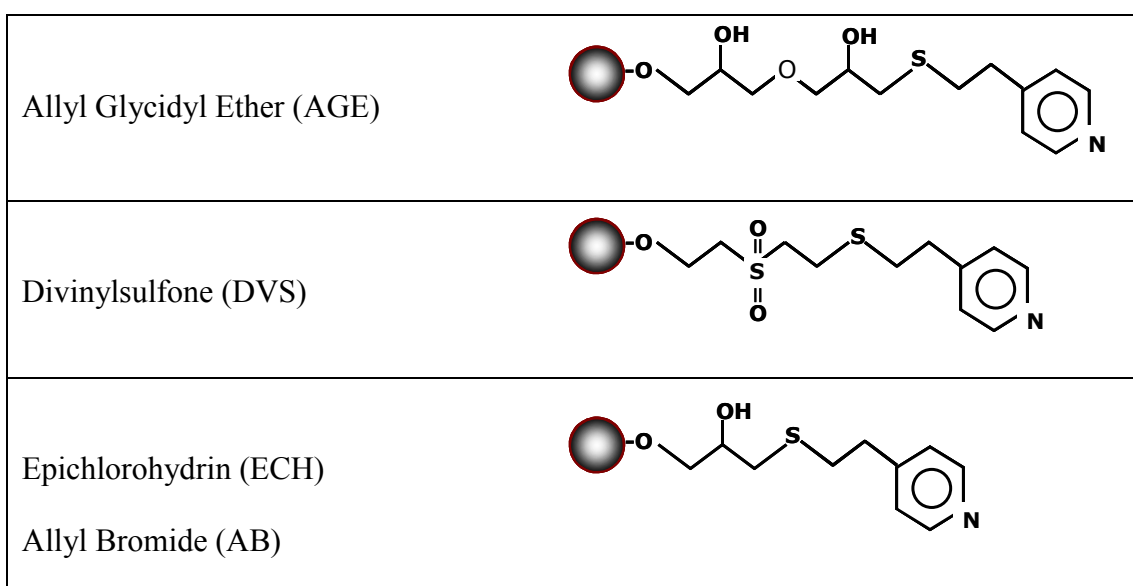
Fig. 2.4 Finished mercaptoethylpyridine-linked magnetic adsorbents prepared with the
indicated activation route.

Table 2.1 Adsorption of total protein and Ig from rabbit antiserum to magnetic MEP
adsorbents prepared with the indicated activation route.

Activation chemistry	Adsorbed protein (mg g^{-1})	Adsorbed Ig (mg g^{-1})
AGE	245	110
DVS	480	89
ECH	527	181
AB	347	40

The performance of the four different types of magnetic adsorbents was tested by
conducting small-scale batch binding studies in rabbit anti-serum. These studies
provided a quick screening of the supports with respect to their ability to bind

immunoglobulins without constructing binding isotherms and furthermore gave
information on the selectivity of the binding.
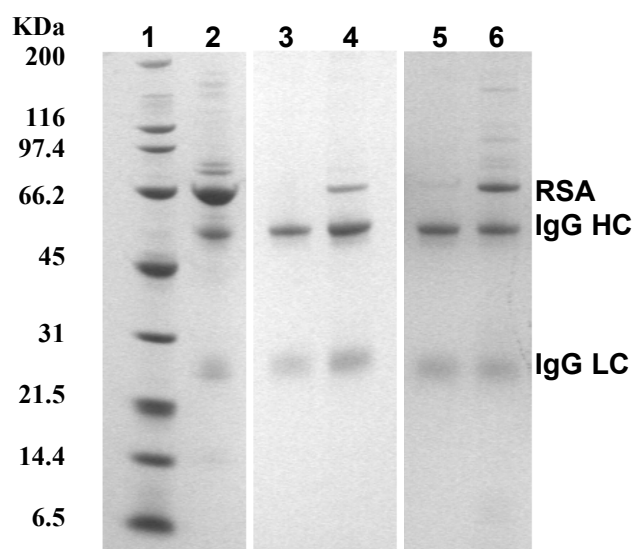
Fig. 2.5 Reducing SDS-PAGE of fractions from purification of IgG from rabbit antiserum. The lanes are: marker (1), antiserum (2) and elutions from supports activated with AGE (3), DVS (4), ECH (5) and AB (6). RSA=rabbit serum albumin, Ig G=immunoglobulin G, HC=heavy chain, LC=light chain.

Determination of the amount of bound material (Table 2.1) indicated that the
adsorbents activated by ECH had a very high binding capacity whereas AB-activated
adsorbents bound Ig very poorly despite having a higher capacity for other proteins.
The adsorbents prepared through the AGE activation route bound Ig at reasonable
levels and the results suggest that the degree of non-specific binding was lower for
this type (Table 2.1). The higher selectivity of this type of adsorbent was confirmed
by SDS-PAGE analysis of the eluted fraction (Fig. 2.5), which indicated a higher
purity as compared to, e.g., the elution fraction from the ECH-activated adsorbent,
where a band corresponding to the main contaminant in the serum, rabbit serum
albumin, can still be seen.

Poorer results than expected were obtained with the adsorbent containing the sulfone
group in the spacer arm. The combination of a spacer arm introduced by DVS
activation with the MEP ligand attached to a cellulose base matrix has previously
been reported (Boschetti, 2002) to give an increase in the binding capacity for IgG as
compared to adsorbents where the sulfone group was absent. However, this was not
the case for our base supports, and therefore, the adsorbents prepared by AGE
activation were selected for further work.

(a)　　　　　　　　　　　　　　　　**(b)**
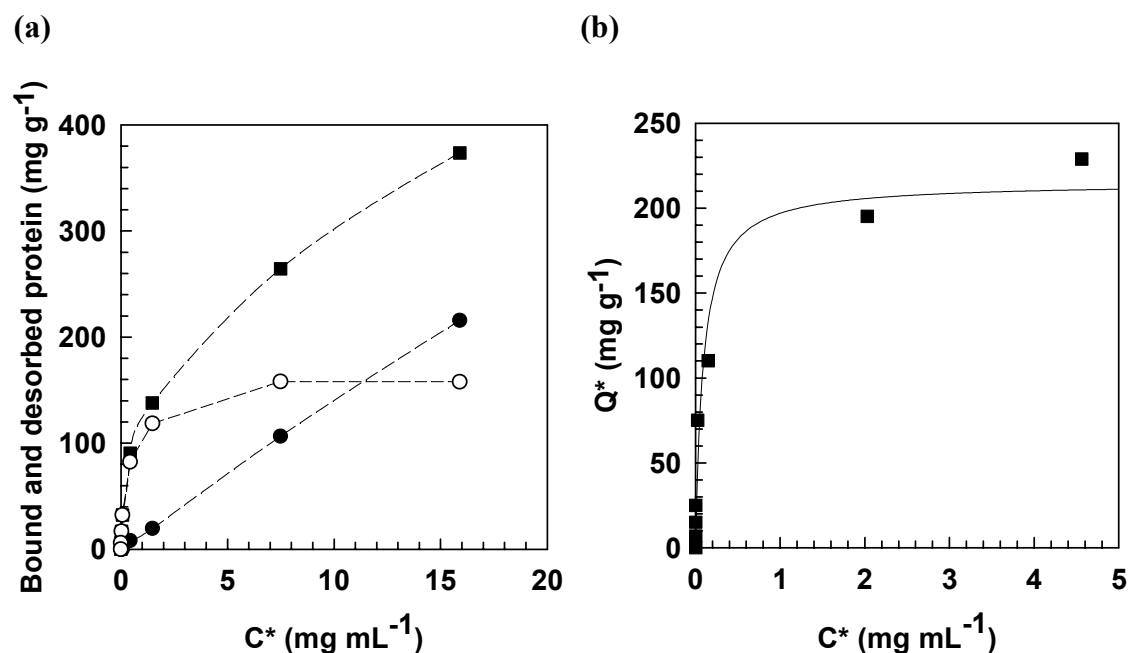
Fig. 2.6 (a) Binding isotherm for total protein from rabbit antiserum on MEP supports (■) followed by washing (●) and elution (○) of the protein bound to the adsorbents. **(b)** Binding isotherm for Ig in rabbit antiserum on MEP supports. The solid line through the data represents the fitted Langmuir curve (Q_{max} = 215 mg g^{-1}, K_d = 0.09 mg mL^{-1}). Binding was performed with a constant concentration of adsorbents: 4.6 g L^{-1}.

2.3.2 Binding properties of AGE activated MEP supports

Further characterisation of AGE-activated MEP magnetic adsorbents with respect to their binding properties was carried out by constructing a binding isotherm in diluted rabbit anti-serum. The results suggested that the adsorbents had a high degree of unspecific protein binding, as shown by the multilayer binding type of isotherm curve obtained from total protein measurements (Fig. 2.6a). However by performing a rapid (30 sec) washing step following binding, it could be seen that a large amount of protein was desorbed, the concentration of which was directly related to the concentration of loaded adsorbents, suggesting a non-specific concentration. In contrast, the amount of protein eluted by lowering the pH followed a different pattern (Fig. 2.6a) suggesting that specifically bound protein was being released. A binding isotherm constructed from measurements of Ig (Fig. 2.6b) supported this contention. Despite the high degree of unspecific protein binding, the results suggest that the

immunoglobulins bind specifically to the adsorbents with a binding capacity of ~75 mg g^{-1}. Furthermore, the Langmuir parameters calculated for this system (Q_{max} = 215 mg g^{-1}, K_d = 0.09 mg mL^{-1} ≈ 1 μM) are in the range of values obtained for other types of affinity systems employing the same type of base supports (Gomes *et al.*, 2006b).

2.3.3 Optimization of binding and elution conditions

Studies of binding conditions

The results above appeared promising. However, the choice of binding and elution conditions used was based on optimization studies done by Guerrier *et al.* (2000) for the purification of human polyclonal IgG using a MEP derivatised commercial chromatography medium (MEP HyperCel). In contrast, our system employs a different type of feedstock, adsorbent size, base matrix and activation chemistry, and furthermore consists of a batch process. Thus it was expected that slightly different conditions might be required for optimal performance in our system. Variation of pH in the binding buffer and feedstock had a strong impact on the amount of protein bound by the adsorbents and a maximum adsorption value was found at pH 8 (Fig. 2.7a), which is in agreement with the results reported by Guerrier *et al.* (2000). The same authors showed that there was no impact of conductivity on adsorption. However, in our system, we observed a slight drop of up to ~25 % in support capacity when low concentrations of sodium chloride (≤ 150 mM) were present (Fig. 2.7b).

Dilution of the feedstock in ammonium sulphate, a lyotropic salt known to enhance thiophilic binding, also had a negative impact on the binding capacity of magnetic MEP adsorbents (Fig. 2.7c), although it has been hypothesised that the presence of the sulfur atom close to the pyridine ring might be involved in Ig binding through a similar mechanism to thiophilic interaction (Boschetti, 2002). From these studies it was concluded that the optimal binding conditions for our system are pH 8 and low ionic strength.

(a)

(b)

(c)

(d)
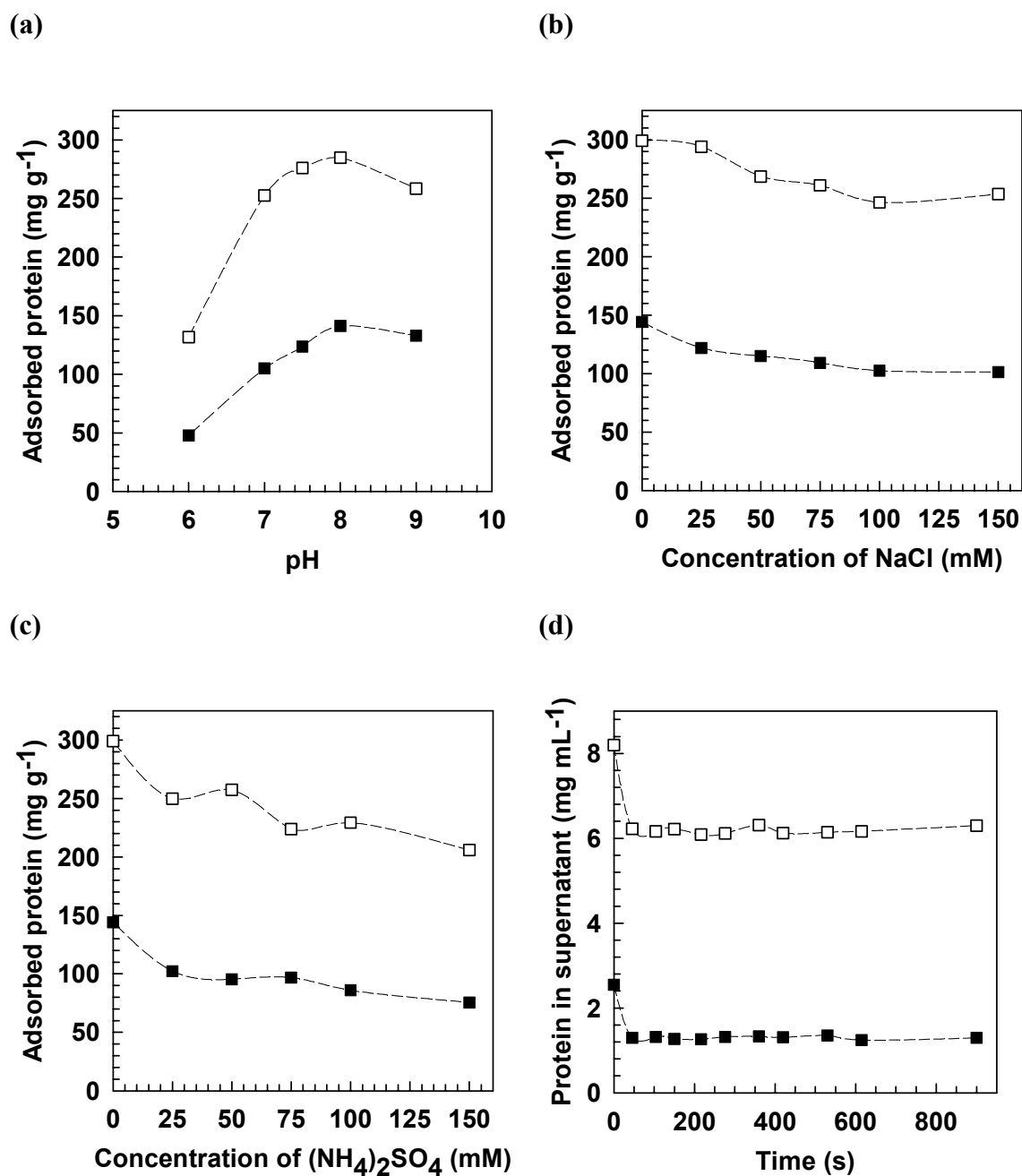
Fig. 2.7 Adsorption of total protein (□) and Ig (■) from rabit antiserum to MEP supports at different conditions: **(a)** pH of binding buffer; **(b)** Concentration of NaCl in binding buffer at pH 8; **(c)** Concentration of $(NH4)_2SO_4$ in binding buffer at pH 8; **(d)** Binding time.

In order to evaluate the time necessary for adsorption to be completed, we monitored the protein content in the supernatant during binding between diluted serum and MEP supports. Binding reached equilibrium within ~45 sec (Fig. 2.7d), which was the

minimum time necessary for handling the samples. Given that the magnetic adsorbents featured in this work are essentially non-porous and have sub-micron sizes, the adsorption kinetics were expected to be fast (Anspach, 1989; Hoffmann, 2002; Ferré, 2005) and our results are in agreement with reports by previous workers for adsorbents based on similar magnetic supports (Heebøll-Nielsen, 2004c; Ferré, 2005). Thus, for subsequent work, at least one minute was employed in all binding steps.

Optimisation of support concentration

The adsorbent concentration used in the batch binding step is a parameter of major importance in HGMF. Given the limited capacity of the HGMS system, i.e., the amount of adsorbent that can be processed by the magnetic filter, the concentration of support employed will determine the volume of feedstock processed in a single cycle.

Recoveries of Ig when applying different concentrations of adsorbent to 10-fold diluted serum are shown in figure 2.8a. In this work, dilution of serum was necessary due to the high concentration of immunoglobulins in the feedstock (~25 mg mL^{-1}) and thus the concentration of adsorbents that would be necessary to bind the entire product. In a batch system like the one used here, there is a physical limitation on the amount of solid supports that can be suspended in a given volume. In preliminary studies conducted in our laboratory, we tested the impact of serum dilution on capacity of the adsorbents by varying the dilution factor and the support concentration proportionally to the concentration of Ig obtained for each dilution. No changes were observed in the support binding capacities, indicating that the binding is not affected by the serum strength (data not shown). In light of this, 10-fold dilution was selected for further examination of the optimum adsorbent concentration during binding.

Addition of 25 mg of support per mL of 10-fold diluted serum removed 48 % of the total protein present and 88 % of the total Ig (Fig. 2.8a). Increasing the support amount to 30 mg resulted in the clearance of 92 % of the Ig initially in the serum (corresponding to a capacity of 81 mg of Ig per g of support) but bound 51 % of total protein. In previous work using other types of magnetic adsorbents at a lower range of concentrations (Hubbuch and Thomas 2002), an impact of support concentration on

binding selectivity has been observed. In that case, it was hypothesised that this resulted from proteins being trapped in the support 'cake', therefore increasing the apparent binding of contaminant proteins. In our system, where up to ~ 30 fold higher support concentrations than by the reported Hubbuch and Thomas (2002) were employed, this effect is expected to be more severe. However, according to figure 2.8a, the binding selectivity does not seem to be affected and the ratio Ig/total protein bound to the adsorbents varies between 0.6 for 6 mg mL^{-1} of adsorbent and 0.5 for 30 mg mL^{-1} of adsorbent.

(a)   **(b)**
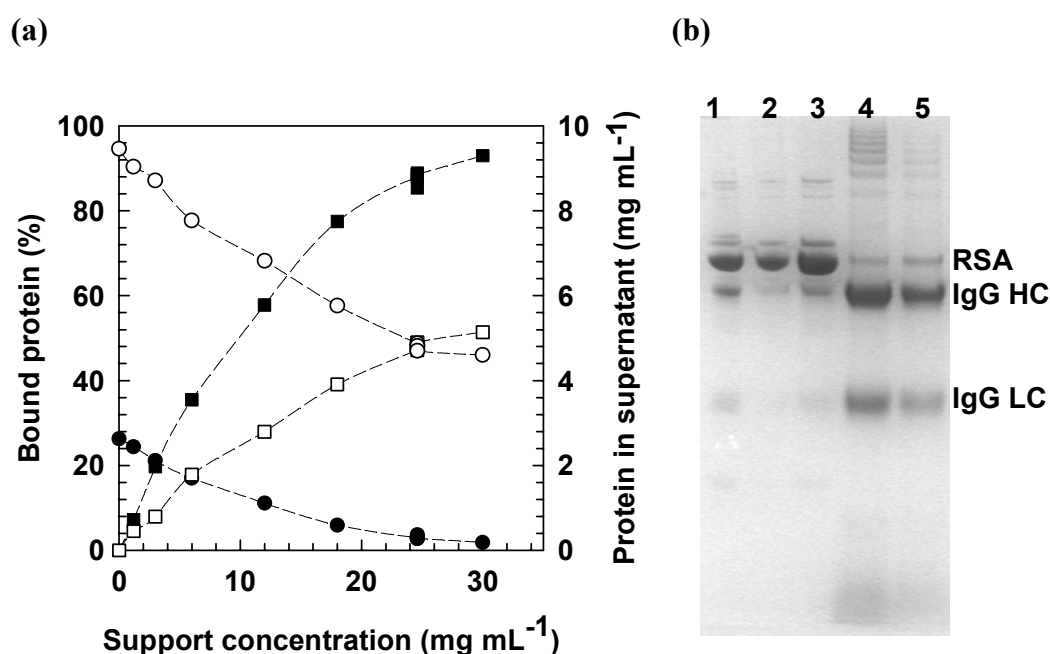
Fig. 2.8 (a) Effect of support concentration on the adsorption of Ig (remaining in solution, ● and bound to adsorbent, ■) and total protein (remaining in solution, ○ and bound to adsorbent, □) from unclarified, 10-fold diluted rabbit antiserum. **(b)** SDS-PAGE analysis of fractions from binding performed with a support concentration of 30 mg mL^{-1} in 10-fold diluted rabbit antiserum (lane 1: rabbit antiserum, lane 2: unbound), wash (lane 3), 1st elution (lane 4) and 2nd elution (lane 5). RSA=rabbit serum albumin, Ig G=immunoglobulin G, HC=heavy chain, LC=Light chain. Elution was mediated by 500 mM sodium acetate, pH 4.

Following an adsorption step using 30 mg support per mL of 10-fold diluted serum, 14 % of the total protein adsorbed was desorbed in a quick washing step with a loss of only 2.7 % of the bound Ig (Table 2.2). Most of the protein washed from the supports

was rabbit serum albumin, as shown by SDS-PAGE analysis of the fraction (Fig 2.8b, lane 3). These results are in agreement with the observations from the initial adsorbent binding studies discussed in section 2.3.2. Under the elution conditions employed here (elution buffer: 500 mM sodium acetate, pH 4; adsorbent concentration: 60 mg mL^{-1}), 58 % of the initially bound Ig was released with a purity of 41 % (after two equivalent elution cycles), i.e., 1.5 fold higher than in serum. Given that the starting material contains a large proportion of the target protein (28 %), high purification factors are not likely to be expected (3.6 would be the theoretical maximum). However, the SDS-PAGE analysis presented in figure 2.8b indicates that purity values in the elution fractions are much higher than the determined by the combination of the turbidimetric method and the BCA assay. A rough examination of the main species present in the elution fractions, i.e., IgG and RSA, by scanning densitometry of the protein gel indicates that at least 97 % of the protein consist of IgG in the first elution and 94 % in the second, which corresponds to an overall purification factor of at least 2.3 with respect to the RSA and IgG present in serum (Table 2.2). The high molecular weight ladder observed in the gel (Fig. 2.8b, lanes 4 and 5) could correspond to polymerised units of IgG.

The turbidimetric assay was tested with immunoglobulin standards from non-immunised rabbits in the same buffer as the one used for elution and no interference was detected under those conditions, i.e., the measured concentration was the same as when the Ig standards were incubated in 50 mM Tris/HCl, pH 8 and in both cases the concentration remained constant for a period of 1 h (data not shown). It has been reported by Bak (2004) that elution fractions obtained with 50 mM sodium acetate, pH 4, from MEP HyperCel (a chromatography medium employing the same ligand that we are working with) contained a precipitate when elution fractions were left to stand. That author suggests that the precipitate probably consisted of lipoproteins (Bak, 2004). In our studies it was observed that at several concentrations of sodium acetate a slight indication of turbidity appeared in the samples after being frozen and thawed and that a decrease in Ig content as measured by immunoturbidimetry also occurred (data not shown). Although a clear formation of precipitates could only be visualised when a concentration of 1 M sodium acetate was used for conducting the

75

elution steps, it seems plausible that some degree of agglomeration at the buffer concentration (500 mM) used during elution affected the measurements of Ig concentration. Furthermore, the BCA assay used in this work for total protein determination is known to be species dependent and it is important to recall that all values are expressed in bovine serum albumin equivalent units. The BCA reagent manufacturer (Pierce) reported that Ig concentrations might be overestimated by 21 % when using BSA standards as reference. Since the elution fraction consists mainly of IgG, it is possible that the total protein content has been overestimated, contributing therefore to an underestimation of the calculated purity values.

Optimisation of elution conditions

Drops in protein recovery, observed when scaling from test tube experiments to HGMF processing (Meyer *et al.*, 2005; Heebøll-Nielsen, 2004a) which appears to be due to the concentration of support in the HGMF system during the desorption steps are often not taken into account during testing. Most desorption optimisation studies in previous work have been done at low concentration of support and therefore the results changed when the conditions were transferred to the HGMF system, where the supports typically would be present at a much higher concentration. This issue has been addressed recently in the work done by Meyer *et al.* (2005) where fairly good predictions of the desorption efficiency could be achieved by simply conducting the bench scale studies at the same concentrations of support that were to be found later in the HGMF system. However, prior to such studies it is necessary that the set-up of the HGMS system is defined and that the conditions for support collection on the magnetic filter are optimised. In our case, dilution of the adsorbents is expected during HGMF wash and elution. The magnetic filter capacity for a suspension of MEP adsorbents in 10-fold diluted serum was determined by a breakthrough experiment to be 98 g L^{-1}, and the volume of the recycle loop including the filter where desorption occurs is 16 mL. Thus it was estimated that the supports will be present at a concentration of ~20-25 mg mL^{-1} in the desorption steps processed by HGMF, as compared to a value of 30 mg per mL of serum in the binding step, determined in the support concentration optimisation studies. Thus, a target

concentration of ~20 mg mL^{-1} loaded adsorbents was selected for optimisation of elution conditions.

(a)

(b)
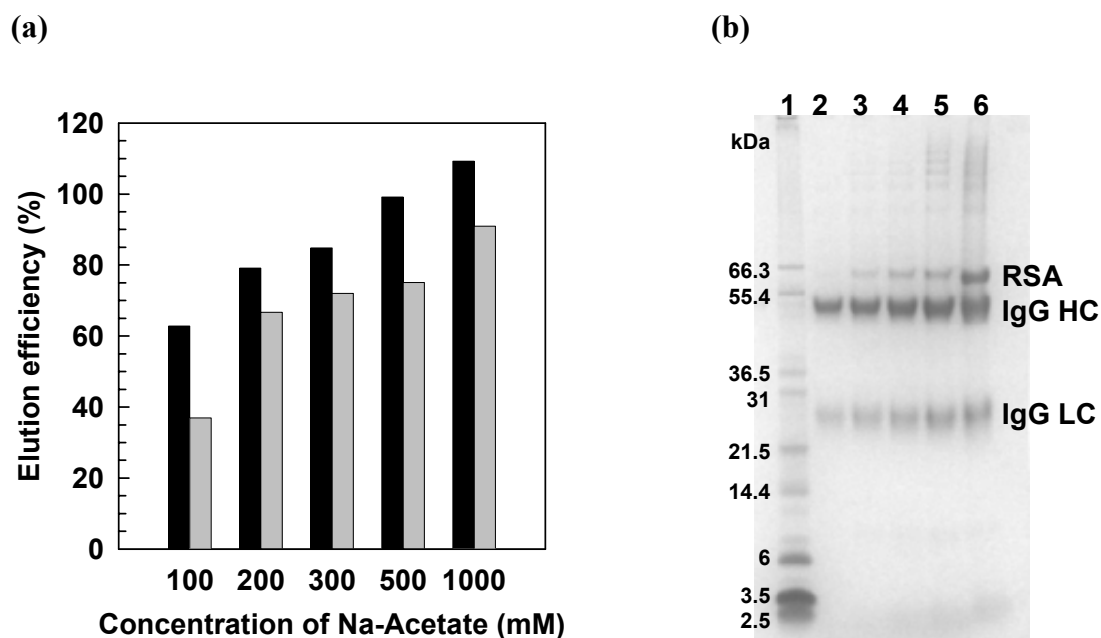
Fig. 2.9 (a) Effect of elution buffer strength on the efficiency of Ig (▭) and total protein elution (▬) from MEP adsorbents present in solution at a concentration of 19 mg mL^{-1}. **(b)** SDS-PAGE analysis of fractions corresponding to the first elution from the supports with sodium acetate concentrations of 100 (lane 2), 200 (lane 3), 300 (lane 4), 500 (lane 5) and 1000 mM (lane 6); Lane 1: molecular weight standards.

Introduction of small changes in pH (± 0.5 units) or use of citrate buffer did not improve the desorption efficiency from protein-loaded adsorbent as compared to the results obtained with sodium acetate at pH 4 (data not shown). We therefore evaluated the buffer strength needed to confer the necessary driving force for Ig release. For that purpose, the magnetic adsorbents were loaded with protein by incubation of 25 mg mL^{-1} in 10-fold diluted serum. Then the wash step and the intended elution tests were performed with the loaded adsorbent at a concentration of 19 mg mL^{-1} (Fig. 2.9). As expected, the desorption efficiency of Ig increased when using higher buffer capacity (Fig 2.9a). When raising the concentration of sodium acetate from 500 to 1000 mM, the elution efficiency based on the amount of Ig remaining bound to the adsorbents after the wash increased from 75 % to 91 % in the first elution step. As mentioned before, the employment of 1000 mM sodium acetate led to a clear formation of a

precipitate after freezing and thawing the sample. For this reason, at the expense of lower elution efficiencies, we decided to conduct further experiments with 500 mM sodium acetate, a choice that will also enable us to compare results with those from test tube experiments presented so far.

At the support concentration employed in these studies, the desorption efficiency was improved both for the wash and for the elution step as compared to the previous tests where higher concentrations were used, whereas the purity of the eluted fractions was not severely affected (Table 2.2). When applying a support concentration of 19 mg per mL of buffer, 76 % of the bound Ig were desorbed compared to only 60 % when 30 mg mL^{-1} in the washing step and 60 mg mg^{-1} in the elution steps were used. The purity values based on the immunoturbidimetric assay seem again to have been underestimated in the elution fractions (*cf.* SDS-PAGE analysis, Fig. 2.9b).

Table 2.2 Desorption efficiency of protein from the MEP adsorbents and purity of the eluted material [a]. Initial ratio of Ig in serum was 28 % by immunoturbidimetric and BCA assay (42 % estimated by scanning densitometry [b]).

Support concentration (mg mL^{-1})		Ig (%)	Total protein (%)	Purity [b] (%)	Purity [c] (%)	Purification factor
Binding: 30 Wash: 30 Elution [d]: 60	Wash	2.73	13.8	n.a.	n.a.	n.a.
	1st Elution	36.8	41.8	44.2	≥ 97 %	1.6 (≥ 2.3 [b])
	2nd Elution	20.7	27.8	37.6	≥ 94%	1.3 (≥ 2.2 [b])
	Balance	**60**	**83**			
Binding: 25 Wash: 19 Elution [d]: 19	Wash	3.82	14.4	n.a.	n.a.	n.a.
	1st Elution	59.0	68.1	42.8	≥ 93%	1.5 (≥ 2.2 [b])
	2nd Elution	13.3	16.7	39.5	n.d.	1.4
	Balance	**76**	**99**			

[a] Binding performed in 1.5 mL of 10-fold diluted serum.

[b] Based on measurements from the immunoturbidimetric and BCA assays for Ig and total protein, respectively.

c From scanning densitometry of IgG and RSA bands in SDS-PAGE gel (Fig. 2.8b & Fig. 2.9b). Since the bands corresponding to the IgG heavy chain are saturated in the elution lanes and RSA is saturated in lane corresponding to serum, the results are indicated as minimum values.

d Elution buffer: 500 mM sodium acetate, pH 4.

n.a. not applicable.

n.d. not determined.

Recovery of immunoglobulins by HGMF processing

Following identification of optimal conditions for recovery and desorption of immunoglobulins, we proceeded with the processing of rabbit anti-serum by HGMF (Fig. 2.10). Addition of magnetic MEP adsorbents 380 mg to 11.5 mL of 10-fold diluted but unclarified rabbit antiserum to a final support concentration of 33 mg per mL serum resulted in a 95.5 % removal of the Ig present in solution (Table 2.3). This result was similar to that found in test tube studies (*cf.* 92 %, Fig. 2.8a). However, an 11 % increase occurred in the removal of total protein (62 % *cf.* 51 % in the clarified undiluted feedstock), which could be an effect of working with an unclarified feedstock or the increase of support concentration (33 mg mL^{-1} *cf.* 30 mg mL^{-1}).

(a)   **(b)**
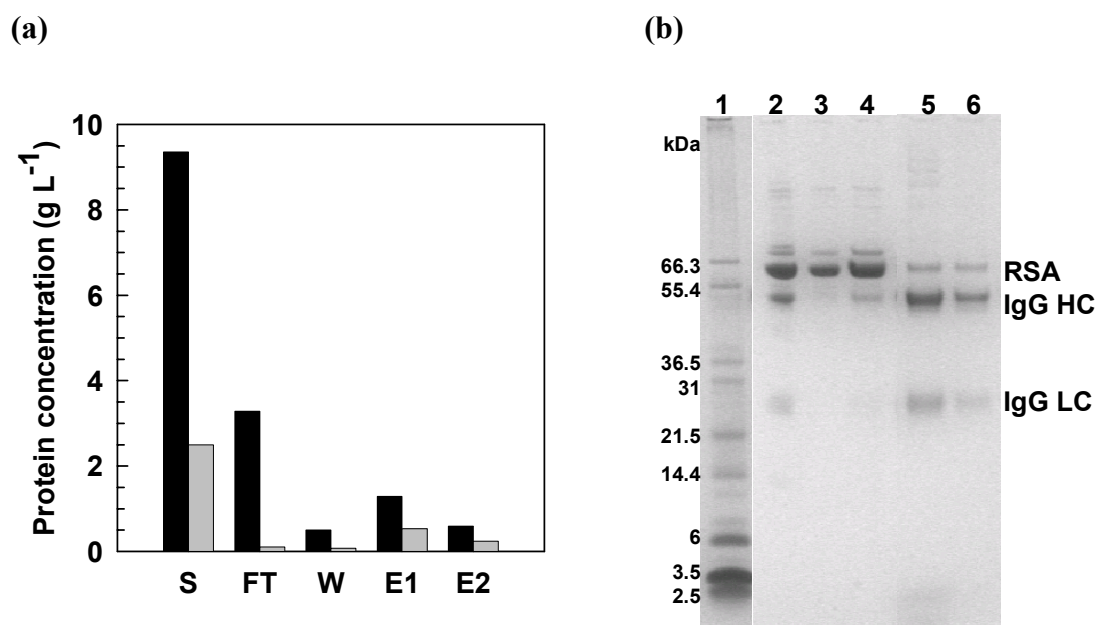
Fig. 2.10 (a) Ig (▭) and total protein (▬) concentration profiles obtained during HGMF processing of 10-fold diluted serum. S=diluted rabbit anti-serum, FT=flowthrough, W=wash, E1=1st elution and E2=2nd elution. **(b)** SDS-PAGE analysis of fractions from the HGMF process (lane 2: rabbit antiserum, lane 3: unbound), wash (lane 4), 1st elution (lane 5) and 2nd elution (lane 6). RSA=rabbit serum albumin, Ig G=immunoglobulin G, HC=heavy chain, LC=light chain. Lane 1: molecular weight standards.

Most of the unspecific bound material was easily desorbed in the HGMF washing step (Fig. 2.10) and the performance was very similar to that seen in test tube studies (13 % *cf.* 14.4 % total protein desorbed and 4.5 % *cf.* 3.8 % Ig desorbed; Table 2.3 &

Table 2.2). Furthermore, the purity in the two eluted fractions and the purification factor of 1.6 was similar to the test tube studies. Visualisation of the proteins in the elution fractions by SDS-PAGE analysis (Fig. 2.10b & Table 2.3) shows a slightly higher concentration of RSA than observed in the screening studies and scanning densitometry of the gel indicated that the IgG was enriched at least 2.1 times with respect to RSA, a result that is still very close to the value of 2.2-2.3 obtained before (Table 2.2). The elution efficiency was undoubtedly the parameter most affected by HGMF processing. In two elution steps, only 58.8 % of the immunoglobulins bound to the adsorbent prior to the washing step were desorbed as compared to 72 % achieved in the bench-scale studies. Performing four more elution steps only led to an 8.2 % increase in desorption of Ig and a 22 % extra desorption of total protein (data not shown).

The fact that the support concentration was slightly higher in the recycle loop (~ 23 mg of support per mL of solution as compared to 19 mg mL^{-1} employed in the bench-scale elution studies) cannot explain the lower desorption efficiency, since less variation in elution efficiencies was observed for support concentration differences in test tube experiments (Table 2.2). Dilution of the elution buffer in the recycle loop by 15 % has been reported for this particular HGMF set-up (Meyer et al, 2005) due to the liquid entrapped in the support cake collected in the magnetic filter. This dilution could be even higher due to mixing in the system, but given that in our elution optimisation studies, the elution buffer strength between 300 and 500 mM sodium acetate had very little an impact on the Ig desorption efficiency (only 3 %), extremely high extents of dilution would be necessary to justify drops of 11 %. The most probable cause for inefficient elution from the adsorbents is believed to be poor re-dispersion of the supports in the recycle loop. In studies performed with a different type of magnetic filters, it was demonstrated that the degree of particle release during the desorption steps in the recycle loop has a large impact on the performance of HGMF, namely on the yields of a purification process (Gomes, 2006a). Cleaning of the magnetic filter, after the supports had been flushed out at the end of the HGMF cycle, in the work presented here, revealed that there were magnetic supports still remaining inside the filter, an observation that confirms that the supports might not

have been efficiently released from the magnetic filter during the desorption steps. It is likely that this reason, combined with the dilution effects discussed above might account for the lower yields as compared to the ones obtained in the bench-scale studies.

Table 2.3 Recovery of immunoglobulins from rabbit anti-serum by HGMF processing using mercaptoethylpyridine-linked magnetic adsorbents.

	Ig (mg)	Ig yield (%)	Total protein (mg)	Total protein yield (%)	Ig desorption efficiency (%)	Total protein desorption efficiency (%)	Purification factor	Dilution factor
Load [a]	28.7	100	107.6	100	n.a.	n.a.	1	1
Flowthrough	1.3	4.5	41.1	38.2	n.a.	n.a.	n.a.	n.a.
Washes	1.3	4.5	8.6	8.0	4.5	13.0	n.a.	n.a.
1st elution	12.1	42.1	29.2	27.1	44.2	43.9	1.6 (≥ 2.1 [b])	4.6
2nd elution	4.2	14.6	10.0	9.3	14.6	15.0	1.6 (≥ 2.1 [b])	10.2
Balance		**66**		**83**	**64**	**72**	**—**	**—**

[a] 33 mg mL^{-1} of adsorbents in 11.5 mL of 10-fold diluted serum.

[b] Determined by scanning densitometry IgG and RSA bands in SDS-PAGE gel in figure 1.10b. Since the bands corresponding to the IgG heavy chain are saturated in the elution lanes and RSA is saturated in lane corresponding to serum, the results are indicated as minimum values.

n.a. not applicable.

Feedstocks containing the target protein present in very high concentrations are a challenge for HGMF processing. As was necessary here, 10-fold dilution of the serum was required to bring the target concentration down to a level where a reasonable concentration of magnetic supports could be used. Heebøll-Nielsen (2003) also reported a similar problem during the processing of a protein expressed in the form of inclusion bodies in which 12 mg mL^{-1} adsorbents were necessary during adsorption. Nevertheless, it might be physically possible to work at higher support concentrations than the ones employed here, although this might lead to an increase of the fluid viscosity, which would in turn reduce the efficiency of particle capture on the magnetic filter. However, there are several other matters that need to be addressed. For example, the amount of support that can be used in one cycle is dependent on the filter capacity and working at high support concentration will limit the volume of feed that can be processed per cycle. This limitation will not only have an effect on the

productivity of the process, but will also compromise the concentrating power of the process. The implications of this were seen in the present HGMF system, where dilution factors of 4.6 and 10.2 were obtained for the fractions, corresponding to the first and second elution steps, respectively. The final concentration of the purified protein is also dependent on the size of the recycle loop where the desorption steps occur and the latter can be optimised by employing filters with higher particle capacity and reducing the relative size of supporting equipment, such as tubing and valves. However, the use of solutions with high buffer capacity will be necessary in order to compensate for the dilution effect caused by the liquid entrained in the support cake. The cost associated with the use of more concentrated buffers and the effect that these might have on the stability of the purified proteins are issues that will need to be taken into consideration.

However, application of the system we present here to the purification of antibodies from other feedstocks should not incur the severe problems related to the use of high support concentration, since most monoclonal antibodies are nowadays produced in mammalian cell culture at lower yields. It has been reported for high productive cell lines that levels of recombinant immunoglobulins were between 0.3 and 0.6 mg mL^{-1} (Bianchi and McGrew, 2003; Jones *et al.*, 2003), and these are concentrations that have typically been dealt with successfully in previous systems processed by HGMF (Ferré 2005; Gomes, 2005b; Heebøll-Nielsen *et al.*, 2004a, 2004b; Hubbuch and Thomas, 2002). Furthermore, the use of HGMF is expected to have great advantages compared to traditional direct capture strategies. In the work presented here, the processing time was lower than 35 min for two elution cycles, even though the HGMF processing was not conducted under optimised time conditions. Considering that the processing times when applying higher volumes will increase only for some of the operations, such as loading of the magnetic particle suspension and buffers, the example we present for HGMF processing of rabbit anti-serum at a small scale gives a realistic picture of the low time consumption that this technique permits. An in-depth analysis of HGMF productivity can be found in the book chapter by Franzreb *et al.* (2006).

2.4 Conclusions

In this chapter we have shown that the magnetic adsorbents constructed using the ligand 4-mercaptoethylpyridine (MEP) can be employed for direct capture of IgGs. In the system used, co-adsorbtion of rabbit serum albumin occurred, but this contaminant could be easily desorbed by a single washing step and the subsequently eluted IgG fractions presented a degree of purity of over 90 %.

The feedstock used in this work, rabbit antiserum containing a high concentration of IgG, constituted a challenge for the high-gradient magnetic fishing technique. At the scale used here, it was thus not possible to achieve a high concentration of the purified protein, since in HGMF, the concentration of eluted material is dependent on the capacity of the magnetic filter, the combined volume of the filter and recycle loop used during elution. This case study shows that improvement of magnetic filters along with design of high capacity adsorbents is necessary. However, an adverse effect of high filter capacity has been identified. In order to deal with the high concentration of particles in the filter, high salt concentration buffers might be necessary. There were strong indications that dilution effects caused by liquid entrapped in the collected supports have a negative impact on elution efficiency. Overall, the results in this work indicate that HGMF might be more suitable for recovery of proteins from dilute feedstocks, as is the case for most antibody bioreactor based containing feedstocks. The processing time of 45 min for a complete HGMF purification cycle and the comparable results obtained in test tube studies using serum confirm that HGMF is a fast and robust technique.

Acknowledgments

References

Anspach, F.B., Johnston, A., Wirth, H.J., Unger, K.K., Hearn, M.T. (1989) High-performance liquid chromatography of amino acids, peptides and proteins. XCII Thermodynamic and kinetic investigations on rigid and soft affinity gels with varying particle and pore sizes. *J. Chromatogr.*, 4(476), 205-225.

Bak, H. (2004) *New downstream processes for antibodies: From rabbit serum to Ig-fraction*. Ph.D. Thesis. Technical University of Denmark, Denmark.

Bianchi, A., McGrew, J.T. (2003) High-level expression of full-length antibodies using trans-complementing expression vectors. *Biotechnol. Bioeng.*, 84, 439-444.

Boschetti, E. (2002) Antibody separation by hydrophobic charge induction chromatography. *Trends Biotechnol.*, 20(8), 333-337.

Burton S.C. (1996) Preparation of chemically modified bead cellulose resins and their application to protein purification. Ph.D. Thesis. Massey University, Palmerston North, New Zealand.

Burton, S.C., Harding, D. R. K. (1997a) Bifunctional etherification of a bead cellulose for ligand attachment with allyl bromide and allyl glycidyl ether. *J. Chromatogr. A*, 775, 29-38.

Burton, A.C., Harding, D.R.K. (1998) Hydrophobic charge induction chromatography: salt independent protein adsorption and facile elution with aqueous buffers. *J. Chromatogr. A*, 814, 71-81.

Ferré, H. (2005) *Development of novel processes for continuous protein refolding and primary recovery - A case study on the major histocompatibility complex class I receptor and its individual subunits*. Ph.D. Thesis. Technical University of Denmark, Denmark.

Franzreb, M., Ebner, N., Siemann-Herzberg, M., Hobley, T.J., Thomas, O.R.T. (2006a) Product recovery and high-gradient magnetic fishing. *Process-scale bioseparations for the biopharmaceutical industry* (Ed. Shukla, A., Gadam, S., Etzel, M.) Marcel Dekker, New York (in press).

GenMab (no date) Introduction to the company [online]. Available from: http://www.genmab.com/html/intro_to_abs.shtml [Accessed 21 February 2005].

Gomes, C.S.G., Ebner, N., Thomas, O.R.T., Franzreb, M., Hobley, T.J. (2006a) Protein purification using high-gradient magnetic fishing: Impact of magnetic filter performance. *Chapter 4*.

Gomes, C.S.G., Heebøll-Nielsen, A., Petersen, T.L., Thomas, O.R.T., Hobley, T.J. (2006b) Control of protein hydrolysis in unclarified liquors: application of high-gradient magnetic fishing (HGMF) employing improved magnetic adsorbents. *Chapter 5*.

Guerrier, L., Girot, P., Schwartz, W., Boschetti, E. (2000) New method for the selective capture of antibodies under physiological conditions. *Bioseparation*, 9, 211-221.

Guerrier, L., Flayeux, I., Boschetti, E. (2001) A dual-mode approach to the selective separation of antibodies and their fragments. *J. Chromatogr. B*, 755, 37-46.

Halling, P.J., Dunnill, P. (1979) Improved nonporous magnetic supports for immobilised enzymes. *Biotechnol. Bioeng.,* 21, 396-416.

Halling, P.J., Dunnill, P. (1980) Magnetic supports for immobilized enzymes and bioaffinity adsorbents. *Enzyme Micro. Technol.,* 2, 2-10.

Heebøll-Nielsen, A., Choe, W.S., Middelberg, A.P.J., Thomas, O. R.T. (2003) Efficient inclusion body processing using chemical extraction and high-gradient magnetic fishing. *Biotechnol. Progr.*, 19(3), 887-898.

Heebøll-Nielsen, A., Dalkiær, M., Hubbuch, J.J., Thomas, O. R.T. (2004a) Superparamagnetic adsorbents for high-gradient magnetic fishing of lectins out of legume extracts. *Biotechnol. Bioeng.,* 87(3), 311-323.

Heebøll-Nielsen, A., Justesen, S.F.L. Hobley, T.J., Thomas, O.R.T. (2004b) Superparamagnetic cation-exchange adsorbents for bioproduct recovery from crude process liquors by high-gradient magnetic fishing. *Sep. Sci. Technol.,* 39(12): 2891-2914.

Heebøll-Nielsen, A., Justesen, S.F.L., Thomas, O.R.T. (2004c) Fractionation of whey proteins with high-capacity superparamagnetic ion-exchangers. *J. Biotechnol.,* 113, 247-262.

Hoffmann, C. (2002) *Einsatz magnetischer Separationsverfahren zur biotechnologischen produktaufarbeitung*. Ph. D. Thesis. Forschunszentrum Karlsruhe, Germany.

Hoffmann, C., Franzreb, M., Höll, W.H. (2002) A novel high-gradient magnetic separator (HGMS) design for biotech applications. *IEEE Trans. Appl. Supercond.,* 12(1), 963- 966.

Hubbuch, J.J., Thomas, O.R.T. (2002) High-gradient magnetic affinity separation of typsin from porcine pancreatin. *Biotechnol. Bioeng.,* 79, 301-313.

Jones, D., Kroos, N., Anema, R., van Montfort, B., Vooys, A., van der Kraats, S., van der Helm, E., Smits, S., Schouten, J., Brouwer, K., Lagerwerf, F., van Berkel, P., Opstelten, D., Logtenberg, T., Bout., A. (2003) High-level expression of recombinant IgG in the human cell line PER.C6. *Biotechnol. Prog.,* 19, 163-168.

Knudsen, K.L., Hansen, M.B., Henriksen, L.R., Andersen, B.K., Lihme, A. (1992) Sulfone-aromatic ligands for thiophilic adsorption chromatograhy: Purification of human and mouse immunoglobulins. *Anal. Biochem.,* 201, 170-177.

Köhler, G., Milstein, C. (1975) Continuous cultures of fused cells secreting antibody of predefined specificity. *Nature,* 256(5517), 495-497.

Langmuir, I. (1918) The adsorption of gases on plane surfaces of glass, mica and platinum. *J. Am. Chem. Soc.,* 44, 1361-1403.

Medarex (no date) *Monoclonal antibodies on the market* [online]. Available from: http://www.medarex.com/Development/Therapeutics.html [Accessed 21 February 2005].

Meyer, A., Hansen, D.B., Gomes, C.S.G., Hobley, T.J., Thomas, O.R.T., Franzreb, M. (2005) Demonstration of a strategy for product purification by high-gradient magnetic fishing: Recovery of superoxide dismutase from unconditioned whey. *Biotechnol. Prog.*, 21, 244-254.

Morrow, J.K. (2002) Economics of antibody production. *Genetic Engineering News*, 22(7), p. 1, 35 and 39.

O'Brien, S. M., Thomas, O. R. T., Dunnill, P. (1996) Non-porous magnetic chelator supports for protein recovery by immobilised metal affinity adsorption. *J. Biotechnol.*, 50, 13-26.

Pierce Biotechnology (no date) *Instructions: BCA protein assay reagent kit* [online]. Available from: http://www.piercenet.com/files/1296dh4.pdf [Accessed 21 February 2005]

Porath, J., Maisano, F., Belew, M. (1985) Thiophilic adsorption – A new method for protein fractionation. *FEBS*, 185(2), 306-310.

Schwartz, W., Judd, D., Wysocki, M., Guerrier, L., Birck-Wilson, E., Boschetti, E. (2001) Comparison of hydrophobic charge induction chromatography with affinity chromatography on protein A for harvest and purification of antibodies. *J. chromatogr.*, 908, 251-263.

van Dijk M.A., van de Winkel, J.G.J. (2001) Human Antibodies as next generation therapeutics. *Curr. Opin. Chem. Biol.*, 5, 368-374.

3. Filter capacity predictions for the capture of superparamagnetic microparticles by High-Gradient Magnetic Separation (HGMS)

Niklas A. Ebner[1], Cláudia S.G. Gomes[2], Timothy J. Hobley[2], Owen R.T. Thomas[2,3] and Matthias Franzreb[1]

[1] Institute for Technical Chemistry, Water- and Geotechnology Division, Forschungszentrum Karlsruhe GmbH, 76344 Eggenstein-Leopoldshafen, Germany.

[2] Center for Microbial Biotechnology, Technical University of Denmark, 2800 Lyngby, Denmark.

[3] Department of Chemical Engineering, The University of Birmingham, Edgbaston, Birmingham B15 2TT, United Kingdom.

Abstract

Experimental and theoretical methods to predict maximum and working filter capacities for the capture of superparamagnetic microparticles through High-gradient Magnetic Separation (HGMS) are presented. For this, various combinations of nine different HGMS filter matrices and two types of superparamagnetic microparticles were employed in breakthrough experiments. By calculating the separated particle mass per filter mesh area, the influences of wire diameter and wire mesh spacing on the particle build-up density were clearly demonstrated. Further, a simple experimental method for estimating average build-up densities in HGMS is introduced. Together with known physical parameters of the filter matrix and the background field, the use of such average build-up densities allows good predictions of the operational working filter capacities to be obtained.

3.1 Introduction

High-gradient magnetic separation has been used in combination with specially functionalized superparamagnetic adsorbent microparticles in a recently developed process known as High-gradient Magnetic Fishing for successful purification of various biomacromolecules (e.g. proteins) 'fished' directly out of crude unclarified biological suspensions (Hubbuch *et al.*, 2001; Hubbuch and Thomas, 2002; Heebøll-Nielsen *et al.*, 2003, 2004a, 2004b; Meyer *et al.*, 2005; Ferré, 2005; Ebner, 2005). In High-gradient Magnetic Fishing, the ability to predict maximum and working filter capacities of various different types of HGMS matrices for product-loaded superparamagnetic adsorbent particles is of great importance as it enables a first approximation of the amount of particle/biosuspension that can be treated within a typical operating cycle to be estimated. However, whereas the capture of paramagnetic particles on single-wires has been extensively studied both experimentally and theoretically (Gerber and Birss, 1983; Svoboda, 1987), far less work has been done on the separation of highly magnetic particles using 'real' multi-wire arrangements. Friedlaender (1978) and co-workers were the first to observe the accumulation of paramagnetic and ferrimagnetic (Takayasu *et al.*, 1983) microparticles onto single wires, and in later work (Leitermann, 1984) they examined the build-up of ferrimagnetic particles within multi-wire arrangements and grids. The data they obtained cannot be employed to describe the collection of the adsorbent materials employed in the present study for two main reasons. The first relates to the adsorbent microparticles possessing superparamagnetic rather than para- or ferrimagnetic properties. All previously described particle build-up behaviours in HGMS matrices are for para- and ferromagnetic materials and neither case is appropriate for superparamagnetic particles. Second, the authors (Leitermann, 1984) relied on optical measurements for judging the performance of the HGMS filters, but pointed to a major weakness of this approach, i.e. that a clear relationship between the optical size of particle build-up and the observed filter capacity could not be found. They reasoned that the density of particle build-up varies greatly under different conditions. In this paper we address for the first time the experimental and theoretical

prediction of particle build-up density around an HGMS wire for superparamagnetic microparticles.

Furthermore, the way in which HGMS has been applied for the recovery of bio-products is fundamentally different to its more common mode within the mineral and steel industries, in that practically complete particle removal is guaranteed in the former. The main reason for this form of operation is one of process economics. The functionalised magnetic adsorbent particles being captured within HGMS filters are loaded up with target bio-molecules. More often than not these species are of high value, and thus any adsorbent particle loss during HGMS represents diminished product recovery and consequent loss in revenue. Most HGMS theories predicting particle trajectories and separation efficiencies are of limited use in the above cases, as separation efficiencies will be very close to 100 %. Such high separation efficiencies are guaranteed through the use of comparatively low filtration velocities (i.e. of the order of 20 m h^{-1}). Filtration velocity is not however a major determinant of overall process performance in High-gradient Magnetic Fishing, because much more time is spent for the combined steps of product sorption, washing and elution as compared to the magnetic filtration step. In contrast, the particle holding capacity of a given filter is of great importance, as it directly affects both the overall process productivity and degree of product concentration that can be achieved. With the increasing interest in using HGMS for separation tasks within biotechnology, a simple method for estimating the particle holding capacities of magnetic filters would be a very useful tool for aiding the design of HGMS-based bioprocesses.

3.2 Materials and Methods

3.2.1 HGMS apparatus

The background magnetic field of $2.6 \cdot 10^5$ A m^{-1} ($B_0 = 0.32$ T) for HGMS experiments was generated using an HGF-10 switch 'on/off' permanent magnet system (Steinert GmbH, Cologne, Germany) described by Hoffmann *et al.* (2002). A non-magnetic (stainless steel 304) stainless steel filter housing containing cassettes of various different magnetic filter matrices (see Fig. 3.1) was inserted into the air gap of the HGF-10's yoke. The filter matrix cassettes consisted of layered stacks of alternating rectangular shaped (58 mm x 80 mm) ferromagnetic (stainless steel 430) and non-ferromagnetic (stainless steel 304) wire meshes (Haver & Boecker, Oelde, Germany). The ferromagnetic meshes formed the magnetic filter elements and the non-magnetic meshes acted as spacers. The wire mesh stacks were perpendicular to the magnetic field and parallel to the liquid flow so that half of the ferromagnetic wires were axially configured, while the other half were in the transverse configuration.
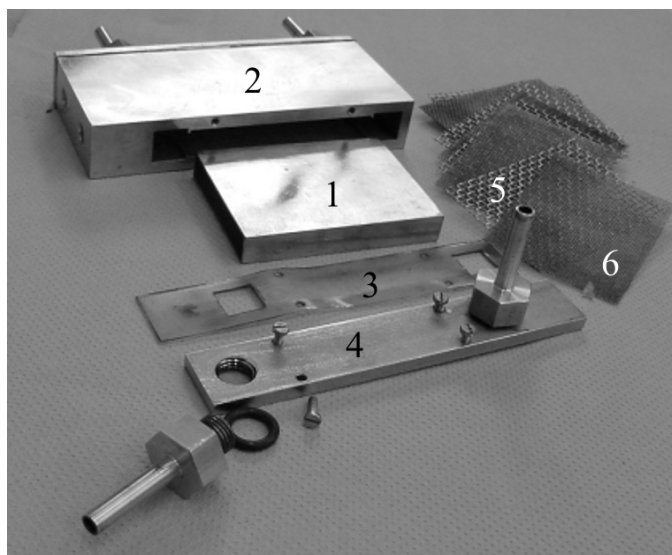
Fig. 3.1 Stainless steel filter housing (1) with cassette holder (2), seal (3), covers with inlets and outlets (4), and spacer (5) and filter (6) elements.

Three different filter elements (a-c) and four different spacers (A-D) were employed in this study, and their properties are summarized in table 3.1.

Table 3.1 Geometric properties of the filter elements and spacers used.

Filter components	wire diameter (mm)	wire mesh spacing (mm)
filter element		
a	0.315	1.00
b	0.250	0.63
c	0.090	0.20
spacer element		
A	0.900	5.00
B	0.500	2.55
C	0.250	1.00
D	0.125	0.50

The following combinations of filter elements and spacers were assembled into discrete cassettes which were subsequently tested for support filtration capacity: Aa (4+5), Ab (4+5), Ba (6+6), Bb (8+7), Bc (8+7), Ca (10+10), Cb (10+9), Cc (14+14), and Db (12+13). The values in parentheses respectively give the number of alternating spacer and filter elements fitted within the cassette holder.

3.2.2 Experimental procedures

Magnetic adsorbents

Two types of superparamagnetic adsorbent beads, PGF and M-PVA, were employed in this study, and brief descriptions of these are presented in table 3.2. The PGF base supports were prepared in two steps: (i) manufacture of sub-micron sized superparamagnetic iron oxide particles (Hubbuch and Thomas, 2002) and (ii) particle coating with 6 g L^{-1} polyglutaraldehyde according to the procedure described in O'Brien *et al.* (1996) and modified by Gomes (2006). Surface modification of both M-PVA and PGF to produce iminodiacetic acid derivatised adsorbents was performed according to Heebøll-Nielsen (2003). Strictly speaking neither of the two particle types are fully superparamagnetic, however, for all practical intents and purposes their very low remnant magnetizations can be neglected in this work.

Filter breakthrough experiments

In all HGMS experiments, suspensions of PGF or M-PVA (5.0 g L^{-1}) were pumped upward through the filter cassettes at 6.6 L h^{-1} (equating to a velocity v_0 of 19 m h^{-1}) and filtrate samples were collected with a fraction collector in aliquots of 15 mL. Shortly after visibly observed particle breakthrough had occurred in each experiment the flow was stopped, and the exact time to reach 5 % breakthrough was then determined by measuring the particle mass in the last few collected fractions from each run. As the particles were suspended in desalinated water, this was done by weighing the particles in each fraction after evaporating the solvent in a drying oven. In all subsequent calculations the filtration times at 5 % breakthrough were employed. In addition to visual observation of particle breakthrough in the exit stream, sporadic measurement of earlier fractions for untimely particle loss was also performed. In all cases, however, the separation efficiency was better than 99 %.

Table 3.2 Properties of superparamagetic adsorbent particles (beads)

Properties of beads	PGF	M-PVA
Basic bead material	polyglutaraldehyde coated ferrite	polyvinyl- alcohol + ferrite
Functional group	iminodiacetic acid	iminodiacetic acid
Density (kg m^{-3})	2800	1800
Mean diameter ($x_{3,0}$) (μm)	0.7	1.6
Shape	irregular	spherical
Magnetization at $B_0 = 0.32$ T (A m^2 kg^{-1})	44	39
Remanent magnetization (A m^2 kg^{-1})	0.33	0.13
Manufacturer	In-house	Chemagen AG, Baesweiler, Germany

Determination of particle settling densities

For the estimation of the settling densities of superparamagnetic adsorbent particles under the influence of strong magnetic field gradients, 1 L of each particle suspension (10 g L^{-1}) was poured into an Imhoff funnel. Thereafter, the lower end (deepest point of particle settlement) of the Imhoff funnel was placed in the room temperature bore of a superconducting magnet (Cryogenics Ltd., UK), 1.5 cm above the plane of the strongest field. The magnet was operated at a field of 4.0 T in its centre, giving a field of ~2 T and a field gradient of 40 T m^{-1} pointing in the direction of gravity within the

region where the particles settle. After settling had taken place and a stationary state was reached, the sediment density under the influence of the magnetic field was determined by dividing the introduced particle mass by the sediment volume.

3.2.3 Capacity data Conversion

In the course of developing a mathematical model for predicting filter capacities under a given set of operating conditions one has to clearly distinguish between the 'working capacity' of a filter for particles and its 'maximum capacity'. As stated in the introduction, large adsorbent particle losses cannot be tolerated in biotechnological applications, and it is for this reason that we define the 'working capacity' of the filter as the particle loading per unit filter volume attained when the exit particle concentration reaches just 5 % breakthrough. However, although these working capacities can be determined experimentally, the mathematical model developed here assumes, as a starting point, a homogeneous maximum particle build-up throughout the filter corresponding to the maximum filter capacity. In the first instance, therefore, it was necessary for us to find a mathematical relationship, allowing the inter-conversion of working and maximum capacities into one another.

From general studies with other types of deep filters (Herzig, 1970; Franz, 1997) it is known that the breakthrough, c/c_0, at the end of an HGMS filter can be described by:

$$\frac{c}{c_0} = \frac{\exp{(\sigma_S^{-1} c_0 v_0 \lambda_0 \tau)}}{\exp{(\sigma_S^{-1} c_0 v_0 \lambda_0 \tau)} + \exp{(\lambda_0 L_F)} - 1} \qquad \text{(Eq. 3.1)}$$

where c_0 and c are respectively the particle concentrations of the suspension entering and leaving the filter, σ_S is the saturation or maximum capacity of the filter, v_0 is the liquid velocity in the filter, λ_0 is the filter coefficient of the unloaded filter, and τ is the displacement filter time, which equals the filtration time, t, minus the time, t_F, the suspension needs to cover the filter length, L_F. Transformation of equation 3.1 with respect to t gives:

$$t = t_F + \ln\left(\exp\left((\lambda_0 L_F) - 1 \right) / \left(\frac{c_0}{c} - 1 \right) \right) \cdot \frac{\sigma_S}{c_0 v_0 \lambda_0} \qquad \text{(Eq. 3.2)}$$

Equation 3.2 describes the time that the filter will theoretically need to run before an effluent particle concentration of c is reached. A theoretical breakthrough time, t_B, (100 % breakthrough) can additionally be defined by:

$$t_B = \left((\sigma_S L_F) / (v_0 c_0) \right) + t_F \qquad \text{(Eq. 3.3)}$$

In equation 3.3, t_B is the time elapsed before the particle amount entering the filter matches the maximal amount of particles that can be retained within it. On the assumption that the particles are completely retained by the filter, the utilization fraction, U_F (i.e. the actual filter capacity, σ, divided by the maximal filter capacity, σ_S), to which the maximum filter loading is reached corresponds to the ratio of filtration time to the time of theoretical breakthrough:

$$U_F = \frac{\sigma}{\sigma_S} = \frac{t}{t_B} = \frac{t_F + \ln\left(\exp\left((\lambda_0 L_F) - 1 \right) / \left(\frac{c_0}{c} - 1 \right) \right) \cdot \frac{\sigma_S}{c_0 v_0 \lambda_0}}{\left((\sigma_S L_F) / (v_0 c_0) \right) + t_F} \qquad \text{(Eq. 3.4)}$$

If the feed concentration, c_0, is not too high ($c_0 \ll \sigma_S$), the term t_F can be considered to be negligible, and thus equation 3.4 becomes:

$$U_F = \frac{1}{\lambda_0 L_F} \ln\left(\exp\left((\lambda_0 L_F) - 1 \right) / \left(\frac{c_0}{c} - 1 \right) \right) \qquad \text{(Eq. 3.5)}$$

where U_F is only dependent on the normalized particle concentration in the effluent, c/c_0, and the dimensionless product, $\lambda_0 L_F$. The fraction to which the maximum filter capacity is used at the moment when an effluent concentration of c/c_0 is attained, is given by the equation 3.5. Thus the mathematical relationship between the working capacity at 5 % breakthrough and the maximum capacity can be expressed as:

$$\sigma_{5\%} = U_{F,5\%} \cdot \sigma_S \qquad\qquad \text{(Eq. 3.6)}$$

In equation 3.5 λ_0 is dependent on the filter wire's particle capture radius, R_{ca}, the filling factor, F_v (ratio of collecting wire volume to filter cassette volume), a geometry coefficient, f_M, and the wire radius, a. In HGMS literature, analytical approximations can be found which allow the calculation of λ_0 in the hydrodynamic flow regime to be applied (see appendix 3-A).

3.3 Results and Discussion

Table 3.3 presents the filter capacities determined at 5 % breakthrough for the eighteen combinations of adsorbent particle and filter matrix together with values for the porosity of the nine different filters.

Table 3.3 Filter capacities σ (5 % breakthrough) and porosities.

Matrix	PGF beads capacity (g L^{-1} filter)	M-PVA beads capacity (g L^{-1} filter)	Filter porosity (%)
Aa	72	279	86.1
Ba	90	281	85.8
Ca	140	311	80.9
Ab	93	291	86.5
Bb	87	315	86.2
Cb	125	291	82.7
Db	137	374	81.5
Bc	100	305	87.1
Cc	100	359	83.1

Analysis of the data reveals the following: First, the working particle holding capacities of the different filters are typically three to four fold higher for the M-PVA *cf.* the PGF beads. Second it can be seen that, for the same filter elements, but with decreasing spacer sizes, the working capacities increase regardless of particle type (compare for example Aa, Ba and Ca). Third, there is no obvious relationship between matrices with a constant spacer size, but different filter elements.

In an attempt to develop a clearer picture, one first needs to distinguish between influences on the maximum filter capacity and those due to the interplay between the

short length of the experimental filter employed and the loading profile developing within it. As was shown earlier in section 3.2.3, this can be done by using equation 3.6. The experimental maximum filter capacities $\sigma_{S,exp}$ can be calculated (see Table 3.4) simply by dividing the measured 5 % breakthrough filter capacities by the respective fractions to which their maximum filter capacities are utilized.

Next, the influence of the total number of filter elements must be accounted for. This cannot be done by simply dividing the maximum filter capacities by the number of filter elements, given that the capacity is defined for a hypothetical matrix of 1 L volume, whereas the actual number of filter elements corresponds to the much smaller 'real' matrix. In order to obtain a reasonable definition of the loading of a single filter element the latter must be defined by the surface area of the wire elements.

Table 3.4 Maximum filter capacities $\sigma_{S,EXP}$.

Matrix	PGF beads capacity (g L^{-1} filter)	M-PVA beads capacity (g L^{-1} filter)
Aa	260	431
Ba	225	398
Ca	218	377
Ab	189	398
Bb	150	405
Cb	173	341
Db	170	417
Bc	120	340
Cc	109	379

Accordingly therefore, the maximum filter capacities are first multiplied by the filter volume to give an absolute mass of particles. This particle mass is then divided by the number of filter elements and the filter element area, yielding the surface loadings (Table 3.5) of single filter elements for each matrix and particle type.

Assuming unhindered particle deposition, it would be expected that the filter element types a, b, and c would have constant surface loadings independent of spacer diameter. Inspection of table 3.5 shows that this is clearly not the case. In fact, the influence of the spacer employed, on the achievable surface loading of a given filter element, is sufficiently strong to prevent particle build-up for a given element from

achieving its maximum theoretical size, presumably by hindering growth from opposed filter elements.

Table 3.5 Surface loadings of single filter elements.

Matrix	PGF beads surface loading (g m^{-2})	M-PVA beads surface loading (g m^{-2})
Aa	520	862
Ba	376	664
Ca	218	238
Ab	379	794
Bb	250	675
Cb	192	379
Db	130	321
Bc	172	487
Cc	78	270

A very simplified model of the geometry and restrictions of the particle build-up is presented in figure 3.2. Here, we assume a layer of particle build-up growing into the free space between the filter elements formed by the spacers. The thickness of the spacer corresponds to two spacer wire diameters. This space is, however, infiltrated by two expanding particle build-up layers growing in opposite directions and the maximum expansion possible for each layer equates to one spacer wire diameter d_s. As the magnetic field is perpendicular to the filter element plane, no build-up is allowed within the region occupied by the filter element itself. The latter assumption does not take account of the sinusoidal-like tracking of the wires of the filter elements.
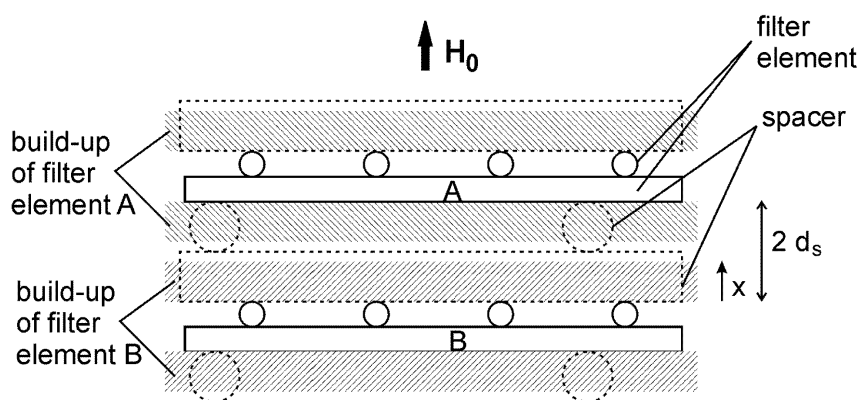
Fig. 3.2 Simplified model of the geometry and restrictions of the particle build-up.

Given the complexity illustrated by the above schematic model (Fig. 3.2), predicting the influence of spacer size on filter capacity is clearly a difficult task. On the one hand, reducing the spacer diameter will allow more filter elements to be used within the cassette, which in turn should result in an increased magnetic particle holding capacity. On the other hand, however, small spacer diameters will lead to a greater degree of overlapping of the potential particle deposit areas, resulting in reduced filter capacities. It is likely, therefore, that there is an optimum spacer size, given that in our simplified model the absence of a spacer would result in having no available build-up space and therefore zero capacity. However, given that the particle build-up density decreases with increasing distance away from the wire, making the spacer size too large will ultimately lead to a reduction in particle holding capacity.

As a pre-requisite to estimating the optimum spacer size, a quantitative description of the local particle build-up density must first be found. This can be accomplished by plotting the achieved area-related build-up masses, m_A, against the diameter of the spacer wires employed, the latter being synonymous with the maximum degree of expansion of particle build-up allowed. According to the schematic model shown in figure 3.2 each filter element forms two build-up layers, and the combined surface loadings for these two layers yields the values shown in table 3.5. To examine the density of particle build-up requires that one only needs to consider one of these layers, and so the values in table 3.5 should be halved. Figure 3.3 shows how m_A values for the different combinations of filter element and particle type vary as a function of expansion of particle build-up.

Calculated trends of m_A can be obtained from the empirical correlation:

$$m_A = m_{A\max}\, x/(K + x) \tag{Eq. 3.7}$$

where x is the allowable expansion of particle build-up perpendicular to the filter element plane (Fig. 3.2), $m_{A\max}$ is the maximum area related build-up mass which can be reached for sterically unhindered particle collection, and K is a parameter describing the attainment of maximum build-up, having the same dimensions as x.
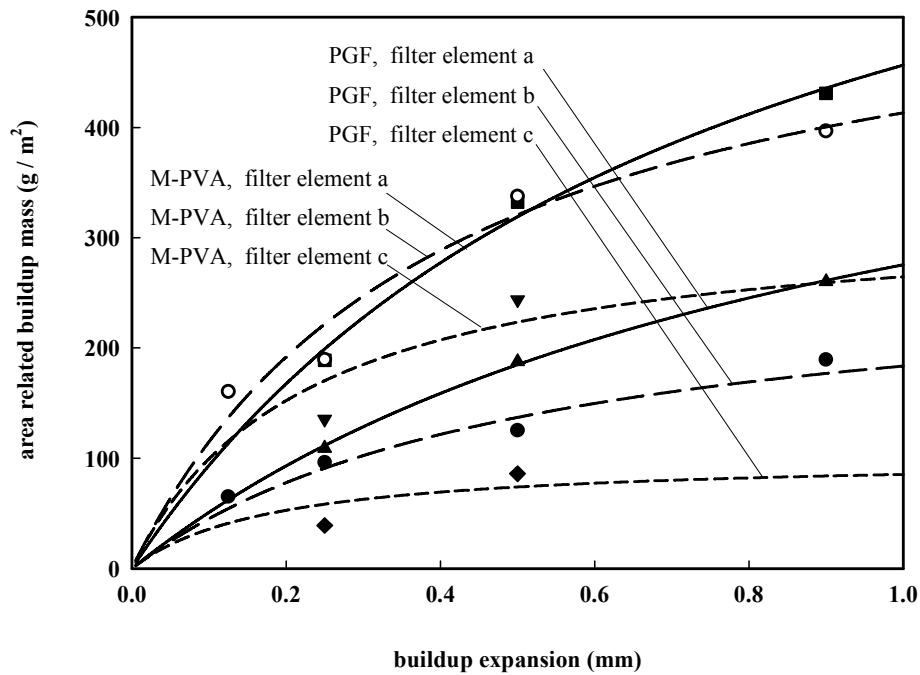
Fig. 3.3 Variation of area related build-up masses (m_A) with expansion of particle build-up (PGF: filter element ▲=a, ●=b, ◆=c; M-PVA: filter element ■=a, ○=b, ▼=c) and correlation (Eq. 3.7).

The meaning of K becomes clear from the observation that when an expansion of x allowed by the spacer equals K, the area-related build-up mass reaches half of its maximum value (i.e. $m_A = \frac{1}{2} \cdot m_{Amax}$).

In order to find the values of the parameters m_{Amax} and K for the different filter element and particle types, least square fits were conducted using the software TableCurve^{TM}2Dv3 (Systat Software Inc., USA). For the filter element types a and b this could be done directly, but in the case of filter element type c an additional assumption had to be made, given the limited number of experimental data points available (see appendix 3-B). The resulting correlation parameters are summarized in table 3.6.

Table 3.6 Fitting parameters for equation 3.7

Matrix	PGF K (mm)	PGF m_{Amax} (g m^{-2})	M-PVA K (mm)	M-PVA m_{Amax} (g m^{-2})
a	0.959	540	0.758	802
b	0.514	278	0.406	581
c	0.182	101	0.226	324

On inspection of figure 3.3 and equation 3.7 it becomes obvious that the differential increase in the area related build-up mass, dm_A, with respect to a differential increase in the expansion of particle build-up, dx, is proportional to the local build-up density, $\rho(x)$. This interrelationship can be described by:

$$\frac{dm_A(x)}{dx} = \rho(x)$$

(Eq. 3.8)

With the aid of equations 3.7 and 3.8 it is possible to find a relationship describing the local build-up density that we had initially aimed to find:

$$\rho(x) = m_{A\max} K / (K + x)^2$$

(Eq. 3.9)

Using the above equation together with the parameters listed in table 3.6, density build-up profiles are derived as a function of distance away from the wire filter element surfaces (see Fig. 3.4).
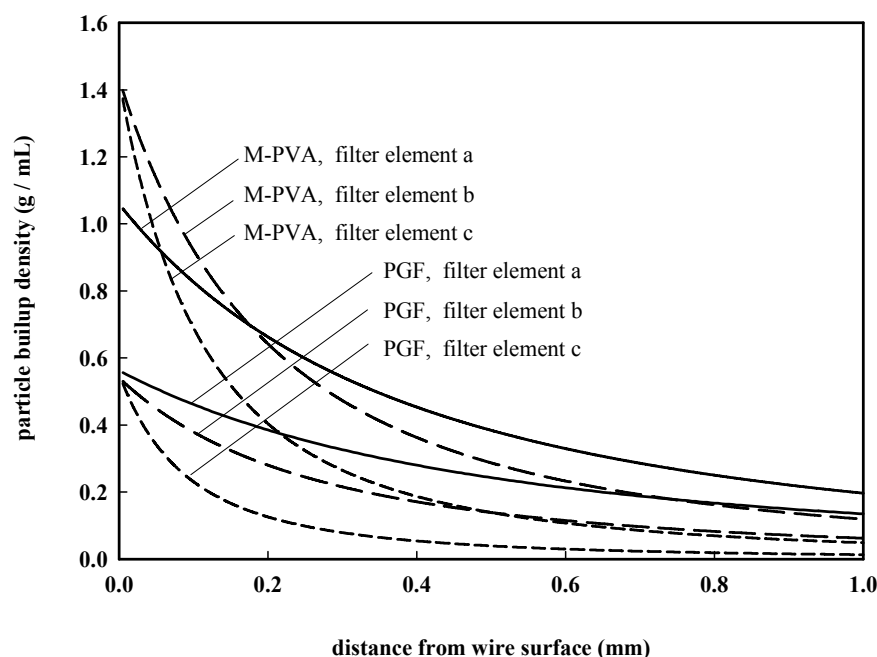
Fig. 3.4 Particle build-up densities (from equation 3.9) as a function of the distance away from the wire surface for all combinations of particles and spacer elements employed.

Although the derivation of equation 3.9 required that several approximations and simplifying assumptions were made, to our knowledge this is the first time that density variations in the build-up regions have been both experimentally and theoretically described. Close inspection of the build-up density plots illustrated in figure 3.4 reveals a number of interesting observations that merit attention: (i) The maximum build-up densities next to the wire surface are 1.4 g mL^{-1} and 0.55 g mL^{-1} for M-PVA and PGF particles, respectively. The value for M-PVA is identical to the theoretically calculated maximum build-up density based on the assumption of monodisperse spherical particles arranged in a hexagonal closed packed structure. Comparison of the observed (0.55 g mL^{-1}) and theoretical (2.2 g mL^{-1}) maximum build-up densities for the PGF particles indicates less dense packing of this material. This observation can be understood given the PGF particles' irregular shape, and, as we will show later (see Table 3.7), the PGF particles possess a reduced tendency to form compact sediments.

(ii) For a given particle type, the observed maximum build-up densities at the wire's surface appear to be roughly similar regardless of the filter element employed. That

102

said, the lower packing density observed for M-PVA on filter element 'a' probably reflects the latter's larger wire diameter (Table 3.3, 315 µm), which results in reduced gradients and consequently lower magnetic forces compared to the narrower wire diameters of elements 'b' (250 µm) and 'c' (90 µm). It should be noted that the compliance of the maximum build-up densities for different filter element types is not inherent in correlation 3.9. Indeed, the maximum build-up density is influenced by both fitting parameters forming the limit value:

$$\rho\big|_{x \to 0} = \frac{m_{A\,\max}}{K}$$

(Eq. 3.10)

(iii) The magnetic field distortion of thick wires stretches further out than that of thin wires. This effect can be easily be appreciated in figure 3.4, where the slopes of build-up density vs. distance away from the wire steepen as the wire diameter of the filter elements is reduced.

In summary, it would appear that the density trends described by equation 3.9 are entirely consistent with physical restrictions and HGMS theory, and may form the basis of a useful tool for optimizing matrix design. If the parameters $m_{A\max}$ and K for a given particle/filter element combination are known, then the maximum filter capacities of matrices formed by this filter element and different spacers can be predicted from the following equation:

(Eq. 3.11)

$$\sigma_{S,th} = \frac{m_A}{d_s + d_{fc}} = \frac{m_{A\,\max} \cdot \dfrac{d_s}{K + d_s}}{d_s + d_{fc}}$$

where d_S and d_{fc} are the wire diameters of the spacer and filter elements respectively. This above equation can be simply understood from the fact that in order to achieve an area-related build-up mass of m_A in a matrix, a distance of $d_S + d_{fc}$ will be required. Equation 3.11 can be used to find the theoretical optimum of the spacer wire diameter for a given particle/filter element combination. To illustrate this, figure 3.5 confirms

103

the existence of a distinct optimum spacer wire diameter (corresponding to 1-2 times the filter element wire diameters) delivering a theoretical maximum filter capacity.
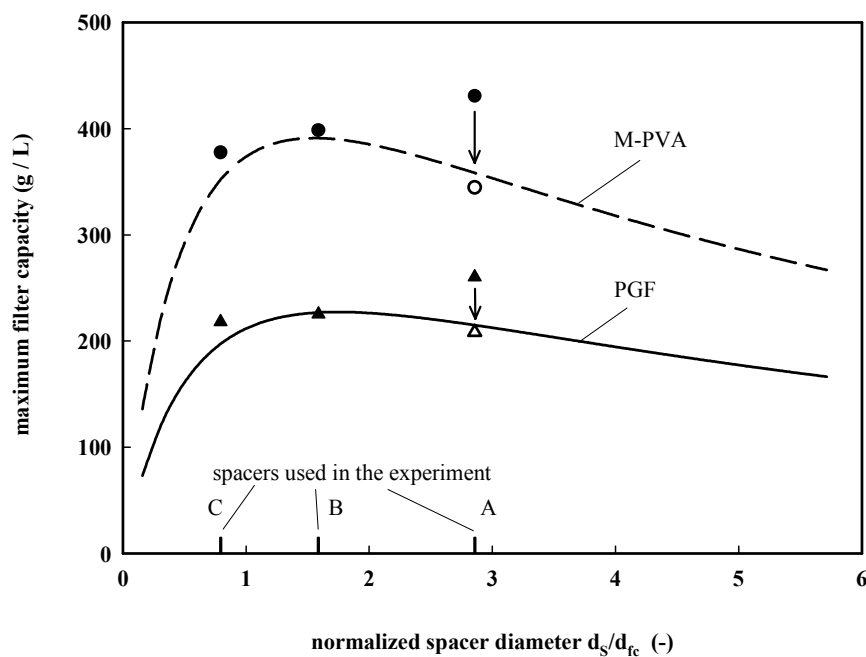
Fig. 3.5 Maximum filter capacity for filter element 'a' as a function of normalized spacer diameter. The lines represent the fit of the theoretical model (Eq. 3.11). Experimental data are indicated by the filled symbols (M-PVA, ●; PGF, ▲) and corrected values (see text) by the open symbols (M-PVA, ○; PGF, △).

Whereas the experimental values obtained with spacers B and C and both particle types are in good accord with the theoretical line, there appears to be considerable deviation for the data sets involving spacer A. This is probably because the packing of the small filter cassettes employed does not always fit the assumption inherent in equation 3.11 - that an equal number of spacer and filter element elements is used. This assumption fits for the spacer/filter element combinations Ba (6+6) and Ca (10+10), but not for combination Aa (4+5). For Aa, five filter elements could be inserted in the cassette, even though the 'theoretical' thickness of a combination of spacer 'A' and filter element 'a' ($2d_S + 2d_{fc}$) comes to 2.4 mm, indicating that only

four filter element layers should fit in a 10 mm wide cassette[1]. Given that equation 3.11 assumes just four of filter elements (*cf.* the five actually present in the Aa combination), a simple correction of the capacity values by a factor of 4/5 was deemed appropriate. This resulted in a surprisingly good fit of the data points (Fig. 3.5, open symbols) to the theoretical curves for both particle types. In most practical cases however, where filter matrices are likely to comprise large numbers of spacer and filter elements, the need for any correction of mismatch in the number of spacers vs. filter elements will be unnecessary.

It should be noted that the good quantitative agreement visible in figure 3.5 is simply because experimental values were used to determine the parameters of equation 3.7. The main benefit of the derivations described above is given by the novel possibility of being able to describe the effect of variations in matrix composition upon capacity with a set of just two parameters. Indeed, close inspection of table 3.6 reveals that for most practical purposes only one parameter (m_{Amax}) may suffice given that the value of K appears, at least to a first approximation, to correspond to twice the filter element wire diameter ($2 \cdot d_{fc}$). This relationship is not surprising given that a wire's diameter influences the steepness of decline in field gradient within its vicinity. Further, the gradient of field decay directly influences the distance (extending from the wire's surface) of maximum particle build-up. The latter effect is also described by the parameter K. In summary, it can be said that the procedure of conducting a number of systematic breakthrough experiments with filter matrices composed of different spacer/filter elements provides deep insight into particle build-up at the wires within HGMS filters. A correlation describing the local build-up density has been found which ultimately enables an optimum spacer size to be calculated. Disadvantages of the approach detailed above are that it is laborious and slow. Accordingly, towards the end of this paper we additionally introduce a simple procedure, which allows educated guesses of the working filter capacities of different matrices to be made.

---

[1] The reason for this is that the wire mesh is rolled during the manufacturing and therefore, although the wires have to cross in the mesh, the mesh thickness is actually slightly less than two wire diameters.

In section 3.2.2 we described settling experiments in which suspensions of M-PVA and PGF particles were poured into Imhoff funnels which were subsequently positioned within the heterogeneous field region of a superconducting magnet. Table 3.7 presents measured sediment densities after 24 h of settling under gravity, and following an additional 1 h under the influence of an applied magnetic field.

Table 3.7 Particle sediment densities measured in an imhoff funnel.

	PGF		M-PVA	
	24 h under gravity	24 h under g + 1h in magnet	24 h under gravity	24 h under g + 1h in magnet
Density (g mL^{-1})	0.109	0.217	0.303	0.370

Clearly, comparison of the magnetic conditions employed here with those experienced in the vicinity of a wire surface in an HGMS indicates that even a superconductor is unable to generate field gradients of the same order of magnitude as those produced in an HGMS. However, it is known from centrifugation, that after a certain point of compaction is reached, any additional increase of centrifugal force only results in minor further compaction. Accordingly, in the present context, the simple experiment described above has been used to provide a lower limit to how settled assemblies of the beads can be compacted by the influence of magnetic forces in an HGMS.

The particle sediment densities under the influence of a magnet observed above provide a first approximation of the average build-up densities that can be expected within the filter matrix. Given the comparatively low field gradient used in the above settling experiments (*cf.* that existing within the magnetized filter matrices), the actual particle build-up densities within the filter are likely to be higher than those listed in table 3.7. Additionally, it should be noted that the density values obtained from sedimentation experiments solely reflect the M-PVA and PGF particle properties (e.g. particle–particle interactions) in the absence of any possible influences arising from the separation matrix.

Nevertheless, when used in combination with the filter matrix porosities ε_F and utilization fractions, these settling density values allow an estimation of the expected working filter capacities:

$$\sigma_{approx} = U_F \cdot \varepsilon_F \cdot \rho_{approx} \qquad \text{(Eq. 3.12)}$$

In the approximation (Eq. 3.12), the tendency for the particle sediment densities to be lower than the actual build-up density within the filter matrix is partially offset by the inherent use of the whole free matrix space for the capacity calculation. Figure 3.6 shows the resulting comparisons of predicted and measured capacities at 5 % breakthrough for both particle types and all matrices. For the PGF particles, the approximation predicts the measured working capacities remarkably well; only the capacities for filter element c were over-predicted. In the case of M-PVA particles, all predicted capacities underestimate the measured values by up to 25 %.
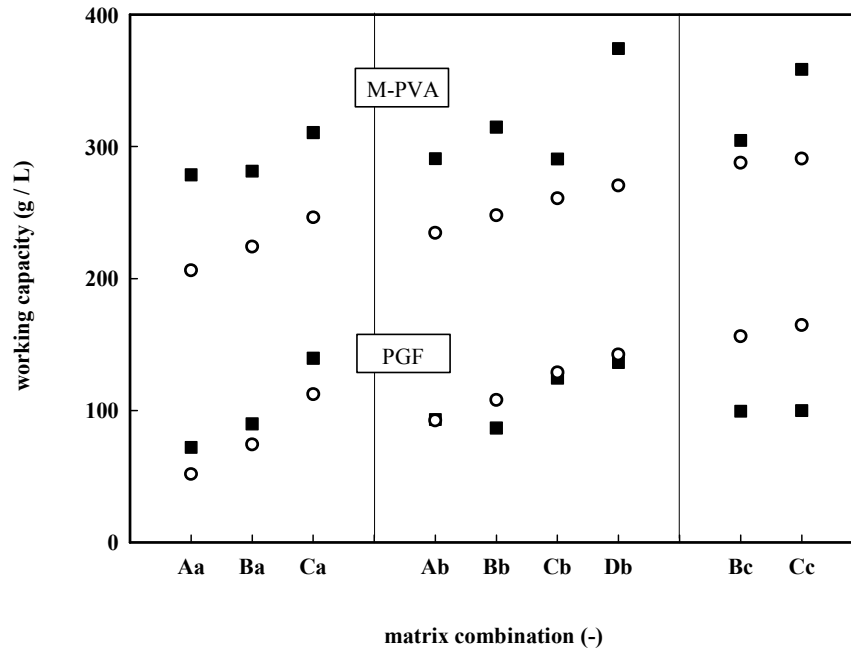
Fig. 3.6 Comparison of predicted (○) and measured (■) capacities at 5 % breakthrough for both particle types and all employed matrices.

3.4 Conclusions

In this work two methods have been presented which allow estimation of HGMS matrix capacities for magnetic particles. The first of these requires more effort and results in correlations for particle build-up densities and maximum filter capacities, whereas the second is simpler and takes into account particle agglomeration and compaction.

The premise for the applicability of both models is of HGMS operation in a regime where the maximum achievable capacity is primarily dominated by the available space and the ability of the particles to form dense build-ups. Thus, the consideration of interparticular interactions is much more important for the success of the predictions than e.g. trying to solve force balances between magnetic and hydrodynamic forces within the matrix. Clearly such a premise cannot be applied to all HGMS applications, but it definitely holds for emerging applications employing magnetic microsorbents in biotechnology, where the prevention of particle loss and the maximization of filter capacity are especially crucial.

Appendix 3-A

In order to determine the utilization fractions U_F, only transversely oriented wires (i.e. perpendicular to the magnetic field and flow) within the filter elements are considered, as these are primarily responsible for particle capture and therefore determining a given filter's capacity. Based on this assumption the initial performance of the filter may be written as (Gerber and Birss, 1983):

$$\frac{c}{c_0} = \exp(-f_{M,T} \cdot F_{V,T} \cdot R_{ca} \cdot \frac{L_F}{a})$$

(Eq. 3.13)

Rearrangement of equation 3.1 for the initial filter performance at $\tau = 0$ and comparison with equation 3.13 gives the following expression for the filter coefficient λ_0:

$$\lambda_0 = \frac{f_{M,T} \cdot F_{V,T} \cdot R_{ca}}{a}$$

(Eq. 3.14)

In their search for the value of the coefficient $f_{M,T}$ in transverse filters, Gerber and Birss (1983) state two extreme cases. In the first, for ordered isolated wires in transverse orientation, theory yields a value for $f_{M,T}$ equal to $2/\pi$. In the second case, of a totally random wire orientation with the field being perpendicular to the flow, a value for $f_{M,T}$ of 0.12 can be found. A filter mesh with a sinusoidal-like arrangement of wires, having angles between the wire axis and the field of approximately 45° to 90°, lies somewhere between the above extremes. Given the absence of an exact value for $f_{M,T}$ in the above case, we selected an intermediate value of $1/\pi$ (lying midway between $2/\pi$ and 0.12).

$F_{V,T}$ is the volume fraction of the transverse filter element wires. Values of $F_{V,T}$ and of the wire radii are shown in table 3.8 and 3.1, respectively. R_{ca} is the normalized particle capture radius and, following Gerber and Birss (1983), can be calculated from the expression:

$$R_{ca} \approx \frac{3}{4} \sqrt{3} \left(\frac{v_m}{v_0} \right)^{\frac{1}{3}} \left[1 - \frac{2}{3} \left(\frac{v_m}{v_0} \right)^{-\frac{2}{3}} \right]$$

(Eq. 3.15)

where v_0 is the filter velocity, and v_m is the so-called magnetic velocity. In the case of strongly magnetic particles, the magnetic velocity, v_m, may be written as (Watson, 1973):

$$v_m = \frac{2 \cdot \mu_0 \cdot M_W \cdot M_P \cdot b^2}{9 \cdot \eta \cdot a}$$

(Eq. 3.16)

where μ_0 is the magnetic field constant ($4\pi \cdot 10^{-7}$ V s A^{-1} m^{-1}), a is the wire radius, b is the particle radius (see Table 3.2), η is the dynamic viscosity (set to $1.002 \cdot 10^{-3}$ Pa s), and M_W and M_P are the magnetization of the wire and of the particles, respectively.

Table 3.8 Filter coefficients, dimensionless product $\lambda_0 L_F$ and filter capacity utilization for the filter matrices used.

Matrix	$F_{V,T}(\%)$	PGF			M-PVA		
		$\lambda_0\,(\text{m}^{-1})$	$\lambda_0 L_F\,(-)$	$U_F\,(\%)$	$\lambda_0\,(\text{m}^{-1})$	$\lambda_0 L_F\,(-)$	$U_F\,(\%)$
Aa	2.9	51.2	4.1	27.7	104.3	8.3	64.7
Ba	3.4	61.4	4.9	39.9	125.1	10.0	70.6
Ca	5.7	102.3	8.2	64.0	208.5	16.7	82.3
Ab	2.7	72.5	5.8	49.2	137.7	11.0	73.3
Bb	3.2	87.0	7.0	57.7	165.3	13.2	77.7
Cb	4.8	130.5	10.4	71.8	248.0	19.8	85.2
Db	6.9	188.5	15.1	80.5	358.1	28.7	89.7
Bc	1.5	211.7	16.9	82.6	342.9	27.4	89.3
Cc	3.1	423.2	33.9	91.3	685.5	54.8	94.6

At the given field strength, H_0, of $2.6 \cdot 10^5$ A m^{-1}, M_w was determined as $3.67 \cdot 10^5$ A m^{-1}, and M_P values for the M-PVA and PGF particles were $7.0 \cdot 10^4$ A m^{-1} and $1.2 \cdot 10^5$ A m^{-1} respectively. The theoretical filter capacity utilization fractions, U_F, at 5 % breakthrough for all filter matrices and both particle types, are given in table 3.8.

Appendix 3-B

Filter element type c was used in combination with only two of the four available spacer types (i.e. A, B, C & D) to form the matrices Bc and Cc, and consequently only two capacity values were obtained experimentally. In order to obtain reasonably reliable values of the parameters m_{Amax} and K for filter element c with this limited data set, an additional assumption was introduced in this particular case. In section 3.3 we argued that for the same type of particles, a roughly constant build-up density is achieved at the wire's immediate surface, independent of its diameter, given that the magnetic force generated will always be strong enough to compact the particle build-up up to its maximum value. This assumption is especially valid in the above case given higher field gradients existing around narrower wires in filter element c *cf.* for example filter element b. Expressing this assumption as an equation we get:

$$\frac{K_c}{m_{A\max,c}} = \frac{K_b}{m_{A\max,b}} \qquad\text{(Eq. 3.17)}$$

Combining equations 3.17 and 3.7 gives an expression for the area-related build-up mass of filter element c with only one remaining fitting parameter $m_{A\max,c}$:

$$m_{A,c} = \frac{m_{A\max,c} \cdot x}{\dfrac{K_b}{m_{A\max,b}} \cdot m_{A\max,c} + x}$$

(Eq. 3.18)

This parameter was obtained from the experimental data using by a least square method employing TableCurve^{TM} 2Dv3, Systat Software Inc., USA. Thereafter, K values for filter element c (cited in Table 3.6) where calculated with the aid of equation 3.17.

Acknowledgments

References

Ferré, H. (2005) Development of novel processes for continuous protein refolding and primary recovery - A case study on the major histocompatibility complex class I receptor and its individual subunits. Ph.D. Thesis. Technical University of Denmark, Denmark.

Franz, M. (1997) Entwicklung und experimentelle ueberprüfung eines modells der magnetische filtration von magnetithaltigen schwermetall-hydroxiden. Ph.D. Thesis. University of Karlsruhe, Germany.

Friedlaender, F.J., Takayasu, M., Rettig, J.B., Kentzer, C.P. (1978) Particle flow and collection process in single wire HGMS studies. *IEEE Trans. Magn.*, Mag-14(6), 1158-1164.

Gerber, R., Birss, R.R. (1983) *High gradient magnetic separation*. Research Studies Press, UK.

Gomes, C.S.G., Heebøll-Nielsen, A., Petersen, T.L., Thomas, O.R.T., Hobley, T.J. (2006) Control of protein hydrolysis in unclarified liquors: application of high-gradient magnetic fishing (HGMF) employing improved magnetic adsorbents. *Chapter 5*.

Heebøll-Nielsen, A., Choe, W.S., Middelberg, A.P.J., Thomas, O. R.T. (2003) Efficient inclusion body processing using chemical extraction and high-gradient magnetic fishing. *Biotechnol. Progr.*, 19(3), 887-898.

Heebøll-Nielsen, A., Dalkiær, M., Hubbuch, J.J., Thomas, O.R.T. (2004) Superparamagnetic adsorbents for high-gradient magnetic fishing of lectins out of legume extracts. *Biotechnol. Bioeng.,* 87(3), 311-32.

Heebøll-Nielsen, A., Justesen, S.F.L., Hobley, T.J., Thomas, O.R.T. (2004) Superparamagnetic cation-exchange adsorbents for bioproduct recovery from crude process liquors by high-gradient magnetic fishing. *Sep. Sci. Technol.,* 39(12), 2891-2914.

Herzig, J.P., Leclerc, D.M., Le Goff, P (1970) Flow of suspensions through porous media. *Ind. Eng. Chem.*, 62(5), 8-35.

Hoffmann, C., Franzreb, M., Höll, W.H. (2002) A novel high-gradient magnetic separator (HGMS) design for biotech applications. *IEEE Trans. Appl. Supercond.*, 12(1), 963- 966.

Hubbuch, J.J., Matthiesen, D.B., Hobley, T.J., Thomas O.R.T. (2001) High gradient magnetic separation versus expanded bed adsorption: A first principle comparison. *Bioseparation*, 10, 99-112.

Hubbuch, J.J., Thomas, O.R.T. (2002) High-gradient magnetic affinity separation of trypsin from crude porcine pancreatin. *Biotechnol. Bioeng.*, 79, 301-313.

Leitermann, W., Friedlaender, F.J., Gerber, R., Hwang, J.Y., Emory, B.B. (1984) Collection of micron-sized particles at high velocities in HGMS. *IEEE Tran. Magn.*, Mag-20(5), 1174-1176.

Meyer, A., Hansen, D.B., Gomes, C.S.G., Hobley, T.J., Thomas, O.R.T., Franzreb, M. (2005) Demonstration of a strategy for product purification by high-gradient magnetic fishing: Recovery of superoxide dismutase from unconditioned whey. *Biotechnol. Progr.*, 21, 244-254.

O'Brien, S.M., Thomas, O.R.T., Dunnill, P. (1996) Non-porous magnetic chelator supports for protein recovery by immobilised metal affinity adsorption. *J. Biotechnol.*, 50, 13-25.

Svoboda, J. (1987) Magnetic methods for the treatment of minerals. *Developments in Mineral Processing* (Ed. Fuerstenau, D.W.), 8, Elsevier Sci. Publ. Co., Amsterdam.

Takayasu, M., Gerber, R., Friedlaender, F.J. (1983) The collection of strongly magnetic particles in HGMS. *J. Magn. Magn. Mater.*, 40, 204-214.

Watson, J.H.P. (1973) Magnetic filtration. *J. Appl. Phys.*, 44(9), 4209-4213.

4. Protein purification using High Gradient Magnetic Fishing: Impact of Magnetic Filter Performance

Cláudia S.G. Gomes[1], Niklas A. Ebner[2], Owen R.T. Thomas[1,3], Matthias Franzreb[2] and Timothy J. Hobley[1]

[1] Center for Microbial Biotechnology, Technical University of Denmark, 2800 Lyngby, Denmark.

[2] Institute for Technical Chemistry, Water- and Geotechnology Division, Forschungszentrum Karlsruhe GmbH, 76344 Eggenstein-Leopoldshafen, Germany.

[3] Department of Chemical Engineering, The University of Birmingham, Edgbaston, Birmingham B15 2TT, United Kingdom.

Abstract

High gradient magnetic separation employing derivatised magnetic adsorbents offers the potential for rapid processing of large volumes of crude bioprocess feedstreams. This technology is now known as high-gradient magnetic fishing (HGMF). The best way to approach large scale magnetic filter based bioprocessing is possibly a strategy employing a cycle of loaded adsorbent capture, wash and elution, which is repeated many times. Thus, adsorbent capture and release from the filter must be efficient. In this work we examine multicycle processing using magnetic filters. Studies using a biotech friendly magnetic filter containing different combinations of matrices with well-defined wire orientations were conducted in a 40-ml cassette using immobilised metal affinity adsorbents constructed from two types of magnetic particle, PGF (polyglutaraldehyde ferrite) and PVA (polyvinyl-alcohol ferrite). Ultimately, one filter was selected and tested for the purification of lactoperoxidase from crude cheese whey using cation exchange magnetic adsorbents. The HGMF system was operated in a controlled multicycle processing mode at a scale of 0.8 L of whey/cycle, permitting an evaluation of the impact of filter performance on the yield of the target protein.

4.1 Introduction

High-gradient magnetic fishing (HGMF) is a technique used for the recovery of biological macromolecules that employs functionalized magnetic adsorbents and a magnetic filter. This integrated process consists of a batch binding step with the adsorbents followed by their collection using high-gradient magnetic separation (HGMS) (Hubbuch and Thomas, 2002). The magnetic support capacity of high-gradient magnetic filters is recognised as a crucial parameter in HGMS-based processes (Svoboda, 1987). However, in despite of this, it has not been given much attention. Some of the few exceptions are the work of Nesset and Finch (1981), and more recently, the work of Ebner *et al.* (2006). Even less attention has been given to release of magnetic particles from a magnetic filter. Potential release in an industrial application of HGMF or HGMS is likely to be of importance since it will determine the real working capacity of a filter when operated in a multicycle mode. Support remaining in the filter after a cycle will reduce the amount that can be loaded in the following cycles and might also lead to the need for filter disassembly and cleaning after only a few cycles.

In the treatment of industrial slurries, one of the traditional applications of HGMS, poor flushing of magnetic matrices is a serious problem, not only because it affects the performance of the filter over a series of cycles but also because it often culminates in clogging. Clogging of magnetic filters results in costly shut-down periods for cleaning or replacement of the matrix (Svoboda, 1987). This issue has been mainly dealt with on a problem-solving basis. That said, a few authors, namely Svoboda and Corrans (1985) and Reffle *et al.* (1979), have specifically addressed this problem, with the former having developed a model based on the Derjaguin-Landau-Verwey-Overbeek (DLVO) theory. Svoboda and Corrans (1985) conclude that adjustment of hydrodynamic conditions is not sufficient to ensure complete removal of particles captured on magnetic filters and argue that changing the conditions that affect particle-wire interactions will ensure removal of particles from stagnant areas. In fact they show that pH has a high impact on particle release. However, changing solution conditions is not an option when using magnetic filters for bioprocessing

since those conditions are determined by other factors, such as the interaction between magnetic adsorbents and biological molecules.

The application of HGMS to biotechnology should not encounter many of the problems that occur in industrial slurry treatment – for example, the magnetic material (the adsorbents) used in biotechnology is produced in controlled conditions and is therefore more homogeneous in terms of size, shape, magnetic and surface properties, in contrast to the assortment of materials that HGMS has to face in its conventional applications. Nevertheless there is a need for good filter performance in bioprocessing and a different set of problems can be foreseen. The high cost of the magnetic material, that in this case is not a waste and needs to be re-used for a large number of cycles, and also the significant value of the products from such processes, demand high degree of recovery from the magnetic filters. Furthermore, efficient cleaning in place is a mandatory requirement for any technique used in bioprocessing. In this work we present results from filter screening tests with respect to adsorbent capture and release, and discuss the impact of filter flushing efficiency on HGMF processing for biotechnological applications.

4.2 Materials and methods

4.2.1 Materials

Magnetic (stainless steel 430) and non-magnetic (stainless steel 304) meshes used as filter fillings were gifts from Susan Venneker (Haver & Boecker, Oelde, Germany). Crude sweet whey was provided by Chr. Hansen A/S (Hørsholm, Denmark). Bovine serum albumin standards (Fluka, 82516), glutaraldehyde (50 %, photographic grade), allyl glycidyl ether, epichlorohydrin, N–bromosuccinimide and iminodiacetic acid were obtained from Sigma-Aldrich Chemi GmbH (Steinheim, Germany). All other chemicals were analytical grade. A neodymium-iron-boron magnet block (B ~ 0.7 T) was obtained from Danfysik A/S (Jyllinge, Denmark) and used for separating magnetic particles in all cases except those involving high gradient magnetic fishing (HGMF). The un-derivatised polyvinyl-alcohol base supports (PVA) were obtained from Chemagen AG (Baesweiler, Germany).

4.2.2 Preparation of superparamagnetic adsorbents

The PGF base supports were prepared in two steps: (i) manufacture of sub-micron sized superparamagnetic iron oxide particles (Hubbuch and Thomas, 2002) and (ii) particle coating with 6 g L^{-1} polyglutaraldehyde according to the procedure described in O'Brien et al. (1996) and modified by Gomes (2006).

The activation of PGF-based supports to produce cation exchange adsorbents was performed according to a procedure described by Heebøll-Nielsen (2004). It consists of a double activation with epichlorohydrin subsequently functionalized with sulphite.

PGF-based metal chelate affinity adsorbent type was prepared by activation with allyl glycidyl ether, followed by bromination of the allyl groups with N–bromosuccinimide. The final adsorbents were obtained by introducing the ligand iminodiacetic acid (IDA) onto the surface of the supports through the active allyl groups. The full procedure used for the preparation of magnetic metal chelators is described in Heebøll-Nielsen (2003). Another type of magnetic adsorbents based on commercial PVA-coated base supports (Chemagen AG) was constructed using the same activation and functionalisation procedures. The IDA functionalised adsorbents were not loaded with metal ions.

4.2.3 Bench-scale batch binding studies

Batch binding studies employing a range of adsorbent concentrations were performed using a stock of 7.7 g L^{-1} of magnetic adsorbent previously equilibrated in 10 mM sodium phosphate equilibration buffer, pH 7. The stock was aliquoted in test tubes over a range of volumes between 0.1 and 1.5 mL. The supernatant was removed after magnetic settlement and 1 mL of unconditioned and pH adjusted (pH 7) crude whey was added to each test tube. The final concentration of adsorbents during binding thus ranged between 0.77 and 11.6 g L^{-1}. Binding was allowed to proceed for 10 minutes under vigorous mixing, after which the supernatants were collected following magnetic settlement.

Multicycle bench studies were performed in a similar way. However in this case 24.3 mg of magnetic cation exchangers previously equilibrated in 10 mM sodium

phosphate equilibration buffer, pH 7 were mixed with 5 mL of crude cheese whey and the supernatant was collected after 10 min binding. The supports were washed with 1 mL of equilibration buffer (giving a support concentration of 24.3 mg mL^{-1}, which is similar to the expected support concentration in the recycle loop of our HGMF system) for 10 min followed by two elution cycles with 1 mL each of equilibration buffer complemented with 1 M NaCl. This procedure was performed consecutively without cleaning of the adsorbents for four more cycles. All fractions were analysed for protein content and lactoperoxidase activity.

4.2.4 HGMF apparatus and system set-up

A laboratory type 'on-off' permanent magnet based high-gradient magnetic separator (Steinert HGF-10, Steinert Elektromagnetbau GmbH, Köln, Germany) designed for biological applications was employed (Hoffmann et al., 2002). The separator was set to have a 2.5 cm gap between the poles with a magnetic flux density of 0.32 T. A high-gradient magnetic filter was placed vertically in the 2.5 cm gap between the poles of the magnet.

(a)   **(b)**
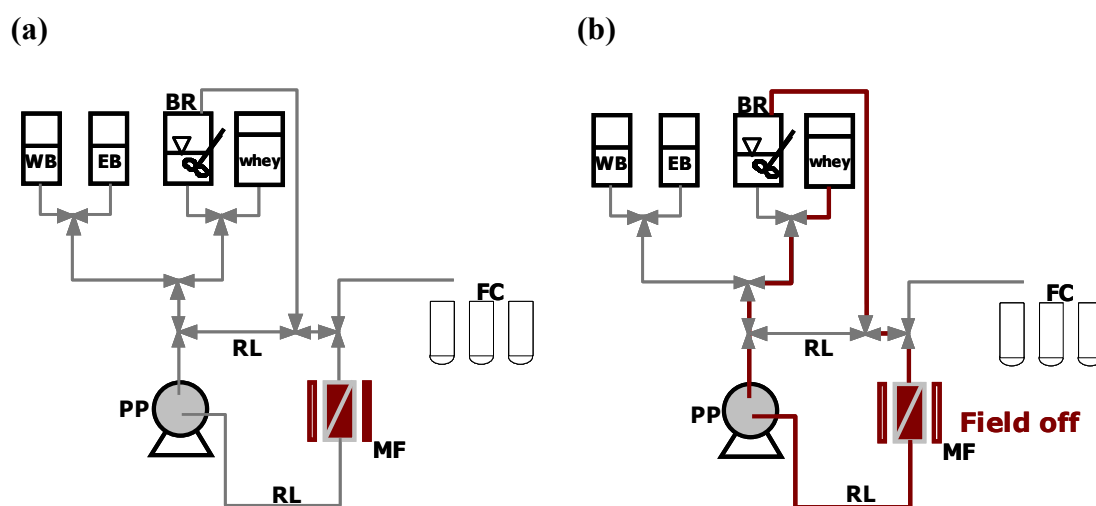
Fig. 4.1 (a) Schematic representation of the HGMF system set-up for multicycle processing. MF = magnetic filter, FC = fraction collector, PP = peristaltic pump, WB = washing buffer container, EB = elution buffer container, RL = recycle loop, BAR = batch adsorption reactor. **(b)** Flow path during .the support recovery step between cycles.

Other components of the HGMF system (Fig. 4.1) included: a batch adsorption reactor equipped with an overhead stirrer; two buffer containers; a container for whey; a fraction collector (SuperFrac 2211, LKB, Bromma, Sweden); a single peristaltic pump (Masterflex$^®$ Easy Load$^®$ model 7518-00, Cole Parmer Instrument Co., Vernon Hills, IL, USA) equipped with a 6.4 mm i.d. Norprene$^®$ A-60-F tube; and a set of four three-way solenoid switching valves (Burkert-Contromatic A/S, Herlev, Denmark) that were used to control the flow path direction and velocity. This system allowed the following steps to be performed: (i) loading of magnetic adsorbent suspension from the batch adsorption reactor through the filter to the fraction collector; (ii) loading of elution or washing buffer through the filter to the fraction collector; and (iii) recirculation of filter contents within a closed recycle loop for recovery of the supports at the end of each cycle. The total volume of the system recycle loop and filter was either 102 mL or 123 mL and is noted where relevant in the text. The HGF-10 magnet, pump and valves were controlled by LabView software (Student Edition 6i, National Instruments Corporation, Austin, TX, USA).

Magnetic filter

The high-gradient magnetic filter consisted of a stainless steel 316 canister containing a 46 mL ($8 \times 5.8 \times 1$ cm) cassette filled with parallel magnetisable sheets of stainless steel 430 woven wire cloth, separated by spacers of stainless steel 316 woven wire cloth. All wires were placed perpendicularly oriented with respect to the magnetic field and have two different but defined orientations with respect to the fluid. The following combinations of filter elements and spacer elements were used, with the number of filter elements and spacers indicated between brackets: Aa (4+5), Ab (4+5), Ba (6+6), Bb (8+7), Bc (8+7), Ca (10+10), Cb (10+9), Cc (14+14), and Db (12+13). The characteristics of the filter components are summarised in table 4.1.

Table 4.1 HGMF magnetic meshes and non-magnetic spacers used.

Magnetic mesh element	wire diameter (mm)	wire size (mm)
a	0.315	1.00
b	0.250	0.63
c	0.090	0.20
Spacer element		
A	0.900	5.00
B	0.500	2.55
C	0.250	1.00
D	0.125	0.50

4.2.5 Lactoperoxidase recovery by HGMF processing

Lactoperoxidase recovery by HGMF processing was conducted as described above, but using appropriate buffers (see adsorbent characterisation in section above) and with the following operational changes. Magnetic cation exchange adsorbents (2.52 g) were equilibrated in 10 mM sodium phosphate equilibration buffer, pH 7 and mixed with 600 mL of cheese whey (unconditioned, pH 6.4) in the batch adsorption reactor (Fig. 4.1). After 600 s of binding, the suspension was loaded to the magnetic filter and the protein loaded magnetic adsorbents were retained while the depleted whey was collected. The magnetic filter used for whey processing was the one defined as Aa in section 4.2.4, and had a voidage of 86 %.

The supports loaded to the filter were washed by filling the recycle loop (123 mL) with equilibration buffer (10 mM sodium phosphate, pH 7) and recycling the suspension for 180 s at 80 m h^{-1} (with change of flow direction every 60 s) while the magnetic field was switched 'off'. The flow rate was then decreased to 20 m h^{-1} and the field switched 'on' in order to re-collect the supports on the filter, a process that took 180 s. Two elution steps were performed using equilibration buffer supplemented with NaCl 1 M, followed by equilibration of the supports in the same fashion as used during elution. A new batch of cheese whey was used to release the supports and flush them from the filter into the binding container, thus reusing the supports. Before flushing the recycle loop was filled with whey fed from the appropriate container (see Fig. 4.1). Flushing was done by recycling the supports in the recycle loop at 80 m h^{-1} for 180 s (60 s in each direction) while the field was 'off', followed by discharging the suspension into the batch adsorption reactor at the same

velocity until a total of 600 mL was loaded to the system. The whey left in the system was displaced into the binding reactor using equilibration buffer. The suspension consisting of cheese whey and released adsorbents from the magnetic filter were kept mixed for 10 min before a new cycle of load, wash, and two elution steps was initiated. Three complete cycles, each consisting of loading, washing, elutions and particle release, were performed in total, without any use of mechanical vibration to the filter. A second experiment consisting of one cycle only was performed in exactly the same conditions as described above with the addition of mechanical vibration to the filter during the desorption steps.

4.2.6 Screening of magnetic filters

The filters constructed with the mesh and spacer components presented in table 4.1 were tested for their loading capacity and flush efficiency using the HGMS system set-up described in section 4.2.4 with a recycle loop and filter combined volume of 102 mL. For each filter type, 3 to 5 consecutive cycles of loading and flushing were conducted. In each cycle 5 g L^{-1} of metal chelating supports suspended in distilled water were loaded at 20 m h^{-1} to the filter up to 5 % breakthrough, followed by recycling for support release and then flushing of the system. This was done in the following way: after filling the filter to 5 % breakthrough, the magnetic field was switched 'off' and the suspension was re-circulated in the recycle loop three times (60 s in each direction), at a flow rate of 80 m h^{-1}, after which the supports were flushed out of the system by simply changing the flow path by triggering the appropriate valves (Fig. 4.1). This step was repeated two more times using the same amount of water for flushing (~0.7 L). Finally a new suspension of supports was loaded again, thus initiating another cycle. The amount of support loaded to 5 % breakthrough and the amount of support released from the filter were determined by visual monitoring and gravimetric analysis of the effluent.

Repetitions of 5 % breakthrough capacity studies using empty filters were performed as described above with the exception that the filters were dismantled and cleaned between experiments.

Definition of terms and calculations

Filter loading capacity is the amount of magnetic supports that can be loaded to a magnetic filter in a given HGMS cycle n. It is determined by measuring the volume of support suspension that can be loaded to the filter until 5 % breakthrough is reached, and by multiplying that volume by the initial concentration of support in suspension and dividing by the total volume of the filter. The term working capacity is often used for the loading capacity when operating in multicycle mode and usually excludes the first loading cycle.

The filter holding capacity is the total amount of support that is accumulated in a filter after loading to 5 % breakthrough, divided by the filter volume. This capacity is the sum of the loading capacity determined in a given HGMS cycle n and the support remaining after flushing of the filter (divided by the filter volume) from the previous cycle n-1. In the first loading cycle, i.e., when a suspension of supports is loaded to an empty filter, the loading capacity and the holding filter capacity are the same.

The flushing efficiency of a filter is the percentage of the total accumulated support that can be flushed from the filter at the end of a cycle.

4.2.7 Analytical methods

Total protein was measured with a BCA protein assay (Pierce Rockford, IL, USA), which was used as recommended by the manufacturer except that it was scaled for use in a Cobas Mira spectrophotometric robot. All protein concentrations were expressed in mg bovine serum albumin (BSA) equivalents. lactoperoxidase activity was determined using the TMB-ONE ready-to-use substrate (Kementech A/S, Copenhagen), an assay based on the oxidation of 3,3'-tetramethyl benzidine by lactoperoxidase. The reaction was followed by measuring the change in absorbance at 600 nm after mixing 15 µL of sample with 185 µL of the reagent, during which the temperature was kept constant at 37 °C. The assay was conducted using a Cobas Mira. The units of lactoperoxidase activity were defined as the change in absorbance per second per mL of sample. Magnetic particle content was determined using a gravimetric method. The magnetic particles in a suspension of defined volume were separated from the liquid phase by magnetic settlement and the supernatant discarded.

122

In the case of the adsorbents that had been in contact with biological material, the particles were washed three times with elution buffer, three more times with 1 M NaOH followed by three washes with Milli-Q water. The particles were resuspended in 1 mL of Milli-Q water, transferred to 5-mL pre-weighed pyrex tubes and dried to constant weight by incubating at 95-100 °C overnight. The tubes were cooled to room temperature in a desiccator for at least 2 h and weighed again. The particle concentration was determined from the difference between the final and initial weighed tubes and the exact volume of the original sample suspension.

Fig. 4.2 Effect of cation exchange magnetic adsorbent concentration on the removal of lactoperoxidase (LPO) (open symbols) and total protein (closed symbols) from crude whey in bench scale studies. Binding performed at pH 7 ($\square$ and $\blacksquare$) and pH 6.4 (Δ and $\blacktriangle$). The starting concentrations of lactoperoxidase and total protein in whey were 0.26 ΔA_{600} s^{-1} mL^{-1} and 10.4 g L^{-1}, respectively.

4.3 Results and discussion

4.3.1 Determination of conditions for Multicycle processing of cheese whey

Recovery of the enzyme lactoperoxidase from cheese whey was selected as a model system in this work, using cation exchange adsorbents that were constructed as

described by Heebøll-Nielsen (2004). A simulation of a HGMF multicycle process was performed at bench-scale with a magnet block and vigorous mixing. First the amount of adsorbents needed to bind the lactoperoxidase was determined (Fig. 4.2). Since lactoperoxidase has a high isoelectric point (approximately 9.8 (Ekstrand, 1989)), compared to most of the other whey proteins, these adsorbents bind the enzyme with no need for conditioning of the feedstock, whose natural pH and conductivity was 6.4 and 5 mS cm^{-1}, respectively. Furthermore, the adsorption properties in bench scale trials with whey were similar to those reported by Heebøll-Nielsen (2004) for clarified whey and were not affected by slight changes of pH (Fig. 4.2). However, as shown in figure 4.2, the amount of lactoperoxidase that can be removed from solution seems to reach a plateau at ~ 90 % removal when the support concentration exceeds ~7.5 g L^{-1}. This plateau effect might be a consequence of using unclarified whey containing casein precipitates and lipids.

(a)   **(b)**
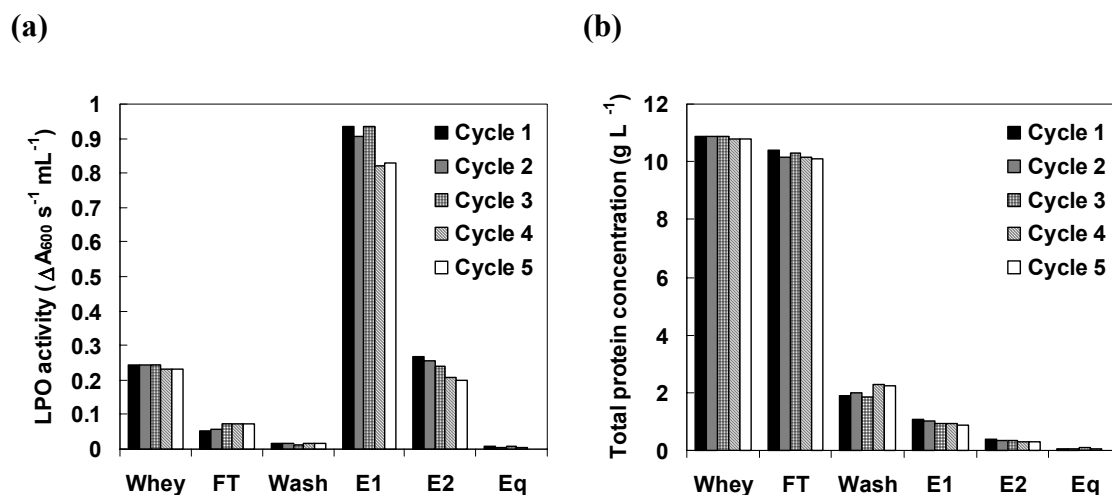
Fig. 4.3 Simulation of a HGMF whey processing experiment done at bench scale using magnetic cation exchangers (adsorbent concentration: 4.9 g L^{-1} in binding step and 24.3 g L^{-1} in desorption steps) and a magnet block. The adsorbents were subjected to 5 consecutive process cycles using crude whey. Lactoperoxidase (LPO) activity **(a)** and total protein concentration **(b)** determined for the fractions: flowthrough (FT), wash, 1st elution (E1), 2nd elution (E2) and equilibration (Eq).

Based on the previous results, further experiments working with the unclarified and unconditioned feedstock employed adsorbent concentrations of 4 - 5 g L^{-1} which

permitted the binding of ~ 80 % of the lactoperoxidase initially present in whey. In bench scale studies, the adsorbents could be reused for 3 cycles of binding and elution of lactoperoxidase without a decrease of efficacy, even though no cleaning step was used between cycles (Fig. 4.3). In the fourth and fifth cycles, small reductions in performance were seen (Fig. 4.3).

4.3.2 Multicycle processing of whey using HGMF

An automated multi-cycle HGMF process was employed for recovering lactoperoxidase from whey based on the conditions identified above. A concentration of 4.2 g L^{-1} of adsorbents was used in the adsorption reactor container. The results for the first cycle (Fig. 4.4, Table 4.2) show that 23 % of the initial lactoperoxidase activity and 85 % of the total protein flowed through the magnetic filter (*cf.* Fig. 4.2). No breakthrough of adsorbents was observed. In the subsequent washing step, 2.6 % of the total protein initially present in whey was removed from the adsorbents with a loss of only 1.8 % of lactoperoxidase activity. The enzyme was partially recovered during two elution steps, with a yield of 43 % after the first step and a total of 59 % after the second (Table 4.2).

After equilibrating the adsorbents in the recycle loop, these were flushed out of the filter, by filling the recycle loop with fresh whey and circulating the suspension at 80 m h^{-1} through the magnetic filter, with the field off. The supports were then fed to the batch adsorption reactor containing sufficient whey to give the same total volume during binding as in the first cycle (Fig. 4.1b). Results from the second processing cycle and a subsequent third cycle show that the activity of lactoperoxidase in the flowthrough increased dramatically to 69 % and further to 82 % of the initial activity present in whey in the beginning of each cycle, respectively (Fig. 4.4 and Table 4.2). Subsequently the yields in the elution fractions from the second and third cycles dropped, and the value of the combined fractions of the two elutions in the last cycle was only 22.5 %. These results cannot be explained by inefficient performance of the adsorbents since the bench-scale studies described above, which were performed under the same conditions as for the HGMF process described here, showed very little change over 3 cycles (Fig. 4.3).

A possible explanation for inferior performance of the HGMF system with respect to binding and elution of protein is poor performance of the magnetic filter. In fact when examining the flushing at the end of each cycle, it was observed that only 2.6 % and 3.3 % of the supports collected on the filter during loading were recovered at the end of the first and second cycles, respectively. This means that very few adsorbents were released from the filter to take part in binding in the batch reactor. The implication is that a significant proportion of whey protein binding to the adsorbents occurred to those adsorbents still remaining on the wires of the magnetic filter from the previous cycle. In such a situation the fast binding kinetics that characterise non-porous adsorbents do not apply to the mass sitting on the adsorbent wires and instead, part of the adsorbents are inaccessible to the protein in solution, especially in the more dense areas close to the wire. The packed adsorbent cake may be partially porous, however much longer contact time with the whey solution would be needed than the short time (180 s) employed for flushing of the adsorbents at the end of each cycle.
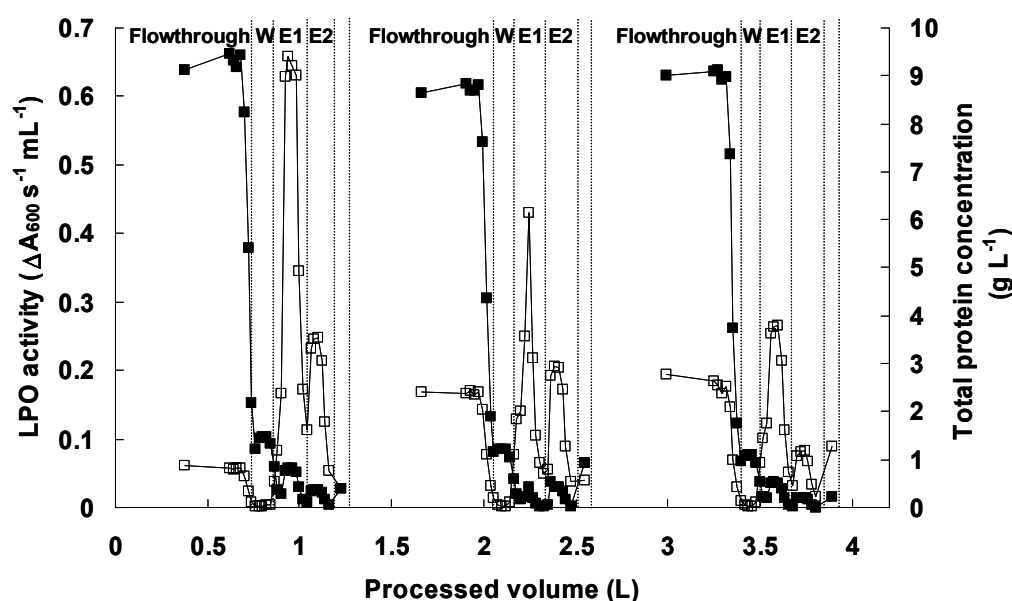
Fig. 4.4 Lactoperoxidase (LPO) activity (□) and total protein (■) profiles obtained during HGMF processing of cheese whey in three consecutive cycles. Each cycle consists of the following steps: flowthrough, wash (W), first elution (E1) and second elution (E2). Initial concentrations of lactoperoxidase and whey protein were 0.25 U ml^{-1} and 10.3 mg ml^{-1}, respectively.

The need for proper dispersion and mixing of adsorbents during wash and elution has been reported before for HGMF processing of trypsin from whey using benzamidine-linked magnetic adsorbents (Heebøll-Nielsen, 2002). Nevertheless, close inspection of table 4.2 shows that in the third cycle, the lactoperoxidase desorption efficiency (based on the amount bound to the adsorbents) is very high (96 %) and the overall balance of the enzyme for the cycle is close to 200 %.

Table 4.2 Yield, elution efficiency and purification factor calculations for the lactoperoxidase (LPO) activity and protein concentration resulting from the 3-cycle processing of cheese whey by HGMF.

Step	LPO yield (%)	LPO desorption efficiency (%)	Protein yield (%)	Protein desorption efficiency (%)	Accumulated protein (%)	
					LPO	Total protein
Load	100	n.a.	100	n.a.		
Flowthrough	23	n.a.	85	n.a.	77	15
Wash	1.8	2.3	2.6	17		
Elution 1	43	56	1.3	8.6		
Elution 2	16	21	0.6	3.7		
Equilibration	1.9	2.5	0.7	4.5	14	9.8
Balance	86	82	90	34		
Load	100	n.a.	100	n.a.		
Flowthrough	69	n.a.	89	n.a.	45	21
Wash	3.2	11	2.3	20		
Elution 1	17	56	0.4	3.2		
Elution 2	13	43	0.64	5.6		
Equilibration	2.9	9.4	1.6	14	9.2	16
Balance	105	119	94	43		
Load	100	n.a.	100	n.a.		
Flowthrough	82	n.a.	93	n.a.	27	23
Wash	2.6	15	1.9	30		
Elution 1	17	96	0.8	12		
Elution 2	5.5	31	0.3	4.7		
Equilibration	9.0	50	0.5	8.5	-7	19
Balance	116	191	97	56		

n.a. not applicable.

This could perhaps be due to some partial activation of the enzyme by removing contaminants and inhibitors. Similar results (119 % yield mass balances) have been reported before for purification of lactoperoxidase from whey and, although not proven, it was argued that the lactoperoxidase gained some activity during purification (Heebøll-Nielsen, 2004). If true, one would expect that the desorption

efficiency would be the same from cycle to cycle in the current work. However, it increases dramatically from cycle 2 to 3 and a simple mass balance to the amount of lactoperoxidase accumulated on the adsorbents at the end of each of the cycles shows a decrease in the accumulation (Table 4.4). This suggests that the lactoperoxidase activity retained in previous cycles is being released in the following ones, perhaps due to rearrangements of the adsorbent cake and slow diffusion during the steps of turning the field on and off. The desorption efficiency for total protein increased much less than for lactoperoxidase, reaching a value of 56 % in the third cycle and in all cycles the amount of total protein bound is higher than the amount desorbed. Quantification of the amount of total protein bound to the adsorbents after a complete cycle indicates that there is accumulation of protein on the adsorbents. Thus, the effects observed over the 3-cycle HGMF process presented here were attributed to poor release and resuspension of the adsorbents from the magnetic filter recycle loop both during binding and desorption. (*cf.* Fig. 4.3).

4.3.3 Screening of magnetic filters for improved performance

The results above clearly show that efficient release of the adsorbents from the magnetic separator is critical for maintaining the performance of the purification process in a given cycle and also over a number of cycles, which may be needed to process a large volume of feedstock. With this in mind, we tested a range of different types of magnetic filters in order to identify better candidates for use in bioprocessing.

The filters used here consisted of arrays of wires with a defined orientation constructed by using alternate layers of mesh (magnetic) components and spacer (non-magnetic) components (Table 4.1). Examination of these filters was conducted in a multicycle mode using the process set up described in section 4.2.4 (see also Fig. 4.1a). However the magnetic adsorbents used now were IDA functionalised metal chelate affinity types, and furthermore, they were suspended in distilled water and fed to the magnetic filter with a constant linear flow rate of 20 m h^{-1}. When the adsorbent concentration in the filter effluent reached a concentration corresponding to 5 % breakthrough, loading was stopped and they were released by conducting three sequential recirculation steps, each one followed by flushing of the supports from the

system. We observed that in each flushing step, a high concentration of supports were released from the system immediately after recirculation and then decreased slowly until the water was transparent, indicating that no suspended support remained in the system. However, high amounts of adsorbent could still be seen during the second and the third flushing. For this reason we made sure that the conditions for the recirculation (velocity, direction of the flow and time), and for pumping the adsorbents out of the system (velocity, volume of water) were kept constant in all experiments. Following a first cycle with load and flushing steps we proceeded with 2 to 5 consecutive cycles without conducting dismantling and cleaning of the filter between cycles. In this set-up, which simulates the multicycle bioprocess studied above with whey, the amount of adsorbent loaded to the filter and remaining after flush in each cycle could be accurately quantified. These experiments were conducted for eight different types of filters using two types of adsorbent base particles (polyglutaraldehyde, PGF, and polyvinyl alcohol coated, PVA). An example of the results from loading filter capacity at 5 % breakthrough and amount of support remaining in the filter obtained over several consecutive cycles is presented for one of the filter combinations studied here (Cb) in figure 4.5a for PGF base supports and figure 4.5b for PVA base supports.

The loading capacity determined at 5 % breakthrough dropped after the first cycle for all filters and adsorbents tested. This drop appeared to be closely connected to the amount of adsorbent remaining in the filter after the first cycle, as exemplified in figure 4.5. It could be expected that the sum of the loading capacity in the second cycle and the amount of support remaining on the filter from the first cycle, would be the same as the loading capacity in the first cycle. Based on the results obtained in the experiments described above, we calculated the amount of supports that 'fitted' on a filter in each cycle during multicycle mode, and compared those with the results from several loading experiments to an empty filter, i.e., with first cycle loading experiments. Averages of the filter loading capacities of an empty filter and averages of the filter holding capacity in multicycle mode are presented in figure 4.6 for the eight filters and two support types examined.
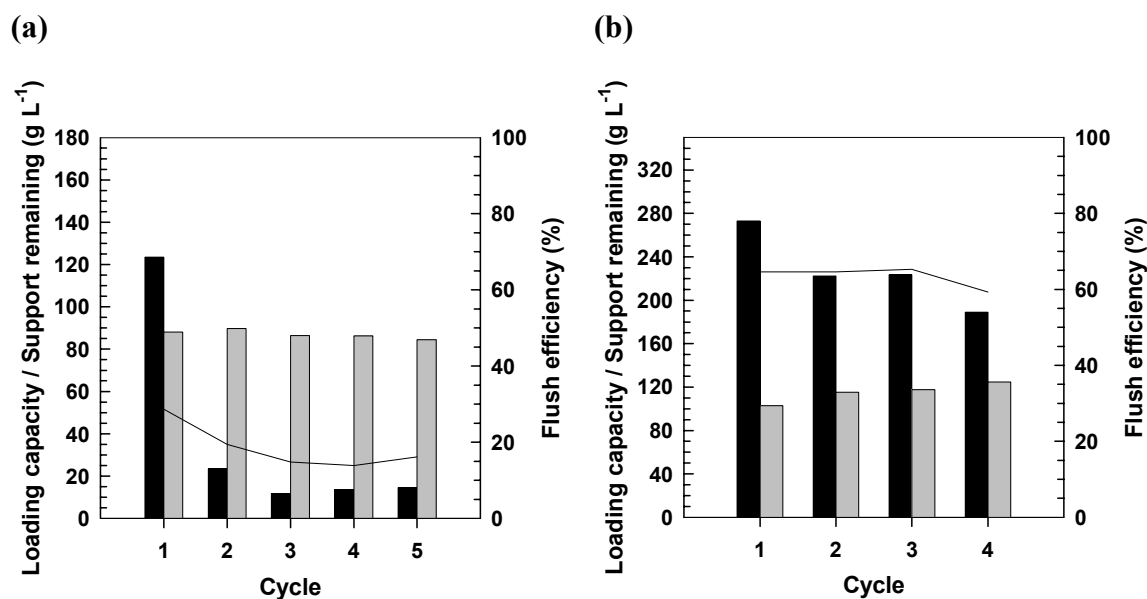
Fig. 4.5 Normalised amount of **(a)** PGF based and **(b)** PVA based IDA derivatised support loaded to the magnetic filter type Cb up to 5 % breakthrough (■) and remaining on the filter after flushing (▭). The lines represent the flush efficiency based on the support amount initially present at each cycle. **Note:** The amount of support on the filter represented here is the loading capacity, i.e., the amount of support that can be added to the filter up to 5 % breakthrough (in mass of captured support per volume of filter) at a given loading cycle. The remaining support is calculated from the loaded amount, the accumulated amount from the previous cycle and the amount flushed in the current cycle.

(a)   **(b)**
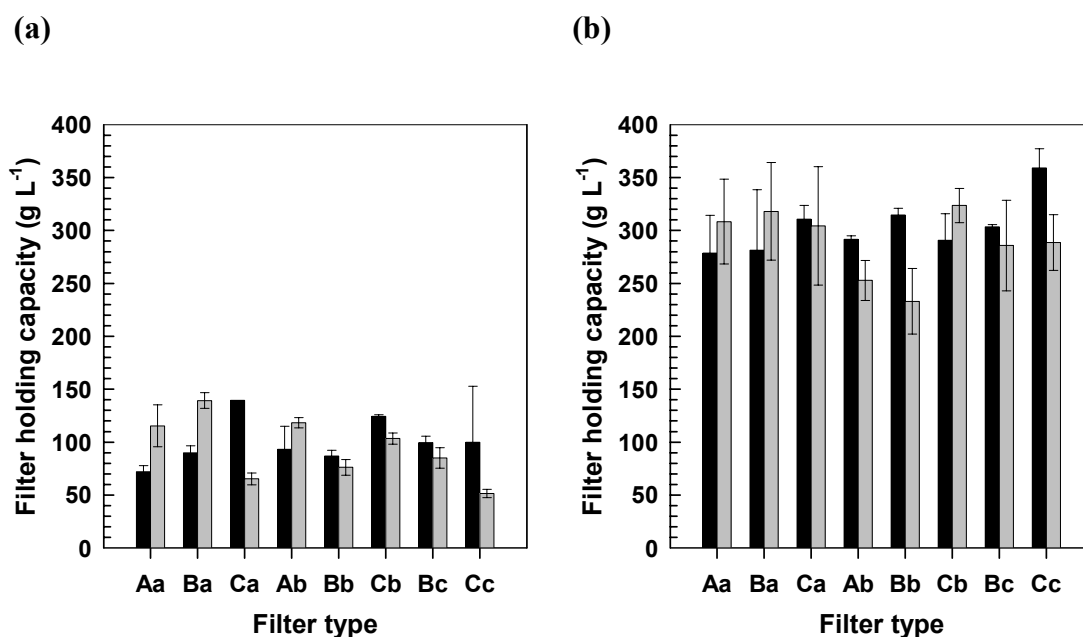
Fig. 4.6 Filter loading capacity at 5 % breakthrough for the first cycle[1] (■), and the average of the filter holding capacity following a multicycle process (excluding the first cycle) (▬) using **(a)** PGF and **(b)** PVA adsorbents.

When comparing the average of total holding capacity (i.e., the total amount of adsorbents accumulated in the filter after each loading cycle) for cycles 2 and onwards with the loading capacity determined on empty filters (Fig. 4.6a & Fig. 4.6b), the outcome is different for the two sets of results. It is possible that the patterns of support capture in the filter are changed by the presence of supports from the previous cycle in the filter leading to different packing of the adsorbents collected on the wires. However, when comparing these results for the PVA case (Fig. 4.6b) they seem to be generally more consistent within the standard deviations than for the PGF case. Examination of the capacity results obtained with the PGF type of adsorbents (Fig. 4.6a) might indicate that there it a tendency for filters with matrices Aa and Ba to become more filled with adsorbents after multiple loading cycles, while matrices consisting of the spacer C seem to have a tendency to pack less adsorbents than during

---

[1] The average and standard deviation results for filter capacity in the first cycle were determined from two individual experiments using empty filters.

the first cycle. When looking at the wire diameters and mesh size of the matrix versus spacer (Table 4.1), the overall level of coarseness of the filter is mainly due to the spacer. It has been shown before (Ebner, 2005), that the use of spacers composed of thick wires (e.g. spacer A) leads ultimately to a decrease of the filter capacity due to a lower density of the particle build-up in regions facing away from the magnetic wire. On the contrary, loading of particles to filters containing spacers made of thin wires (e.g. C types) will result in a denser magnetic particle packing. Therefore, the increase in total amount of adsorbents that can be packed inside the filter during multicycle processing as compared to loading capacity of an empty filter for the more coarse filter (spacer A, Fig. 4.6) could be the result of an improvement of the filter space usage due to mechanical filtration effects promoted by previously collected particles. For filters employing fine spacers (spacer C, Fig. 4.6a & Fig. 4.6b), mechanical filtration (rather than magnetic capture) is proposed to lead to the occurrence of completely blocked regions, giving rise to very high interstitial fluid velocities, i.e., via the formation of channels. These high local velocities would then result in rapid adsorbent breakthrough after the first cycle and thus a lower holding capacity of the filter would be observed when compared to the holding capacity of the empty filter. Supporting this theory is the result of visual inspection of the filter at the end of multicycle tests. After carefully dismantling the filter, it could be seen that the adsorbents remaining were not evenly distributed, and instead, were agglomerated in different areas.

The working capacity, i.e., the amount of support that can actually be loaded to the filter during multicycle processing, can be approximated by averaging the 5 % breakthrough loading capacity values obtained after these stabilise (in most cases after the second cycle). These results, presented in figure 4.7a are not consistent between the two sets of supports and do not follow any particular trend. For example, the working capacity for PGF adsorbents drops when moving from Ba to Ca filters, but the PVA support capacity increases when making this change (Fig. 4.7a). The filter loading capacity determined at 5 % breakthrough is also influenced by operating parameters, such as magnetic field, magnetic velocity and velocity of the fluid, and this influence varies for different types of supports (Ebner, 2005). Magnetic

properties, size and shape of the supports determine the value of the filter coefficient, a parameter that affects the loading profile of a filter (i.e., the shape of the breakthrough curve). Therefore, when 5 % of the loaded concentration reaches the outlet of the filter, this will have different meanings in terms of filter occupation. For example, for a steep curve, the filter particle filling would be close to the maximum possible occupation of the filter given by 100 % breakthrough. Since 5 % capacity is not an independent property of the filter/particle system examined, it cannot be used for a direct quantitative comparison. However when examining the extreme cases of filter coarseness used, i.e., the use of spacers A and C, it can be seen that, for the PGF system, the working capacity is consistently lower when using the spacer C as compared to use of A (Fig. 4.7a). This effect is not observed for the PVA system in distilled water (Fig. 4.7a), probably due to the better flushing characteristics of these supports (Fig. 4.7a & Fig. 4.7b).

(a)   **(b)**
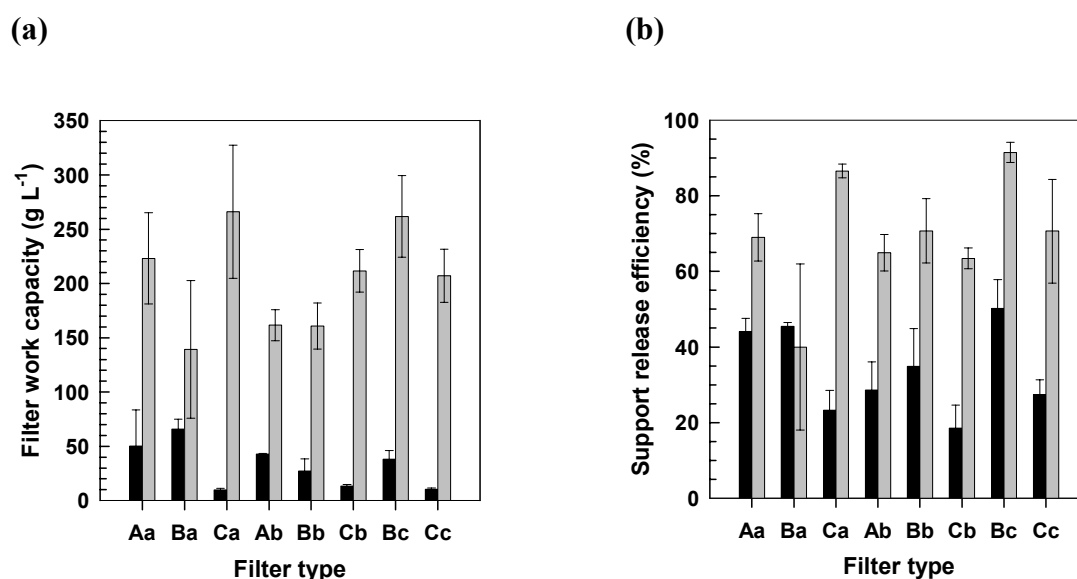
Fig. 4.7 Working capacity **(a)** and average values of flushing efficiency **(b)** for the PGF (■) and PVA (▭) adsorbents.

In light of the results above, it seems clear that filters constructed with the spacer type C are not suitable for working with PGF supports. Furthermore, when using PGF based supports in a biological feedstock, it is expected that occurrence of blocked regions and the impact of these on the working capacity becomes more severe.

Although such an impact is not observed on the working capacity determinations for PVA supports in distilled water, it is possible that when employing these adsorbents in a biologic feedstock, these effects might be seen.

The filter capacities both in empty filters and in multicycle mode are almost three times higher for PVA supports than PGF (Fig. 4.6 & Fig. 4.7a). Moreover, as mentioned earlier, for the PVA case, the average loading capacity from multicycling for each filter combination is essentially the same as the loading capacity of the first cycle (Fig. 4.7b). It has been shown in previous work (Ebner, 2005), that the PVA adsorbent have a better packing capability than PGF types due to being more monodispersed and can thus pack more regularly in the filter. In addition, the filter coefficient for the PVA system was consistently higher than for the PGF supports (Ebner, 2005), which characterises the system as having a sharper loading front. Therefore, not only are higher capacities expected when employing PVA adsorbents, but also flushing is better, and there is less effect from the coarseness of the filter. In fact, the flushing efficiencies (i.e., the percentage of the initially present support flushed out of the filters) for the PVA adsorbents varied from a lowest average value of 37 % to 91 % for filters Ba and Bc, respectively, and were thus much higher when compared to the PGF supports (between 27 % and 50 % for filters Bc and Cc, respectively) (Fig. 4.7a). Although the flushing efficiency results were different for the two types of supports employed here, we investigated the particular properties of the filter that have an impact on flushing, such as voidage of the filter, diameter and aperture of the spacer and mesh, ratio between the two, number of intersections of the wires from the mesh but no correlation was found. It is possible that a combination of different factors contribute to the results. A possible explanation, in agreement with the support agglomeration observed at the end of the multicycle experiments, is the occurrence of channelling in the filter during flushing. It can be expected that increasing the linear flow rate of liquid through the filter will improve flushing efficiency. Such effects have been reported and discussed by Svoboda and Corrans (1985). When this was examined with filter type Aa loaded with PVA adsorbents in the current work, it was possible to achieve a flushing efficiency of 99.7 % by increasing the linear flow rate from 80 to 178 m h^{-1} (Fig. 4.8). However there is a

limit to the flow rates achievable in a given setup, and depending on the loading conditions, feedstocks used, etc, formation of channels in the filter may hamper complete adsorbent release even with PVA types. Preliminary experiments (Fig. 4.8) using a pneumatic filter vibrator and PVA supports show that it is possible to obtain flushing efficiencies higher than 98 % at the same linear fluid velocity used for flushing the magnetic filter in the studies described above (i.e. 80 m h^{-1}). When employing vibration combined with high flow rates, the release of the collected supports in the filter is extremely efficient (101 % for 178 m h^{-1}).
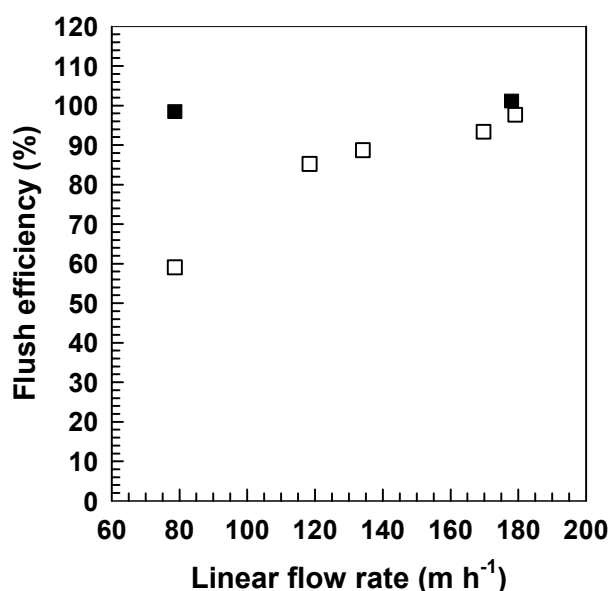
Fig. 4.8 Flush efficiency of PVA metal chelator adsorbents from a magnetic filter (type Aa) at different flow rates with (■) and without (□) mechanical vibration.

4.3.4 Improved HGMF process

Although the screening tests using support suspensions in water give an indication of how filters will perform according to their geometry, other parameters have to be taken into account. For example, properties of the feedstock might have a large impact on capacity and flushing. One of the main advantages of using HGMF filters is the high voidage (81-87 %, in this work). However, once the filter starts filling up, the voidage will decrease and mechanical filtration effects are expected to occur. For a very crude feedstock with a high content of solids, the best choice for a filter might

simply be the most coarse available. This was the case for processing crude cheese whey in this work and the reason for choosing the filter type Aa, which also had good flushing properties (Fig. 4.7 & Fig. 4.8). However, these considerations need to be studied case by case.
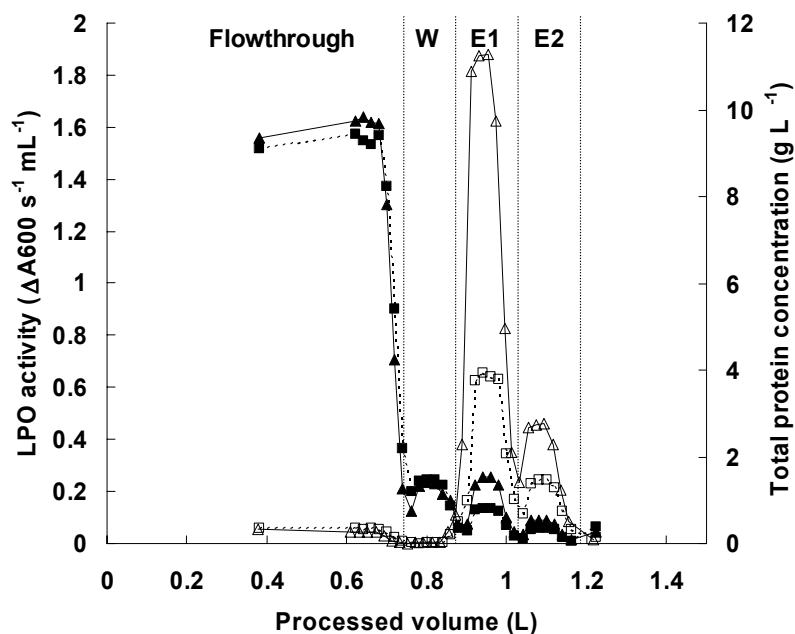
Fig. 4.9 Lactoperoxidase (LPO) activity ($\triangle$) and total protein ($\blacktriangle$) profiles obtained during HGMF processing of cheese whey employing mechanical vibration of the filter in the desorption steps. Lactoperoxidase (LPO) activity ($\square$) and total protein ($\blacksquare$) corresponding to the first cycle in figure 4.1 are also represented. The cycle consists of the following steps: flowthrough of unbound proteins during filter loading, wash (W), first elution (E1) and second elution (E2).

Simple mechanical vibration of the filter was also tried as a means of improving adsorbent release. The results (Fig. 4.9 & Table 4.3) of a complete HGMF cycle with mechanical vibration during particle release can be compared to the results from the first HGMF cycle presented in Table 4.2. It can be seen that the recovery of lactoperoxidase in the elution step is greatly increased when vibration is used. In fact, the elution efficiencies are similar to those obtained in bench scale runs (Fig. 4.3 & Table 4.3), where very efficient resuspension of magnetically settled adsorbents was used. Mechanical vibration during HGMF processing enabled the release of 82 % of

the supports at the end of the cycle as compared to the value of 2.6 % reported in the absence of vibration. A clear correlation between the elution yields and the amount of support recovered at the end of the cycle can be observed in figure 4.9. The amount of lactoperoxidase released during elution is very much higher when using vibration in each of the adsorbent re-dispersion steps than without.

Table 4.3 Yield and purification factor for lactoperoxidase (LPO) and protein calculated from HGMF processing of cheese whey employing mechanic vibration of the filter.

	Step yield (%)				Purification factor Bench-scale	Purification factor HGMF
	LPO[a] Bench-scale	LPO HGMF	Protein[a] Bench-scale	Protein HGMF		
Load	100	100	100	100	1	1
Flowthrough	25 ± 4	14	94 ± 1	85	0.3	0.2
Wash	1.2 ± 0.1	1.6	3.5 ± 0.1	2.4	0.7	0.7
1st elution	76 ± 1	77	1.8 ± 0.2	2.3	33	40
2nd elution	21 ± 1	22	0.66 ± 0.07	0.9	29	28
Equilibration	0.5 ± 0.1	0.7	0.11 ± 0.04	0.5	2.9	1.6
Balance	**124**	**115**	**100**	**91**	n.a.	n.a.

[a] Average and standard deviation for the three first runs (see Fig. 4.3).

n.a. not applicable.

4.4 Conclusions

This work shows that the performance of magnetic filters is a parameter that deserves more attention if they are to be used in downstream processing of biological molecules. In particular, poor flushing of magnetic adsorbents from magnetic filters in HGMF has a large effect on elution performance and also on capacity during multicycle processing of lactoperoxidase from whey. Binding and elution results were clearly better when improved particle release conditions were employed, namely the use of vibration of the magnetic filter. Furthermore, the results suggest that the use of fine spacers might not be suitable when used with PGF adsorbent types. However, the properties of the adsorbents also have a large role in filter capacity and ease of flushing. In particular, PVA types had much superior performance than PGF types, presumably due to differences in shape as well as size distribution.

Acknowledgments

References

Ebner, N., Gomes, C.S.G., Hobley, T.J., Thomas. O.R.T., Franzreb, M. (2006) Filter capacity predictions for the capture of superparamagnetic microparticles by high-gradient magnetic separation (HGMS). *Chapter 3*.

Ekstrand, B. (1989) Antimicrobial factors in milk – A review. *Food Biotechnol.*, <u>3</u>, 105-126.

Gomes, C.S.G., Heebøll-Nielsen, A., Petersen, T.L., Thomas, O.R.T., Hobley, T.J. (2006) Control of protein hydrolysis in unclarified liquors: application of high-gradient magnetic fishing (HGMF) employing improved magnetic adsorbents. *Chapter 5*.

Heebøll-Nielsen, A (2002) *High gradient magnetic fishing – support functionalisation from unclarified bioprocess liquors*. Ph.D. Thesis. Technical University of Denmark, Denmark.

Heebøll-Nielsen, A., Choe, W.S., Middelberg, A.P.J., Thomas, O. R.T. (2003) Efficient inclusion body processing using chemical extraction and high-gradient magnetic fishing. *Biotechnol. Progr.*, <u>19</u>(3), 887-898.

Heebøll-Nielsen, A., Justesen, S.F.L. Hobley, T.J., Thomas, O.R.T. (2004) Superparamagnetic cation-exchange adsorbents for bioproduct recovery from crude process liquors by high-gradient magnetic fishing. *Sep. Sci. Technol.,* <u>39</u>(12): 2891-2914.

Hoffmann, C., Franzreb, M., Höll, W.H. (2002) A novel high-gradient magnetic separator (HGMS) design for biotech applications. *IEEE Trans. Appl. Supercond.*, 12(1), 963- 966.

Hubbuch, J.J., Thomas, O.R.T. (2002) High-gradient magnetic affinity separation of typsin from porcine pancreatin. *Biotechnol. Bioeng.*, 79, 301-313.

Nesset, J.E., Finch, J.A. (1981) The static build-up model of particle accumulation on single wires in HGMS: experimental confirmation. *IEEE Trans. Magn.*, Mag-17 (1), 53-57.

O'Brien, S. M., Thomas, O. R. T., Dunnill, P. (1996) Non-porous magnetic chelator supports for protein recovery by immobilised metal affinity adsorption. *J. Biotechnol.*, 50, 13-26.

Reffle, J., Krautwurm, V., Schewe, H., Hoffmann, H. (1979) Investigation of the matrix cleaning process in HGMS. *J. Magn. Magn. Mater.*, 13, 11-12.

Svoboda, J. (1987) Magnetic methods for the treatment of minerals. *Developments in Mineral Processing* (Ed. Fuerstenau, D.W.), 8, Elsevier Sci. Publ. Co., Amsterdam.

Svoboda, J., Corrans, I.J. (1985) The removal of particles from the matrix of a high-gradient magnetic separator. *IEEE Trans. Magn.*, Mag-21 (1), 53-57.

5. Control of protein hydrolysis in unclarified liquors: application of high-gradient magnetic fishing (HGMF) employing improved magnetic adsorbents

Cláudia S. G. Gomes[1], Anders Heebøll-Nielsen[1], Trine L. Petersen[1], Owen R.T. Thomas[1,2], Timothy J. Hobley[1]

[1] Center for Microbial Biotechnology, Technical University of Denmark, 2800 Lyngby, Denmark.

[2] Department of Chemical Engineering, The University of Birmingham, Edgbaston, Birmingham B15 2TT, United Kingdom.

Abstract

In this work we introduce a new process for controlling protein hydrolysis processes by employing high-gradient magnetic fishing (HGMF). Our system enables enzymatic hydrolysis to be halted at a desired degree of hydrolysis and the enzyme to be recovered. The system used to demonstrate this concept is the control of tryptic hydrolysis of bovine cheese whey. We show how benzamidine linked magnetic adsorbents at low concentrations (5 g L^{-1}) combined with HGMF processing can rapidly and effectively remove (99.1 %) and recover (51 %) small amounts of trypsin (0.15 g L^{-1}) added to cheese whey, thereby limiting the extent of hydrolysis. The degree of hydrolysis was controlled to either 2 % or 4 % by varying the time between adding the trypsin and employing HGMF. The development and construction of improved superparamagnetic adsorbents for this test is also presented here. The benzamidine linked adsorbents with the best binding properties (maximum binding capacity, 178 mg g^{-1} and dissociation constant, 0.16 μM) were prepared by activating polyglutaraldehyde-coated superparamagnetic particles with heterobifunctional allyl glycidyl ether and N-bromosuccinimide, followed by coupling with *p*-amino benzamidine.

5.1 Introduction

The use of enzymic modification in the food industry for improving qualities such as digestability, flavour, and texture will undoubtedly continue to gain in popularity in the future. However, the control of enzymatic hydrolysis reactions, occurring in complex biological suspensions, and involving exogenously added soluble enzymes, is not a simple affair. The most commonly applied methods for removing the activity of an added enzyme catalyst, namely heat treatment or exposure to extremes of pH, are often detrimental to the end-product. Furthermore, in many cases the reuse of enzyme catalysts is highly desirable. This is especially true when the cost for 'one-shot' use of the free enzyme are high and/or technical difficulties associated with the need to inactivate or remove the catalyst are encountered. Though numerous important industrial processes using immobilised enzyme catalysts have been established, the technical problems associated with the use of immobilised enzymes have still not been solved. Conventional immobilised enzyme catalysts typically employ porous support materials, and are effectively limited to the conversion of only small molecule reactants in clean liquors.

Recently, we described the bioseparation technique known as high-gradient magnetic fishing (HGMF) and demonstrated its advantages for the selective recovery of various macromolecular target species directly out of complex bioprocess liquors (Hubbuch *et al.*, 2001; Hubbuch and Thomas, 2002; Heebøll-Nielsen *et al.*, 2003, 2004a; 2004b, 2004c). The fast adsorption and short processing times that characterise HGMF suggest that the technique could be potentially useful in recovering an enzyme catalyst from an industrial process liquor following modification of the latter. Adsorbents designed for HGMF are based on non-porous support materials and therefore, these are resistant to fouling and allow much faster adsorption equilibria as minimal diffusional limitations are observed (Zulqarnain, 1999; Heebøll-Nielsen *et al.*, 2004c; Ferré, 2006).

An example of an industrially relevant enzyme modification process is the tryptic hydrolysis of bovine whey. Cheese whey is produced in vast quantities as a by-product from the dairy industry; for 1997 a world-wide output of $1.18 \cdot 10^{11}$ kg was

estimated with a further increase projected (Geberding and Byers, 1998). Whey has been used as a source of protein for human food products and animal feed. However, increased functional properties can be obtained by exposing the bulk protein to controlled, partial proteolysis (Adler-Nissen, 1979; Pintado *et al.*, 1999), and in addition, certain whey protein species can be converted into bioactive peptides upon hydrolysis with digestive proteases (Pihlanto-Leppälä, 2001). For example, degradation of α-lactalbumin and β-lactoglobulin with trypsin or other pancreatic enzymes yields peptide fragments with opioid activities or angiotensin I-converting enzyme inhibiting effects. The latter peptides may be employed as anti-hypertensive additives for functional foods and pharmaceuticals ('nutraceuticals').

In this work we describe the development of improved benzamidine-linked superparamagnetic adsorbents and show how these can be employed as a gentle and highly effective means of controlling trypsin-mediated hydrolysis reactions within unclarified bovine whey using a HGMF system consisting of a cyclically operated 'on-off' permanent magnet separator fitted with a magnetic filter device composed of a woven stainless steel matrix of high voidage.

5.2 Materials and Methods

5.2.1 Materials

FeCl$_3$·6H$_2$O and DMSO (99.5 %) were obtained from Merck (Darmstadt, Germany). FeCl$_2$·4H$_2$O was bought from Mallinckrodt Baker B.V. (Deventer, the Netherlands). NaBH$_4$, divinyl sulphone (DVS), arginine, and 3-amino propyl triethoxy silane, glutaraldehyde (50 %, photographic grade), 1,4-butanediol diglycidyl ether (BDE), allyl glycidyl ether (AGE), N-bromosuccinimide (NBS), *p*-amino benzamidine (*p*-AB) dihydrochloride salt, bovine pancreatic trypsin (T8003), porcine pancreatin (P1500), bovine serum albumin standards (Fluka, 82516), L-leucine, N-α-benzoyl-DL-arginine-*p*-nitroanilide (BAPNA) and trinitrobenzene sulphonic acid (TNBS) were purchased from Sigma-Aldrich Chemie GmbH (Steinheim, Germany). The bicinchoninic acid (BCA) protein assay kit was bought from Pierce Chemicals (Rockford, IL, USA). All other chemicals were analytical grade.

The mesh of stainless steel 430 wires (~100 μm diameter, KnitMesh type 9029), used for constructing the 5-mL magnetic filter, was a gift from C. Barnes (KnitMesh Ltd., South Croydon, Surrey, UK). Woven wire cloths of stainless steels 316 (material DIN 1.4301, 0.9 mm Ø wires, 5 mm mesh) and 430 (material DIN 1.4016, 0.315 mm Ø wires, 1 mm mesh) were obtained as gifts from Susan Venneker (Haver & Boecker, Oelde, Germany). The crude bovine sweet whey type I was kindly donated by Waagner Nielsen (The Royal Veterinary and Agricultural University, Copenhagen, Denmark). The crude bovine sweet whey type II was provided by Chr. Hansen A/S (Hørsholm, Denmark). Unless mentioned, all experiments in the current work were performed using whey type I.

5.2.2 Batch-wise support separation

A neodymium-iron-boron magnet block (B ~ 0.7 T) from Danfysik A/S (Jyllinge, Denmark) was used to separate magnetic particles from liquid phases during preparation of the magnetic adsorbents, equilibration of adsorbents, binding studies in whey and bench-scale hydrolysis control studies. In the bench-scale adsorption and desorption studies done with pure trypsin solutions and porcine pancreatin, a side-pull permanent magnet rack ($B \leq 0.15$ T, PerSeptive Diagnostics, Cambridge, MA, USA) was employed.

5.2.3 Preparation of superparamagnetic adsorbents

Preparation and activation of base matrix

Sub-micron sized superparamagnetic iron oxide particles were prepared by a procedure based on alkaline precipitation of Fe^{2+} and Fe^{3+} followed by silanisation with 3-aminopropyltriethoxysilane, using the chemicals and methods of Hubbuch and Thomas (2002), and subsequently coated by polyglutaraldehyde as described by O'Brien *et al.* (1996). Polyglutaraldehyde-coated supports were activated (at 100 mg scale) with DVS or BDE as has been described by Heebøll-Nielsen *et al.* (2004a) and O'Brien *et al.* (1996), respectively. In the former procedure DVS was added at regular intervals over 10 min to the particles suspended in 0.5 M Na_2CO_3 containing 18 mM $NaBH_4$ to a total of 80 mmol g^{-1} particles and the reaction allowed to proceed for 1 h,

whereas the latter involved reaction with 45 % (v/v) BDE under reducing, alkaline conditions (15.3 mM $NaBH_4$, 0.1 M NaOH) for 6 h. The procedure for attachment of AGE (Heebøll-Nielsen *et al.*, 2003) is a modification of an activation route suggested by Burton and Harding (1997a). Following suspension of the supports (up to 0.5 g scale) in a solution containing 0.15 M NaOH and 36 mM $NaBH_4$ in 50 % (v/v) DMSO at a particle concentration of 25 g L^{-1}, AGE was added to a final concentration of 50 % (v/v), and the reaction was allowed to proceed for 48 h at ambient temperature. Allyl derivatised particles were washed extensively with water, and the double bonds of the allyl groups brominated with NBS to produce bromohydrin moieties. This step was performed at room temperature in a 0.14 M aqueous solution of NBS at a charge of 10 mmol g^{-1} supports, which was expected to constitute a large molar excess. The bromination reaction between NBS and the allyl double bonds was assumed to progress rapidly and efficiently, and was terminated by magnetic settling and removal of the supernatant after 1 h at room temperature. Brominated supports were washed extensively in water before the final derivatisation step.

Ligand coupling

Matrices activated with BDE or DVS were derivatised with the trypsin inhibitors arginine and *p*-AB·2 HCl dissolved in aqueous sodium carbonate under reducing conditions (Hubbuch and Thomas, 2002; Heebøll-Nielsen *et al.*, 2004a, respectively). For BDE the coupling time and temperature were 18 h and 60 °C, whereas coupling to DVS activated supports took place at room temperature for 24 h. The bromohydrin moieties of the brominated AGE-reacted supports were reacted with arginine or *p*-AB·2 HCl in 100 g L^{-1} solutions in 0.5 M Na_2CO_3 for 72 h at room temperature. During the reactions the support concentrations were 15 g L^{-1}. For all three chemistries tested, control particles were prepared for which no ligand was added to the coupling solutions; it was assumed that the reactive groups would be hydrolysed under the alkaline conditions. The prepared adsorbents were washed extensively with water and then with storage buffer (20 mM sodium phosphate, 1.0 M NaCl, pH 6.8), before storing the supports at 4 °C until required.

Larger scale preparation of benzamidine-linked superparamagnetic adsorbents

For manufacturing of 4 g, 40 fold greater batches, of adsorbents activated with AGE and further derivatised with *p*-amino benzamidine the following modifications were introduced: the particle concentration in the polyglutaraldehyde coating step was increased from 1 g L^{-1} to 6 g L^{-1} and in the *p*-amino benzamidine coupling step, the particle concentration was 24 g L^{-1} instead of 15 g L^{-1}, while the other reagent concentrations were kept constant.

5.2.4 Adsorbent characterisation

The binding properties of the adsorbents were investigated in small-scale batch binding experiments at room temperature, using a range of support concentration-to-trypsin ratios in equilibration buffer, porcine pancreatin extract, and crude and clarified cheese whey. In all studies, the adsorbents were previously equilibrated by resuspension in 100 mM Tris/HCl, 10 mM $CaCl_2$, pH 7.5. The amounts of adsorbed trypsin were calculated by difference and adsorption isotherms were subsequently plotted and fitted with the Langmuir model (Langmuir, 1918), represented by equation 5.1. The equilibrium concentration of the adsorbed and bulk-phase protein are represented by Q* and C* respectively, K_d is the dissociation constant and Q_{max} is the maximum binding capacity of the adsorbents. The fit of the data to the Langmuir equation was done with the aid of the software SigmaPlot (Systat Software, Inc., Point Richmond, CA, USA).

$$Q^* = Q_{max} \frac{C^*}{K_d + C^*}$$

Eq. 5.1

Trypsin binding in a monocomponent system

Trypsin solutions (1 mL) at a range of concentrations (0 to 2 g L^{-1}) were prepared in equilibration buffer and added to 1 mg of equilibrated adsorbent. After 30 min of vigorous mixing, the adsorbents were magnetically separated from the liquid phase and the supernatant was recovered for total protein and trypsin activity determination.

Recovery of trypsin from porcine pancreatin extract

Protein interaction with the supports was further examined in small-scale studies to determine adsorption of trypsin and bulk protein from an extract of pancreatin. AGE-activated adsorbents derivatised with benzamidine or control particles without immobilised inhibitors were first equilibrated as above, then aliquotted to give 1.2-1.6 mg of supports in a series of tubes, before adding 1.00 mL volumes of pancreatic extract diluted up to 200-fold. The extract was prepared by magnetically stirring 100 g L^{-1} of pancreatin in the equilibration buffer for 90 min on ice before clarifying by centrifugation for 2 min at 13,000 rpm. After 30 min of binding the supernatants of the magnetically settled supports were analysed for trypsin activity and total protein.

Optimal elution conditions were found in similar experiments: In this case only the benzamidine-functionalised adsorbents, in 0.8 mg aliquots, were employed with an extract containing 20 g L^{-1} of pancreatin. Following 30 min of binding each of five reaction tubes were briefly washed three times with binding buffer (1 mL) before conducting three consecutive desorption steps by adding 1 mL of an elution buffer and mixing the tubes for 30 min for competitive elution, or 5 min for elution by changing pH. The five elution buffers were: Binding buffer supplemented with 5 mM arginine or benzamidine; 10 mM glycine/HCl, pH 2.6, 5 mM $CaCl_2$; 50 mM glycine/HCl, pH 2.6, 5 mM $CaCl_2$; or 10 mM glycine/HCl, pH 2.6, 0.10 M NaCl, 5 mM $CaCl_2$. After each washing or elution step the particles were settled, and the supernatants withdrawn and analysed for trypsin activity and concentration of total protein.

Trypsin binding in crude bovine sweet whey

For batch binding experiments performed in whey, a range of previously equilibrated AGE activated *p*-AB magnetic adsorbent amounts up to a maximum of 16.5 mg were mixed with 1 mL of partially clarified (filtered through a Whatman filter type 1 followed by a centrifugation at 5000 rpm for 10 min.) or crude whey spiked with 0.1, 0.15 or 0.2 g L^{-1} trypsin. The supernatants were collected after 30 min binding and analysed for protein content and trypsin activity. Time-dependent binding experiments were also performed in whey by resuspending the adsorbents to a final

concentration of 4.5 g L^{-1} in 10 mL containing 0.15 g L^{-1} trypsin and collecting samples over a period of 10 min, while mixing the suspension with an overhead stirrer. The samples were processed very quickly after collection (~ 10 sec) by settling the magnetic supports and recovering the supernatants for analysis.

5.2.5 Tryptic hydrolysis of whey

All hydrolysis experiments were performed using crude whey, at constant temperature (25 °C) and at constant pH (7.5). The whey was placed in a water bath at 25 °C and mixed by an overhead stirrer. When the whey reached 25°C, the pH was adjusted to 7.5 with 0.5 M sodium hydroxide (whey type I) or 1 M sodium hydroxide (whey type II) and a solution of 4 g L^{-1} trypsin in 100 mM Tris/HCl, 10 mM CaCl$_2$, pH 7.5 was added to a final concentration of 0.15 g L^{-1} trypsin. The pH was kept constant by the addition of sodium hydroxide 0.5 M, controlled by a pH-stat assembly from Radiometer (Copenhagen, Denmark), which consisted of a pH-meter PHM82, a titrator TTT80 and an auto-burette ABU80 (whey type I), or by the manual addition of sodium hydroxide 1 M (whey type II). The hydrolysis reaction was followed for periods of up to 6 h and samples were taken for SDS-PAGE analysis and determination of the degree of protein hydrolysis, trypsin activity and total protein concentration. Control hydrolysis experiments were performed in parallel under identical conditions, but in the absence of added trypsin.

5.2.6 Bench scale hydrolysis control studies with magnetic adsorbents

Tryptic hydrolysis of 50-mL and 100-mL whey (type I) aliquots was performed as described above. After 11 min, AGE-activated p-AB adsorbents were added to the hydrolysate to a final concentration of 4.5 g L^{-1} and kept in suspension using an overhead stirrer. After 4 min binding, the adsorbents were separated by magnetic settlement on a magnet block (for the 50-mL aliquot) or by pumping the suspension (for the 100-mL aliquot) through a 4-mL high-gradient magnetic filter exposed to an external magnetic field of 0.56 T generated by a Steinert HGF-10 high-gradient magnetic separator described later in section 5.2.7. The magnetic filter consisted of a 1 cm inner diameter plastic canister filled with a rolled mesh of stainless steel 430

wires yielding a voidage of 0.89, and was placed vertically in the 1.5 cm gap between the poles of the magnet. The suspension was pumped at a flow rate of 24 m h^{-1} by a peristaltic pump (model 503U, Watson-Marlow, Cornwall, England).

Following removal of magnetic adsorbents from the hydrolysate, the supernatant or magnetic filter permeate was recovered and kept at the same conditions as before, i.e., mixed by an overhead stirrer at 25 °C and pH 7.5. Throughout these experiments, samples were taken for SDS-PAGE and determination of the degree of protein hydrolysis, trypsin activity and total protein concentration.

5.2.7 Hydrolysis control and enzyme recovery using HGMF processing

HGMF apparatus and system set-up

The system employed for HGMF processing is depicted in figure 5.1. A laboratory type 'on-off' permanent magnet based high-gradient magnetic separator (Steinert HGF-10, Steinert Elektromagnetbau GmbH, Cologne, Germany) designed for biological applications was employed (Hoffmann *et al.*, 2002). The separator was set to have a 2.5 cm gap between the poles with a magnetic flux density of 0.32 T.

A high-gradient magnetic filter was placed vertically in the 2.5 cm gap between the poles of the magnet and consisted of a non-ferromagnetic (stainless steel 316) canister containing a 46 mL cassette filled with parallel magnetisable sheets of stainless steel 430 woven wire cloth, separated by spacers of stainless steel 304 woven wire cloth, giving a voidage of 86 % (Filter type Aa; see Ebner *et al.*, 2006). Other components of the HGMF system included: a batch adsorption reactor equipped with an overhead stirrer; two buffer containers; a fraction collector (SuperFrac 2211, LKB, Bromma, Sweden); a single peristaltic pump (Masterflex$^{®}$ Easy Load$^{®}$ model 7518-00, Cole Parmer Instrument Co., Vernon Hills, IL, USA) equipped with a 6.4 mm i.d. Norprene$^{®}$ A-60-F tube; and a set of four three-way solenoid switching valves (Bürkert-Contromatic A/S, Herlev, Denmark). The latter were used to control the flow path direction within the system enabling the following steps to be performed: (i) loading of magnetic adsorbent suspension from the batch adsorption reactor through the filter to the fraction collector; (ii) loading of elution or washing buffer through the

filter to the fraction collector; iii) recirculation of filter contents within a closed recycle loop. The total volume of the system recycle loop used in this study was 123 mL. The HGF-10 magnet, pump and valves were controlled by LabView software (Student Edition 6i, National Instruments Corporation, Austin, TX, USA).

The system used for the preliminary small scale HGMF processing employing a 5-mL magnetic filter is described in Heebøll-Nielsen (2004b). The magnetic separator was operated at 0.4 T and the volume of the recycle loop employed for washing and desorption operations was 15 mL.
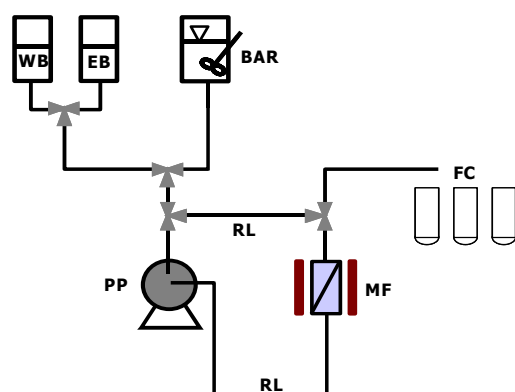
Fig. 5.1 Schematic diagram of the HGMF system employed in this work. MF = magnetic filter, FC = fraction collector, PP = peristaltic pump, WB = washing buffer container, EB = elution buffer container, RL = recycle loop, BR = batch adsorption reactor.

HGMF-mediated hydrolysis control

Tryptic hydrolysis was performed in 0.4 L of whey in a batch adsorption reactor in the presence of 0.15 g L^{-1} trypsin, at 25°C and pH 7.5. At a defined time (24 or 58 min), benzamidine-functionalised magnetic adsorbents, previously equilibrated with 100 mM Tris/HCl, 10 mM $CaCl_2$, pH 7.5, were added to the hydrolysate to a final concentration of 5.6 g L^{-1} or 7.6 g L^{-1}. After 6 min binding, all of the suspension was loaded to the 46-mL magnetic filter at a superficial linear velocity of 24 m h^{-1} (230 mL min^{-1}) while the magnetic field was 'on'. The magnetic adsorbents were collected on the filter, and the flowthrough (i.e. hydrolysate) was returned to the adsorption reactor (now free of adsorbents) where it was kept under hydrolysis conditions for ~4 h more, during which time sampling was continued.

149

Recovery of trypsin by HGMF processing

After binding of trypsin in whey to benzamidine-functionalised magnetic adsorbents, and collection of the latter on the high-gradient magnetic filter, a HGMF processing cycle was conducted. Two washing steps and four elution steps were used in order to recover the trypsin. First, the system (Fig. 5.1) was filled with washing buffer (100 mM Tris/HCl, 10 mM $CaCl_2$, pH 7.5) while the magnetic field was 'on'. Second, the 123-mL recycle loop was closed, the field was turned 'off', and the supports were recycled for 5 min (with change of flow direction every 1 min) at a superficial linear velocity in the filter of 80 m h^{-1} while the latter was mechanically vibrated. Third, the flow rate was decreased to 24 m h^{-1}, the field was turned 'on' and the supports were collected on the filter by recycling the suspension upwards with respect to the filter for 3 minutes. Fourth, with the field still 'on' the washing fractions were collected by loading washing buffer into the system for the second washing step. Steps one to four were then repeated using elution buffer instead of wash buffer, i.e., by loading the appropriate buffer to the system, recycling the supports in the recycle loop, collecting the supports and finally collecting the eluate by loading the next buffer. The buffer used to elute the trypsin from the adsorbents was 0.1 M glycine supplemented with 20 mM $CaCl_2$ at pH 2.6.

Prior to processing 0.4 L of whey, a small-scale HGMF process was performed in order to confirm the ability to use HGMF for trypsin recovery. The small-scale test was done in the same fashion as described above with the following modifications. The cheese whey (60 mL) was hydrolysed in presence of 0.1 g L^{-1} trypsin and 5 mM $CaCl_2$ by incubation for 60 min at 37 °C. The degree of hydrolysis was not monitored and the pH was adjusted before and after incubation to 7.5. After incubation, 55 mL of the hydrolysate was mixed with 275 mg of benzamidine-functionalised magnetic adsorbents previously equilibrated to binding conditions. Protease adsorption was allowed for 10 min, and the suspension was then applied to the HGMF system at a flowrate of 24 m h^{-1}. Washing and elution (2 cycles) were performed for 5 min recirculation at a flow-rate of 48 m h^{-1} and application of mechanical vibration.

5.2.8 Determination of the degree of hydrolysis

The degree of hydrolysis (DH) was determined by the trinitro-benzene-sulphonic acid (TNBS) method described by Adler-Nissen (1979), with small modifications as mentioned below. This method is based on the quantification of free amino groups that are released during hydrolysis of proteins. Duplicate aliquots (1 mL) of sample were pre-treated by mixing them with 5 mL of 1 % SDS previously heated to 95°C and kept at this temperature for at least 10 min to ensure that the trypsin was inactivated. Aliquots (0.125 mL) of the pre-treated samples were diluted in 1 mL 0.213 M phosphate buffer (pH 8.2) and mixed with 1 mL of a freshly prepared 0.1 % TNBS solution for 60 min at 50 °C in the dark. The reaction was stopped by adding 2 mL 0.1 N HCl to the samples and leaving them at room temperature for 20 min. The samples were diluted by the addition of 4 mL milli-Q water and were left for 10 min at room temperature. A HP845 UV Visible System Spectrophotometer was used for measuring the absorbance of the samples and standards at 340 nm. Standards of leucine in the concentration range of 0-3 mM were treated in exactly the same way as the samples. The 0 mM leucine standard was used as the absorbance blank. DH values were calculated using equation 5.2 (Adler-Nissen, 1979).

$$DH(\%) = 100 \left(\frac{h}{h_{tot}} \right)$$

Eq. 5.2

Here h is hydrolysis equivalents, i.e., the number of peptide bonds cleaved during a hydrolysis process and h_{tot} the total number of peptide bonds in a given protein. Values of h were obtained by comparison with a standard curve of L-leucine concentration (mM) versus absorbance at 340 nm followed by dividing the obtained values by the total protein concentration in the samples. Hydrolysis equivalents are therefore expressed in mM leucine equivalents per gram protein. A recommended h_{tot} value (mmol equivalents g^{-1} protein) of 8.8 for whey concentrate (Adler-Nissen, 1986) was used in our calculations.

5.2.9 Other analytical methods

Total protein was measured with a BCA protein assay (Pierce Rockford, IL, USA), which was used as recommended by the manufacturer. All protein concentrations were expressed in mg bovine serum albumin (BSA) equivalents. Activity of trypsin was analysed by hydrolysis of BAPNA (Erlanger *et al.*, 1961) as described by Hubbuch and Thomas (2002). One sample volume was mixed with a reagent solution consisting of 1 volume 0.04 M BAPNA in DMSO and 7 volumes of 100 mM Tris/HCl buffer at pH 7.6, and the activity was calculated from the recorded change in absorbance at 405 nm. Both the BCA and trypsin assays were scaled for use with a Cobas Mira robot spectrophotometer (Roche Diagnostic Systems, Rotkreutz, Switzerland). Based on BCA and BAPNA assays, the specific activity of trypsin was estimated to be 19.5 U mg^{-1} (determined by standard curves based on purified trypsin at binding conditions; the correlation coefficient R^2 was 0.996).

Visualization of the protein composition of whey hydrolysates was done by reducing SDS-PAGE analysis in NuPAGE® Novex Bis-Tris gels, using NuPAGE® MES SDS as the running buffer and Coomassie staining. Precast SDS-PAGE gels, buffers, stain and markers (Mark 12™) were purchased from Invitrogen (Groningen, The Netherlands) and used according to the manufacturers instructions. Prior to SDS-PAGE analysis, the samples (50 μL aliquots) were precipitated by the addition of 50 μL of TCA followed by incubation on ice for a minimum period of 20 min. The pellet was washed with 5 mM HCL in acetone and then with pure acetone (50 μL each). The pellet was finally resuspended in 100 μL of NuPAGE® LDS sample loading buffer.

Magnetic particle content was determined using a dry weight method. The magnetic particles in a suspension of defined volume were separated from the liquid phase by magnetic settlement and the supernatant discarded. In the case of the adsorbents that had been in contact with biological material, the particles were washed three times with elution buffer, three more times with 1 M NaOH followed by three washes with Milli-Q water. The particles were resuspended in ≤ 1 mL of milli-Q water, transferred to 5-mL pre-weighed pyrex tubes and dried to constant weight by incubating at 95 - 100 °C overnight. The tubes were cooled to room temperature in a desiccator for at

least 2 h and weighed again. The particle concentration was determined from the difference between the final and initial weighed tubes and the exact volume of the original sample suspension.

5.3 Results and discussion

5.3.1 Adsorbent preparation and characterisation

In recent work we have shown how benzamidine-derivatised magnetic supports can be employed successfully to recover trypsin by HGMF from both crude porcine pancreatin (Hubbuch, 2001; Hubbuch and Thomas, 2002) and cheese whey feedstocks (Hubbuch, 2001). One of the aims of the current work was to develop improved types of magnetic adsorbents for removal and recovery of trypsin. With that purpose, a range of magnetic affinity adsorbents were constructed and characterised with respect to their binding properties for trypsin. The traditional preparation of affinity adsorbents involves an initial activation step, in which a bifunctional molecule is attached to the matrix via one reactive end, leaving the terminal group available for reaction with a ligand molecule. This further serves to introduce a spacer arm of a suitable length between the support surface and the ligand, allowing the ligand to interact with a specific site in the target protein. We used two activation agents, BDE and DVS, that have been successfully employed with superparamagnetic supports to produce affinity adsorbents with both high capacities and tight protein-ligand interaction (O'Brien *et al.*, 1996; Hubbuch *et al.*, 2001; Hubbuch and Thomas, 2002). However, both BDE and DVS are homobifunctional reagents and there is a risk that the reactive group attached during activation may undergo premature hydrolysis during this initial step in the reaction sequence. Following up on the work of Burton and Harding (1997a, b), who demonstrated how activation with AGE could increase the ligand density compared to that which could be achieved using either BDE or epichlorohydrin, another well-described epoxy activation agent, we selected this chemical route as a third strategy for the activation of our magnetic adsorbents. AGE is a heterobifunctional molecule, which in common with BDE, becomes affixed to the matrix via a reactive oxirane ring (Fig. 5.2). In contrast to the epoxy-groups attached to the particle surface by BDE-activation, reaction with AGE results in

immobilisation of more stable, terminal allyl groups. The double bonds of the allyl moieties can easily be brominated with NBS under mild aqueous conditions resulting in formation of bromohydrin groups suitable for nucleophilic substitution reactions (Fig. 5.2). AGE and BDE activation chemistries have been employed in the construction of metal affinity magnetic adsorbents derivatised with iminodiaceticacid and the first resulted in adsorbents of superior performance (Heebøll-Nielsen *et al.*, 2003).
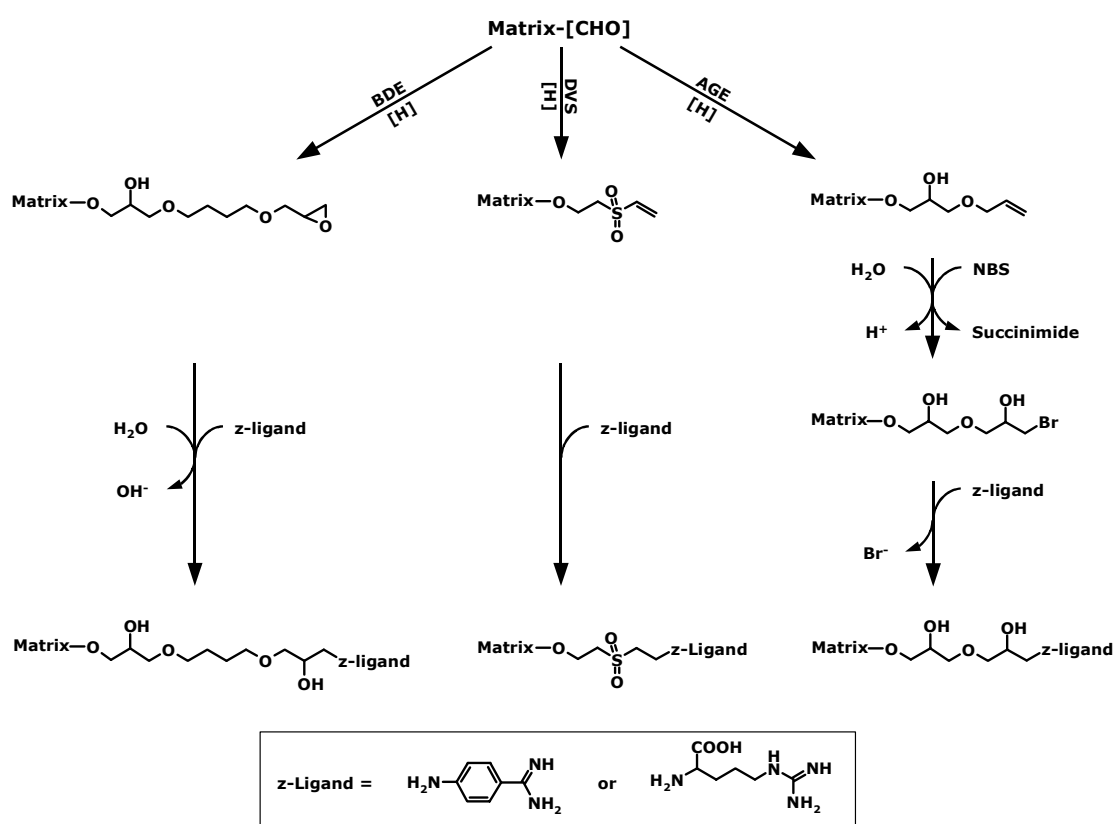
Fig. 5.2 Activation with BDE, DVS and AGE, and subsequent coupling of ligand molecules carrying a nucleophilic group (denoted 'z') to the activated matrices.

The activated supports were further functionalised with arginine or benzamidine, two classic affinity ligands for trypsin (Hermanson *et al.*, 1992) resulting in the production of six different types of adsorbents. The adsorbents were compared by conducting small-scale binding studies and obtaining the trypsin adsorption isotherms for each adsorbent (Fig. 5.3). The estimated Langmuir parameter values for the isotherms,

summarised in table 5.1, are useful for comparing adsorption data, as they give a direct indication of the potential utility of the supports.

(a)   **(b)**

(c)
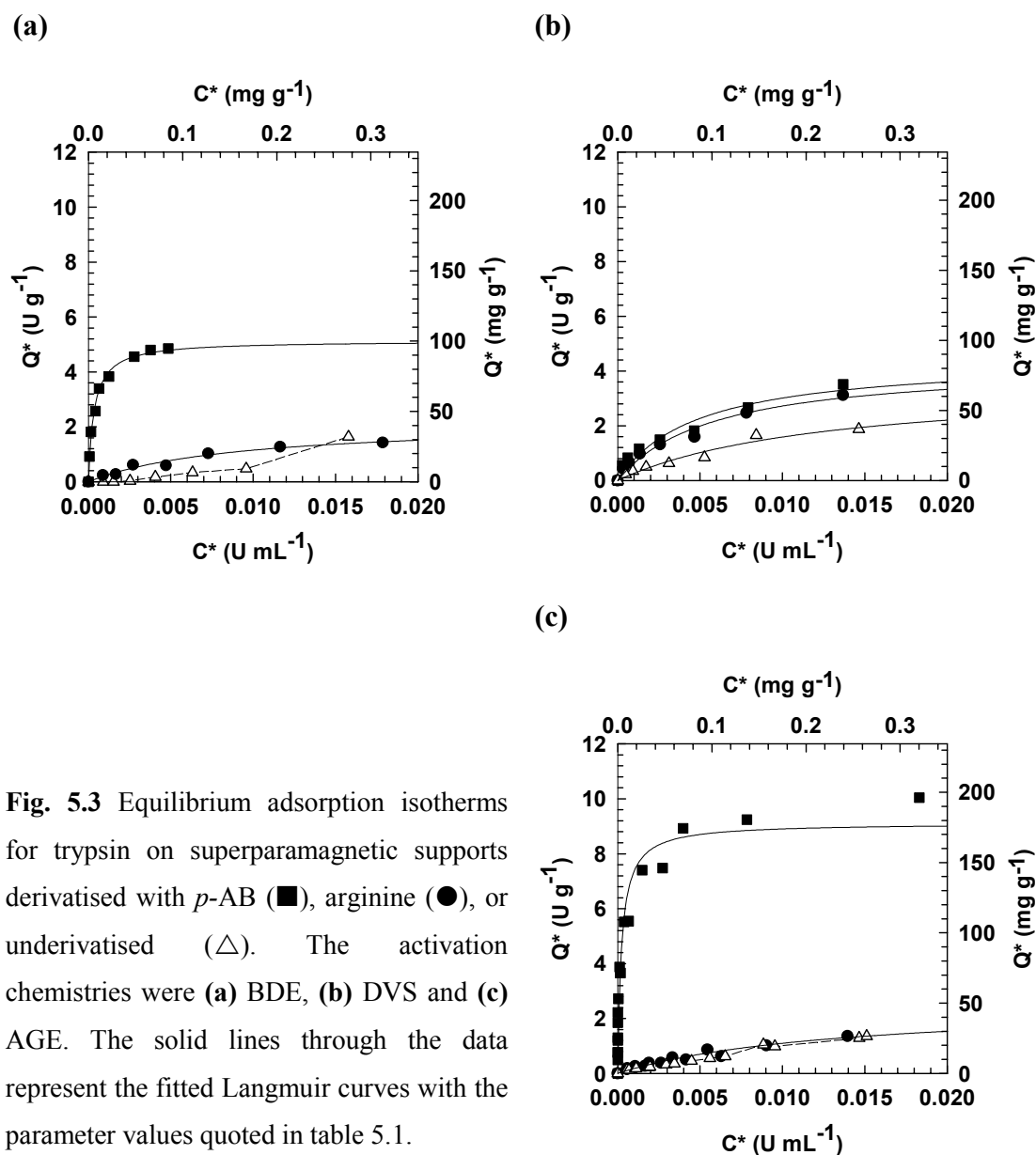
Fig. 5.3 Equilibrium adsorption isotherms for trypsin on superparamagnetic supports derivatised with *p*-AB (■), arginine (●), or underivatised (△). The activation chemistries were **(a)** BDE, **(b)** DVS and **(c)** AGE. The solid lines through the data represent the fitted Langmuir curves with the parameter values quoted in table 5.1.

Despite its use as a commercial trypsin ligand, arginine did not perform satisfactorily when attached to the activated supports. Slightly better results for arginine were observed when the inhibitor was coupled to a DVS activated matrix (Fig. 5.3b). In this case a maximum capacity of 84 mg g^{-1} was observed. However, the high dissociation constant resulted in an unsatisfactory initial slope of the isotherm curve. Moreover,

this support type was only slightly different from its corresponding control, which also adsorbed trypsin with some apparent specificity (K_d = 8.7 µM). Derivatisation of PG-coated superparamagnetic supports with bacitracin following activation with DVS have been shown to yield a four-fold higher ligand density than was possible with either epichlorohydrin or BDE (Hubbuch et al., 2001). It was therefore expected that DVS would yield trypsin affinity supports with significantly improved characteristics compared to the BDE-p-AB adsorbents employed by Hubbuch and Thomas (2002). However, this was surprisingly not the case with the DVS-p-AB adsorbents presenting a Q_{max}/K_d value 16 fold lower than the value obtained for BDE-p-AB adsorbents (Fig. 5.3a). The poor performance may be caused by insufficient spacer capacity of the five atoms introduced in the reaction sequence (Fig. 5.2).

Table 5.1 Langmuir binding parameters for adsorption of trypsin

Activation chemistry	Ligand	Q_{max} (mg g^{-1})	K_d (µM)	Q_{max}/K_d (L g^{-1})
BDE	None	n.a.	n.a.	n.a.
BDE	Arginine	43	5.6	0.27
BDE	p-AB	100	0.24	15
DVS	None	71	8.7	0.28
DVS	Arginine	84	3.9	0.74
DVS	p-AB	87	3.3	0.92
AGE	None	n.a.	n.a.	n.a.
AGE	Arginine	50	9.0	0.19
AGE	p-AB	178	0.16	38

n.a. Not applicable. The data could not be fitted to the Langmuir model.

Superior results were found for the AGE-p-AB combination (Fig. 5.3c) which produced an adsorbent with Q_{max} = 178 mg g^{-1} and K_d = 0.16 µM, yielding a high value of 38 L g^{-1} for the initial slope (Q_{max}/K_d). Comparison to the control supports prepared by reacting AGE-activated particles under coupling conditions in the absence of ligand molecules further indicated that the spacer arm alone did not interact with the enzyme, as little protein was seen to bind. Immobilisation of benzamidine via the AGE-route confirmed the advantages of this chemistry over BDE (Burton and Harding, 1997a, b; Heebøll-Nielsen, 2003), as the maximum capacity was increased nearly two-fold, while still retaining very tight interaction. The dissociation constants were very similar in both cases, suggesting that the 7 atom

spacer introduced by AGE (compared to the 12-atom spacer of BDE) allowed specific interaction between immobilised benzamidine and the active site of trypsin.

The AGE-*p*-AB adsorbent, due to its best performance in terms of trypsin binding in a pure system, was selected for further studies using porcine pancreatin extract as a source of trypsin. The isotherm constructed from batch binding experiments using this more complex system (Fig. 5.4a) shows that, despite a small deviation of the data from the Langmuir model, the adsorbents presented comparable binding properties as when tested with the monocomponent system (Fig. 5.3c), i.e., a slightly higher maximum capacity of 225 mg g^{-1} and a tight interaction with trypsin, as indicated by the low K_d value (0.3 μM).

Following binding of trypsin from porcine pancreatin, desorption of unspecifically bound or entrapped material on the AGE-*p*-AB adsorbents was investigated, as well as determination of optimal conditions for desorbing bound trypsin. Desorption of most of the non-specifically bound protein (72 %) occurred in the first washing step with equilibration buffer (100 mM Tris/HCl, 10 mM CaCl$_2$, pH 7.5) with a loss of only 11 % of the bound trypsin activity (Fig. 5.4b). Two more washes were less efficient, increasing the total amount of desorbed protein only up to 88 % at the expense of a constant loss of trypsin (25 % of the activity after 3 washes). Desorption of trypsin from AGE-*p*-AB supports after a three-step wash was considerably more efficient by changing pH than by competitive elution (Fig. 5.4c & Fig. 5.4d). When the equilibration buffer was supplemented with either arginine (Buffer A) or benzamidine (Buffer B), very poor elution efficiencies were observed and after three elution steps only 20 % of trypsin activity was desorbed from the supports, although 60 % of the protein was desorbed when applying the benzamidine buffer. Lowering the pH to 2.6 (Buffer C) resulted in 97 % desorption of trypsin, with 90 % released in the first elution cycle. Increase of buffer strength (Buffer D) or addition of NaCl (Buffer E) did not improve the elution efficiency any further.
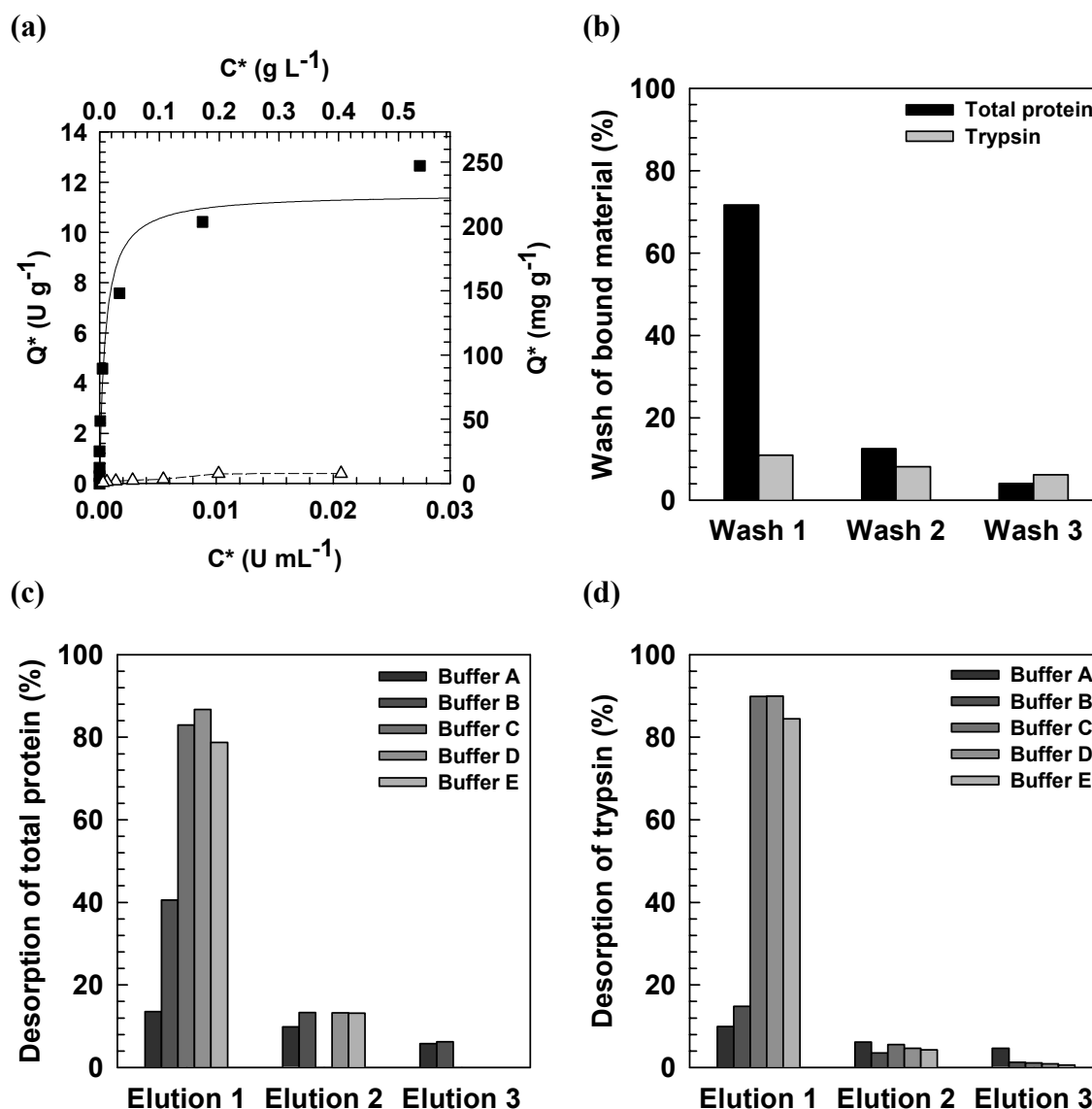
Fig. 5.4 Studies of *p*-AB magnetic support behaviour with trypsin from porcine pancreatin: **(a)** Equilibrium adsorption isotherm for trypsin from porcine pancreatin on superparamagnetic *p*-AB supports (■) and underivatised AGE-activated supports (△). The solid line through the data represent the fitted Langmuir curve (Q_{max} = 11.5 U g^{-1} or 225 mg g^{-1}; K_d = 0.0005 U mL^{-1} or 0.3 μM); **(b)** Desorption of trypsin and total protein from benzamidine-linked magnetic supports under washing conditions after binding in porcine pancreatin; Elution of **(c)** bound protein and **(d)** bound trypsin activity from porcine pancreatin to benzamidine-linked magnetic supports. Supports were washed 3 times before applying the following buffers: binding buffer supplemented with arginine (Buffer A) or benzamidine (Buffer B), 10 mM glycine/HCl, pH 2.6 (Buffer C), 50 mM Glycine/HCl, pH 2.6 (Buffer D) and 50 mM Glycine/HCl supplemented with 0.1 M NaCl, pH 2.6 (Buffer E).

The tests performed to the AGE-*p*-AB adsorbents in porcine pancreatin confirmed the good binding properties of the supports regarding specificity and capacity as was observed in the studies with pure trypsin. Furthermore the behaviour of the supports regarding desorption selectivity and efficiency, i.e., preferential release of unspecifically bound material during wash conditions and efficient release of trypsin under the appropriate elution conditions, indicate that these supports are suitable for applying to the test of controlling trypsin mediated hydrolysis and enzyme recovery.

Recovery of trypsin from cheese whey

Small-scale studies were performed to determine the amount of AGE-*p*-AB supports necessary to remove trypsin from a whey hydrolysate. The concentrations of 0.10 and 0.15 g L^{-1} trypsin spiked in whey used in these studies are within the range of enzyme:protein ratio (approximately 1-2 % w/w) that is commonly employed in hydrolysis of whey (Margot *et al.*, 1997; Pintado *et al.*, 1999; Schlothauer *et al.*, 1999). The crudeness of whey did not seem to have any impact on the performance of AGE-*p*-AB adsorbents (Fig. 5.5a). Almost complete removal of trypsin (97.5 %) from the 0.15 g L^{-1} trypsin solution in clarified whey was achieved by the addition of 5.3 g L^{-1} support and only 4.4 g L^{-1} support was necessary to remove 99.7 % of the trypsin present in crude whey. Further increases of the support concentration results in a higher extent of unspecific binding (Fig. 5.5a). Removal of trypsin from crude whey using 5.5 g L^{-1} adsorbents was achieved in approximately 4 min (Fig. 5.5b). However, when only 0.1 g L^{-1} of trypsin was spiked in crude whey, almost the same amount of adsorbents was needed to remove trypsin, i.e, 5.5 g L^{-1} of support to remove 95 % of the trypsin activity. The differences between the behaviour of the adsorbents under the different conditions could only be observed when constructing isotherms (Fig. 5.5c). In all cases the adsorbents presented a lower maximum binding capacity for trypsin in whey (Table 5.2) than for trypsin in equilibration buffer (Table 5.1) and in porcine pancreatin (Fig. 1.4a). The presence of solid matter in whey had little effect on the binding properties of the adsorbents as shown by the similar Langmuir parameters for the experiments conducted with clarified and crude whey (Q_{max}/K_d = 10.5 and 11.6 L g^{-1}, respectively). However, despite the fact that we are working with high affinity

adsorbents, when working at a lower concentration of trypsin, the adsorbents bind less tightly (Q_{max}/K_d = 4.3 L g^{-1}), possibly due to increased competition from other proteins in whey that bind non-specifically to the surface of the adsorbents. The presence of lipids or competing enzymes in whey might also help explaining the differences observed in adsorbent performance.

(a)

(b)

(c)
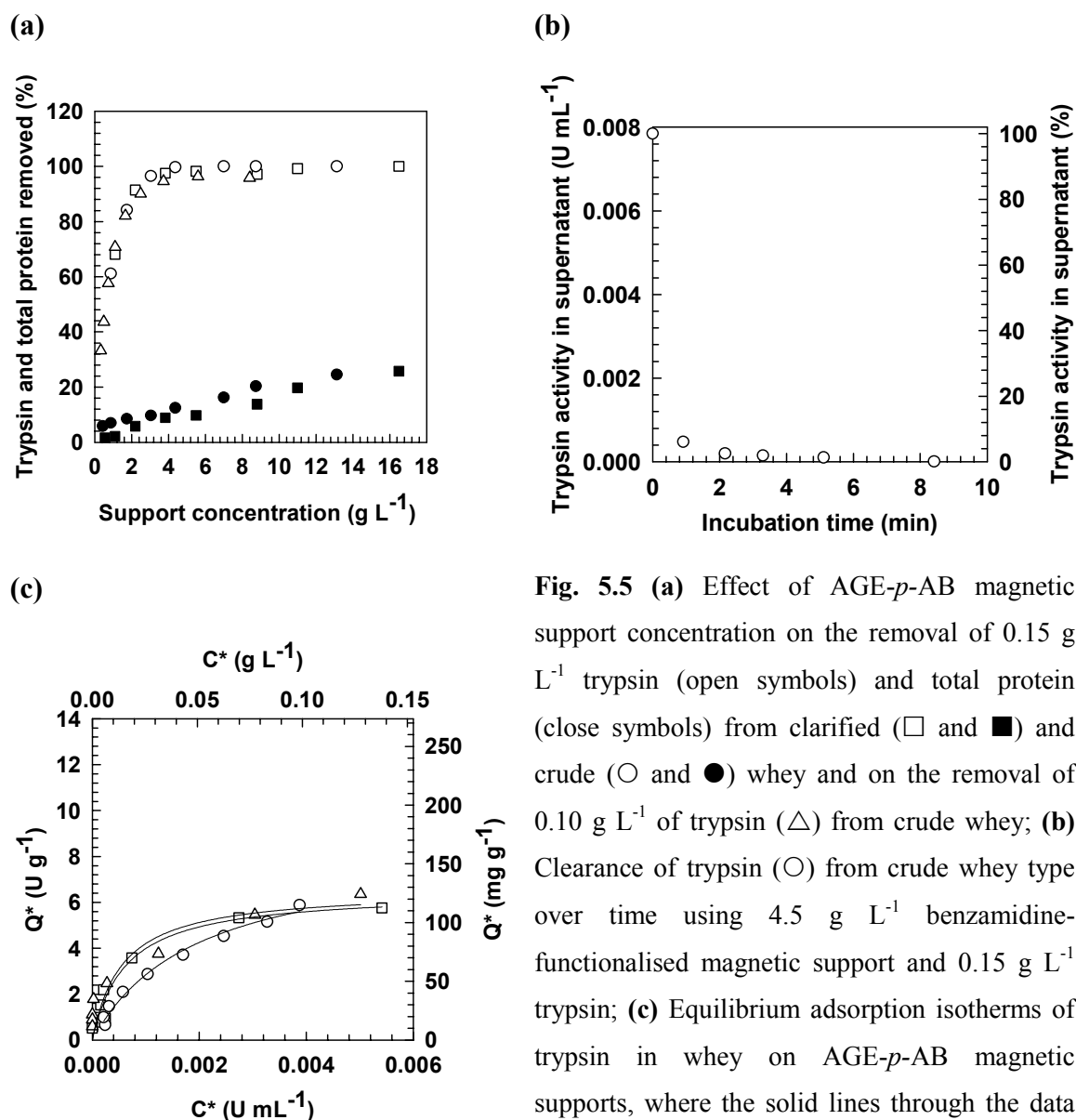
Fig. 5.5 (a) Effect of AGE-*p*-AB magnetic support concentration on the removal of 0.15 g L^{-1} trypsin (open symbols) and total protein (close symbols) from clarified (□ and ■) and crude (○ and ●) whey and on the removal of 0.10 g L^{-1} of trypsin (△) from crude whey; **(b)** Clearance of trypsin (○) from crude whey type over time using 4.5 g L^{-1} benzamidine-functionalised magnetic support and 0.15 g L^{-1} trypsin; **(c)** Equilibrium adsorption isotherms of trypsin in whey on AGE-*p*-AB magnetic supports, where the solid lines through the data represent the fitted Langmuir curves.

Table 5.2 Langmuir parameters for binding isotherms of AGE-*p*-AB adsorbents and tryspin in whey.

Type of whey	Trypsin conc. (g L^{-1})	Q_{max} (mg g^{-1})	K_d μM	Q_{max}/K_d (L g^{-1})
Clarified	0.15	126	0.42	10.5
Crude	0.15	128	0.38	11.6
Crude	0.10	165	1.3	4.3

5.3.2 Preliminary HGMF testing

A preliminary experiment for testing the efficiency of trypsin recovery from a whey hydrolysate when processed by HGMF was conducted and the results are shown in figure 5.6 and table 5.3. A 5 g L^{-1} AGE-*p*-AB adsorbent concentration was used to remove 0.10 g L^{-1} of trypsin from whey, based on the results obtained in the batch binding studies described above. Trypsin was recovered from the whey hydrolysate using a 10 min adsorption step prior to loading the adsorption suspension to a 5 mL high-gradient magnetic filter. In this case, ~97 % of the trypsin could be removed and the adsorbent free hydrolysate collected, which contained 86 % of the protein originally present. The trypsin was subsequently recovered by the magnetic filter employing the optimal desorption conditions determined by the porcine pancreatin studies, i.e., one wash with equilibration buffer followed by two elution steps with 10mM glycine/HCl, pH 2.6. The latter yielded 75 % of the added protease. Because desorption was mediated by a change in pH to 2.6, the loss of 25 % trypsin was thought to be partly due to inactivation. We thus performed stability tests to trypsin in 10mM glycine/HCl, pH 2.6 at room temperature and observed a decrease in the measured trypsin activity over time[1]. For example, assuming that the total time for handling an elution step (i.e., release of trypsin from adsorbents in the HGMF recycle loop, collection of the adsorbents on the filter and collection of the elution fraction from the HGMF system) was approximately 10 minutes, ~6 % of an initial trypsin activity of 0.005 U mL^{-1} would be lost by inactivation. Another reason for the poor

---

[1] The estimated first-order inactivation function for trypsin based on activity measurements of 0.3 g L^{-1} trypsin in 10 mM glycine/HCl, pH 2.6 at room temperature was the following: Trypsin (U mL^{-1}) = 0.016 exp(-0.0065 t/min).

recovery might be an insufficient number of elution cycles. Parallel studies done in test tubes under the same conditions as with the HGMF above, except with 1.5 g L^{-1}, showed that 95 % of trypsin could be desorbed in two elution steps (data not shown). However elution in the HGMF was performed at an adsorbent concentration of 18 g L^{-1} due to concentration of the adsorbents in the small filter-recycle loop used. The ~10-fold higher adsorbent concentration in the magnetic filter than in the test tube experiments, may lead to a lower desorptive driving force. Introduction of further elution buffer to the system might thus be expected to desorb the remaining material bound to the supports, and therefore we decided to conduct more than two elution steps in future experiments.
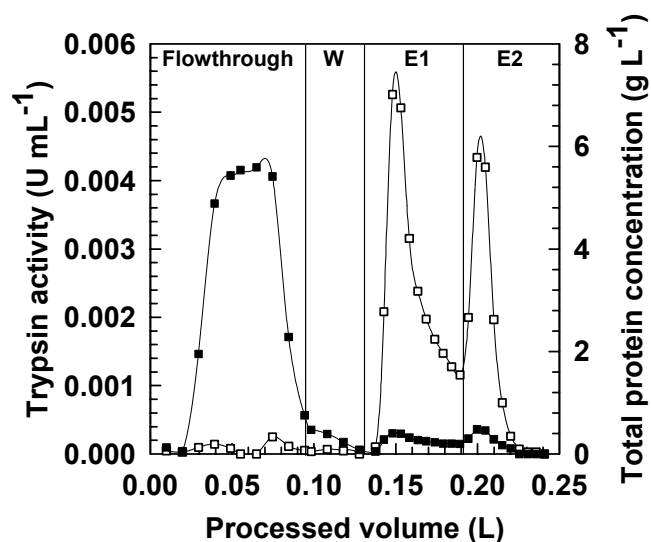
Fig. 5.6 Trypsin activity ($\square$) and protein concentration ($\blacksquare$) profiles obtained during HGMF processing with a 5 mL filter of whey hydrolysate following incubation with 0.10 g L^{-1} trypsin. Wash and elution fractions are represented by W and E, respectively.

It is conceivable that the shear created by the high flow velocity used during elution was insufficient to release all particles from the filter so that part of the adsorbents still existed as a tightly packed inaccessible mass. Such behaviour has been demonstrated previously (Hubbuch and Thomas, 2002; Gomes *et al.*, 2006). An indication that this might have been the case is that only 87 % of the adsorbents could be accounted for after elution, when the adsorbents were recovered from the filter. The filter was not loaded fully to the determined capacity (of 65 g L^{-1} at 10 % breakthrough; Heebøll-Nielsen *et al.*, 2004b), instead only 50 g L^{-1} filter matrix was applied to ensure that an adsorbent-free hydrolysate would be obtained after

processing. This may have an influence on the release efficiency of the supports in the desorption steps.

5.3.3 Control of cheese whey protein hydrolysis

Before studying the strategy of using HGMF to control trypsin hydrolysis, we conducted a series of control studies where the hydrolysis occurring in the substrate was monitored. The concept of using the degree of hydrolysis (DH) as a measure of the extent of protein hydrolysis for control purposes is not new (Adler-Nissen, 1982, 1986). Adler-Nissen (1979) defined DH as the percentage of peptide bonds cleaved, and there are several methods available for determining this, such as the pH-stat and various colorimetric based methods (*o*-phthaldialdehyde, OPA; ninhydrin and trinitrobenzene sulphonic acid, TNBS). In the work done by Panasiuk *et al.* (1998), it was suggested that results obtained using OPA and TNBS are the most correct. Moreover, in a recent comparison of pH-stat, OPA and TNBS methods, the latter was shown to be the most suitable for an accurate quantification of DH in whey protein hydrolysates (Spellman *et al.*, 2003), and it is for this reason that TNBS was employed for the determination of DH in the current work.

Tryptic hydrolysis curves for whey proteins

Hydrolysis experiments were conducted in the two different types of whey used in this work. The first, type I, was used for all preliminary experiments including testing of the supports and bench-scale hydrolysis control studies. The second, type II, will be introduced later in this work.

Trypsin was added to both types of whey to a final concentration of 0.15 g L^{-1}. Within the enzyme:protein range commonly used for protein whey hydrolysis (approximately 1-2 % w/w, as mentioned above) this value was chosen for practical reasons, since preliminary studies indicated that at room temperature this concentration would enable us to observe significant changes in the DH within a reasonable time frame, i.e, between 4 to 6 hours. Under these conditions the DH of whey type I increased up to ~ 5 % within the first hour of incubation and continued increasing at a slower rate during the last 5 hours of incubation reaching a value of ~ 8 % (Fig. 5.7a). The

progression of hydrolysis in whey type II had a different outcome and DH was observed to increase steadily, reaching a value of ~ 7 % within 5 h (Fig. 5.7b). In the absence of 'added' trypsin to whey type I, a DH value of ~ 2 % was measured after 5 hours, whereas in whey type II, the DH attained a plateau value of ~1 % after ~ 1 h and remained at this level throughout the duration of the experiment (Fig. 5.7a & Fig. 5.7b). Another distinction between the two types of whey was that the activity of the incubated trypsin decreased steadily over time when in whey type I, whereas in whey type II the activity decreased slightly in the first hour and then stabilised. This might partially explain the differences observed in the hydrolysis curves obtained for whey type I and type II.

(a)   **(b)**
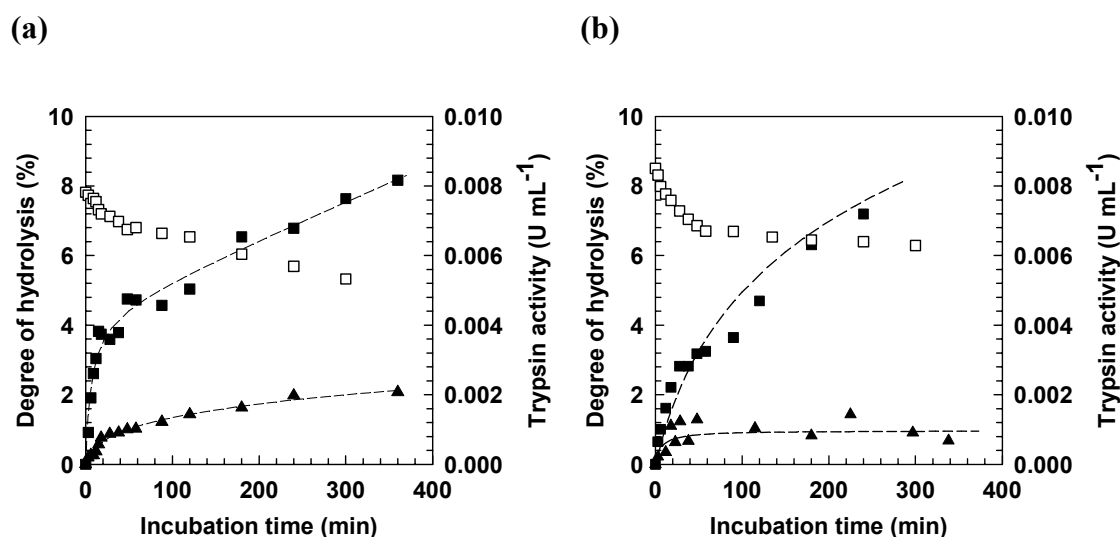
Fig. 5.7 Hydrolysis curves for whey proteins type I **(a)** and type II **(b)** incubated at 25 °C and pH 7.5 with 0.15 g L^{-1} trypsin (■) and in the absence of trypsin (▲). Trypsin activity in the hydrolysate over time (□).

The theoretical maximum DH in cheese whey was estimated to be 11 % based on the lysine and arginine composition of the substrate (11.20 and 3.01 g free amino acid per 100 g protein, respectively, as recommended by Adler-Nissen, 1986), given that trypsin specifically catalyses the cleavage of peptide bonds on the carboxylic side of lysine and arginine only. Our results are in agreement with the estimated DH value and furthermore, when we measured the degree of hydrolysis of whey type I initially

incubated with 0.5 g L^{-1} trypsin 24 and 48 h later[2], we obtained values of 9.5 and 10 %, respectively.
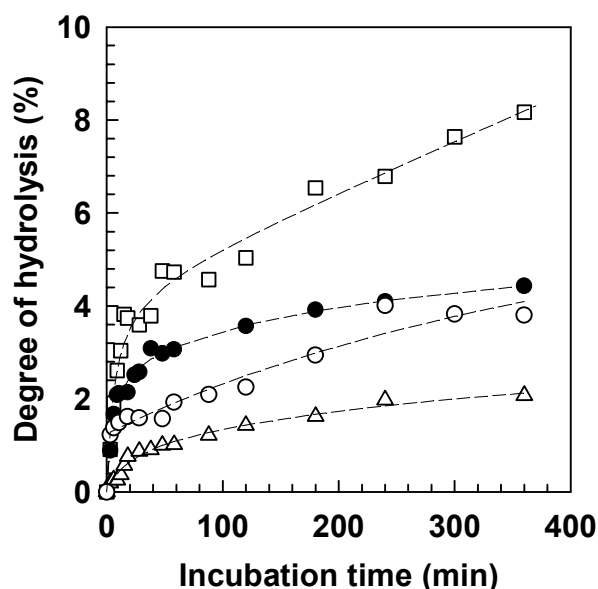
Fig. 5.8 Progression of degree of hydrolysis in whey (type I) incubated with 0.15 g L^{-1} trypsin, then after 11 min mixing with benzamidine-functionalised magnetic support for 4 min followed by removal of the supports by magnetic settlement (●) or with a high-gradient magnetic filter (○). Hydrolysis curve (□) and baseline curve (△) from figure 5.7a used as reference.

Hydrolysis control studies

Addition of AGE-*p*-AB adsorbents to whey hydrolysate after 11 min of incubation with 0.15 g L^{-1} of trypsin followed by removal of the supports resulted in a slowdown of the hydrolysis curves in two cases examined in which separation of the supports was done using a magnet block or the HGM filter (Fig. 5.8). In the first case the amount of adsorbents added (4.5 g L^{-1}) were sufficient to remove almost all the trypsin present in the hydrolysate (99 % removed) and the slow increase in DH observed after adsorbent removal was of the same extent as the baseline, i.e., of the DH curve obtained in the absence of 'added' trypsin. However, the termination of trypsin-mediated hydrolysis is not very sharp and a slight increase could still be seen in the initial period after removal of the adsorbents. This increase was due to the finding that it took approximately 10 min to remove completely the supports after the 4-min binding period when using the bar magnet. Interestingly we have observed in preliminary experiments that adding the magnetic adsorbents does not halt hydrolysis

---

[2] The pH was not kept constant at 7.5 after the initial 5h.

until the loaded adsorbents are removed from solution. Loading of the suspension of AGE-*p*-AB adsorbents after 4-min binding to an HGM filter results in a sharper halt in hydrolysis since this separation process took only 3 minutes. However monitoring of the flowthrough showed that in this experiment only 70 % of trypsin activity had been removed and the remaining activity caused the continued slow increase of DH (Fig. 5.8).

5.3.4 Integrated system: Control of whey protein hydrolysis by HGMF and recovery of trypsin

Following the investigation and optimisation of the different processes involved in this work, an integrated system was set up in order to control cheese whey protein hydrolysis by HGMF processing. With this system it was possible to remove trypsin activity by binding the enzyme to magnetic adsorbents followed by a rapid separation of the adsorbents and subsequent recovery of the enzyme from the supports. A 46 mL HGMF filter was employed, permitting the capture of approximately 3.6 g of adsorbent[3]. Under the conditions used here, scale-up of the adsorbent manufacture was required.

Scale-up of production of AGE-p-AB adsorbents

The manufacture of AGE-*p*-AB adsorbents was scaled-up to 4 g (40 times) and the performance of the new adsorbents was tested in two simple studies of binding to trypsin in equilibration buffer and in whey type II. For the pure system, the values for the Langmuir parameters Q_{max} and K_d were calculated to be 225 mg g^{-1} and 1.2 μM respectively. Despite the higher value for Q_{max} as compared to the AGE-*p*-AB adsorbents presented previously in this work (Q_{max} = 178 g L^{-1}, Table 5.1), a higher value for K_d was obtained (as compared to 0.16 μM; Table 5.1). Nevertheless, the

---

[3] The filter was characterised by conducting breakthrough experiments with a suspension of magnetic supports, loaded at 22 m h^{-1} in presence of a magnetic field density of 0.32 T. The capacity calculated at 5 % breakthrough was 79 g L^{-1}. This value provides an indication of the maximum limit for filter load. Furthermore, when loading a suspension of magnetic adsorbents in whey to the magnetic filter at 24 m h^{-1} and 0.32 T, corresponding to a filter capacity of 65 g L^{-1}, no breakthrough was observed.

adsorbents produced in the larger batch sizes were observed to have suitable characteristics for trypsin removal from crude whey. When crude whey was spiked with 0.2 g L^{-1} trypsin a support concentration of only 4.9 g L^{-1} was needed to remove 99.8 % of the added trypsin and only 8 % of the total protein. From these screening studies it was concluded that a minimum support concentration of 5 g L^{-1} was required to remove the 0.2 mg L^{-1} of added trypsin employed for the hydrolysis of crude whey.

Hydrolysis control by HGMF

Hydrolysis experiments were conducted by incubating trypsin in whey type II under the same conditions as described above. In two parallel studies, the AGE-*p*-AB adsorbents were added to the hydrolysate in the batch reactor after 24 min (using 5.6 g L^{-1} adsorbents) in one case and 58 min (using 7.6 g L^{-1} adsorbents) in the other, in order to permit different degrees of hydrolysis to be reached. After 6 min of binding, the supports were pumped through the HGMF filter and collected within 2 min. When the flowthrough was examined it was found that 99.1% or 99.9 % of the added trypsin had been removed following processing with 5.6 g L^{-1} or 7.6 g L^{-1} adsorbents, respectively. Although 5 g L^{-1} would be sufficient, higher amounts of adsorbent were employed to guarantee complete removal of trypsin from the hydrolysate. In both cases little further hydrolysis was seen (Fig. 5.9a) and the resulting DH values were 2 % and 4 % for the processes controlled after 24 min and 58 min, respectively. Additionally, no further change in pH was observed after HGMF processing, providing further evidence that hydrolysis had been terminated. The control of whey protein cleavage by adding adsorbents and removing them by HGMF could also be clearly seen when samples were analysed by SDS-PAGE (Fig. 5.9b). When no adsorbents were used, the band corresponding to β-lactoglobulin became greatly diminished over time (Fig. 5.9b, lanes 2–12). In contrast, no such decrease in β-lactoglobulin was observed after addition and subsequent removal of the AGE-*p*-AB supports (Fig. 5.9b, lanes 17–24). The preferential hydrolysis of β-lactoglobulin by trypsin is consistent with the reports of Pintado *et al.* (1999).

(a)

(b)
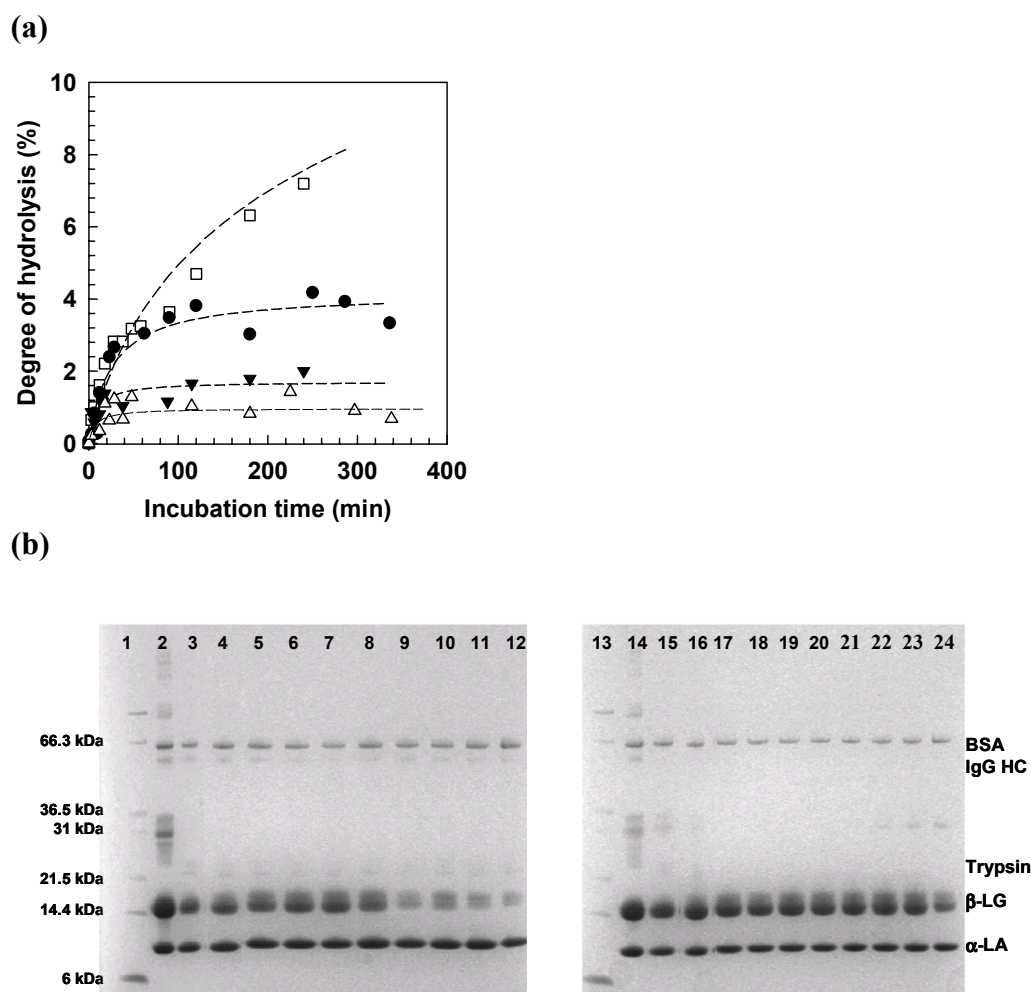
Fig. 5.9 (a) Progression of hydrolysis in whey incubated with 0.15 g L^{-1} trypsin, mixing with AGE-*p*-AB after 24 min (▼) and 52 min (●) and processing by HGMF. Hydrolysis curve (□) and baseline curve (△) from figure 5.7b, whey type II, used as reference; Reducing SDS-PAGE analysis of samples taken during trypsin hydrolysis of whey **(gel on the left)** without adsorbents added and **(gel on the right)** with adsorbents added after 24 min of hydrolysis and HGMF processing. Lanes 1 and 13, molecular weight markers; lanes 2 and 14, whey. The remaining lanes correspond to samples removed after the following incubation times: **(gel on the left)** – 0 min (lane 3), 9 min (lane 4), 38 min (lane 5), 48 min (lane 6), 58 min (lane 7), 120 min (lane 8), 180 min (lane 9), 240 min (lane 10), 300 min (lane 11) & 360 min (lane 12); **(gel on the right)** – 0 min (lane 15), 9 min (lane 16), 32 min (lane 17), 38 min (lane 18), 48 min (lane 19), 58 min (lane 20), 88 min (lane 21), 120 min (lane 22), 180 min (lane 23), & 240 min (lane 24). Abbreviations: β-LG, β-lactoglobulin; α -LA, α -lactalbumin; IgG-HC, immunoglobulin heavy chain.

The final degree of hydrolysis was in agreement with the predicted value based on results obtained from previous hydrolysis studies (Fig. 5.7b). Despite the 8-fold increase in processed volume of whey, compared to bench experiments where a magnet bar was used to separate the magnetic adsorbents, the hydrolysis could be stopped more efficiently using HGMF. Furthermore, the 4-fold increase in processed volume when compared to the experiment done with the 5-mL HGMF filter (Fig. 5.8) had no negative impact on the precision achieved for the final degree of hydrolysis. Although, this work has not demonstrated any negative effects due to scaling-up on the outcome of the hydrolysis control process, this is a problem that can be anticipated when industrial-scale volumes are to be processed. Higher loading times of the adsorbent suspension and therefore slower separation of the trypsin-bound supports from the hydrolysate will probably influence the precision of the HGMF process in stopping hydrolysis at the desired DH value if a batch reactor was used. A solution would be to use continuous processing, a possibility that has been previously demonstrated for HGMF by Ferré (2006).

Recovery of trypsin by HGMF processing

After binding of trypsin and subsequent collection of the adsorbents on the magnetic filter essentially no trypsin passed out of the filter to contaminate the whey flowthrough, i.e., 99.1 % of trypsin present in the hydrolysate was removed (Table 5.3). Following filter loading, two washes were performed and 43 % of the nonspecifically bound proteins were desorbed with little loss of adsorbed trypsin. Most protein was washed from the supports during the first wash (Fig. 5.10 and Table 5.3). The second wash was introduced to guarantee that higher amounts of unspecifically bound material, would not affect the purity of the eluted material. Trypsin was subsequently eluted in four consecutive steps yielding a recovery of 50 % of the bound enzyme and purification factors of 10.9 and 8.3 for the first and second elution fractions, respectively. These purification factors were similar to those obtained when HGMF was performed employing the 5 mL HGMF filter (Fig. 5.6 & Table 5.3).
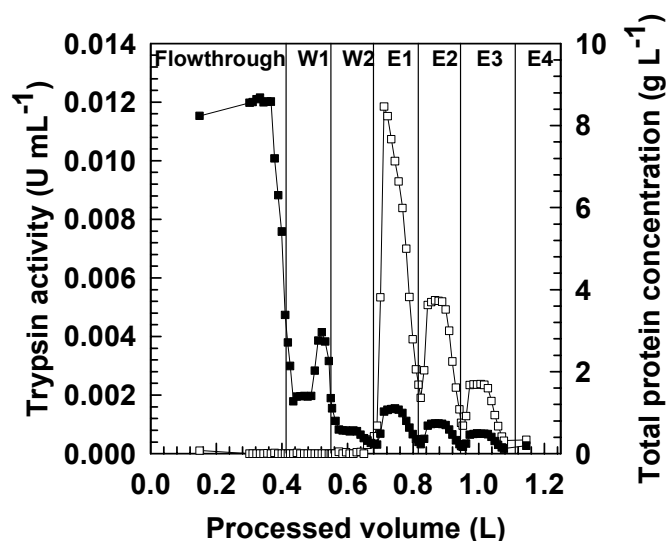
Fig. 5.10 Trypsin activity (□) and protein concentration (■) profiles obtained during HGMF processing (with a 46 mL filter) of whey (type II) hydrolysate after incubation with 0.15 g L^{-1} trypsin for 24 min. Wash and elution fractions are represented by W and E, respectively.

It was argued in a previous section that trypsin might not be recovered totally from the adsorbents in a two-elution step HGMF process due to insufficient buffer power in the system. Although this is probably true and this effect is more dramatic when working with larger filters due to the larger extents of mixing in the system, such effects were not observed in the current experiment despite the use of a larger filter with a different geometry. Very little trypsin (1.8 %) was recovered in the last elution step, suggesting that higher recoveries will not be possible. Furthermore, when the supports were stripped with 1 M sodium hydroxide at the end of the HGMF cycle, and the sample analysed by SDS-PAGE, no band corresponding to trypsin could be detected (data not shown). It is reasonable to partially attribute the loss of trypsin to inactivation of the enzyme, since the mass calculation of the mass balance is based on activity measurements. This argument has been discussed in section 5.3.2., but does not explain why the lower total trypsin yield (Table 5.3; 51 % *cf.* 75 %) occurs when HGMF processing is performed with the 46-mL instead of the 5-mL filter). One possible reason could be that different types of whey were used for the two HGMF studies at different scale. The cause for the inactivation still remains unclear since no loss of trypsin has been observed in bench-scale batch binding studies.

The results (Table 5.3) indicate that trypsin was not concentrated in any of the elution steps. In HGMF the concentration of the eluted proteins is dependent on the size of the recycle loop where the desorption steps are performed and the amount of target protein inside the filter (which is in turn dependent on the working protein binding capacity of the supports and the filter holding capacity for the supports). In this work, the filter was loaded to a capacity of 50 g L^{-1} based on the total volume of the filter, which corresponds to 63 % of the total capacity of the filter determined at slightly different conditions[4]. Loadings in this range were used in both HGMF processes presented in this work (65 % of the total capacity was used for the 5 mL filter), in order to ensure that all adsorbents were trapped inside the filter and could thus be optimised. Decreasing the volume of the recycle loop might improve the resulting concentration factor and it is likely that significant advantages with regard to the ratio of filter volume to recycle loop volume could be achieved by further scaling-up since there are restrictions on reducing the length of the recycle loop in the smaller apparatus used here. However in such a situation of high adsorbent and protein concentrations, other problems might need to be considered, such as the need to raise the buffer capacity during elution, as it has recently been reported (Meyer *et al.*, 2005). Even in the work conducted here, the support concentrations in the recycle loop were 20 g L^{-1}, i.e., 3.4 times higher than the concentration in the binding reactor.

The lower concentration factors observed (0.5 and 0.3) in the smaller scale process (Table 5.3) are due to the binding process having occurred with a lower trypsin:adsorbent concentration ratio. Previous results in this work (Fig. 5.5a & Table 5.2) indicate that the binding properties of AGE-*p*-AB are dependent on the trypsin concentration in solution and that nearly the same amount of supports are necessary to remove trypsin present in whey in concentrations of 0.10 or 0.15 g L^{-1}. In such a system the enzyme concentration is a parameter that could be optimised to maximise adsorbent protein loading capacity and therefore improve HGMF productivity. However, the impact of this parameter needs to be evaluated in both processes integrated in this work: hydrolysis and HGMF since variation of enzyme

---

[4] See footnote 3.

concentration will affect the hydrolysis rates. In this case much higher hydrolysis rates may be problematic since it would probably require faster loading of the hydrolysate suspension containing the enzyme to the HGMF system. Other parameters affecting HGMF processing can however be optimised independently of the hydrolysis process, such as the support concentration used for a given trypsin concentration, contact time in the binding step, and binding and desorption buffer conditions.

Table 5.3 Recovery of trypsin from whey by HGMF processing a two different scales using benzamidine-linked magnetic adsorbents. Results are summarised for a process employing a 5-mL HGMF filter and a 46-mL filter for processing 60 mL and 0.4 L of whey, respectively.

Step	Trypsin activity (U)		Trypsin yield (%)		Total protein (mg)		Protein yield (%)		Purification factor		Concentration factor	
Magnetic filter (mL)	5	46	5	46	5	46	5	46	5	46	5	46
Load	0.28	3.50	100	100	0.34	4.09	100	100	1	1	1	1
Flowthrough	0.008	0.03	2.86	0.9	0.30	3.35	85.8	81.9	n.a.	n.a.	n.a.	n.a.
Washes	0.002	0.02	0.82	0.5	0.009	0.32	2.69	7.8	n.a.	n.a.	n.a.	n.a.
1st elution	0.13	0.97	46.9	27.5	0.014	0.10	4.13	2.5	11.4	10.9	0.5	0.9
2nd elution	0.07	0.50	25.1	14.2	0.009	0.07	2.72	1.7	9.3	8.3	0.3	0.5
3rd and 4th	—	0.29	—	8.3	—	0.08	—	1.8	—	4.5	—	0.1
Balance			75	51.4			95	95.7				

n.a. Not applicable.

5.4 Conclusions

In this work we demonstrated that high-gradient magnetic fishing can be used as a tool for controlling enzymatic hydrolysis processes. At a desired time after initiating hydrolysis, magnetic adsorbents derivatised with appropriate ligands can be added to the reaction mixture and rapidly removed in a magnetic filter, thereby stopping hydrolysis. Subsequently the enzyme catalyst can be recovered in a semi-purified state. In view of the generic nature of HGMF, the technique presented is likely to have widespread applicability for hydrolysis control or the removal of enzyme contaminants causing product instability in a wide range of bioprocess feedstocks. Furthermore, high capacity adsorbents capable of interacting very tightly with target proteins – a necessary requirement for optimal operation of HGMF based separation processes – were constructed. The significant improvements yielded by AGE-activation of non-porous superparamagnetic supports over more well-described

technologies, such as BDE and DVS, show that this method may be a general way to produce affinity supports with these desirable characteristics.

Acknowledgements

References

Adler-Nissen, J. (1979) Determination of the degree of hydrolysis of food protein hydrolysates by trinitrobenzenesulfonic acid. *J. Agr. Food Chem.*, 27, 1256-1262.

Adler-Nissen, J. (1982) Limited enzymic degradation of proteins: A new approach in the industial application of hydrolases. *J. Chem. Technol. Biotechnol.*, 32, 138-156.

Adler-Nissen, J. (1986) *Enzymic Hydrolysis of Food Proteins*. Elsevier, UK.

Burton, S.C., Harding, D.R.K. (1997a) Bifunctional etherification of a bead cellulose for ligand attachment with allyl bromide and allyl glycidyl ether. *J. Chromatogr. A*, 775, 29-38.

Burton, S.C., Harding, D.R.K. (1997b) High density ligand attachment to brominated allyl matrices and application to mixed mode chromatography of chymosin. *J. Chromatogr. A*, 775, 39-50.

Ebner, N., Gomes, C.S.G., Hobley, T.J., Thomas. O.R.T., Franzreb, M. (2006) Filter capacity predictions for the capture of superparamagnetic microparticles by high-gradient magnetic separation (HGMS). *Chapter 3*

Erlanger, B.F., Kokowsky, N., Cohen, W. (1961) The preparation and properties of two new chromogenic substrates of trypsin. *Arch. Biochem. Biophys.*, 95, 271-278.

Ferré, H. (2006) *Development of novel processes for continuous protein refolding and primary recovery - A case study on the major histocompatibility complex class I receptor and its individual subunits*. Ph.D. Thesis. Technical University of Denmark, Denmark.

Geberding, S.J., Byers, C.H. (1998) Preparative ion-exchange chromatography of proteins from dairy whey. *J. Chromatogr. A*, 808, 141-151

Gomes, C.S.G., Ebner, N., Thomas. O.R.T., Franzreb, M., Hobley, T.J. (2006) Protein purification using high-gradient magnetic fishing: Impact of magnetic filter performance. *Chapter 4*.

Heebøll-Nielsen, A., Choe, W.S., Middelberg, A.P.J., Thomas, O.R.T. (2003) Efficient inclusion body processing using chemical extraction and high-gradient magnetic fishing. *Biotechnol. Progr.*, 19(3), 887-898.

Heebøll-Nielsen, A., Dalkiær, M., Hubbuch, J.J., Thomas, O.R.T. (2004a) Superparamagnetic adsorbents for high-gradient magnetic fishing of lectins out of legume extracts. *Biotechnol. Bioeng.,* 87(3), 311-323.

Heebøll-Nielsen, A., Justesen, S.F.L., Hobley, T.J., Thomas, O.R.T. (2004b) Superparamagnetic cation-exchange adsorbents for bioproduct recovery from crude process liquors by high-gradient magnetic fishing. *Sep. Sci. Technol.,* 39(12): 2891-2914.

Heebøll-Nielsen, A., Justesen, S.F.L., Thomas, O.R.T. (2004c) Fractionation of whey proteins with high-capacity superparamagnetic ion-exchangers. *J. Biotechnol.*, 113, 247-262.

Hermanson, G.T., Mallia, A.K., Smith, P.K. (1992) *Immobilized affinity ligand techniques*. Academic Press, London.

Hoffmann, C., Franzreb, M., Höll, W.H. (2002) A novel high-gradient magnetic separator (HGMS) design for biotech applications. *IEEE Trans. Appl. Supercond.,* 12(1), 963- 966.

Hubbuch, J.J. (2001) *Development of adsorptive separation systems for recovery of proteins from crude bioprocess liquors*. Ph.D. Thesis. Technical University of Denmark. ISBN 87-88584-57-7.

Hubbuch, J.J., Thomas, O.R.T. (2002) High-gradient magnetic affinity separation of trypsin from porcine pancreatin. *Biotechnol. Bioeng.,* 79, 301-313.

Hubbuch, J.J., Matthiesen, D.B., Hobley, T.J., Thomas, O.R.T. (2001) High gradient magnetic separation versus expanded bed adsorption: a first principle comparison. *Bioseparation*, 10(3), 99-112.

Langmuir, I. (1918) The adsorption of gases on plane surfaces of glass, mica and platinum. *J. Am. Chem. Soc.*, 44, 1361-1403.

Margot, A., Flaschel, E., Renken, A. (1997) Empirical kinetic models for tryptic whey-protein hydrolysis, *Process. Biochem.*, 32, 217-223.

Meyer, A., Hansen, D.B., Gomes, C.S.G., Hobley, T.J., Thomas, O.R.T., Franzreb, M. (2005) Demonstration of a strategy for product purification by high-gradient magnetic fishing: Recovery of superoxide dismutase from unconditioned whey. *Biotechnol. Progr.*, 21, 244-254.

O'Brien, S.M., Thomas, O.R.T., Dunnill, P. (1996) Non-porous magnetic chelator supports for protein recovery by immobilised metal affinity adsorption. *J. Biotechnol.*, 50, 13-26.

Panasiuk, R., Amarowicz, R., Kostyra, H., Sijtsma, L. (1998) Determination of α-amino nitrogen in pea protein hydrolysates: a comparison of three analytical methods. *Food Chem.*, 62(3), 363-367.

Pihlanto-Leppälä, A. (2001) Bioactive peptides derived from bovine whey proteins: opioid and ace-inhibitory peptides. *Trends. Food. Sci.. Tech.*, 11, 347-356.

Pintado, M.E., Pintado, A.E., Malcata, F.X. (1999) Controlled whey protein hydrolysis using two alternative proteases. *J. Food Eng.*, 42, 1-13.

Schlothauer, R.-C., Schollum, L.M., Singh, A.M., Reid, J.R. (1999) Bioactive whey protein hydrolysate. *PCT patent application WO99/65326*.

Spellman, D., McEvoy, E., O'Cuinn, G., Fitzgerald, R.J. (2003) Proteinase and exopeptidase hydrolysis of whey protein: Comparison of the TNBS, OPA and pH stat methods for quantification of degree of hydrolysis. *Int. Dairy J.*, 13, 447-453.

Zulqarnain, K. (1999) *Scale-up of affinity based separation based on magnetic support particles*. Ph. D. thesis. University College London, UK.

6. Conclusions

The work presented here covers aspects of the two main operations that characterise the integrated technique, high-gradient magnetic fishing: adsorption to magnetic adsorbents and collection of adsorbents on magnetic filters.

Preparation of a new type of magnetic adsorbents was performed using the activated magnetic supports (based on polyglutaraldehyde coated ferrite, PGF) developed by Heebøll-Nielsen (2002). The adsorbents were functionalised with the ligand 4-mercaptoethylpyridine (MEP) and a selected type was used for the recovery of immunoglobulin G (IgG) from rabbit antiserum by HGMF. The biological system used herein constituted a challenge to the application HGMF, since the target protein was present in very high concentrations (~ 25 g/L), necessitating the use of a large amount of magnetic adsorbents (33 g/L) to bind 95 % of the IgG after 10-fold dilution of the anti-serum. Even at these conditions it was possible to recover IgG in a purified form (>90 % purity) demonstrating for the first time the promise that HGMF holds for recovery and purification of antibodies. However, biological systems like the one studied here substantiate the need for more efficient magnetic filters, which leads to the next part of this thesis.

A better understanding of high-gradient magnetic filter performance has been achieved by screening a range of filter types with defined wire orientation. A model, taking into consideration the density of magnetic adsorbents collected around the ferromagnetic wires of a filter, magnetic properties and physical constraints, has been introduced. A simpler model for a less accurate estimation of filter capacity has been suggested. An important finding in this work is the better packing characteristics of adsorbents with narrower size distribution and regular shape (polyvinyl-alcohol based, PVA), which leads to higher filter capacities, contrary to the irregular PGF based adsorbents. The PVA adsorbents were also found to be more easily released from the magnetic filter when it was flushed at the end of a processing cycle.

In an attempt to evaluate adsorbent capture and release in HGMF for real-life processing situations, a model system employing multicycle mode was adopted using

cheese whey and PGF cation exchangers for binding and elution of lactoperoxidase. A worst-case scenario approach was used for studying the impact that poor release properties from the magnetic filter would have on binding and elution of proteins during HGMF processing. A clear impact of poor release properties was shown, demonstrating the importance of this parameter. Employment of mechanical vibration was sufficient to improve greatly binding and elution. Screening of several types of magnetic filters with different sizes of magnetic meshes and spacers was performed under controlled loading and flushing conditions over several cycles. The results suggest that the spacer size is determinant for the performance of the filter under the conditions applied, and that finer spacers are not suitable when used with PGF adsorbents.

Finally a new application of HGMF for bioprocessing was demonstrated. Improved affinity magnetic adsorbents (*p*-benzamidine linked adsorbents) were used to rapidly bind and remove an enzyme catalyst (trypsin) from a protein hydrolysate (cheese whey) stopping the enzyme activity when the desired degree of hydrolysis was achieved. This was possible due to the fast binding enabled by these types of adsorbents and by the rapid loading of the adsorbent/hydrolysate suspension through a high voidage HGMF filter. Furthermore, HGMF processing permitted the recovery of the enzyme in a semi-purified state.

In conclusion, HGMF has shown its potential for applicability to additional bioprocessing situations, and some of its critical parameters have been investigated.

Reference

Heebøll-Nielsen, A. (2002) *High gradient magnetic fishing: Support functionalisation and application for protein recovery from unclarified bioprocess liquors*. Ph.D. Thesis. Technical University of Denmark, Denmark.

Appendix A

Controlling enzyme reactions in unclarified bioprocess liquors using high-gradient magnetic fishing (HGMF)

Controlling enzyme reactions in unclarified bioprocess liquors using high-gradient magnetic fishing (HGMF)

Cláudia S.G. Gomes[1], Trine L. Petersen[1], Timothy J. Hobley[1], Owen R.T. Thomas[1,2,*]
[1]Center for Microbial Biotechnology, BioCentrum-DTU, Technical University of Denmark, Building 223, Søltofts Plads, DK-2800, Lyngby, Denmark, and [2]Department of Chemical Engineering, The University of Birmingham, Edgbaston, Birmingham B15 2TT. *Corresponding author. Tel.: +44-121-414-5278; Fax: +44-121-414-5377; Email: o.r.t.thomas@bham.ac.uk

Abstract
The use of enzymic modification in the food industry for improving qualities such as digestability, flavour, and texture will undoubtedly continue to gain in popularity in the future. For instance, whey protein hydrolysate, a food grade ingredient prepared from whey protein by controlled proteolysis, is set to become one of the most significant food additives of the next decade. However, the control of enzymatic hydrolysis reactions, occurring in complex biological suspensions, and involving exogenously added soluble enzymes, can be a tricky affair. We show here how benzamidine-linked magnetic adsorbents at low concentrations (5.6 g L^{-1}) combined with high-gradient magnetic fishing can be used to rapidly and effectively remove (>99%) and recover (>50%) small amounts of trypsin (0.15 g L^{-1}) added to cheese whey, thereby limiting and controlling the extent of hydrolysis to a desired level (in this study ~ 2 & 4%).

Keywords: affinity separation; batch adsorption; benzamidine; superparamagnetic adsorbents; trypsin; whey protein hydrolysates

1. Introduction
The most commonly applied methods for 'killing' an added enzyme catalyst, namely heat treatment or exposure to extremes of pH, are often detrimental to the end-product. Furthermore, in many cases the incentive of applying reusable enzyme catalysts is highly desirable. This is especially true when the costs for 'one-shot' use of the free enzyme are high and/or technical difficulties associated with the need to inactivate or remove the catalyst are encountered. Though numerous important industrial processes using immobilised enzyme catalysts have been established, the technical problems associated with the use of immobilised enzymes have still not been solved. Conventional immobilised enzyme catalysts typically employ porous support materials, and are effectively limited to the conversion of only small molecule reactants in clean liquors. Most industrial feedstocks, including those within the dairy industries, are 'dirty' and much more complex than this, *i.e.* they may be viscous, contain suspended insoluble particles and/or colloidal fouling materials. Recently we invented the bioseparation technique known as high-gradient magnetic fishing (HGMF) and demonstrated its advantages for the selective recovery of various macromolecular target species directly out of 'dirty' bioprocess liquors (Hubbuch et al., 2001; Hubbuch and Thomas, 2002; Heebøll-Nielsen et al., 2003, 2004a; 2004b, 2004c). In this work we extend HGMF's repertoire and show it can be employed as a gentle and highly effective means of controlling protease-mediated hydrolysis reactions within unclarified bioprocess liquors. The example chosen to illustrate the HGMF approach is the control of tryptic hydrolysis of crude bovine whey using benzamidine-functionalised superparamagnetic adsorbents, and a cyclically operated 'on-off' permanent magnet separator fitted with a magnetic filter device composed of a woven stainless steel matrix of high voidage.

2. Materials and Methods
2.1. Materials
Woven wire cloths of stainless steels 316 (0.9 mm Ø wires, 5 mm mesh) and 430 (0.315 mm Ø wires, 1 mm mesh) were obtained as gifts from Susan Venneker (Haver & Boecker, Oelde,

Germany). The crude sweet whey used in the kinetic studies was kindly donated by Waagner Nielsen (The Royal Veterinary and Agricultural University, Copenhagen, Denmark). In all other experiments we employed a crude sweet whey provided by Chr. Hansen A/S (Hørsholm, Denmark). The materials, allyl glycidyl ether (AGE), N-α-benzoyl-DL-arginine-p-nitroanilide (BAPNA), bovine pancreatic trypsin, bovine serum albumin, glutaraldehyde, L-leucine, p-aminobenzamidine (pABA) and trinitrobenzene sulphonic acid (TNBS) were all obtained from Sigma (St. Louis, MO, USA). All other chemicals were analytical grade.

2.2. Batch-wise support separation
A neodymium-iron-boron magnet block (B ~ 0.7 T) from Danfysik A/S (Jyllinge, Denmark) was used to separate magnetic particles from liquid phases during preparation of the magnetic adsorbents, binding studies, equilibration of adsorbents and bench-scale hydrolysis control studies.

2.3. Preparation of benzamidine-linked superparamagnetic adsorbents
Sub-micron sized polyglutaraldehyde-coated superparamagnetic iron oxide particles were prepared as described by Hubbuch and Thomas (2002). These base particles were subsequently functionalised with the synthetic protease inhibitor, benzamidine, in a two-step procedure detailed by Heebøll-Nielsen (2002) involving activation with allylglycidyl ether and subsequent reaction with pABA

2.4. Characterization of benzamidine-linked superparamagnetic adsorbent performance
The binding properties of the benzamidine-functionalised adsorbents were investigated in small-scale batch binding experiments at room temperature, using a range of 'support concentration' / 'trypsin' ratios in equilibration buffer and crude cheese whey. In all studies, the adsorbents were thoroughly equilibrated by resuspension in 100 mM Tris/HCl, 10 mM CaCl$_2$, pH 7.5 and separated using a magnet block. Trypsin solutions (1 mL) at a range of concentrations (0 to 2 g L^{-1} were prepared in equilibration buffer and added to 1 mg of adsorbent. After 30 min of vigorous mixing, the adsorbents were magnetically separated from the liquid phase and the supernatant was recovered for protein and trypsin activity determination. For batch binding experiments performed in whey, a range of magnetic support amounts up to a maximum of 16.5 mg were mixed with 1 mL of whey spiked with 0.2 g L^{-1} trypsin. The supernatants were collected after 30 min binding and analysed for protein content and trypsin activity. Time-dependent binding experiments were also performed in whey by resuspending the adsorbents to a final concentration of 4.5 g L^{-1} in 10 mL of whey containing 0.15 g L^{-1} trypsin and collecting samples over a period of 10 min, while mixing the suspension with an overhead stirrer. The samples were processed very quickly after collection (~ 10 s) by settling the magnetic supports and recovering the supernatants for analysis. The amounts of adsorbed trypsin were calculated by difference and an adsorption isotherm was subsequently plotted and fitted with the Langmuir model (Langmuir, 1918), represented by equation 1. The equilibrium concentration of the adsorbed and bulk-phase protein are represented by Q* and C* respectively, K$_d$ is the dissociation constant, and Q$_{max}$ is the maximum binding capacity of the adsorbents.

$$Q* = Q_{max} \frac{C*}{K_d + C*}$$ Eq. 1

2.5. Tryptic hydrolysis of whey
All hydrolysis experiments were performed using crude whey, at constant temperature and pH (i.e. 25 °C, pH 7.5). The whey was placed in a water bath at 25 °C and mixed by an overhead stirrer. When the whey reached 25°C, the pH was adjusted to 7.5 with 1 M NaOH and a solution

of 4 g L^{-1} trypsin in 100 mM Tris-HCl, 10 mM $CaCl_2$, pH 7.5 was added to give a final concentration of 0.15 g L^{-1} trypsin. The pH was kept constant by the manual addition of 1 M NaOH. The hydrolysis reaction was followed for periods of up to 6 h and samples were taken for SDS-PAGE and determination of the degree of protein hydrolysis, trypsin activity and total protein concentration. Control hydrolysis experiments were performed in parallel under identical conditions, but in the absence of added trypsin.

2.6. HGMF processing

2.6.1. HGMF apparatus and system set-up

The system employed for HGMF processing is depicted in Fig. 1. A 0.32 T laboratory type 'on-off' permanent magnet based high-gradient magnetic separator (Steinert HGF-10, Steinert Elektromagnetbau GmbH, Köln, Germany) designed for biological applications was employed (Hoffmann et al., 2002). A high-gradient magnetic filter was placed vertically in the 2.5 cm gap between the poles of the magnet and consisted of a stainless steel 316 canister containing a 46 mL cassette filled with parallel magnetisable sheets of stainless steel 430 woven wire cloth, separated by spacers of stainless steel 316 woven wire cloth, giving a voidage of 86%. Other components of the HGMF system included: a batch adsorption reactor equipped with an overhead stirrer; two buffer containers; a fraction collector (SuperFrac 2211, LKB, Bromma, Sweden); a single peristaltic pump (Masterflex® Easy Load® model 7518-00, Cole Parmer Instrument Co., Vernon Hills, IL, USA) equipped with a 6.4 mm i.d. Norprene® A-60-F tube; and a set of four three-way solenoid switching valves (Burkert-Contromatic A/S, Herlev, Denmark). The latter were used to control the flow path direction and velocity within the system enabling the following steps to be performed: (i) loading of magnetic adsorbent suspension from the batch adsorption reactor through the filter to the fraction collector; (ii) loading of elution or washing buffer through the filter to the fraction collector; iii) recirculation of filter contents within a closed recycle loop. The total volume of the system recycle loop used in this study was 123 mL. The HGF-10 magnet, pump and valves were controlled by LabView software (Student Edition 6i, National Instruments Corporation, Austin, TX, USA).
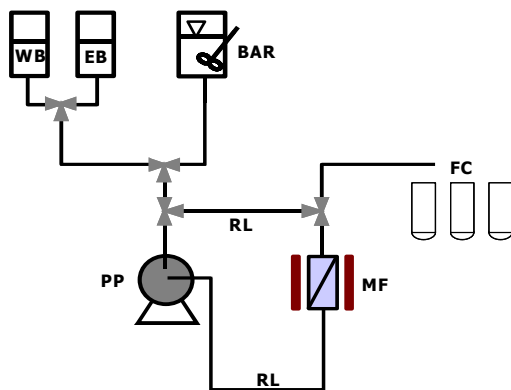
Fig. 1. Schematic diagram of the HGMF system employed in this work. MF = magnetic filter, FC = fraction collector, PP = peristaltic pump, WB = washing buffer container, EB = elution buffer container, RL = recycle loop, BAR = batch adsorption reactor.

2.6.2. HGMF-mediated hydrolysis control

Tryptic hydrolysis was performed in 0.4 L of whey in the batch adsorption reactor in the presence of 0.15 g L^{-1} trypsin, at 25°C and pH 7.5. At a defined time (24 or 58 min), benzamidine-functionalised magnetic adsorbents, previously equilibrated with 100 mM Tris/HCl, 10 mM $CaCl_2$, pH 7.5, were added to the hydrolysate to a final concentration of 5.6 g L^{-1} or 7.6 g L^{-1}. After 6 min binding, all of the suspension was loaded to the magnetic filter at a superficial linear

velocity of 24 m h^{-1} (230 mL min^{-1}) while the magnetic field was 'on'. The magnetic adsorbents were collected on the filter, and the flowthrough (*i.e.* hydrolysate) was returned to the adsorption reactor (now free of adsorbents) where it was kept under hydrolysis conditions for ~4 h more, during which time sampling was continued.

2.6.3. Recovery of trypsin

After adsorption of trypsin in whey on to benzamidine-functionalised magnetic adsorbents, and collection of the latter within the high-gradient magnetic filter, an HGMF processing cycle was conducted. Two washing and four elution cycles were used in order to recover the trypsin. The system was filled with washing buffer (100 mM Tris/HCl, 10 mM CaCl$_2$, pH 7.5) while the magnetic field was 'on'. The 123 mL recycle loop was then closed, the field turned 'off', and the supports were recycled for 5 min (with change of flow direction every 1 min) at a superficial linear velocity in the filter of 80 m h^{-1}, while the latter was mechanically vibrated. Subsequently the flow rate was reduced to 24 m h^{-1}, the field was switched back 'on' again, and the supports were collected on the filter by recycling the suspension upwards with respect to the filter for 3 min. Next, with the field still 'on' the washing fractions were collected by loading washing buffer into the system for the second washing step. All of the above steps were then repeated using elution buffer instead of wash buffer, i.e., by loading the appropriate buffer to the system, recycling the supports in the recycle loop, collecting the supports and finally collecting the eluate by loading the next buffer. The buffer used to elute the trypsin from the adsorbents was 0.1 M glycine supplemented with 20 mM CaCl$_2$ at pH 2.6.

2.7. Analytical methods

Trypsin activity was analysed by hydrolysis of BAPNA (Erlanger et al., 1961) as described by Hubbuch and Thomas (2002). One sample volume was mixed with a reagent solution consisting of 1 volume 0.04 M BAPNA in DMSO and 7 volumes of 100 mM Tris/HCl buffer at pH 7.6, and the activity was calculated from the recorded change in absorbance at 405 nm. Total protein was measured with a BCA protein assay (Pierce Rockford, IL, USA), which was used as recommended by the manufacturer. All protein concentrations were expressed in mg BSA equivalents. Both the BCA and trypsin assays were scaled for use with a Cobas Mira robot spectrophotometer (Roche Diagnostic Systems, Rotkreutz, Switzerland).

The degree of hydrolysis (DH) was determined essentially as described by Adler-Nissen (1979), but with some minor modifications. This method is based on the TNBS-based quantification of free amino groups that are released during hydrolysis of proteins. Duplicate aliquots (1 mL) of sample were pre-treated by mixing them with 5 mL of 1% (w/v) SDS previously heated to 95°C and kept at this temperature for at least 10 min to ensure that the trypsin was inactivated. Aliquots (0.125 mL) of the pre-treated samples and standards (L-leucine in the concentration range of 0 to 3 mM) were diluted in 1 mL of 0.213 M phosphate buffer (pH 8.2) and mixed with 1 mL of a freshly prepared 0.1% TNBS solution for 1 h at 50 °C in the dark. Reactions were stopped by the addition of 2 mL of 0.1 N HCl. After 20 min at room temperature 4 mL of distilled deionised water was added to each tube. After a further 10 min at room temperature the absorbance of each sample and standard was measured at 340 nm in a HP845 UV-visible spectrophotometer. DH values were calculated using equation 2 (Adler-Nissen, 1979).

$$DH(\%) = 100 \left(\frac{h}{h_{tot}} \right) \qquad \text{Eq. 2}$$

Here, h is the number of hydrolysis equivalents, i.e., the number of peptide bonds cleaved during a hydrolysis process, and h$_{tot}$ is the total number of peptide bonds in a given protein. Values of h were expressed in mM leucine equivalents per gram protein. A recommended h$_{tot}$ value (mmol

equivalents g^{-1} protein) of 8.8 for whey concentrate (Adler-Nissen, 1986) was used in our calculations.

The protein composition of whey hydrolysates was analysed by reducing SDS-PAGE in precast NuPAGE® Novex 4-12% Bis-Tris gels (Invitrogen, Groningen, The Netherlands) in accordance with the manufacturers instructions. Prior to SDS-PAGE analysis, the samples (50 μL aliquots) were treated with trichloroacetic acid on ice for >20 min, and the resulting protein precipitates were then washed sequentially with 5 mM HCL in acetone and then with pure acetone, before drying and resuspending with 100 μL of NuPAGE® LDS sample loading buffer (Invitrogen, Groningen, The Netherlands).

The magnetic particle content in samples was determined by a dry weight method (Heebøll-Nielsen et al. 2003, 2004a). In the case of the adsorbents that had been in contact with biological material, the particles were first washed three times with elution buffer, three more times with 1 M NaOH and finally with three washes of Milli-Q water.

3. Results and Discussion

3.1. Hydrolysis of whey

The concept of using the degree of hydrolysis (DH) as a measure of the extent of protein hydrolysis is not new (Adler-Nissen, 1982, 1986). Adler-Nissen (1979) defined DH as the percentage of peptide bonds cleaved, and there are several methods available for determining it, such as the pH-stat and various colorimetric based methods (o-phthaldialdehyde, OPA; ninhydrin and TNBS). In the work done by Panasiuk et al. (1998), it was suggested that results obtained using OPA and TNBS are the most correct. Moreover, in a recent comparison of pH-stat, OPA and TNBS methods, the latter was shown to be the most suitable for an accurate quantification of DH in whey protein hydrolysates (Spellman et al., 2003), and it is for this reason that TNBS was employed for the determination of DH in the current work.

When trypsin was added to whey at a final concentration of 0.15 g L^{-1}, DH was observed to increase steadily, reaching a value of ~ 7% within ~5 h (Fig. 2). In the absence of 'added' trypsin DH attained a plateau value of ~1% after ~ 1 h and remained at this level throughout the duration of the experiment (<6 h. Fig. 2). The theoretical maximum DH in cheese whey was estimated to be 11% based on the lysine and arginine composition of the substrate (11.20 and 3.01 g free amino acid per 100 g protein, respectively, as recommended by Adler-Nissen, 1986), given that trypsin specifically catalyses the cleavage of peptide bonds on the carboxylic side of lysine and arginine only. Although higher rates of trypsin hydrolysis could probably be achieved by using incubation temperatures of 55°C, or concentrations of enzyme greater than 0.15 g L^{-1}, the hydrolysis rate observed in Fig. 2 gives a wide operating window within which to clearly demonstrate hydrolysis control.

3.2. Characterisation of benzamidine-linked superparamagnetic adsorbents

In this work, magnetic supports have been functionalised with benzamidine, a classic affinity ligand for trypsin. In recent work we have shown how benzamidine-derivatised magnetic supports can be employed successfully to recover trypsin by HGMF from both crude porcine pancreatin (Hubbuch, 2001; Hubbuch and Thomas, 2002) and cheese whey feedstocks (Hubbuch, 2001). More recently, Heebøll-Nielsen (2002) developed and compared improved types of benzamidine-functionalised magnetic adsorbents that use different spacer arms between the base matrix and the ligand. The best of those supports, employed a 7-atom hydrophilic spacer introduced by activation of the base matrix with allyl glycidyl ether prior to coupling of the ligand, and this strategy was therefore selected in the current work.
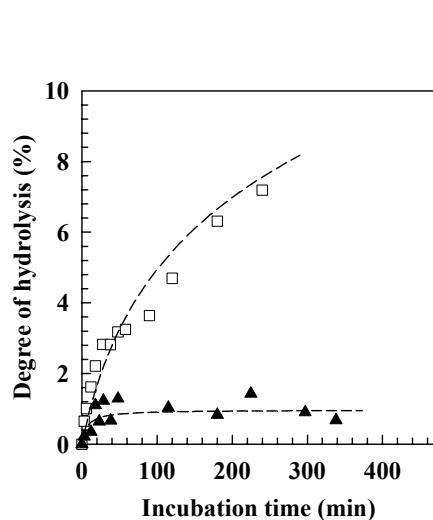
Fig. 2. Hydrolysis curves for whey proteins incubated at 25 °C and pH 7.5 with 0.15 g L^{-1} trypsin (□) and in the absence of trypsin (▲).
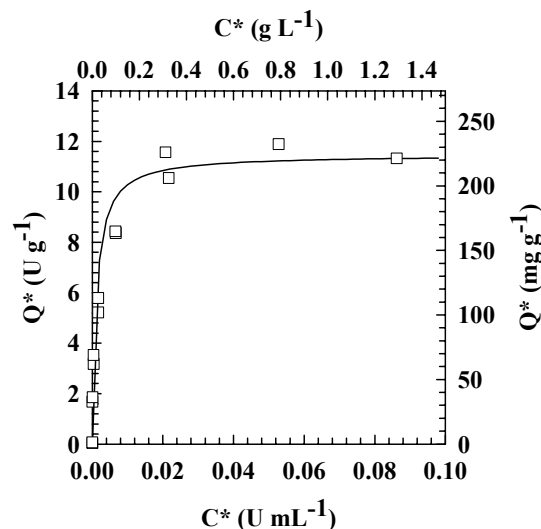
Fig. 3. Equilibrium adsorption isotherm for pure trypsin on benzamidine-functionalised magnetic supports. The solid line through the data represents the fitted Langmuir curve (Q_{max} = 11.5 U g^{-1} or 225 mg g^{-1}; K_d = 0.0015 U mL^{-1} or 1.2 μM).

An equilibrium isotherm for the binding of pure trypsin to benzamidine-linked superparamagnetic adsorbents is shown in Fig. 3. Highly satisfactory Langmuir binding parameters were demonstrated, and the same materials also displayed excellent characteristics for trypsin removal from crude whey (Fig. 4). When crude whey was spiked with 0.2 g L^{-1} trypsin (0.0111 U mL^{-1}) a support concentration of only 4.9 g L^{-1} was needed to remove 99.8 % of the 'added' trypsin.
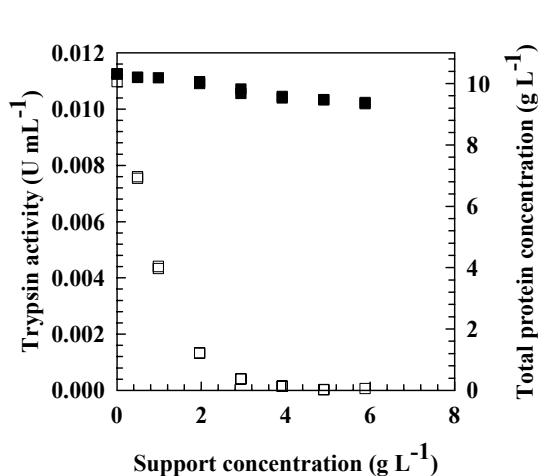
Fig. 4. Effect of benzamidine-functionalised magnetic support concentration on the removal of trypsin (□) and total protein (■) from crude whey. Trypsin was added at 0.2 g L^{-1}.
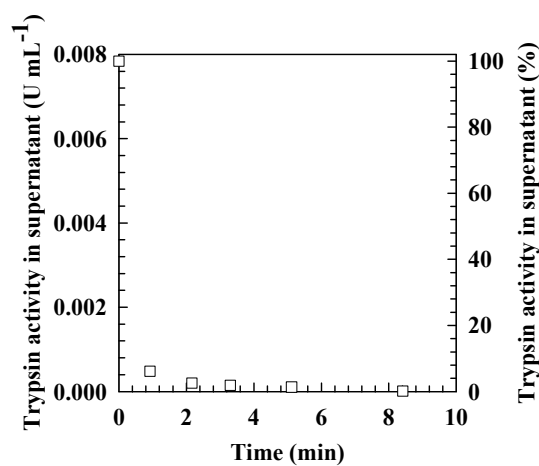
Fig. 5. Clearance of typsin (□) from crude whey over time using 4.5 g L^{-1} benzamidine-functionalised magnetic support and 0.15 g L^{-1} trypsin.

Fig. 5 shows that 98.7% and 99.9% of the initially added trypsin could be removed with binding times of just 5 and 8 min respectively. From these screening studies it was concluded that a minimum support concentration of 5 g L^{-1} was required to remove the 0.2 mg L^{-1} of added trypsin

employed for the hydrolysis of crude whey, and that ~5 min contact time with the benzamidine-linked adsorbents would be sufficient for near complete removal of trypsin from the whey.
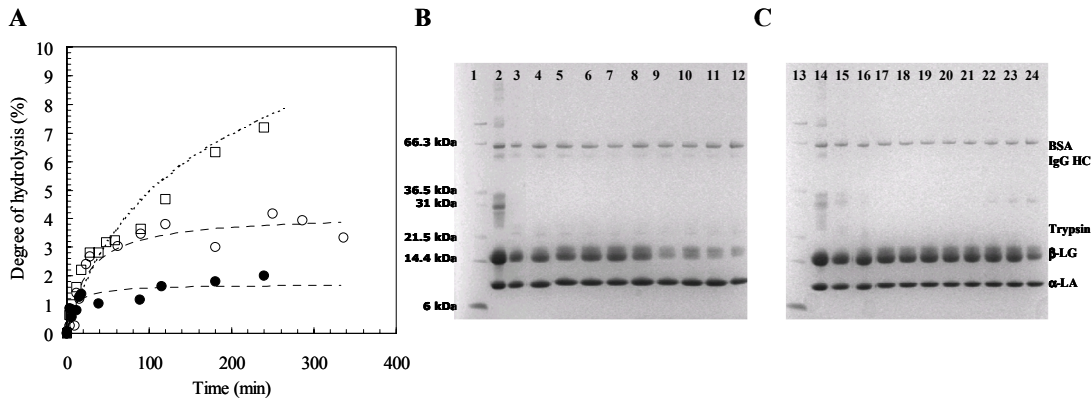
Fig. 6. (A) Progression of hydrolysis in whey incubated with 0.15 g L^{-1} trypsin, mixing with benzamidine-linked adsorbents after 24 min (●) and 52 min (○) and processing by HGMF. Reference trypsin hydrolysis curve (□) from Fig. 2; Reducing SDS-PAGE analysis of samples taken during trypsin hydrolysis of whey **(B)** without adsorbents added and **(C)** with adsorbents added after 24 min of hydrolysis and HGMF processing. Lanes 1 and 13, molecular weight markers; lanes 2 and 14, whey. The remaining lanes correspond to samples removed after the following incubation times: **(B)** – 0 min (lane 3), 9 min (lane 4), 38 min (lane 5), 48 min (lane 6), 58 min (lane 7), 120 min (lane 8), 180 min (lane 9), 240 min (lane 10), 300 min (lane 11) & 360 min (lane 12); **(C)** – 0 min (lane 15), 9 min (lane 16), 32 min (lane 17), 38 min (lane 18), 48 min (lane 19), 58 min (lane 20), 88 min (lane 21), 120 min (lane 22), 180 min (lane 23), & 240 min (lane 24). Abbreviations: β-LG, β-lactoglobulin; α-LA, α-lactalbumin; IgG-HC, immunoglobulin heavy chain.

### 3.3. Hydrolysis control by High-Gradient Magnetic Fishing

The benzamidine-linked magnetic supports were shown above to be efficient for the removal of trypsin from crude cheese whey, and were thus employed for examining the control of hydrolysis by HGMF. To evaluate the performance of this process, hydrolysis experiments were conducted by incubating trypsin in whey under the same conditions as described above. In two parallel studies, the benzamidine-linked adsorbents were added to the hydrolysate in the batch reactor after 24 min (using 5.6 g L^{-1} adsorbents) in one case and 58 min (using 7.6 g L^{-1} adsorbents) in the other, in order to permit different degrees of hydrolysis to be reached. After 6 min of binding, the supports were pumped through the HGMF filter and collected within 2 min. When the flowthrough was examined it was found that 99.1% or 99.9% of the added trypsin had been removed following processing with 5.6 g L^{-1} or 7.6 g L^{-1} adsorbents respectively. In both cases little further hydrolysis was seen (Fig. 6A) and the resulting DH values were 2% and 4% for the processes controlled after 24 min and 58 min respectively. Additionally, no further change in pH was observed after HGMF processing, providing further evidence that hydrolysis had been terminated. The control of whey protein cleavage by adding adsorbents and removing them by HGMF could also be clearly seen when samples were analysed by SDS-PAGE (Fig. 6B & C). When no adsorbents were used, the band corresponding to β-lactoglobulin became greatly diminished over time (Fig. 6B, lanes 2 –12). In contrast, no such decrease in β-lactoglobulin was observed after addition and subsequent removal of the benzaminidine-linked supports (Fig. 6C, lanes 17–24). The preferential hydrolysis of β-lactoglobulin by trypsin is consistent with the reports of Pintado et al. (1999).

3.4. Recovery of trypsin by High-Gradient Magnetic Fishing

Binding of added trypsin with magnetic adsorbents and rapid removal from whey using a magnetic filter permitted hydrolysis to be halted. However, the application of HGMF enables further processing and the recovery of the trypsin bound to the adsorbents, which are trapped within the magnetic filter. Following filter loading, two washes were performed and 43% of the nonspecifically bound proteins were desorbed with little loss of adsorbed trypsin (Fig. 7 & Table 1). Trypsin was then eluted in four consecutive steps yielding a recovery of ~50 % of the bound enzyme.
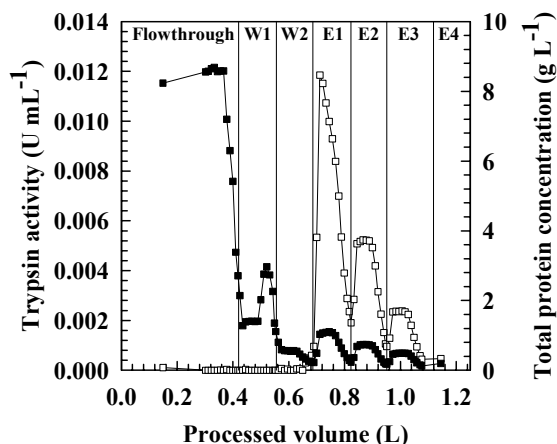

Fig. 7. Trypsin activity (□) and protein concentration (■) profiles obtained during HGMF processing of whey hydrolysate following incubation with 0.15 g L^{-1} trypsin for 24 min. Wash and elution fractions are represented by W and E, respectively.

Table 1. Recovery of trypsin from whey by HGMF processing using benzamidine-linked magnetic adsorbents.

Step	Trypsin activity (U)	Trypsin yield (%)	Total protein (g)	Protein yield (%)	Purification factor	Concentration factor
Load	3.5	100	4.09	100	1	1
Flowthrough	0.03	0.9	3.35	81.9	n.a.	n.a.
Washes	0.02	0.5	0.32	7.8	0.3	n.a.
Elutions	1.76	50	0.25	6.0	8.2	0.4
Balance		*51.4*		*95.7*		

n.a. not applicable

When the supports were stripped at the end of the HGMF cycle, and samples analysed by SDS-PAGE, no band corresponding to trypsin could be detected, suggesting that all of the enzyme had been eluted, and that the apparent loss of trypsin activity was most likely due to inactivation of the enzyme. The results indicate that trypsin was not concentrated during elution (Table 1). In HGMF processing the concentration of the eluted proteins is dependent on the size of the recycle loop in which desorption steps are performed, and on the amount of target protein within the filter (which is in turn dependent on the working protein binding capacity of the supports and the filter holding capacity for adsorbent particles). In this work, the filter was loaded to a capacity of 50 g L^{-1}, which corresponds to just 63% of the total capacity of the filter[1]. Optimisation of the loading conditions and/or decreasing the volume of the recycle loop should improve the concentrating power, and it is furthermore likely that significant advantages could be achieved on scaling-up, as this would enable the ratio of filter volume to recycle loop volume to be increased. There are

---

[1] The capacity calculated at 5% breakthrough was 79 g L^{-1} when a suspension of magnetic supports was applied at 22 m h^{-1} to the filter placed in a magnetic field of 0.32 T.

restrictions on reducing the length of the recycle loop that can be employed in the small apparatus we have used in this study.

4. Conclusions
In this work we have demonstrated that high-gradient magnetic fishing can be used as a tool for controlling enzymatic hydrolysis processes. At a desired time after initiating hydrolysis, magnetic adsorbents derivatised with appropriate ligands can be added to the reaction mixture and rapidly removed in a magnetic filter thereby stopping hydrolysis. Subsequently the enzyme catalyst can be recovered in a semi-purified state. In view of the generic nature of HGMF, the technique presented is likely to have widespread applicability for hydrolysis control or the removal of enzyme contaminants causing product instability in a wide range of bioprocess feedstocks.

References
Adler-Nissen, J. (1979) Determination of the degree of hydrolysis of food protein hydrolysates by trinitrobenzenesulfonic acid. *J. Agr. Food Chem.*, 27, 1256-1262.

Adler-Nissen, J. (1982) Limited enzymic degradation of proteins: A new approach in the industial application of hydrolases. *J. Chem. Technol. Biotechnol.*, 32, 138-156.

Adler-Nissen, J. (1986) *Enzymic Hydrolysis of Food Proteins*. Elsevier, UK.

Erlanger, B.F., Kokowsky, N., and Cohen, W. (1961) The preparation and properties of two new chromogenic substrates of trypsin. *Arch. Biochem. Biophys.*, 95, 271-278.

Heebøll-Nielsen, A. (2002) *High Gradient Magnetic Fishing: Support functionalisation and application for protein recovery from unclarified bioprocess liquors*. Thesis (PhD). Technical University of Denmark. ISBN 87-88584-82-8.

Heebøll-Nielsen, A., Choe, W.S., Middelberg, A.P.J. and Thomas, O. R.T. (2003) Efficient inclusion body processing using chemical extraction and high-gradient magnetic fishing. *Biotechnol. Progr.*, 19(3), 887-898.

Heebøll-Nielsen, A., Dalkiær, M., Hubbuch, J.J. and Thomas, O. R.T. (2004a) Superparamagnetic adsorbents for high-gradient magnetic fishing of lectins out of legume extracts. *Biotechnol. Bioeng.*, 87(3), 311-323.

Heebøll-Nielsen, A., Justesen, S.F.L. Hobley, T.J. and Thomas, O.R.T. (2004b) Superparamagnetic cation-exchange adsorbents for bioproduct recovery from crude process liquors by high-gradient magnetic fishing. *Sep. Sci. Technol.*, 39(12): 2891-2914.

Heebøll-Nielsen, A., Justesen, S.F.L. and Thomas, O.R.T. (2004c) Fractionation of whey proteins with high-capacity superparamagnetic ion-exchangers. *J. Biotechnol.*, 113, 247-262.

Hoffmann, C., Franzreb, M. and Höll, W.H. (2002) A novel high-gradient magnetic separator (HGMS) design for biotech applications. *IEEE Trans. Appl. Supercond.*, 12(1), 963- 966.

Hubbuch, J.J. (2001) *Development of adsorptive separation systems for recovery of proteins from crude bioprocess liquors*. Thesis (PhD). Technical University of Denmark. ISBN 87-88584-57-7.

Hubbuch, J.J., Matthiesen, D.B., Hobley, T.J. and Thomas, O.R.T. (2001). High gradient magnetic separation versus expanded bed adsorption: a first principle comparison. *Bioseparation*, 10(3), 99-112.

Hubbuch, J.J., and Thomas, O.R.T. (2002) High-gradient magnetic affinity searation of typsin from porcine pacreatin. *Biotechnol. Bioeng.*, 79, 301-313.

Langmuir, I. (1918) The adsorption of gases on plane surfaces of glass, mica and platinum. *J. Am. Chem. Soc.*, 44, 1361-1403.

Panasiuk, R., Amarowicz, R., Kostyra, H. and Sijtsma, L. (1998) Determination of α-amino nitrogen in pea protein hydrolysates: a comparison of three analytical methods. *Food Chem.*, 62(3), 363-367.

Pintado, M.E., Pintado, A.E. and Malcata, F.X. (1999) Controlled whey protein hydrolysis using two alternative proteases. *J. Food Eng.*, 42, 1-13.

Spellman, D., McEvoy, E., O'Cuinn, G., and Fitzgerald, R.J. (2003) Proteinase and exopeptidase hydrolysis of whey protein: Comparison of the TNBS, OPA and pH stat methods for quantification of degree of hydrolysis. *Int. Dairy J.*, 13, 447-453.

Appendix B

Demonstration of a strategy for product purification by high-gradient magnetic fishing: Recovery of superoxide dismutase from unconditioned whey

Biotechnol. Progr., <u>21</u>, 244-254

Demonstration of a Strategy for Product Purification by High-Gradient Magnetic Fishing: Recovery of Superoxide Dismutase from Unconditioned Whey

Andrea Meyer,[†,‡,||] Dennis B. Hansen,[‡,⊥] Cláudia S. G. Gomes,[‡] Timothy J. Hobley,[‡] Owen R. T. Thomas,*[,‡,§] and Matthias Franzreb*[,†]

Institute for Technical Chemistry, Water- and Geotechnology Division, Forschungszentrum Karlsruhe, Hermann v. Helmholtz Platz 1, 76344 Eggenstein-Leopoldshafen, Germany; Center for Microbial Biotechnology, BioCentrum-DTU, Technical University of Denmark, Building 223, Søltofts Plads, DK-2800, Kgs. Lyngby, Denmark; and Department of Chemical Engineering, The University of Birmingham, Edgbaston, Birmingham B15 2TT, U.K.

A systematic approach for the design of a bioproduct recovery process employing magnetic supports and the technique of high-gradient magnetic fishing (HGMF) is described. The approach is illustrated for the separation of superoxide dismutase (SOD), an antioxidant protein present in low concentrations (ca. $0.15-0.6$ mg L^{-1}) in whey. The first part of the process design consisted of ligand screening in which metal chelate supports charged with copper(II) ions were found to be the most suitable. The second stage involved systematic and sequential optimization of conditions for the following steps: product adsorption, support washing, and product elution. Next, the capacity of a novel high-gradient magnetic separator (designed for biotechnological applications) for trapping and holding magnetic supports was determined. Finally, all of the above elements were assembled to deliver a HGMF process for the isolation of SOD from crude sweet whey, which consisted of (i) binding SOD using Cu^{2+}-charged magnetic metal chelator particles in a batch reactor with whey; (ii) recovery of the "SOD-loaded" supports by high-gradient magnetic separation (HGMS); (iii) washing out loosely bound and entrained proteins and solids; (iv) elution of the target protein; and (v) recovery of the eluted supports from the HGMF rig. Efficient recovery of SOD was demonstrated at ∼50-fold increased scale (cf. magnetic rack studies) in three separate HGMF experiments, and in the best of these (run 3) an SOD yield of >85% and purification factor of ∼21 were obtained.

1. Introduction

In our laboratories we have recently introduced a new robust isolation technique for macromolecules ($1-7$) termed High-Gradient Magnetic Fishing (HGMF). In a typical HGMF process, the target species is first bound onto functionalized magnetic supports in a simple batch adsorption reactor and the product-loaded adsorbents are subsequently separated from the nonmagnetic components using high-gradient magnetic separation (HGMS) technology, adapted from the mineral processing and wastewater industries. The use of a simple and readily scaleable batch-binding step for product adsorption makes this technique particularly interesting for the treatment of high volume feedstocks, such as whey. Previously we have focused on the construction and characterization of

magnetic supports followed by a simple demonstration of their use in an HGMF process (*3, 5, 6*). To date, however, it has not been demonstrated how an HGMF process can be developed systematically for the recovery of a particular target molecule of interest.

The cheese industry produces excessive amounts of whey as a byproduct, e.g., 1.18×10^{11} kg of whey was produced worldwide in 1997, rising by 3% each year (*8, 9*), and many scientists in collaboration with dairy companies are looking for new ways to make use of this excess. In this context interest in recovering high-value milk proteins from this waste material for use in food, cell culture, and for pharmaceutical purposes has grown constantly in recent years (*9*). One interesting target molecule in whey is the enzyme superoxide dismutase (SOD), which is present in low concentrations of the order of $0.15-0.6$ mg L^{-1} (*10−13*). SOD is present in almost all tissues of eukaryotes and is responsible in vivo for catalyzing a vital reaction, namely, the dismutation of highly reactive superoxide anion radicals. A technique for the isolation of SOD from sweet whey is of interest, given that the antioxidant properties of the enzyme may make it suitable for treating inflammatory diseases (*14*). Although Holbrook and Hicks (*15*) described a procedure for the isolation of SOD from milk, the purpose of their study was one of characterization rather than efficient

---

* To whom correspondence should be addressed. O.R.T.T.: Tel. +44 121 414 5278. Fax +44 121 414 5377. Email: o.r.t.thomas@ bham.ac.uk. M.F.: Tel. +49 7247 82 3595. Fax +49 7247 86 6660. Email: matthias.franzreb@itc-wgt.fzk.de.
† Forschungszentrum Karlsruhe.
‡ Technical University of Denmark.
§ University of Birmingham.
|| Current address: Procter & Gamble Service GmbH, Sulzbacher Strasse 40, 65823 Schwalbach am Taunus.
⊥ Current address: Alpharma ApS, Dalslandsgade 11, DK-2300, Copenhagen, Denmark.

exploitation of the technique for preparative purposes. To date, most work on preparative recovery of SOD has used blood as the source material, primarily owing to the several-hundred-fold higher concentration of the enzyme in this feedstock (*10, 13, 16*).

In this paper we demonstrate how an HGMF process can be designed when faced with the task of recovering a "new" target molecule from a "new" feedstock. Simple screening studies conducted with a clarified version of the intended feed and a selection of different candidate ligands supported on conventional commercially available chromatographic matrices were first used to identify a suitable ligand for binding of the target molecule. In the next phases magnetic supports functionalized with the chosen ligand were manufactured, and their binding and desorption performance were subsequently characterized/optimized in small-scale studies, using the unconditioned (i.e., crude and unclarified) feedstock. Finally, using optimized conditions acquired from the small-scale experiments, we demonstrate the piecing together of an HGMF process. The particular example we have chosen for illustrating the design of an HGMF process is the recovery of SOD from crude sweet whey.

2. Materials and Methods

2.1. Materials. The "430" stainless steel wire matrix (KnitMesh type 9029) employed in HGMS and HGMF experiments and the unconditioned crude sweet whey used throughout this study were received as gifts from Colin Barnes (KnitMesh, South Croydon, Surrey, U.K.) and Waagner Nielsen (Royal Veterinary and Agricultural University, Copenhagen, Denmark), respectively. The bicinchoninic acid (BCA) protein assay kit was purchased from Pierce Chemicals (Rockford, IL), TMB-ONE ready-to-use substrate was supplied by Kem-En-Tec A/S (Copenhagen, Denmark), and superoxide dismutase assay kit (cat. no. 574600) was obtained from Calbiochem-Novabiochem (San Diego, CA). Bovine serum albumin (BSA, Fraction V powder, A9647), superoxide dismutase (from bovine erthyrocytes, S2515), lactoperoxidase (from bovine milk, L2005), lactoferrin (from bovine milk, L9507), immunoglobulin (from bovine milk, I5506), α-lactalbumin (from bovine milk, L5385), β-lactoglobulin (from bovine milk, L0130), lysozyme (from human milk, L6394), and catalase (from bovine liver, C9322) were all acquired from the Sigma Chemical Company (St. Louis, MO), as were the chemicals (aminopropyl)triethoxysilane, glacial acetic acid, glutaraldehyde (50% photographic grade), sodium borohydride, allyl glycidyl ether, *N*-bromosuccinimide, and iminodiacetic acid (disodium salt). The salts iron(II) chloride hexahydrate and iron(III) chloride tetrahydrate were supplied by J. T. Baker (Deventer, The Netherlands). Methanol (GPR grade) was purchased from BDH Laboratory Supplies (Poole, Dorset, U.K.). All other chemicals were obtained from either Merck (Darmstadt, Germany) or the Sigma Chemical Company.

2.2. Ligand Screening. Screening of a suitable ligand to recover SOD from whey was performed on a Gradifrac system (Amersham Biosciences, Uppsala, Sweden) using 1-mL HiTrap chromatography columns (Amersham Biosciences, Sweden) packed with two types of media, namely, Heparin Sepharose HP and Chelating Sepharose HP. Prior to use the latter immobilized metal affinity chromatography (IMAC) columns were charged with either Cu^{2+}, Ni^{2+}, or Zn^{2+} ions using 0.1 M solutions of copper sulfate, nickel chloride, or zinc chloride, respectively. Before loading, all columns were equilibrated with an appropriate buffer, i.e., 10 mM sodium phosphate, pH 7 for heparin columns and 10 mM potassium phosphate,

1 M NaCl, pH 6.4 for IMAC (*17*). Thirty column volumes (CVs) of clarified whey (prepared by filtering through a 0.45-μm polyethersulfone membrane (PALL Cooperation, Ann Arbor, MI)) were then applied to columns at a superficial linear flow velocity of 1.58 m h^{-1}. Following loading, columns were washed with 10 CV of the appropriate equilibration buffer and thereafter eluted at 0.79 m h^{-1} with 10 CV of the same buffer supplemented with either 1 M NaCl (for heparin) or 1 M NH$_4$Cl (for IMAC). All collected fractions were analyzed for protein content and SOD activity as described under Analytical Methods.

2.3. Preparation of Cu^{2+}- Charged Magnetic Metal Chelator Particles. The detailed methods for the preparation of Cu^{2+}-charged "type II" magnetic metal chelator particles used in this work have been presented elsewhere (*3, 6*). These magnetic support materials employ the tridentate chelating agent, iminodiacetic acid (IDA), which is covalently attached to the coated particle surfaces via a 7-atom hydrophilic spacer arm. Immediately prior to use the IDA-linked supports were charged with Cu^{2+} ions exactly as described by Heebøll-Nielsen et al. (*6*), i.e., by washing them three times in a 0.1 M copper sulfate solution, followed by three washes in 10 mM potassium phosphate, 1 M NaCl, pH 6.4. Four separate batches of Cu^{2+}-IDA magnetic adsorbents were fabricated: one using ~13 g IDA per g of magnetic supports in the coupling reaction, designated LS for "low substitution", and three "high substitution" batches (HS$_1$, HS$_2$, and HS$_3$) prepared using a 4-fold higher IDA to particle ratio during coupling of the chelating agent. To minimize possible inconsistencies arising from batch-to-batch differences, adsorbent particles from just a single batch were used in each experiment. Throughout all stages of adsorbent preparation, a ~0.7 T neodymium−iron−boron permanent magnet block (Danfysik A/S, Jyllinge, Denmark) was used for recovery of magnetic support particles from suspension.

2.4. BSA Binding Tests. Batches of magnetic adsorbent particles were subjected to a simple quality control test, which involved characterization of their BSA adsorption properties. Seven-milligram portions of magnetic chelator supports (charged with Cu^{2+} or uncharged) were (i) magnetically retrieved from storage buffer (20 mM sodium phosphate, pH 6.8 containing 1 M NaCl), (ii) equilibrated thoroughly by resuspension in a binding buffer composed of 10 mM potassium phosphate, pH 6.4, supplemented with 1.0 M NaCl, (iii) reseparated, and then (iv) incubated at room temperature (22 °C) with 1-mL aliquots of BSA solutions (of varying concentration and made up in binding buffer) on an IKA VXR-S17 vibrating shaker (IKA Labortechnik, Staufen, Germany) operated at ~800 rpm. After 600 s of incubation the supports were separated and the supernatants were assayed for residual protein content (see Analytical Methods). The amounts of adsorbed BSA were calculated by difference, and adsorption isotherms were subsequently plotted and fitted to the Langmuir (*18*) and bi-Langmuir models. In the simple monomodal Langmuir expression (eq 1), the equilibrium concentrations of the adsorbed and bulk-phase protein are represented by Q^* and C^*, respectively. Binding is fully described by two terms, a dissociation constant, K_d, and Q_{max}, the maximum capacity for the adsorbed protein. In the bi-Langmuir model (eq 2), two types of binding sites are assumed, namely, "tight" and "weak", and these are described by the dissociation constants K_{dA} and K_{dB}, respectively. The corresponding maximum protein binding capacity at each of these sites are given by Q_{maxA} and

Q_{maxB}, and the sum of the two capacities equals the total capacity, Q_{max}.

$$Q^* = Q_{max}\frac{C^*}{K_d + C^*} \qquad (1)$$

$$Q^* = Q_{maxA}\frac{C^*}{K_{dA} + C^*} + Q_{maxB}\frac{C^*}{K_{dB} + C^*} \qquad (2)$$

Collected data were fitted to these models using the χ^2 minimization procedure of Microcal Origin software version 4.1.

2.5. SOD Batch Adsorption/Desorption Studies. Small-scale SOD batch binding and elution studies were carried out in 2-mL eppendorf-style tubes using whey and defined amounts of the aforementioned Cu^{2+}-IDA linked magnetic adsorbent. As a starting point for method development the basic buffer employed in these experiments was the same as that used in the chromatographic screening study described earlier, i.e., 10 mM potassium phosphate, pH 6.4. This was supplemented with up to 1 M NaCl for equilibration/binding and washing operations or with various concentrations of ammonium chloride (0.2−1 M NH$_4$Cl) for elution. Between each step, the supports were separated magnetically, using side-pull magnetic racks (Perseptive Biosystems, Framingham, MA), to allow the supernatant to be removed before the new buffer was added. The supports were equilibrated in binding buffer prior to resuspending in whey and incubating for 600 s at ~800 rpm on a vibrating shaker. After the batch binding step, the supernatants were collected, and the supports were subsequently washed twice with 1 mL of the appropriate washing buffer for 30 s. Finally, bound proteins were desorbed in either one or two successive rounds of elution, by incubating the washed "product-loaded" supports with elution buffer for 600 s at 800 rpm on a vibrating shaker, before magnetically retrieving the particles, and removing the supernatant(s). All of the above operations were carried out at a temperature of ~22 °C.

2.6. High-Gradient Magnetic Fishing System Setup. A schematic illustration of the HGMF system employed in this work is shown in Figure 1. A distinction of the present study, cf. our previous work on HGMF, is that it is the first to feature a magnet system designed specifically for use in bioprocessing (*19*). A photograph of this laboratory-type permanent magnet separator (Steinert HGF-10, Steinert Elektromagnetbau GmbH, Köln, Germany) is shown in Figure 1, and a schematic illustration of how it works is presented in Figure 2. The magnetic flux density in the 1.5 cm air-gap between the poles was determined with the aid of a gaussmeter (Lakeshore model 410, Westerville, OH) fitted with a transverse probe, as 0.56 and 0.03 T in the "on" and "off" positions, respectively. A filter canister (4.4 mL, 56 mm long × 10 mm i.d.) was filled with a rolled mat of woven mesh composed of "430" stainless steel fibers (~110 μm thickness) to occupy ~11% of the working volume (i.e., to give a voidage of 0.89 and void volume of 3.9 mL) before positioning vertically between the pole shoes. The process setup consisted of (i) a stirred batch adsorption reactor; (ii) the magnet and the filter canister mentioned above; (iii) two peristaltic pumps (Masterflex L/S Easy-Load model 7518-00, Cole Parmer Instruments Co., Vernon Hills, IL, MA); and (iv) a model 2212 Helirac fraction collector (LKB Bromma, Bromma, Sweden). The different flow directions used for particle loading, washing, product elution, and particle recovery were controlled
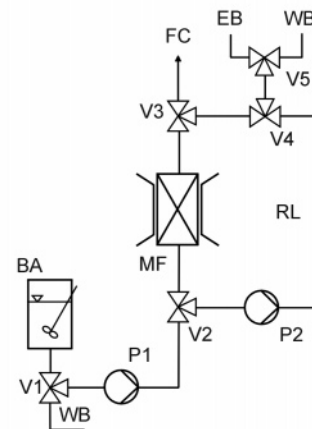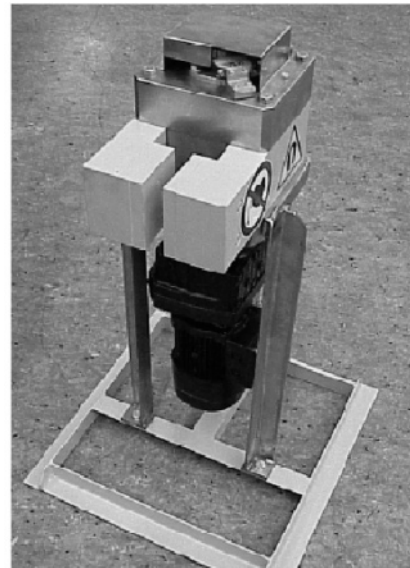

Figure 1. Photograph of the laboratory type (Steinert HGF-10) switch on−off permanent magnet separator (top) and schematic representation of the high-gradient magnetic fishing system (bottom). Key: BA, batch adsorption reactor; EB, elution buffer; FC, fraction collector; MF, magnetic filter; RL, recycle loop; P1 and P2, pumps; V1−V5, valves; WB, wash buffer.

by manual three-way (2 mm i.d.) Teflon valves (Kebo Lab A/S, Albertslund, Denmark). During loading of the magnetic filter with the field on, the particle/feedstock suspension was fed through valves 1−3 via pump 1. For washing and protein elution, a recycle-loop was created by changing valves 2 and 3 so that after filling the loop via valve 4, the liquid could be pumped in a circle with pump 2 after switching the field off. The field was then switched back on, and after changing valve 3, the washed off or eluted material was collected. Finally, switching off the field while pumping allowed the supports to be recovered from the HGMF rig.

Prior to carrying out HGMF recovery of SOD the support trapping characteristics of the magnetic filter were examined in breakthrough studies, which were conducted using magnetic support particles (amine-terminated intermediates and finished adsorbents) suspended in various liquors (i.e., different buffers or whey) at a final concentration of 7 g L^{-1}. With the field switched on these suspensions were fed to the magnetized filter at a linear flow rate of 24 m h^{-1}. The breakthrough of particles in the filter effluent was monitored by gravimetric measurement of the particle mass in collected samples, as detailed in Analytical Methods.
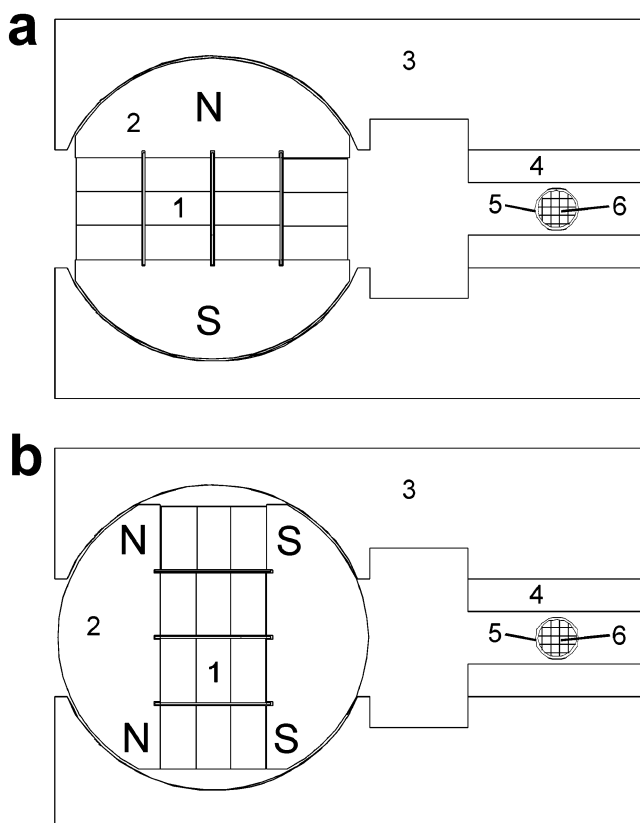
a

b

Figure 2. Schematic top view of the switch on−off permanent magnet system and the separation unit. (a) Field on position. (b) Field off position. Key: 1, blocks of permanent magnet material; 2, circular shaped subyoke; 3, iron yoke; 4, pole shoe; 5, separation unit housing; 6, separation matrix.

The extent of in-system mixing during transition from one buffer to another in an HGMF experiment was determined in the following way. A UV1 detector (Amersham Biosciences, Uppsala, Sweden) was inserted into the HGMF system immediately after valve V3 (Figure 1). The filter canister was filled to 10% breakthrough capacity with amine-terminated magnetic particles suspended in buffer 1 (20 mM Tris-HCl buffer, pH 8) as described above. After loading, the system was washed with the field switched on. Then, with the field still on buffer 2, i.e., buffer 1 supplemented with 0.5 M NaCl and 10% (v/v) acetone, was applied to the canister until the acetone concentration measured by the UV monitor reached 1% (v/v), i.e., 10% breakthrough. At this point, pumping was stopped, and valves V3 and V4 were closed to isolate the recycle loop (Figure 1), before switching the field off and chasing the particles out of the filter and around the loop in the reverse direction, at 92 m h^{-1} for 600 s. Supports were subsequently recaptured within the filter by switching the field back on, and the washings were sent out of the HGMF rig to the fraction collector. The recycle loop was then refilled with the same volume of buffer 2 as that determined in the previous cycle, and a second run was performed in a manner identical to that just described for the first. The conductivities of the first and second buffer pools collected from the HGMF recycle loop were measured off-line using a Meterlab model CDM210 conductivity meter (Radiometer, Brønshøj, Copenhagen), and the NaCl concentration in each was determined by reference to a standard curve constructed using 0−0.5 M NaCl suspended in 20 mM Tris-HCl pH 8 containing 10% acetone (v/v). Comparison of the NaCl concentration in the first and second buffer pools emerging from the

HGMF system employed in this study, with the buffer initially applied, showed 15% and 3% drops, respectively.

Between experiments the filter canister was disconnected from the HGMF system and cleaned by flushing in both directions with water at high flow rate for a period of at least 600 s.

2.7. Recovery of SOD from Whey using the HGMF Process. Equilibrated Cu^{2+}-charged magnetic metal chelator supports were resuspended in sufficient whey to give a particle concentration of 7 g L^{-1} and thereafter mixed at room temperature with an overhead stirrer for 600 s. Subsequently, the particle/whey suspension was pumped upward through the magnetic filter canister at a linear flow rate of 24 m h^{-1}, while the magnetic field was switched on. Shortly before particle breakthrough was expected (determined in the preceding filter characterization experiments) pumping was stopped. The recycle loop was then filled with washing buffer (10 mM potassium phosphate, 30 mM NaCl, pH 6.4) and after turning the field off, the suspension was pumped through the recycle loop under reversed flow at a velocity of 92 m h^{-1} for 120 s to wash out entrained and/or loosely adsorbed materials. The particles were subsequently recaptured, by turning on the magnetic field, and the "dirty" washing buffer was pumped out of the HGMF rig. A second cycle of washing was performed before commencement of SOD elution. Bound SOD was desorbed from the particles in two cycles of 600 s each, in a fashion analogous to the washing procedures just described, by filling the recycle loop with elution buffer (100 mM potassium phosphate, 0.8 or 1.2 M NH$_4$Cl, pH 6.4), and rapidly circulating the particles around the closed system loop.

2.8. Analytical Methods. Particle concentration was determined by dry weight measurements. Samples containing magnetic particles were applied to (predried and weighed) 0.45-μm filters (PALL Corporation, Ann Arbor, MI) and filtered under vacuum while being flushed with large amounts of water to release entrained salts or solids. Afterward the filters were dried in a microwave oven at 300 W for 600 s. After cooling in a desiccator the filters were weighed, and the particle concentration in the samples was calculated from the difference in weight of the filter before and after sample application.

Soluble protein (expressed in BSA equivalents), SOD, and lactoperoxidase (LPO) contents in samples were determined using, respectively, the bicinchoninic acid (BCA) protein assay, superoxide dismutase assay kit, and TMB-ONE ready-to-use substrate. All three assays were scaled for use in a Cobas Mira spectrophotometric robot (Roche Diagnostics, Switzerland).

The basis for the commercial SOD assay employed here, and first described by Nebot et al. (*20*), is that SOD accelerates the alkaline autoxidation of 5,6,6a,11b-tetrahydro-3,9,10-trihydroxybenzo[*c*]fluorene (BXT-01050) to a chromophore possessing an apparent ϵ_{max} at 525 nm. The ratio of the autoxidation rates measured in the presence and absence of SOD gives a measure of SOD activity, and 1 unit of SOD activity is defined as that which doubles the autoxidation rate of the control blank (*20*). Although interference arising from the presence of biological mercaptans in samples is eliminated by the incorporation of the mercaptan scavenger 1-methyl-2-vinylpyridinium trifluoromethanesulfonate in the assay, the presence of certain proteins can also cause significant artifacts (*20* and references therein). Accordingly, prior to employing the SOD assay on samples of crude whey and fractions collected during SOD purification, we tested it on the following purified proteins: β-lactoglobulin (3

Table 1. Summary of Data from Recovery of SOD from Clarified Sweet Whey on Heparin Sepharose HP and M^{2+}-Charged Chelating Sepharose HP HiTrap Screening Columns

purification step	% yield	specific activity (U mg^{-1})	purification factor	yield factor[a]
clarified whey	100	0.075	1.0	1.0
Heparin Sepharose HP	67.3	1.30	17.4	11.7
Cu^{2+}-Chelating Sepharose HP	70.5	2.72	36.4	25.1
Ni^{2+}-Chelating Sepharose HP	2.8	0.92	12.3	0.34

[a] Yield factor = fractional yield × purification factor (ref 23).

g L^{-1}), immunoglobulin (1 g L^{-1}), α-lactalbumin (0.7 g L^{-1}), serum albumin (0.3 g L^{-1}), lactoferrin (0.02−0.35 g L^{-1}), LPO (0.01−0.03 g L^{-1}), and lysozyme (<0.001 g L^{-1}), with each being used at concentrations reflecting their reported contents in bovine whey (*21, 22*). Of these, only LPO was observed to interfere with the assay; its presence in samples resulted in a concentration-dependent "false positive" SOD activity. For the determination of "true" SOD activity in samples (i.e., due to SOD alone), the correction of the apparent SOD activity for false positive contributions due to the presence of LPO proved necessary and was carried out as follows: (i) The precise LPO content in a given sample was determined with the LPO assay (see below). (ii) The false positive contribution of that amount of LPO to the sample's apparent SOD activity was then calculated by reference to a standard curve of apparent SOD activity vs LPO content. (iii) The true SOD activity was subsequently obtained simply by subtracting the estimated contribution due to LPO from the SOD measurements on the sample. For crude bovine whey correction of the apparent SOD activity (0.857 ± 0.026 U mL^{-1}, $n = 7$) for false positive interference from endogenous LPO gave a mean value for the true SOD activity of 0.784 ± 0.023 U mL^{-1} ($n = 7$), i.e., ∼91% of the measured SOD activity was judged to be true and just 8% as arising from LPO. A similar value for the true SOD activity in whey was obtained using a different approach, i.e., adding sufficient catalase to knock out the false positive interference caused by LPO (*20*). When catalase was added to crude whey at 50, 100, and 150 U mL^{-1} of sample, the apparent SOD activity dropped to 92.9 ± 0.5% ($n = 3$) of its initial value.

In the assay for LPO activity, LPO catalyzes the oxidation of 3,3′,5,5′-tetramethyl benzidine. The formation of the deep blue product was followed at 37 °C by monitoring the change in absorbance at 600 nm. In contrast to the false positive activity shown by LPO in the SOD assay, pure SOD registered no apparent LPO activity, even when used at a concentration as high as 0.52 g L^{-1}.

In this work we have employed "yield factors" (fractional yield × purification factor) recommended by Hearle et al. (*23*) to aid selection of the best combinations of SOD purity and recovery.

3. Results and Discussion

3.1. Ligand Selection. Both heparin affinity (*24, 25*) and immobilized metal affinity principles (*26*) have been employed previously for the chromatographic purification of SODs from various sources, but a comparative evaluation of these two techniques for SOD isolation from whey has not been reported until now. The results of chromatographic screening studies performed on HiTrap immobilized metal affinity chromatography (IMAC) and heparin columns (Table 1) confirm that the best yield, purification, and yield factors were obtained by IMAC
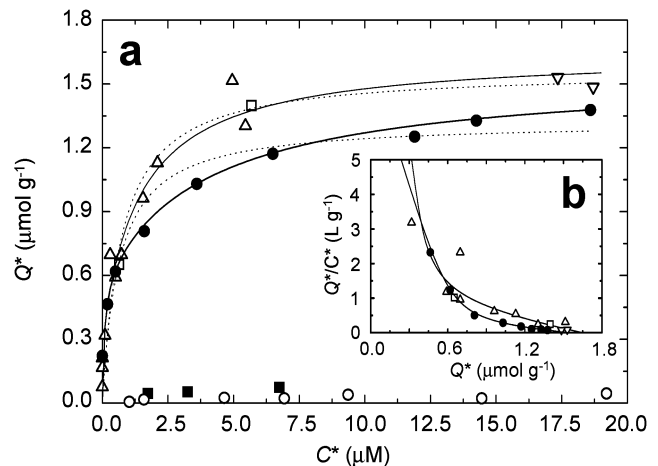

Figure 3. (a) Equilibrium adsorption of BSA on magnetic chelator particles. (b) Scatchard plots showing heterogeneous adsorption of BSA to Cu^{2+}-charged magnetic chelators. Key: (●) Cu^{2+}-charged LS, (△) HS$_1$, (□) HS$_2$, and (▽) HS$_3$ magnetic chelators; Uncharged (○) LS and (■) HS$_2$. Broken and solid lines through the data represent the fit of Langmuir (eq 1) and bi-Langmuir (eq 2) isotherms, respectively, with the parameters cited in Table 2.

on Cu^{2+}-IDA Sepharose HP, with the second best performance being obtained by the Heparin Sepharose HP matrix. Conversely, the performance of both Ni^{2+}- and, to an even greater extent, Zn^{2+}-charged IMAC columns for which no binding was detected (results not shown) was very poor and did not warrant further study. In view of the superior binding performance of the Cu^{2+}-IDA support, combined with the ready availability, low cost, and robustness of the synthetic metal chelating agent, iminodiacetic acid (IDA), the latter was chosen in preference to heparin as the ligand for construction of magnetic adsorbents with selectivity for SOD.

3.2. BSA Binding Tests. Following their manufacture and prior to use in studies with unconditioned whey, the various batches of Cu^{2+}-IDA magnetic adsorbent particles were first subjected to a performance/quality control test, which involved determining adsorption isotherms with bovine serum albumin (BSA), a protein known for its ability to bind to Cu^{2+}-IDA supports (*27*). Figure 3 shows the adsorption isotherms obtained with the various batches of magnetic chelator particles used in this study. Strong and high capacity binding of BSA was observed with the Cu^{2+}-charged supports. This adsorption behavior was clearly mediated by the presence of chelated Cu^{2+} ions, as only very low levels of BSA binding were noted for uncharged supports (Figure 3a). The Cu^{2+}-charged BSA binding data were fitted to Langmuir (eq 1) and bi-Langmuir (eq 2) models, and resulting parameters obtained for the curves presented in Figure 3 are shown in Table 2. The gross similarity of the three Cu^{2+}-charged high sub batches (HS$_1$, HS$_2$, and HS$_3$) was confirmed by the observation that their BSA binding data collapsed along common Langmuir and bi-Langmuir fit curves (Figure 3a). Evidently the LS adsorbent possessed somewhat reduced sorption performance for BSA compared to its HS counterparts. Although at first glance the simple Langmuir isotherm yielded apparently satisfactory fits (Figure 3a, broken lines), Scatchard (*28*) analysis (Figure 3b) gave strongly curved plots consistent with at least two different types of binding affinities. Not surprisingly, therefore, remodeling the data to the bi-Langmuir isotherm (Figure 3a and b, solid lines) resulted in superior fits. The Langmuir fits grossly underestimated the tightness of BSA binding (initial slopes of the

Table 2. Estimated Parameters[a] for Adsorption of BSA on Type II Cu²⁺-Charged Magnetic Metal Chelators

support type	Langmuir model (eq 1)			bi-Langmuir model (eq 2)					
	Q_{max} (μmol g⁻¹)	K_d (μM)	initial slope (L g⁻¹)[b]	Q_{maxA} (μmol g⁻¹)	K_{dA} (μM)	Q_{maxB} (μmol g⁻¹)	K_{dB} (μM)	Q_{max} (μmol g⁻¹)[c]	initial slope (L g⁻¹)[d]
LS	1.26	6.4	0.197	0.58	0.076	0.95	4.1	1.53	7.86
HS	1.56	7.4	0.211	0.33	0.023	1.32	1.5	1.65	15.15

[a] Figure 3 adsorption isotherm data were fitted using the χ^2 minimization procedure of Microcal Origin software version 4.1; [b] Initial slope = Q_{max}/K_d. [c] $Q_{max} = Q_{maxA} + Q_{maxB}$. [d] Initial slope = $Q_{maxA}/K_{dA} + Q_{maxB}/K_{dB}$.

isotherms), and differences between the LS and HS adsorbents were totally obscured (Table 2, initial slopes of ~0.2 L g⁻¹ for both Cu²⁺-charged supports). By contrast the bi-Langmuir model not only revealed that BSA binding of both adsorbent types was much tighter, but also that the Cu²⁺-HS material was roughly twice as potent as the Cu²⁺-LS variant (Table 2, initial slopes = 15.2 vs 7.9 L g⁻¹).

3.3. Characterization/Optimization of Substeps That Make Up HGMF. Having selected a suitable ligand, manufactured magnetic adsorbents featuring it, and confirmed the suitability of the latter materials for protein recovery by immobilized metal affinity adsorption, the next tasks en route to construction of an HGMF-based SOD extraction process were systematic characterization and optimization of each of the substeps (i.e., product adsorption, adsorbent collection, adsorbent washing, and product desorption). With the exception of the adsorbent collection study (3.3.3), all of this work was performed at small scale, i.e., using eppendorf vials and permanent magnet racks. The equilibration, wash, and elution conditions previously employed to good effect in the recovery of SOD from clarified whey by chromatography on Cu²⁺-Chelating Sepharose HP (see Table 1) were initially applied in these experiments, but were systematically altered as optimal conditions for each of the steps in HGMF (i.e., binding, washing, and elution) were identified.

3.3.1. SOD Adsorption. Numerous other whey proteins present at concentrations much higher (*21, 29*) than that of SOD, e.g., serum albumin (*27*), immunoglobulins (*30, 31*), lactoferrin (*30, 32, 33*), LPO (*31, 34*), lysozyme (*33, 35*), α-lactalbumin (*7, 36*), and β-lactoglobulin (*7, 35*) are also known for their ability to bind to immobilized metal affinity adsorbents. Not surprisingly, therefore, when suspended in whey, the Cu²⁺-charged magnetic adsorbents bind much more of these species than SOD. SDS−PAGE analysis (results not shown) confirmed that lactoferrin, LPO, and immunoglobulin were substantially enriched in eluates from Cu²⁺-charged supports after having been contacted with crude whey. α-Lactalbumin and β-lactoglobulin had also been bound in significant amounts, albeit less specifically, but BSA had not been adsorbed. Given SOD's very low concentration in whey (0.15−0.6 mg L⁻¹) and that it runs in exactly the same position as the most abundant whey protein species, β-lactoglobulin (present at 3 g L⁻¹), under both reducing and nonreducing conditions, visual detection of the target enzyme in Coomassie blue and silver stained SDS-polyacrylamide gels was not possible. Attempts to detect SOD's presence in crude samples using specific zymographic (a two-stage technique that involves protein separation by electrophoresis, followed by in situ assay of enzyme activity) methods (*37*) developed for and tested on systems rich in endogenous SODs (e.g., bovine blood, *E. coli* extracts) were likewise compromised by the very low levels of SOD in all whey-derived samples.

In view of the above in small-scale batch binding experiments, we first determined the optimal magnetic adsorbent concentration for SOD recovery from unconditioned whey. Figure 4 shows that virtually complete removal of the SOD present in the crude whey feedstock could be achieved by using the LS adsorbent at a concentration of close to 12 g L⁻¹, whereas the use of HS particles allowed the same result to be achieved at lower support concentrations (typically ~7 g L⁻¹). Importantly, despite huge competition for binding sites on the Cu²⁺-charged LS and HS supports from the other metal chelate binding proteins present in whey, complete removal of SOD was attained at the expense of only a ~15% drop in the concentration of total whey protein (Figure 4). Clearly therefore, preferential adsorption of SOD vs other whey proteins had been achieved with both adsorbent types. For all further experiments on development of a HGMF process, HS supports were selected in preference to the LS materials, and these were employed at the minimum concentration required for quantitative removal of SOD from whey, i.e., 7 g L⁻¹. The impact of this choice on the performance of the resulting HGMF process is highly significant. For example, in HGMF use of the LS adsorbent for the above task would entail >1.7-fold faster exhaustion of the magnetic filter's capacity for adsorbent particles and a >40% reduction in the volume of feedstock that could be treated per cycle.

3.3.2. Switch On−Off Permanent Magnet Separator. Using variable field electromagnets we have previously determined that the magnetic particles described in this work can be collected by HGMS from biological suspensions flowing at 100 m h⁻¹ using moderate field strengths (e.g., ~0.4 T) that are easily supplied by rare earth permanent magnets (*1, 2*). A distinction of the HGMF system featured in this work (section 2.5, Figure 1) is that it is built around a cyclically operated on−off permanent magnet (*19*). This separator was designed with bioprocessing in mind, and this study is the first to report its use for bioproduct purification by HGMF.

The unusual capacity to turn a permanent magnet on and off at will is realized by mounting an arrangement of magnet blocks within the center of a cylindrical iron subyoke, which can be rotated along its central axis, within a fixed iron yoke (Figure 2). In the on position (Figure 2a) the system resembles a conventional magnet yoke and generates a flux density in the gap between the pole shoes of ~0.56 T. Rotation of the cylinder stepwise through 90° (to the off position; Figure 2b) reduces the flux density at the pole region to ~0.03 T, the main reason for this being that the magnetic flux lines are short-circuited by the iron yoke. The main advantages of this particular magnetic separator design over systems employing electric coils include the absence of a dedicated power supply (i.e., no heat generation), low operating costs, and easy accessibility to the magnet field region. Moreover, the small size of the lab prototype (~70 kg) used here makes for an easily transported system, allowing small-scale HGMF trials with real industrial feedstocks to be performed on-site at interested biotech companies.
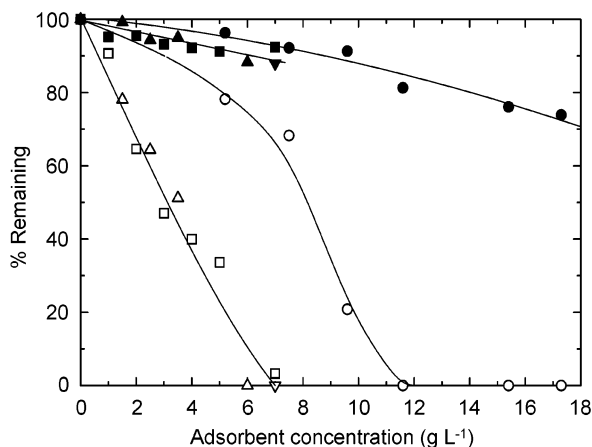
Figure 4. Effect of Cu^{2+}-charged LS and HS type II magnetic chelator particle concentration on the removal of SOD from unconditioned whey. Key: ($\bigcirc$, $\bullet$) LS; ($\blacktriangle$, $\triangle$) HS$_1$; ($\square$, $\blacksquare$) HS$_2$; and ($\triangledown$, $\blacktriangledown$) HS$_3$ Cu^{2+}-magnetic chelators; SOD activity (open symbols); soluble protein content (filled symbols).
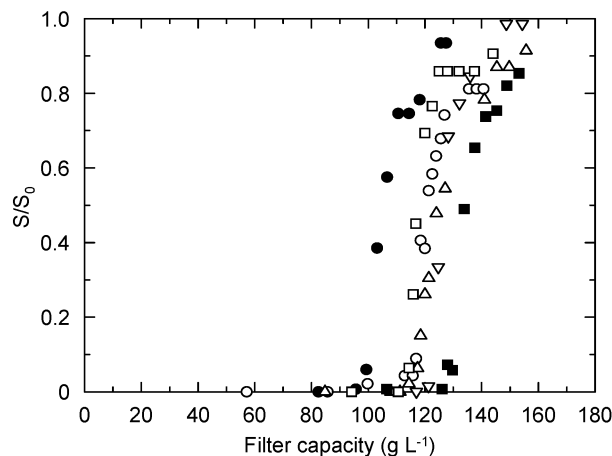

Figure 5. Influence of support surface chemistry and suspending phase on magnetic support capture by HGMS. Key: fresh amine terminated particles suspended in ($\bigcirc$) equilibration/wash buffer, ($\triangle$) elution buffer, and ($\bullet$) unconditioned whey; recycled amine terminated particles suspended in ($\triangledown$) equilibration/wash buffer; fresh HS$_3$ Cu^{2+}-charged magnetic chelators suspended in ($\square$) equilibration/wash buffer and ($\blacksquare$) unconditioned whey. S_0 = support concentration applied to filter; S = support concentration exiting filter. Equilibration/wash buffer: 10 mM potassium phosphate, 1 M NaCl, pH 6.4. Elution buffer: 10 mM potassium phosphate, 0.8 M NH$_4$Cl, pH 6.4.

3.3.3. Adsorbent Collection by HGMS.

Having selected an appropriate concentration of magnetic adsorbent particles to employ during batch binding operation, the next step was to examine their collection by HGMS. The volume of particle-liquid suspension processed per cycle of the HGMF system is constrained by the support holding capacity of the magnetic filter. Under ideal conditions the filter will capture 100% of the incoming magnetic support particles until a certain capacity is reached, after which sudden breakthrough will occur and all new particles entering the filter pass through. In reality, however, some magnetic particles will escape the filter before its total capacity is attained. The filter should therefore be operated in such a way that the highest possible support holding capacity is achieved at the expense of minimal support loss. In much of our previous work on the characterization of magnetic particle breakthrough in simple buffered solutions and under various combinations of magnetic flux density and fluid velocity, instead of "finished" magnetic adsorbent particles, we have employed a defined intermediate in their manufacture, namely, an amine-terminated magnetic particle of very similar size and magnetic properties (1−6). The availability of this "model" magnetic material in much larger amounts than the finished adsorbents permitted more extensive trials to be conducted. In this work we have carried out HGMS breakthrough studies with both types of magnetic supports, i.e., the amine-terminated model material and the Cu^{2+}-charged magnetic chelators, and the results are presented in Figure 5. When suspended in 10 mM potassium phosphate, pH 6.4 based equilibration or elution buffers (containing either 1 M NaCl or 0.8 M NH$_4$Cl, respectively), the particle breakthrough profiles for fresh Cu^{2+}-charged magnetic chelators and both fresh and recycled amine-terminated supports were, for practical purposes, identical, with particle breakthrough occurring shortly after a filter capacity of 110 g L^{-1} was reached. That the breakthrough behavior of the amine-terminated support was unaltered after being subjected to a second HGMS particle capture cycle is testament to the fact that no adsorbent agglomeration occurred during the first and is entirely in keeping with the near ideal superparamagnetic properties (i.e., absence of magnetic memory) displayed by these magnetic support particles (1, 4, 5). In stark contrast to the above, the breakthrough behavior of amine-terminated and Cu^{2+}-charged supports were very different to

one another when the suspending phase was switched from equilibration buffer to unconditioned whey. In the latter feedstock, the breakthrough of amine-terminated particles occurred much earlier (i.e., ~90 g L^{-1} vs 110 g L^{-1} in buffer), whereas that of the Cu^{2+}-charged adsorbents was noticeably delayed (~125 g L^{-1}). The premature breakthrough observed with the amine-terminated supports suspended in the low ionic strength whey feedstock (4.4 mS cm^{-1} vs 80.3 mS cm^{-1} for equilibration/wash buffer) most likely reflects some degree of electrostatic interaction between the positively charged support particles and negatively charged insoluble components present in the feedstock. It is plausible that such an interaction would lead to entrainment of insoluble whey material within the cake of magnetic supports collected in the magnetic filter, increasing the space occupied within the filter, which in turn would result in a loss of the latter's magnetic particle holding capacity. An explanation for the apparent increase in capacity of the magnetic filter for the Cu^{2+}-charged supports when suspended in whey versus equilibration buffer is less obvious. We have previously noted that in addition to changes in suspending solution properties and chemical derivatization of the surfaces of magnetic supports, the adsorption of protein to magnetic adsorbent particles exerts a powerful effect on the zeta potential of the latter (1). For example, following the adsorption of trypsin to benzamidine-linked magnetic particles at the binding pH of 7.5, the magnitude of the net surface charge dropped from −30 to −15 mV. In the present case, it is conceivable that, following adsorption of soluble proteins from the whey suspension, the zeta potential of Cu^{2+}-charged magnetic adsorbents would be expected to move closer to zero. This in turn should permit closer particle−particle approach and could, at least in part, account for the observed increase in particle holding capacity of the filter (Figure 5) compared to the same particles suspended in a protein-free equilibration buffer.

3.3.4. SOD Desorption.

An important feature of the present HGMF system is that once captured within the filter all subsequent operations involve the use of an in-system recycle loop. Although immediately following
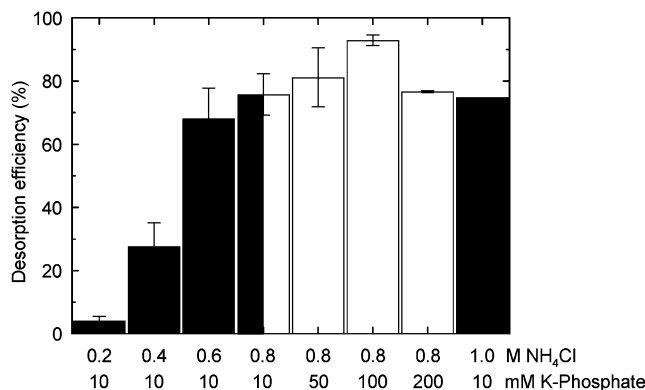
Figure 6. Effect of NH_4Cl concentration and buffer strength on the efficiency of SOD desorption from twice-washed Cu^{2+}-magnetic chelators. Following SOD adsorption supports were washed twice with 10 mM potassium phosphate, 1 M NaCl, pH 6.4, and then eluted with 0.2–1.0 M NH_4Cl in 10 mM potassium phosphate, pH 6.4 or 10–200 mM potassium phosphate buffer pH 6.4 in the presence of 0.8 M NH_4Cl (white bars). The amounts of SOD released are expressed as percentages of the total bound prior to elution. HS_1 and HS_3 particles were used in the "change in $[NH_4Cl]$" and "change in buffer strength" series, respectively. The particle concentration during binding was 7 g L^{-1}, but was raised to 30 g L^{-1} during washing and elution. Over 30% of adsorbed SOD was lost in two washes of 10 mM potassium phosphate, 1 M NaCl, pH 6.4 prior to elution.

collection of adsorbents the particle concentration within current filters can be >100 g L^{-1}, the particle concentration during washing and elution cycles drops considerably, the extent being determined by the size of the recycle loop relative to that of the filter. In this work the void volume of the filter measured 3.8 mL, that of the recycle loop (including valves) is 12.2 mL, and that of the filter and loop combined is 16 mL. Thus, on loading the filter to a capacity of 100–125 g L^{-1} and releasing/recycling the trapped adsorbents into the loop, the mean particle concentration would be expected to be in the range of 20–30 g L^{-1}. With this in mind, in subsequent small-scale experiments conducted with magnetic racks, aiming to identify washing and elution conditions suitable for use in HGMF, the support concentration during binding was maintained at 7 g L^{-1}, but washing and elution were performed at 3- to 4-fold higher adsorbent concentrations, to simulate conditions likely to exist in the recycle loop during HGMF.

Conditions for efficient elution of SOD from washed product-loaded adsorbents were systematically identified in two stages. In the first of these, the effect of NH_4Cl concentration on the efficiency of SOD elution from twice-washed supports was examined (Figure 6, black bars), whereas in the second the impact of increasing buffer strength was studied (Figure 6, white bars). The ease with which SOD was desorbed into the bulk liquid phase was strongly dependent on the ammonium chloride concentration of the latter. For example, efficient recovery of SOD (>75% in one step) from the supports required NH_4Cl concentrations of at least 0.8 M. Variation in the potassium phosphate concentration (10–200 mM potassium phosphate, pH 6.4) in the presence of 0.8 M NH_4Cl (Figure 6, white bars) exerted a less pronounced effect on SOD desorption. A 10-fold increase in potassium phosphate concentration from 10 mM initially to 100 mM raised the relative elution efficiency 1.2-fold, but with further increase to 200 mM this gain was almost completely lost.

3.3.5. Adsorbent Washing. Following adsorption of SOD from whey and prior to elution, we noted alarming

Table 3. Impact of Washing Buffer on Recovery of SOD[a] from Unconditioned Whey Using Magnetic Cu^{2+}-Charged HS_3 Particles[b]

parameter	washing buffer	
	standard[c]	modified[d]
% yield:		
wash 1	27.6	~0.1
wash 2	20.1	~0.5
combined washes	47.7	<0.7
elution 1	25.8	34.0
elution 2	16.7	19.5
combined elutions	42.5	53.5
purification factor:		
combined washes	6.2	<0.2
combined elutions	12.3	12.4
yield factor:[e]		
combined washes	3.0	$<1.3 \times 10^{-3}$
combined elutions	5.2	6.6

[a] The amounts of SOD released are expressed as percentages of the total adsorbed (~99.9%) from the whey. [b] The particle concentration during binding was 7 g L^{-1}, but was raised to 30 g L^{-1} during washing and elution. Elution was performed with 100 mM potassium phosphate, pH 6.4, + 0.8 M NH_4Cl. [c] 10 mM potassium phosphate, pH 6.4 + 1 M NaCl (80.3 mS cm^{-1}) [d] 10 mM potassium phosphate, pH 6.4, + 30 mM NaCl (4.4 mS cm^{-1}). [e] Yield factor = fractional yield × purification factor (ref 23).

levels of product loss (i.e., ~30–50% of that adsorbed) during adsorbent washing steps, which were performed with the standard equilibration buffer (Table 3). Loss of the enzyme from loaded magnetic particles during washing could, however, be reduced down to very low levels (<0.7% of that adsorbed), simply by reducing the concentration of added NaCl from 1 M to 30 mM, thereby lowering the buffer conductivity from 80.3 mS cm^{-1} to a level matching that of the whey feedstock (i.e., 4.4 mS cm^{-1}) used in the batch adsorption step. The positive impact of this change in wash buffer on SOD purification performance (i.e., yield, purification, and yield factor) is clearly observed in Table 3.

3.4. Recovery of SOD from Unconditioned Whey by HGMF. With suitable conditions for the HGMF recovery of SOD from crude whey defined, three separate HGMF runs were conducted. Table 4 presents the data obtained from analysis of the first HGMF run, and a comparison of the three runs is summarized in Table 5. In runs 1 and 3, following the adsorption step SOD-loaded adsorbents were applied to the filter to a capacity of ~80 g L^{-1} such that during washing and elution the particle concentration was ~21 g L^{-1}, whereas in run 2 the filter loading capacity was increased to ~86 g L^{-1}, giving an adsorbent concentration in the recycle loop of nearly 24 g L^{-1}. The ammonium chloride concentration of the elution buffer used for filling the rig's recycle loop was 0.8 M in both elution cycles in runs 1 and 2, but was raised to 1.2 M in run 3. A common pattern was observed in all three runs, which were all conducted with the same batch of Cu^{2+}-charged adsorbents (HS_3). Analysis of the flow through fractions showed that ~85% of the total protein was lost, but that no SOD was detected (Table 4). This was not surprising given that at the adsorbent concentration of 7 g L^{-1} employed in the binding step the target enzyme is completely adsorbed from the crude whey (Figure 4). In two subsequent washing cycles, performed within the closed recycle loop system using the modified wash buffer, further removal of entrained and/or loosely adsorbed protein (>7% of that initially present) was achieved at the expense of only ~0.6% loss of SOD. In run 1, 76.5% of the initially present SOD was recovered in two elution cycles with a purification factor of 14.1 and yield factor of 10.8. SOD is an exceptionally

Table 4. Summary of Data for the Recovery of SOD from Unconditioned Whey in HGMF Run 1

recovery step	volume (mL)	SOD (U)	protein (mg)	specific activity (U mg^{-1})	yield (%)	purification factor	yield factor[a]
whey	52	41.6	531	0.078	100	1.0	1.0
flow through	52	0	450.8				
wash 1	17	0	29.9				
wash 2	17	0.26	8.0	0.033	0.6	0.38	0.002
elution 1	17	17.8	20.7	0.86	42.8	11.0	4.7
elution 2	17	14.0	8.3	1.69	33.7	21.7	7.3
combined elutions	34	31.8	29	1.10	76.5	14.1	10.8
mass balance (%)		77.1	80.0				

[a] Yield factor = fractional yield × purification factor (ref 23). [b] The particle concentration during binding was 7 g L^{-1} but was raised to 21.4 g L^{-1} during washing (10 mM potassium phosphate, pH 6.4, + 30 mM NaCl) and elution (100 mM potassium phosphate, pH 6.4, + 0.8 M NH$_4$Cl).

Table 5. Comparison of HGMF and Small-Scale Purifications of SOD from Unconditioned Whey Performed with Cu^{2+}-Charged HS$_3$ Particles

run	particle concn during elution (g L^{-1})	NH$_4$Cl concentration (M)			yield (%)	purification factor	yield factor[a]
		elution buffer used	during elution 1	during elution 2			
HGMF 1	21.4	0.8	0.68	0.78	76.5	14.1	10.8
HGMF 2	23.7	0.8	0.68	0.78	73.9	13.9	10.3
HGMF 3	21.4	1.2	1.0	1.15	85.7	20.7	17.8
magnetic rack[b]	21.4	1.2	nd	nd	64.7	23.1	14.9

[a] Yield factor = fractional yield × purification factor (ref 23). [b] Small-scale experiment carried out in parallel with HGMF run 3.

robust enzyme (*38*), and so the activity unaccounted for most likely reflects that the missing SOD is still bound to the adsorbents and could be recovered in further elution cycles.

Increasing the particle concentration from 21.4 g L^{-1} in the first run to 23.7 g L^{-1} in the second resulted in slightly inferior purification performance; the purification factor remained essentially unchanged, but both the yield and yield factor dropped very slightly to 73.9% and 10.3 respectively (Table 5). In runs 1 and 2 the elution buffer employed for filling the recycle loop contained ammonium chloride at a concentration of 0.8 M. However, dilution of the incoming elution buffer with traces of the previous solution remaining in the recycle loop caused the actual ammonium chloride concentration to be 0.68 and 0.78 M in elution cycles 1 and 2, respectively. To compensate for this drop in eluting power, a third HGMF run was conducted in which the ammonium chloride concentration of the elution buffer used to fill the recycle loop was raised to 1.2 M. A significant improvement in purification was achieved relative to the two previous runs. More than 85% of the initial SOD was recovered in two elution cycles with an overall purification factor of nearly 21 and yield factor of 17.8. Interestingly lab-scale processing of a 1-mL aliquot (i.e., using a magnetic rack) taken from the batch adsorption reaction corresponding to HGMF run 3 resulted in poorer overall purification performance (i.e., a yield factor of 14.9 vs 17.8), a lower yield (64.7% vs 85.7%), but higher purification factor (23.1 vs 20.7). A possible explanation for the higher elution efficiency observed in HGMF compared to the magnetic rack system is that HGMF affords more effective compaction and dewatering of the adsorbent particle cake within the filter than can be achieved under the influence of a low strength magnet placed alongside an eppendorf tube. Clearly, further experimentation is required to confirm this, but for the present, lab-scale experiments would appear to give reasonably good predictions of the behavior of the HGMF system.

3.5. Strategy for HGMF Process Development. The strategy used here for the design of a HGMF process for SOD capture from whey is a generic approach that can be applied to any new type of macromolecule target

and/or feedstock. Figure 7 shows a schematic representation of the approach, which consists of four main steps prior to arriving at the final process.

In the first step, candidate ligands suitable for binding the target must be identified. In the study described here we have borrowed from chromatography process design in using HiTrap columns. However, rapid small-scale batch binding studies with commercial chromatography media or with commercial or custom-designed magnetic supports would be suitable. A kit of magnetic particles functionalized in different ways would simplify ligand selection, and adaptation to rapid screening methodologies, for example, in 96-well plate format, can be envisaged.

During step 2 a suitable magnetic support must be sourced and characterized. At present custom adsorbent construction may be required, as was used in this work, because of the limited selection of cheap, readily available commercial types. When this situation changes, steps 1 and 2 may be combined. Support binding capacities should preferably be >100 mg g^{-1} (*1*) and ideally >200 mg g^{-1} (*3*) as capacity directly affects the amount of supports that must be used. Dissociation constants in the submicromolar range (*39*) are required in view of the batch adsorption approach employed, and examination of the binding kinetics is necessary for optimization of the batch (or possibly continuous) binding step; typically ~30 s (equivalent to three half-lives) is required for complete binding (*4*). However, optimization of the adsorbent concentration in addition to solution properties (pH, ionic strength, salt type, eluent type) during binding and elution are also worthy of consideration as was observed for the SOD−whey system examined in this work.

Step 3 requires that the magnetic filter be characterized with the feedstock and adsorbents to be used in the final process, given that filter capacity constrains the amount of supports that can be processed in each complete HGMF cycle and that significant differences in the behavior of model materials and finished adsorbents in feedstock and buffers might occur, as was observed in the present study. Magnetic support capture can be influenced by fluid viscosity (but not density), support
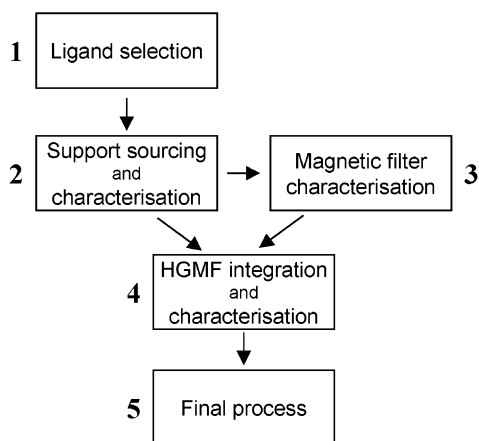
Figure 7. A general strategy for HGMF process design.

size (variation arising between different batches as well as possibly from agglomeration) affecting magnetic velocity, feedstock particulates (increasing drag on the filter cake), processing flow rate, magnetic field strength, and type of filter material (*40*).

Integration of steps 2 and 3 occurs at stage 4 where the process variables already defined are tested, validated against performance in a HGMF process, and where necessary further optimized. At this point, models of the process could conceivably be developed to predict performance robustness, and the advantages of continuous or semicontinuous processing using magnets with multiple yokes and/or filters could be weighed, prior to arriving at an optimal final process in step 5.

4. Conclusions

Magnetic particle-based separation technology applied for bioseparations can be scaled up from laboratory studies in magnetic racks to an integrated magnetic separation-based process, known as high-gradient magnetic fishing (HGMF). The ability to transfer the conditions found in small-scale studies to a HGMF system allows a process for product capture from crude feedstocks to be developed by following a straightforward strategy centered around individual optimization of two key parts: (i) protein adsorption−desorption and (ii) adsorbent capture. Lab-scale optimization of the first key event provides a rapid means of screening a variety of ligand systems, buffers, and feedstock formulations. In the second part, estimation of the filter capacity for support capture requires that the adsorbents to be used in the final process be characterized using a high-gradient magnetic separator. The switch on−off permanent magnet separator used here has proven to be suitable for biotechnological capture processes, and in view of the low operating costs afforded by the use of permanent magnets, further examination of the potential of HGMF at larger scales is warranted. Using the strategy outlined, SOD could be purified from crude whey over 20-fold and in high yield (>85%). The fast processing rates and lack of need for feedstream pretreatment make HGMF an interesting alternative/addition to other separations such as ultrafiltration and ion exchange chromatography used currently for the isolation of milk and whey proteins.

Notation

C^*	protein concentration in the liquid phase (M)
K_d	apparent dissociation constant (M)
K_{dA}	apparent dissociation constant at "tight" sites (M)
K_{dB}	apparent dissociation constant at "weak" sites (M)
Q^*	protein adsorption capacity at equilibrium (mol g^{-1})
Q_{max}	maximum capacity for adsorbed protein (mol g^{-1})
Q_{maxA}	maximum capacity for adsorbed protein at "tight" sites (mol g^{-1})
Q_{maxB}	maximum capacity for adsorbed protein at "weak" sites (mol g^{-1})

References and Notes

(1) Hubbuch, J. J. Development of adsorptive separation systems for recovery of proteins from crude bioprocess liquors. Ph.D. Thesis, Technical University of Denmark, 2001.

(2) Hubbuch, J. J.; Matthiesen, D. B.; Hobley, T. J.; Thomas, O. R. T. High gradient magnetic separation versus expanded bed adsorption: a first principle comparison. *Bioseparation* **2001**, *10*, 99−112.

(3) Heebøll-Nielsen, A. High gradient magnetic fishing: Support functionalisation and application for protein recovery from unclarified bioprocess liquors. Ph.D. Thesis, Technical University of Denmark, 2002.

(4) Hoffmann, C. Einsatz magnetischer Separationsverfahren zur biotechnologischen Produktaufbereitung. Ph.D. Thesis, Forschungzentrum Karlsruhe, Karlsruhe, Germany, 2002.

(5) Hubbuch, J. J.; Thomas, O. R. T. High-gradient magnetic affinity separation of trypsin from crude porcine pancreatin. *Biotechnol. Bioeng.* **2002**, *79*, 301−313.

(6) Heebøll-Nielsen, A.; Choe, W.-S.; Middelberg, A.; Thomas, O. R. T. Efficient inclusion body processing using chemical extraction and high gradient magnetic fishing. *Biotechnol. Prog.* **2003**, *19*, 887−898.

(7) Meyer, A. Einsatz magnettechnologisher Trennverfahren zur Aufbereitung von Molkereiprodukten; Ph.D. Thesis, Forschungzentrum Karlsruhe. Karlsruhe, Germany, 2004.

(8) Gerberding, S. J.; Byers, C. H. Preparative ion-exchange chromatography of proteins from dairy whey. *J. Chromatogr. A* **1998**, *808*, 141−151.

(9) Hahn, R.; Schulz, P. M.; Schaupp, C.; Jungbauer, A. Bovine whey fractionation based on cation-exchange chromatography. *J. Chromatogr. A* **1998**, *795*, 277−287.

(10) Hill, R. D. Superoxide dismutase activity in bovine milk. *Aust. J. Dairy Technol.* **1975**, *30*, 26−28.

(11) Asada, K. Occurrence of superoxide dismutase in bovine milk. *Agric. Biol. Chem.* **1976**, *40*, 1659−1660.

(12) Korycka-Dahl, M.; Richardson, T.; Hicks, C. L. Superoxide dismutase activity in bovine milk serum. *J. Food Prot.* **1979**, *42* (11), 867−871.

(13) Kiyosawa, I.; Matuyama, J.; Nyui, S.; Yoshida, K. Cu-, Zn- and Mn-superoxide dismutase concentration in human colostrum and mature milk. *Biosci. Biotechnol. Biochem.* **1993**, *57* (4), 676−677.

(14) Greenwald, R. A. Superoxide dismutase and catalase as therapeutic agents for human diseases−A critical review. *Free Radical Biol. Med.* **1990**, *8*, 201−209.

(15) Holbrook, J.; Hicks, C. L. Variation of superoxide dismutase activity in bovine milk. *J. Dairy Sci.* **1978**, *61*, 1072−1077.

(16) Eremin, A. N.; Metelitsa, D. I. Purification of superoxide dismutase from red blood cells using reversed micelles of aerosol-OT in heptane. *Appl. Biochem. Microbiol.* **1996**, *32*, 260−264.

(17) Michalski, W. P.; Prowse, S. J. Cu, Zn superoxide dismutase from chicken erythrocytes. *Comp. Biochem. Physiol.* **1991**, *100* (2), 371−375.

(18) Langmuir, I. The adsorption of gases on plane surfaces of glass, mica and platinum. *J. Am. Chem. Soc.* **1918**, *40*, 1361−1403.

(19) Hoffmann, C.; Franzreb, M.; Höll, W. H. A novel high gradient magnetic separator (HGMS) design for biotech applications. *IEEE Trans. Appl. Supercond.* **2002**, *12*, 963−966.

(20) Nebot, C.; Moutet, M.; Huet, P.; Xu, J.-Z.; Yadan, J.-C.; Chaudiere, J. Spectrophotometric assay of superoxide dismutase activity based on the activated autoxidation of a tetratcyclic catechol. *Anal. Biochem.* **1993**, *214*, 442−451.

(21) Creamer, L. K.; MacGibbon, A. K. H. Some recent advances in basic chemistry of milk proteins and lipids. *Internat. Dairy J.* **1996**, *6*, 639−568.

(22) Vasavada, P. C.; Cousin, M. A. Dairy microbiology and safety. In *Dairy Science and Technology Handbook*, *2 Product Manufacturing*; Hui, Y. H., Ed.; VCH Publishers Ltd.: Cambridge, UK, 1993.

(23) Hearle, D. C.; Aguilera-Soriano, G.; Wiksell, E.; Titchener-Hooker, N. J. Quantifying the fouling effects of a biological process stream on chromatographic supports. *Inst. Chem. Eng. Res. Event* **1994**, *1*, 174−176.

(24) Karlsson, K.; Marklund, S. L. Extracellular superoxide dismutase in the vascular system of mammals. *Biochem. J.* **1988**, *255*, 223−228.

(25) Tibell, L. A. E.; Sethson, J.; Buevich, A. Characterization of the heparin-binding domain of human extracellular superoxide dismutase. *Biochim. Biophys. Acta* **1997**, *1340*, 21−32.

(26) Miyato-Asano, M.; Ito, K.; Ikeda, H.; Sekiguchi, S. Purification of copper−zinc-superoxide dismutase and catalase from human erythrocytes by copper-chelate affinity chromatography. *J. Chromatogr. A* **1986**, *370*, 501−507.

(27) Andersson, L.; Sulkowski, E.; Porath, J. Immobilised metal ion affinity chromatography of serum albumins. *Bioseparation* **1991**, *2*, 15−22.

(28) Scatchard, G. The attraction of proteins for small molecules and ions. *Ann. N.Y. Acad. Sci.* **1949**, *51*, 660−672.

(29) Kinghorn, N. M.; Paterson, G. R.; Otter, D. E. Quantification of the major bovine whey proteins using capillary zone electrophoresis. *J. Chromatogr. A* **1996**, *723*, 371−379.

(30) Al-Mashiki, S. A.; Li-Chan, E.; Nakai, S. Separation of immunoglobulins and lactoferrin from cheese whey by chelating chromatography. *J. Dairy Sci.* **1988**, *71*, 1747−1755.

(31) Fukumoto, L. R.; Li-Chan, E.; Kwan, L.; Nakai, S. Isolation of immunoglobulins from cheese whey using ultrafiltration and immobilized metal affinity chromatography. *Food Res. Int.* **1994**, *27*, 335−348.

(32) Lönnerdal, B.; Carlsson, J.; Porath, J. Isolation of lactoferrin from human milk by metal-chelate affinity chromatography. *FEBS Lett.* **1977**, *75*, 89−92.

(33) Torres, A. R.; Peterson, E. A.; Evans, W. H.; Mage, M. G.; Wilson, S. Fractionation of granule proteins of granulocytes by copper chelate chromatography. *Biochim. Biophys. Acta* **1979**, 385−392.

(34) Sciancalepore, V.; Pizzuto, P.; Stefano, G. de. Purification of lactoperoxidase by immobilized copper affinity chromatography. *Latte* **1994**, *19* (11), 1152−1155.

(35) El-Rassi, Z.; Horvath, C. Metal chelate interaction chromatography of proteins with iminodiacetic acid-bonded stationary phases on silica support. *J. Chromatogr.* **1986**, *359*, 241−253.

(36) Blomkalns, A. L.; Gomez, M. R. Purification of bovine alpha-lactalbumin by immobilized metal ion affinity chromatography. *Prep. Biochem. Biotechnol.* **1997**, *27* (4), 219−226.

(37) Misra, H. P.; Fridovich, I. Superoxide dismutase and peroxidase: a positive activity stain applicable to polyacrylamide electropherograms. *Arch. Biochem. Biophys.* **1977**, *183* (2), 511−515.

(38) Fridovich, I. Superoxide dismutases. *Adv. Enzymol.* **1986**, *58*, 61−97.

(39) Chase, H. A. Affinity separations utilising immobilized monoclonal antibodies−A new tool for the biochemical engineer. *Chem. Eng. Sci.* **1984**, *39*, 1099−1125.

(40) Watson, J. H. P. Magnetic filtration. *J. Appl. Phys.* **1973**, *44*, 4209−4213.